Dynamic Loadability of Cable Based Transmission Grids

Olsen, Rasmus Schmidt

Publication date:
2013

Document Version
Publisher's PDF, also known as Version of record

ENERGINET.DK

Technical University of Denmark

DTU

Rasmus Olsen

Dynamic Loadability of Cable Based Transmission Grids

PhD-Thesis

August 2013

DTU Electrical Engineering
Department of Electrical Engineering

Rasmus Olsen

Dynamic Loadability of Cable Based Transmission Grids

PhD-Thesis

August 2013

Dynamic Loadability of Cable Based Transmission Grids
PhD-Thesis

This report was prepared by
Rasmus Olsen

Supervisor
Joachim Holbøll, DTU-Elektro

External Supervisor
Unnur Stella Guðmundsdóttir, Energinet.dk

Department of Electrical Engineering
Centre for Electric Technology (CET)
Technical University of Denmark
Elektrovej building 325
DK-2800 Kgs. Lyngby
Denmark

www.elektro.dtu.dk/cet
Tel: (+45) 45 25 35 00
Fax: (+45) 45 88 61 11
E-mail: cet@elektro.dtu.dk

Energinet.dk
Electricuty Division
Electricity Transmission
Tonne Kjærsvej 65
DK-70000 Fredericia
Denmark

www.energinet.dk
Tel: (+45) 70 10 22 44
Fax: (+45) 76 24 51 80
E-mail: info@energinet.dk

Release date:	August 13, 2013
Category:	1 (Public)
Edition:	First
Comments:	This report is part of the requirements to achieve the Doctor of Philosophy (Ph.D.) degree at the Technical University of Denmark.

Preface

This thesis is the product of three years research within the field of dynamic loadability of cable based transmission grids. The report contains a summary of the three year PhD project which has been conducted in a collaboration between the Danish Transmission System Operator (TSO), Energinet.dk who has fully funded the research, and the Department of Electrical Engineering at the Technical University of Denmark (DTU).

All content of this report has been produced by the author during the three years, either individually or in collaboration with the different professional partners.

The PhD project was carried out at three main locations, the head quarters of Energinet.dk in Erritsø, DTU in Kgs. Lyngby and during a five months external stay at Kinectrics in Toronto, Canada.
At Energinet.dk I gained considerable knowledge about the practical considerations regarding design, installation and dynamic loadability of cables. Energinet.dk has also been the main location where discussions, about how to implement the findings of the project into the real world, have taken place.
At DTU most of the academical discussions within the project have taken place. This includes discussions about pure mathematical issues, cable technology and software technical problems. DTU was also the place where most of the experimental work, for verification of the theoretical models, took place.
For the external stay, which is a mandatory activity to obtain a PhD degree from DTU, I visited Kinectrics in Toronto, Canada. Kinectrics is a large consultancy who employ, among others, one of the experts within loadability calculations, Dr. George Anders. During my stay, I obtained much insight

into dynamic rating techniques, practical issues with loadability calculations and the mathematics behind.

During the PhD project I supervised 2 master projects, as well as 5 special courses at DTU. Furthermore I created and taught a cable course, with approximately 25 students, throughout 13 weeks during the spring of 2011.

The PhD project has until now contributed with 3 journal papers and 4 conference papers. Selected papers can be found in the appendix.

This thesis is divided into 9 chapters, plus list of references, appendices, etc. References to literature are denoted in square brackets, e.g. [1], and equations are denoted in parenthesis, e.g. (1.2) where the 1 refers to the chapter number and the 2 refers to the specific equation in the chapter. Similarly figures and tables are referenced as e.g. figure 1.2 and table 1.2, where the 1 refers to the chapter number and the 2 refers to the specific figure or table in the chapter.

Lyngby, August 13, 2013

Rasmus Olsen

Acknowledgements

I would like to use the opportunity to thank my supervisors Joachim Holbøll, from the Technical University of Denmark, and Unnur Stella Guðmundsd., from Energinet.dk, for many hours of discussion, paper reviewing and supervision. You have both been patient with me and lifted this project to a level which it could not have reached without your significant contributions.

Also a thanks to employees at Department of Electrical Engineering at the Technical University of Denmark, who have given me insight into different areas of research as well as input when difficulties arose. A special thanks to Flemming Juul Pedersen and Jens Christian Jensen who contributed greatly to making my experimental setups possible, and Andrzej Holdyk with whom I have shared many office hours.

Thanks to all employees at Energinet.dk for contributing to a fantastic working environment combined with excellent opportunities for technical discussions. Especially I would like to thank the section of Transmission Lines, where amongst many others Sebastian Dollerup, Thomas Kvarts, Poul Erik Pedersen, Morten Arhenkiel Vilhelmsen and Christian Skovgaard Andersen, deserves thanks for their contributions within both the technical and practical areas of cable manufacturing and installation.

A special thank to my fellow PhD at Energinet.dk, Christian Flytkjær Jensen, with whom I did not only discuss technical issues but also shared an apartment for a significant amount of time during my studies.

I would also like to thank Per Balle Holst, Flemming Bo Christensen and Carsten Rasmussen from Energinet.dk who have followed my project through-

out the three years and during the status meetings contributed significantly to all aspects of my work.

Furthermore a warm thanks to the employees at Kinectrics in Toronto, Canada, especially Mark Fenger, George Anders, Mark Credland, Daniel Suarez, Jeff Hadlow, Sarajit Banerjee and Ivan Boev who made my external stay very memorable as well as contributing significantly to my knowledge within cable testing and thermal modelling.

A deep felt thanks to my friends and family, especially my wife Gitte, who have listened for hours-and-hours about the amazing world of transmission cables. You have supported me in all of my adventures and detours along the way.

Finally I would like to thank all of the people whom I have met during my PhD project. Technical discussions at conferences, workshop, etc., with many of the key players within dynamic rating of transmission cables, have made significant contributions in shaping this thesis.

Abstract

With the decision, made by the Danish parliament in 2009, to underground all of the transmission system below 400 kV and much of the 400 kV system as well, the Danish transmission system operator (TSO), Energinet.dk, initiated this PhD-project as part of the attempt to develop tools for minimising the expected 15 billion Kroner (approximately 2 billion Euro) costs.
The goal of this project is to develop a methodology for implementing dynamic loadability calculations in the decision processes at Energinet.dk, such that the future cable based transmission grid can be optimally dimensioned and utilised.

This thesis starts by investigating different tools for modelling the dynamic behaviour of power cable temperatures and it is found that the thermoelectric equivalent (TEE) method has a good compromise between computational speed and accuracy.
The accuracy of the thermal models is verified by a large scale laboratory experiment. Three 245 kV single phased cables in flat formation are subjected to a highly varying load profile for more than 4 months and very good correlation is found between the measured and modelled conductor temperatures, especially when screen temperature measurements are available as feedback for the model.

Having proven that the temperature of individual cable lines can be estimated with good accuracy, the thermal models are combined with load flow calculations in the power systems simulation software DigSilent PowerFactory (DSPF), which makes the TSO able to predict the future thermal behaviour of all cables in the grid. This integration of load flow (electrical calculations) with TEE (thermal modelling) is in this project denoted electrothermal coordination (ETC).

It is shown in this thesis that ETC can benefit three areas of expertise at the TSO.

Firstly, the real time power system control can, in case of contingencies, use the developed ETC tool to predict the thermal evolution of the grid and determine if any cables in the transmission system are expected to be overheated in the near future or if the system can be allowed to continue operation without interference. This means that ETC allows the operator to control the system based on temperatures (which are the real limiting parameters) instead of current values.
Secondly, the day-ahead planning can use ETC to determine if the settled power market for the coming 36 hours can be allowed or if interference is required due to loadability limitations being exceeded. It is suggested that the current which each cable is capable of conducting continuously for 40 hours (the 40 hours loadability) is calculated and used as the limiting parameter for the load flow studies, instead of the presently used steady state loadability.
Thirdly, it is shown that the transmission grid planner can use ETC to analyse future grid enhancements. Today, new transmission lines are dimensioned such that they can continuously conduct the current which will be experienced during two subsequent outages. However with ETC such restrictions are not necessary to enforce as the temperature can be dynamically modelled.

The developed ETC algorithms are tested on different case studies, including both an adapted version of the IEEE 14-bus test system as well as cases taken from the real Danish transmission system.
It is shown that significant technical as well as economical benefits can be obtained by using ETC in the decision processes instead of steady state loadability values. Furthermore it is shown that the ETC approach increases the reliability of the system as it may allow for harder loading of the individual transmission cables.

It is emphasised that the developed ETC methodology has been developed in close collaboration with the Danish TSO and should thus be seen as ready for implementation, however it should also be acknowledged that the developed tools and algorithms are not limited by national borders and the author encourages utilisation wherever applicable.

Dansk Resumé

I kølvandet på den politiske beslutning om at lægge hele det danske elektriske transmissionsnet på 132/150 kV niveau, samt store dele af 400 kV nettet, i jorden foretog Energinet.dk en række tiltag som skulle hjælpe med at begrænse udgifterne der var budgetteret i størrelsesordnen 15 milliarder kroner. Dette PhD projekt udgør et af disse tiltag.
Målet med projektet er at definere en metode til implementering af dynamiske belastbarhedsberegninger i beslutningsprocesserne hos Energinet.dk, således at det fremtidige kabelbaserede transmissionsystem kan blive dimensioneret og udnyttet optimalt.

Første del af denne afhandling undersøger og diskuterer forskellige værktøjer til dynamisk modellering af temperaturen i transmissionskabler. Modelleringsmetoden termoelektriske ækvivalenter (TEE) vælges som det foretrukne værktøj da dennes kompromis imellem beregningshastighed og nøjagtighed anses for at være bedst.
Nøjagtigheden i beregningerne verificeres endvidere igennem et storskala laboratorieforsøg hvor tre enkeltfasede 245 kV kabler i flad forlægning udsættes for en stærkt varierende belastning henover fire måneder. Sammenligning mellem den simulerede og målte ledertemperatur viste god overensstemmelse, specielt når målinger af skærmtemperaturen var til rådighed som feedback til modellen.

De udviklede modeller til beregning af den dynamiske belastbarhed af transmissionskabler blev integreret med Energinet.dk's systemsimuleringssoftware, DigSilent PowerFactory (DSPF), således at det blev muligt at forudsige den termiske udvikling for alle kabler i transmissionssystemet. Denne interaktion mellem de elektriske beregninger (load flow) og termiske beregninger (TEE) bliver i projektet omtalt som electrothermal coordination (ETC).

Det beskrives i denne afhandling hvordan særligt tre ansvarsområder hos Energinet.dk vil kunne få gavn af ETC.

Det første ansvarsområde er den daglige realtidsdrift af transmissionssystemet. I tilfælde af fejl i nettet vil det udviklede ETC værktøj kunne forudsige hvordan temperaturen i nettet vil udvikle sig henover tid. Dermed kan der tages beslutning om det er nødvendigt at gribe ind eller om det givne belasningsscenarie kan få lov til at fortsætte. Dette betyder at ETC gør det muligt for operatøren at kontrollere nettet på baggrund af temperaturer (hvilke er de reelt begrænsende parametre) i stedet for strømværdier.
Det andet ansvarsområde er i planlægningen af det kommende driftsdøgn (day-ahead planning). Her anbefales det at ETC udnyttes til at beregne den strøm som det er muligt at sende kontinuert igennem de enkelte kabler i 40 timer. Denne 40 timers belastbarhed benyttes til at evaluere om det fastlagte day-ahead elmarked kan få lov til at køre eller om der kræves indblanding fra operatørens side. I dag er indblanding påkrævet hvis load flow beregningerne af det fastlagte elmarked medfører at den kontinuerte belastbarhed for de enkelte kabler bliver overskredet, men med beregning af 40 timers belastbarheden opnås en større fleksibilitet.
Det tredje ansvarsområde der kan få gavn af ETC er i planlægningen af nye transmissionslinier. I dag dimensioneres kablerne således at de kontinuert vil kunne overføre den strøm de kan blive udsat for i tilfælde af to på hinanden følgende komponentudfald. Med implementeringen af ETC er dette ikke nødvendigt da man kan modellere temperaturen dynamisk.

Gennem simulering af en række teoretiske såvel som virkelige scenarier af elsystemer, herunder en tilpasset version af IEEE's 14-bus test system samt udsnit af det danske elnet, bliver det vist at der er betydelige tekniske og økonomiske incitamenter til at implementere ETC. Projektet viser endvidere at ETC metoden kan øge pålideligheden af transmissionsnettet da belastningen af de enkelte kabler kan øges.

Det skal understreges at dette PhD projekt er udarbejdet i tæt samarbejde med Energinet.dk og det udviklede ETC værktøj skal derfor ses som værende klar til implementering i det danske transmissionssystem. Det bør dog også anerkendes at de udviklede algoritmer kan implementeres i andre transmissionssystemer og forfatteren opfordrer derfor til at udnytte det arbejde der præsenteres i denne afhandling så bredt som muligt.

Contents

Expressions, Abbreviations and Symbols

Expressions and Abbreviations

Expression/ Abbreviation	Definition
Ampacity	Maximum calculated current in transmission line permitted by temperature (in opposition to Current carrying capacity). The same definition as loadability used in this thesis
AENS	Average Energy Not Supplied. Measure of reliability
ANN	Artificial Neural Network
ASAI	Average System Availability Index. Measure of reliability
$ASAI_{Current}$	ASAI when system is operated based on steady state loadabilities
$ASAI_{ETC}$	ASAI when system is operated based on electrothermal coordination
ATC	Available Transmission Capability
Backfill	Material put around the cable in the trench to protect the cables against damage and enhance thermal performance of the surroundings

Expression/ Abbreviation	Definition
Bentonite	Clay material which is injected into the cable duct for enhancing the thermal conditions when the cable has to cross under an obstacle
Cable grid	The full transmission network of cables, utilised to transport energy from site of generation to site of consumption
Cable system	Three phases of cable in the AC case (or one or two phases in the DC case), used to transport electric energy from point A to point B. Including all related components such as joints and end point terminations
CAIDI	Customer Average Interruption Duration Index. Measure of reliability
Current carrying capacity	Maximum current in transmission line permitted by physical constraints related to the temperature
Cyclic loadability	Maximum allowed current in a 24 hours load cycle, where the load cycle is assumed to be repeated indefinitely
Distribution cable	Power cables rated below 100 kV
DKK	Danish Kroner. Danish currency, 1 € is approximately 7.5 DKK
DPL	Scripting environment in DSPF, focus on static calculations
DSL	Scripting environment in DSPF, focus on dynamic calculations
DSPF	DigSilent PowerFactory
DSO	Distribution System Operator
DTR	Dynamic Thermal Rating
DTU	Technical University of Denmark
Duct	Pipe in which cables can be pulled to cross obstacles
Dynamic loadability	Maximum allowed current for a specified amount of time
Emergency loadability	Maximum allowed current during emergency operation - typically 1 hour

Expression/ Abbreviation	Definition
ETC	Electrothermal Coordination. Denotes the operation of transmission systems based on temperature instead of current quantities
FACTS	Flexible AC Transmission System
FEM	Finite Element Method. Numerical calculation method where continuous components are divided into small elements
Fibre pipe	Pipe installed in cable trench containing optic fibres for communication and temperature monitoring
FL	Fuzzy Logic
GA	Generic Algorithm
IEC	International Electrotechnical Commission
IEEE	Institute of Electrical and Electronics Engineers
Jacket	Outer covering of individual phases of cables
Load factor	The daily average of the hourly load divided by the maximum daily load
Loadability	Maximum calculated current in transmission line permitted by temperature (in opposition to Current carrying capacity). The same definition as ampacity used in this thesis
Loss-load factor	The daily average of the square of the hourly load divided by the square of the maximum daily load
LP	Linear Programming
Metallic screen	Cable subcomponent with the purpose of maintaining a low voltage along the cable, ensure homogeneous electric field in the insulation and conduct currents in case of faults. The metallic screen is sometimes also used for blocking radial water penetration. When the screen is an extruded metal it is sometimes denoted a metallic sheath

Expression/ Abbreviation	Definition
N situation	System in its complete state. If a component is out for maintenance the system's N state is considered without that component
N-1 situation	System in an incomplete state. If a greater contingency is experienced, the system is in the N-1 situation
Native soil temperature	Temperature in cable burial depth if the soil had been left unaffected
NR	Newton-Raphson
OHL	Overhead line
OPF	Optimal Power Flow
PD	Partial discharge
PE	Poly-ethylene
PVC	Poly vinyl chloride
PMU	Phase Measurement Unit
PT100	Temperature sensor made of platinum, with a nominal resistance of 100 Ω at 0 °C
Rating	Similar to loadability
RS232	Communication protocol
SAIDI	System Average Interruption Duration Index. Measure of reliability
SAIFI	System Average Interruption Frequency Index. Measure of reliability
SCADA	Supervisory Control And Data Acquisition
SR	Step Response. The method to calculate the dynamically evolving temperature in cables as suggested by IEC
Steady state loadability	Calculated current which the cable is capable of carrying indefinitely without exceeding the thermal limits
TEE	Thermoelectric Equivalent. The method to calculate the dynamically evolving temperature in cables as suggested in this PhD project
Temperature Distribution	Temperature dependent on spatial propagation
Temperature Profile	Temperature dependent on time
TGP	Transmission Grid Planner

Expression/ Abbreviation	Definition
Thermocouple, Type-K	Temperature sensor made of chromel and alumel
Transmission cable	Power cables rated 100 kV and above
Transmission grid	The collection of components which transport electric energy on voltage levels higher than 100 kV
Transmission Line	Common name of transmission cables and overhead transmission lines.
Transmission system	A term covering the transmission grid plus the measurement equipment, relays, control structures, etc.
TRM	Transfer Reliability Margin
TRXLPE	Tree-Retardant Cross-Linked Poly-Ethylene
TSO	Transmissions System Operator
TTC	Total Transmission Capability
WAMS	Wide-Area Monitoring System
XLPE	Cross-linked poly-ethylene

List of Symbols

Symbol	Unit	Definition
$\underline{A}$		System matrix of the thermoelectric equivalent method
A	m^2	Area
A	$^{\mathrm{o}}\mathrm{C}$	Mean yearly air temperature
B	$^{\mathrm{o}}\mathrm{C}$	Maximum variation of the air temperature
C_1	$\frac{\mathrm{J}}{\mathrm{K}}$ or $\frac{\mathrm{J}}{\mathrm{m}\cdot\mathrm{K}}$	Thermal capacitance of conductor plus the inner part of the insulation
$C_{1,x}$	$\frac{\mathrm{J}}{\mathrm{K}}$ or $\frac{\mathrm{J}}{\mathrm{m}\cdot\mathrm{K}}$	Thermal capacitance of zone x in the insulation, used in the TEE method
C_3	$\frac{\mathrm{J}}{\mathrm{K}}$ or $\frac{\mathrm{J}}{\mathrm{m}\cdot\mathrm{K}}$	Thermal capacitance of outer part of the insulation plus the screen and the jacket
$C_{3,y}$	$\frac{\mathrm{J}}{\mathrm{K}}$ or $\frac{\mathrm{J}}{\mathrm{m}\cdot\mathrm{K}}$	Thermal capacitance of zone y in the jacket, used in the TEE method
C_4	$\frac{\mathrm{J}}{\mathrm{K}}$ or $\frac{\mathrm{J}}{\mathrm{m}\cdot\mathrm{K}}$	Thermal capacitance of surroundings
$C_{4,z}$	$\frac{\mathrm{J}}{\mathrm{K}}$ or $\frac{\mathrm{J}}{\mathrm{m}\cdot\mathrm{K}}$	Thermal capacitance of zone z in the surroundings, used in the TEE method
C_{elec}	F	Electric capacitance
C_{therm}	$\frac{\mathrm{J}}{\mathrm{K}}$ or $\frac{\mathrm{J}}{\mathrm{m}\cdot\mathrm{K}}$	Thermal capacitance
C_A	$\frac{\mathrm{J}}{\mathrm{K}}$ or $\frac{\mathrm{J}}{\mathrm{m}\cdot\mathrm{K}}$	Thermal capacitance used in the SR method
C_B	$\frac{\mathrm{J}}{\mathrm{K}}$ or $\frac{\mathrm{J}}{\mathrm{m}\cdot\mathrm{K}}$	Thermal capacitance used in the SR method
C_c	$\frac{\mathrm{J}}{\mathrm{K}}$ or $\frac{\mathrm{J}}{\mathrm{m}\cdot\mathrm{K}}$	Thermal capacitance of the conductor
$C_{ground,v}$	$\frac{\mathrm{K}}{\mathrm{m}\cdot\mathrm{W}}$	Thermal capacitance of zone number v in the ground when modelling the native soil temperature
C_i	$\frac{\mathrm{J}}{\mathrm{K}}$ or $\frac{\mathrm{J}}{\mathrm{m}\cdot\mathrm{K}}$	Thermal capacitance of the insulation
C_{i1}	$\frac{\mathrm{J}}{\mathrm{K}}$ or $\frac{\mathrm{J}}{\mathrm{m}\cdot\mathrm{K}}$	Thermal capacitance of the inner part of the insulation
C_{i2}	$\frac{\mathrm{J}}{\mathrm{K}}$ or $\frac{\mathrm{J}}{\mathrm{m}\cdot\mathrm{K}}$	Thermal capacitance of the outer part of the insulation
C_j	$\frac{\mathrm{J}}{\mathrm{K}}$ or $\frac{\mathrm{J}}{\mathrm{m}\cdot\mathrm{K}}$	Thermal capacitance of the jacket

Symbol	Unit	Definition
C_s	$\frac{\mathrm{J}}{\mathrm{K}}$ or $\frac{\mathrm{J}}{\mathrm{m \cdot K}}$	Thermal capacitance of the metallic screen
C_{sur}	$\frac{\mathrm{J}}{\mathrm{K}}$ or $\frac{\mathrm{J}}{\mathrm{m \cdot K}}$	Thermal capacitance of the surroundings
D_e	m	Outer cable diameter
$Ei(x)$		Exponential integral, defined as: $Ei(x) = -\int_{-x}^{\infty} \frac{e^{-t}}{t} dt$
F		Failed state of component, in opposition to O
G_b		Geometric factor for calculation of $r_{backfill,eq}$
I	A	Current
$I_{max,c}$	A	Cyclic loadability
$I_{max,SS}$	A	Steady state loadability
$I_{max,1h}$	A	1 hour loadability
$I_{max,40h}$	A	40 hours loadability
I_{add}	A	Current to be added to I_{Test} at the end of loadability evaluation iteration
I_{Test}	A	Test current for calculating dynamic loadability curve
L	m	Burial depth of cable
M_{vol}	$\%_{vol}$	Moisture content in volume percentage
M_0	s	Coefficient used in the calculation of the thermal response in the SR method
M_c		Cyclic rating factor
M_{weight}	$\%_{weight}$	Moisture content in percentage of total weight
N		Vector of shape functions for FEM simulations
N_0	s^2	Coefficient used in the calculation of the thermal response in the SR method
N_1		Shape function for FEM simulations
N_2		Shape function for FEM simulations
N_3		Shape function for FEM simulations
N_i	$\frac{\text{custumers}}{\text{event}}$	Number of interrupted customers at system failure event number i
N_T	events	Total number of system failure events

Symbol	Unit	Definition
O		Operational state of component, in opposition to F
P	W	Active power
P		Phase angle, used to calculate the soil temperature at cable burial depth
P		Probability
$P_{D,i}$	W	Demanded power in bus number i
P_F		Probability that component is in failed state
$P_{G,i}$	W	Generated power in bus number i
P_i	J	Energy not delivered during system failure event number i
P_L	W	Total transmission losses in the transmission system
$P_{L,k}$	W	Transmission losses in component number k
P_O		Probability that component is in operating state
Q	VAr	Reactive power
Q	J	Thermal energy
Q_{ent}	J	Energy entering the thermal system
Q_{gen}	J	Internally generated energy in the thermal system
Q_{int}	J	Energy stored in the thermal system
Q_{out}	J	Energy leaving the thermal system
R	Ω	Electric resistance
R_{AC}	Ω or $\frac{\Omega}{\mathrm{m}}$	Electrical resistance of conductor to alternating current, including skin and proximity effects
$R_{AC,20}$	Ω or $\frac{\Omega}{\mathrm{m}}$	Electrical resistance of conductor to alternating current at 20 °C, including skin and proximity effects
R_a	Ω or $\frac{\Omega}{\mathrm{m}}$	Electrical resistance of armour to alternating current
$R_{a,20}$	Ω or $\frac{\Omega}{\mathrm{m}}$	Electrical resistance of armour to alternating current at 20 °C
R_{DC}	Ω or $\frac{\Omega}{\mathrm{m}}$	Electrical resistance of conductor to direct current at 20 °C
$R_{DC,a}$	Ω or $\frac{\Omega}{\mathrm{m}}$	Electrical resistance of armour to direct current at 20 °C

Symbol	Unit	Definition
$R_{DC,s}$	Ω or $\frac{\Omega}{\mathrm{m}}$	Electrical resistance of metallic screen to direct current at 20 °C
R_s	Ω or $\frac{\Omega}{\mathrm{m}}$	Electrical resistance of metallic screen to alternating current
$R_{s,20}$	Ω or $\frac{\Omega}{\mathrm{m}}$	Electrical resistance of metallic screen to alternating current at 20 °C
S	VA	Apparent power
S_a	m^2	Nominal cross section of armour
S_c	m^2	Nominal cross section of conductor
S_s	m^2	Nominal cross section of metallic screen
T	h	Length of temperature cycle for modelling native soil temperature
T	s	Total time span on which the reliability indexes are based
T	$\frac{\mathrm{K}}{\mathrm{W}}$ or $\frac{\mathrm{K}}{\mathrm{m}\cdot\mathrm{W}}$	Thermal resistance
T_1	$\frac{\mathrm{K}}{\mathrm{m}\cdot\mathrm{W}}$	Thermal resistance of the dielectric insulation material
$T_{1,x}$	$\frac{\mathrm{K}}{\mathrm{m}\cdot\mathrm{W}}$	Thermal resistance of zone x in the dielectric insulation material
T_2	$\frac{\mathrm{K}}{\mathrm{m}\cdot\mathrm{W}}$	Thermal resistance of the armour bedding of the cable
T_3	$\frac{\mathrm{K}}{\mathrm{m}\cdot\mathrm{W}}$	Thermal resistance of the cable jacket
$T_{3,y}$	$\frac{\mathrm{K}}{\mathrm{m}\cdot\mathrm{W}}$	Thermal resistance of zone y in the jacket material
T_4	$\frac{\mathrm{K}}{\mathrm{m}\cdot\mathrm{W}}$	Thermal resistance of the cable surroundings
$T_{4,z}$	$\frac{\mathrm{K}}{\mathrm{m}\cdot\mathrm{W}}$	Thermal resistance of zone z in the surrounding material
T_A	$\frac{\mathrm{K}}{\mathrm{m}\cdot\mathrm{W}}$	Thermal resistance used in the SR method
T_a	$\frac{\mathrm{K}}{\mathrm{m}\cdot\mathrm{W}}$	Apparent thermal resistance used in the SR method
T_B	$\frac{\mathrm{K}}{\mathrm{m}\cdot\mathrm{W}}$	Thermal resistance used in the SR method
T_b	$\frac{\mathrm{K}}{\mathrm{m}\cdot\mathrm{W}}$	Apparent thermal resistance used in the SR method
$T_{ground,v}$	$\frac{\mathrm{K}}{\mathrm{m}\cdot\mathrm{W}}$	Thermal resistance of zone number v in the ground when modelling the native soil temperature

Symbol	Unit	Definition
T_i	$\frac{\mathrm{K}}{\mathrm{m}\cdot\mathrm{W}}$	Thermal resistance of insulation
T_j	$\frac{\mathrm{K}}{\mathrm{m}\cdot\mathrm{W}}$	Thermal resistance of jacket
T_{sur}	$\frac{\mathrm{K}}{\mathrm{m}\cdot\mathrm{W}}$	Thermal resistance of surroundings
U	V	Voltage
U_i	V	Voltage at bus number i
$U_{max,i}$	V	Maximum allowed voltage at bus number i
$U_{min,i}$	V	Minimum allowed voltage at bus number i
U_o	V	Voltage between conductor and screen
U_{pp}	V	System voltage. Voltage between phases
V	m^3	Volume
$V_{material}$	m^3	Volume of porous material, used for evaluating the specific heat of a moist porous material
V_{water}	m^3	Volume of water, used for evaluating the specific heat of a moist porous material
W_a	$\frac{\mathrm{J}}{\mathrm{s}}$ or $\frac{\mathrm{J}}{\mathrm{s}\cdot\mathrm{m}}$	Joule losses in armour
W_c	$\frac{\mathrm{J}}{\mathrm{s}}$ or $\frac{\mathrm{J}}{\mathrm{s}\cdot\mathrm{m}}$	Joule losses in conductor
W_d	$\frac{\mathrm{J}}{\mathrm{s}}$ or $\frac{\mathrm{J}}{\mathrm{s}\cdot\mathrm{m}}$	Dielectric losses in insulation
W_{d1}	$\frac{\mathrm{J}}{\mathrm{s}}$ or $\frac{\mathrm{J}}{\mathrm{s}\cdot\mathrm{m}}$	Dielectric losses of the inner part of the insulation
W_{d2}	$\frac{\mathrm{J}}{\mathrm{s}}$ or $\frac{\mathrm{J}}{\mathrm{s}\cdot\mathrm{m}}$	Dielectric losses of the outer part of the insulation
W_s	$\frac{\mathrm{J}}{\mathrm{s}}$ or $\frac{\mathrm{J}}{\mathrm{s}\cdot\mathrm{m}}$	Joule losses in screen
W_T	$\frac{\mathrm{J}}{\mathrm{s}}$ or $\frac{\mathrm{J}}{\mathrm{s}\cdot\mathrm{m}}$	Sum of all losses in cable
a	s^{-1}	Coefficient used in the calculation of the thermal response in the SR method
b	s^{-1}	Coefficient used in the calculation of the thermal response in the SR method
c_1		Constant used to calculate thermal response in the TEE method
c_2		Constant used to calculate thermal response in the TEE method
c_3		Constant used to calculate thermal response in the TEE method
c_{therm}	$\frac{\mathrm{J}}{\mathrm{m}^3\cdot\mathrm{K}}$	Specific heat

Symbol	Unit	Definition
$c_{therm,a}$	$\frac{\mathrm{J}}{\mathrm{m}^3 \cdot \mathrm{K}}$	Specific heat of armour material
$c_{therm,backfill}$	$\frac{\mathrm{J}}{\mathrm{m}^3 \cdot \mathrm{K}}$	Specific heat of backfill material
$c_{therm,c}$	$\frac{\mathrm{J}}{\mathrm{m}^3 \cdot \mathrm{K}}$	Specific heat of conductor material
$c_{therm,i}$	$\frac{\mathrm{J}}{\mathrm{m}^3 \cdot \mathrm{K}}$	Specific heat of dielectric insulation material
$c_{therm,j}$	$\frac{\mathrm{J}}{\mathrm{m}^3 \cdot \mathrm{K}}$	Specific heat of jacket material
$c_{therm,s}$	$\frac{\mathrm{J}}{\mathrm{m}^3 \cdot \mathrm{K}}$	Specific heat of metallic screen material
$c_{therm,soil}$	$\frac{\mathrm{J}}{\mathrm{m}^3 \cdot \mathrm{K}}$	Specific heat of native soil
$c_{therm,water}$	$\frac{\mathrm{J}}{\mathrm{m}^3 \cdot \mathrm{K}}$	Specific heat of water
d_a	m	Diameter outside armour
d_c	m	Conductor diameter
d_{cs}	m	Diameter of semiconductive conductor screen
d_i	m	Diameter outside insulation
d_{is}	m	Diameter of semiconductive insulation screen
d_{pk}	m	Distance from cable under investigation, p, to cable k
d'_{pk}	m	Distance from cable under investigation, p, to image of cable k above ground
d_s	m	Diameter outside metallic screen
f	Hz	System frequency
$h_{backfill}$	m	Height of backfill envelope in cable trench
h_{conv}	$\frac{\mathrm{W}}{\mathrm{K} \cdot \mathrm{m}^2}$	Convection constant
i		System failure event number
i		Bus number
k		Component number in the grid
k_p		Factor used for the calculation of the proximity effect
k_s		Factor used for the calculation of the skin effect
l	m	Length of cable section
n		number of conductors in cable
p		Van Wörmer coefficient for dividing the thermal capacitance of the insulation in the SR method, long duration thermal transients

Symbol	Unit	Definition
p^*		Van Wörmer coefficient for dividing the thermal capacitance of the insulation in the SR method, short duration thermal transients
p'		Van Wörmer coefficient for dividing the thermal capacitance of the jacket in the SR method
q	$\frac{\mathrm{J}}{\mathrm{m}^2}$	Energy flux
q_{cond}	$\frac{\mathrm{J}}{\mathrm{m}^2}$	Conductive energy flux
q^x_{cond}	$\frac{\mathrm{J}}{\mathrm{m}^2}$	Conductive energy flux in the x direction
q^y_{cond}	$\frac{\mathrm{J}}{\mathrm{m}^2}$	Conductive energy flux in the y direction
q^z_{cond}	$\frac{\mathrm{J}}{\mathrm{m}^2}$	Conductive energy flux in the z direction
q_{conv}	$\frac{\mathrm{J}}{\mathrm{m}^2}$	Convective energy flux
q_{rad}	$\frac{\mathrm{J}}{\mathrm{m}^2}$	Radiative energy flux
q_s		Ratio: losses in conductor plus losses in screen, divided by losses in conductor
$r_{backfill,eq}$	m	Equivalent radius of the thermal backfill cross section in a cable trench
r_x	m	Outer radius of zone number x in the insulation, used to evaluate thermal response in the TEE method
r_{x-1}	m	Inner radius of zone number x in the insulation, used to evaluate thermal response in the TEE method
r_y	m	Outer radius of zone number y in the jacket, used to evaluate thermal response in the TEE method
r_{y-1}	m	Inner radius of zone number y in the jacket, used to evaluate thermal response in the TEE method
r_z	m	Outer radius of zone number z in the surroundings, used to evaluate thermal response in the TEE method
r_{z-1}	m	Inner radius of zone number z in the surroundings, used to evaluate thermal response in the TEE method

Symbol	Unit	Definition
s		Total number of zones in the insulation, TEE method
s	m	Axial spacing between conductors
s_1	m	Axial separation of two adjacent cables in flat formation not touching
s_2	m	Geometric mean axial distance between cables in flat formation
$s_{systems}$	m	Centre distance between to adjacent cable systems
t	s or h or year	Time
t		Total number of zones in the jacket, TEE method
t_a	m	Thickness of armour
t_i	s	Restoration time for system failure event number i
t_i	m	Thickness of insulation
t_s	m	Thickness of metallic screen
$\underline{u}$		Vector of external influences, used in the TEE method
u		Total number of zones in the surroundings, TEE method
v		Zone number in the soil when modelling the native soil temperature
v_1		Eigenvector of system matrix
v_2		Eigenvector of system matrix
v_3		Eigenvector of system matrix
w		Total number of zones in the soil when modelling the native soil temperature
$w_{backfill}$	m	Width of backfill material in cable trench
x		Zone number in the insulation, TEE method
x	m	Depth for temperature modelling
x		Direction in coordinate system
x_p		Factor used for the calculation of y_p
x_s		Factor used for the calculation of y_s
x_v	m	Depth in the bottom of the zone when modelling the native soil temperature

Symbol	Unit	Definition
x_{v-1}	m	Depth in the top of the zone when modelling the native soil temperature
y		Zone number in the jacket, TEE method
y		Direction in coordinate system
y_p		Proximity effect factor
y_s		Skin effect factor
z		Zone number in the surroundings, TEE method
z		Direction in coordinate system
α		Attainment factor, relation between e.g. conductor and jacket temperature
α_{elec}	$\frac{\Omega}{\mathrm{K}}$	Temperature coefficient of electrical resistivity
α_{20}	$\frac{\Omega}{\mathrm{K}}$	Temperature coefficient of the electrical resistivity of the conductor at 20 °C
$\alpha_{20,a}$	$\frac{\Omega}{\mathrm{K}}$	Temperature coefficient of the electrical resistivity of the armour at 20 °C
$\alpha_{20,s}$	$\frac{\Omega}{\mathrm{K}}$	Temperature coefficient of the electrical resistivity of the metallic screen at 20 °C
δ_{soil}	$\frac{\mathrm{m}^2}{\mathrm{s}}$	Soil thermal diffusivity
ϵ		Emissivity of material
ϵ_0	$\frac{\mathrm{F}}{\mathrm{m}}$	Permittivity in vacuum
ϵ_r		Relative permittivity
λ	$\frac{\text{failures}}{100\text{km}\cdot\text{year}}$	Cable failure rate
λ_1	$\frac{\text{failures}}{100\text{km}\cdot\text{year}}$	Failure rate of cable 1
λ_1		Eigenvalue of system matrix
λ_1		Ratio of losses in the screen to the losses in the conductor
λ_1'		Ratio of losses in the screen to the losses in the conductor, caused by circulating currents in the screen
λ_1''		Ratio of losses in the screen to the losses in the conductor, caused by eddy currents in the screen
λ_2	$\frac{\text{failures}}{100\text{km}\cdot\text{year}}$	Failure rate of cable 2
λ_2		Eigenvalue of system matrix

Symbol	Unit	Definition
λ_2		Ratio of losses in the armour to the losses in the conductor
λ_2'		Ratio of losses in the armour to the losses in the conductor, caused by circulating currents in the armour
λ_2''		Ratio of losses in the armour to the losses in the conductor, caused by eddy currents in the armour
λ_3		Eigenvalue of system matrix
μ	$\frac{\text{repairs}}{\text{year}}$	Cable repair rate
μ		Loss-load factor
μ_1	$\frac{\text{repairs}}{\text{year}}$	Repair rate of cable 1
μ_2	$\frac{\text{repairs}}{\text{year}}$	Repair rate of cable 2
ρ	$\frac{\text{kg}}{\text{m}^3}$	Density of material
ρ_{20}	$\Omega\cdot\text{m}$	Electrical resistivity of conductor at 20 °C
$\rho_{a,20}$	$\Omega\cdot\text{m}$	Electrical resistivity of armour at 20 °C
ρ_{elec}	$\Omega\cdot\text{m}$	Electrical resistivity
$\rho_{s,20}$	$\Omega\cdot\text{m}$	Electrical resistivity of metallic screen at 20 °C
ρ_{therm}	$\frac{\text{K}\cdot\text{m}}{\text{W}}$	Thermal resistivity
$\rho_{therm,backfill}$	$\frac{\text{K}\cdot\text{m}}{\text{W}}$	Thermal resistivity of backfill material
$\rho_{therm,i}$	$\frac{\text{K}\cdot\text{m}}{\text{W}}$	Thermal resistivity of dielectric insulation material
$\rho_{therm,j}$	$\frac{\text{K}\cdot\text{m}}{\text{W}}$	Thermal resistivity of jacket material
$\rho_{therm,soil}$	$\frac{\text{K}\cdot\text{m}}{\text{W}}$	Thermal resistivity of native soil
σ	$\frac{\text{W}}{\text{m}^2\cdot\text{K}^4}$	Stefan-Boltzmann constant approximately equal to $5.67 \cdot 10^{-8}$
$\tan\delta$		Loss factor for insulating dielectric
$\underline{\theta}$	°C	Vector of temperatures
$\underline{\dot{\theta}}$	$\frac{\text{°C}}{\text{s}}$	Vector of time derivative temperatures
θ	°C	Temperature
θ_a	°C	Armour temperature
θ_a'	°C	Armour temperature above native soil temperature at cable burial depth
θ_{air}	°C	Air temperature above ground

Symbol	Unit	Definition
θ_{amb}	°C	Native (undisturbed) ambient soil temperature at cable burial depth
θ_c	°C	Conductor temperature
θ_{c-e}	°C	Conductor temperature rise above jacket temperature
θ'_c	°C	Conductor temperature above native soil temperature at cable burial depth
θ_e	°C	Temperature at cable surface
θ'_e	°C	Jacket temperature above native soil temperature at cable burial depth
$\theta_{material}$	°C	Temperature of porous material, used for calculation of the specific heat of moist porous materials
θ_{max}	°C	Maximum allowed temperature
θ_s	°C	Metallic screen temperature
θ'_s	°C	Metallic screen temperature above native soil temperature at cable burial depth
θ_{water}	°C	Temperature of water, used for calculation of the specific heat of moist porous materials

PART I

Preliminaries

This part of the thesis introduces the PhD project and defines the objectives for the three years of work. Furthermore the structure of this thesis is explained for easing navigation through the document.

Chapter 1

Introduction

The PhD-project which is reported in this document has focussed on defining the loadability (also denoted ampacity) of transmission systems and evaluating different possibilities for implementation of dynamic loadability in cable based transmission systems.
The project has especially focussed on how dynamic thermal rating calculations can be combined with forecasts of the future load and generation needs to estimate the future loadability of cable based transmission grids. It is studied how the reliability of the transmission system can be determined such that a possible implementation of dynamic loadability will not compromise the system performance. Furthermore, the economic benefits of implementing dynamic loadability of transmission systems are discussed in order to show the prospects of the developed methodology.

1.1 Background for Performing the PhD Project

In 2009 the Danish parliament decided to underground major parts of the Danish transmission system. In specific two technical reports, [1] and [2], describe how all transmission lines below 400 kV and large parts of the 400 kV system could be undergrounded within the year 2040 in the most economical way. The recommendations in these reports are to be carried out, through the mandate given by the Danish parliament, by the national Danish transmission system operator, Energinet.dk.

On the background of this political decision Energinet.dk chose to establish

a large research project covering the main problems which inevitably will arise when implementing such radical changes to the transmission system. The research project with the title "DANish Power system with Ac Cables" (DANPAC) includes several PhD projects and all research is focused on optimising the economic solution when restructuring the transmission system. This economic optimisation is required to be based on technically proved concepts (existing or novel) as well as the environmental aspects of implementing the solution are to be taken into account.

DANPAC covers a wide area of research and development activities, such as topology optimisation of the proposed grid, investigation of different backfill materials for cable trenches, possible on-line fault location techniques, optimising the loadability of the grid, etc.
The PhD-project presented in this thesis covers the part concerned with loadability optimisation of cable based transmission systems, and it thus contributes to the results of the greater DANPAC project.

1.2 Loadability and Control of Transmission Systems

The operation of the Danish transmission system is today based on static current limits which means that the current pushed through the individual transmission lines must be kept below a certain value at all times during normal operation.
The current limit is denoted 'continuous loadability' (or 'steady state loadability') of the transmission line and because this defined loadability is allowed continuously all year round, it is calculated based on some unfavourable conditions. The result is that transmission lines for much of the time are over dimensioned, implying that investments are poorly utilised.

As the undergrounding of the Danish transmission system will require large investments, [1] estimates approximately two billion Euros, Energinet.dk seek ways to utilise the assets better.
The idea, from where the present PhD study arouse, is that the operator of the future transmission system should be able to fully utilise the dynamically varying conditions of the transmission grid. This means that instead of operating the transmission system on the basis of static loadability limits, the loadability of the lines should adapt to the real time conditions.

It is the main goal of this PhD study to develop a concept for using dynamic loadability in power system design and operation, and to deliver documentation proving that the reliability of the power system is maintained.

1.3 Content of the PhD Study

The PhD study focusses on identifying the possibilities of implementing a system for dynamic evaluation of the loadability of a transmission systems with high shares of underground cables.

The outcome of the project is to increase the efficiency of the transmission system, both during planning and operation. It is therefore the objective of the PhD project to give directions to how the Danish transmission system can change from being operated based on static loadability limits to being operated based on the real time conditions of the grid.

The focus in the study is on transmission cables, and the main goals of the PhD project are therefore defined as:

- Clarify the possibilities for increasing the loadability of transmission cables based on dynamic calculations
- Study the influence of dynamic loadability on a large cable based transmission grid
- Evaluate the potential of dynamic loadability when implemented in cable based transmission systems operated under market based conditions

The PhD study is aimed at implementation within the Danish TSO and thus the work will be focussed around Danish standards within transmission system operation, choice of cable designs, installation procedures, etc.; however the concepts are to be developed as open as possible such that adaptions and additions are easy to make.

1.4 The Thesis

In order to give a clear and transparent structure, this thesis has been divided into six main parts.
Part I introduces the project and outlines that the main goal is to develop a concept which enhances utilisation of cable based transmission systems via dynamic loadability calculations of power cables.
Part II is concerned with the analysis of loadability calculations in a point-to-point perspective, which includes dynamic thermal modelling of power cables. The second part of the thesis furthermore shows how the thermal models are chosen and enhanced, as well as validity of the models is proven through experimental studies.

Part III uses the findings of the point-to-point loadability analyses in a system perspective. A concept for utilising thermal calculation in the power system design and operation is developed. It is furthermore proven through case studies that it is possible to obtain significant technical advantages by implementing the developed tools.
Part IV shows that the developed concept is capable of enhancing reliability of the transmission system as well as possibly leading to a lowering of both the design and operational costs of the transmission system.
Part V concludes this thesis with a discussion about the advantages, limitations and prospects of the developed concept.
Part VI is a collection of appendixes which include in depth descriptions of the experimental work performed during the PhD project and elaborations of selected theoretical topics. Furthermore, a list of the scientific contributions produced during this PhD project is given, as well as a selection of these written publications is also found in the appendixes.

PART II

Loadability of Power Cables - Models and Experimental Verification

---

Even though this thesis is to investigate loadability on the grid level, it should be recognised that the current flows according to Kirchhoff's laws and the transmission capacity of the system is thus limited by individual lines. Therefore this part of the thesis discusses how state of the art studies evaluate loadability of power cables including introduction to the commonly agreed standardised methods. Moreover suggestions to improved calculation techniques are given such that the loadability calculation methodology can be ready for implementation on the grid level. These improvements are further verified by measurements from a larger experimental setup designed for the specific purpose.

In order to enable an easier understanding of the topic of loadability calculations, this part of the thesis includes a chapter which briefly introduces cable design and installation techniques used in the modern Danish transmission system.

Chapter 2

Transmission Cable Design and Installation

In order to understand the different aspects of loadability and thermal calculations of transmission cables it is vital to be familiar with their design. This chapter is a brief overview of the cable design and installation procedure typically used in the Danish transmission grid. It is thus not to be seen as an exhaustive description of all possibilities, but only as a description of a few selected techniques.

This chapter is primarily based on [3–7], as well as dialog with cable manufacturers, installation technicians, transmission system designers, etc.

2.1 Design of Cables for the Danish Transmission Grid

Many different types of cable design are available on the market, and all manufacturers have their special approach to design and production. Figure 2.1 shows a cross section of a polymer insulated transmission cable as they are typically designed for the Danish transmission grid. However it should be remembered that other designs, including different material choices and possible additional subcomponents, are also available on the market.

It is seen that the cable has six main subcomponents, a conductor, a semiconductive layer, insulation, another semiconductive layer, a metallic screen and an outer covering. The purpose of the different subcomponents is listed in table 2.1 along with typical choices of material.

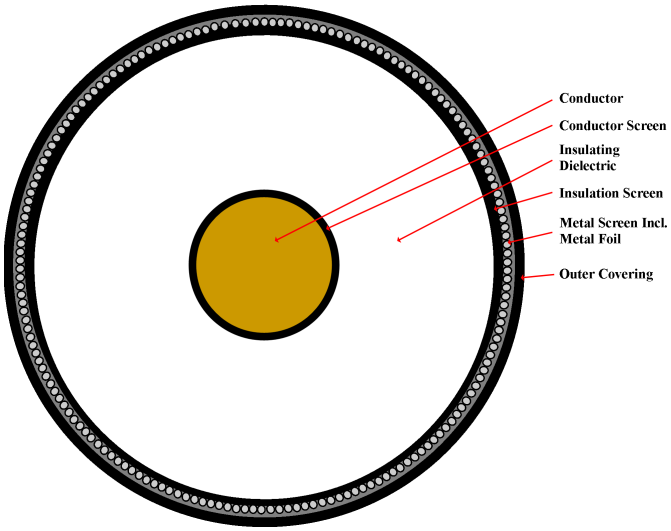

Figure 2.1: Example of a design of a single phase underground transmission cable.

Subcomponent	Purpose	Material
Conductor	Conduct current	- Aluminium - Copper
Conductor Screen	Mitigate possible electric field enhancements at conductor protrusions, etc.	- Carbon doped XLPE - Carbon paper
Insulation	Maintain distance between voltage carrying conductor and ground	- XLPE - Low viscous oil impregnated paper - Mass impregnated paper
Insulation Screen	Mitigate possible electric field enhancements at screen protrusions	- Carbon doped XLPE - Carbon paper
Metallic Screen	Carry ground potential Conduct fault currents Radial water blocking	- Aluminium or copper (Wires and/or foil) - Extruded lead
Outer Covering/Jacket	Mechanical protection	- PVC - PE

Table 2.1: Typical subcomponents of underground transmission cables, including purpose and different material possibilities.

It should be acknowledged that the design of a power cable is a compromise between the materials' electrical, mechanical and thermal properties, as well as manufacturing restrictions, handling issues, environmental issues and economical issues.

2.2 Cable Installation in Denmark

Transmission cables are in Denmark primarily installed by using the open trench technique. A long trench is dug wherein the cables are laid and around the cables is installed an envelope of sand which is to provide mechanical protection against the rocks in the soil and enhance the thermal properties of the cable surroundings. Cable systems in Denmark are buried in either flat or close trefoil formation. This project has focused on modelling the flat formation installation, which looks as seen in figure 2.2, however it is emphasised that the different tools given in this thesis are applicable to trefoil installations as well, with only minor adaptions.
A small pipe is, in figure 2.2, seen to run along the centre phase. This pipe contains optic fibres for communication and temperature monitoring purposes.

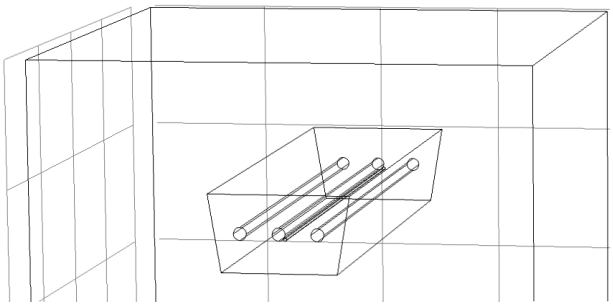

Figure 2.2: Three single phase cables installed in a trench using sand to protect the cable jacket during installation. Taped to the centre phase is seen a pipe which is used for optic communication, and temperature monitoring, fibres.

When it is not possible to create an open trench, such as when crossing under roads, ducts are drilled under the obstacle (still in flat formation) and the cables are pulled through. In order to ensure good thermal properties, the ducts are filled with a clay substance called bentonite.

It should be noted that the installation presented in figure 2.2 is the technique preferred by the Danish TSO. Cables can though also be installed in trays, in duct bays, in tunnels, etc. which are techniques widely used in

other countries. However as it is not the purpose of this study to cover all cable designs and installation techniques, but merely to develop methods and tools, the cable design of figure 2.1 and the installation technique of figure 2.2 is used as the basic case study in the remainder of this thesis.

Chapter 3

Loadability Calculations of Power Cables

Loadability, also denoted ampacity, evaluation of transmission cables have been a research discipline for as long as electrical power systems have existed. Several standardised calculation procedures are available on the market, as well as multiple commercial software are capable of performing loadability calculations for different types of installation.
The present chapter will briefly introduce the standardised procedures for calculation of cable loadability as well as describe the most important results from different recent research studies.

3.1 Definition of Loadability

Loadability of power cables can in basic be divided into two categories, steady state loadability and dynamic loadability.
With inspiration from both standards and more recent research, this study has used the following definitions for the two loadability categories, [8–10].

3.1.1 Steady State Loadability

The steady state loadability of a power cable is defined as the calculated current which can be carried continuously for an infinite period of time without the physical limitations of any part of the cable being exceeded.

3.1.2 Dynamic Loadability

The dynamic loadability of a power cable is defined as the calculated current which can be carried for a limited period of time without the physical limitations of any part of the cable being exceeded.
As it is seen from this definition the dynamic loadabiity is, unlike the steady state loadability, not a specific quantity but is dependent on the time interval on which is was calculated and thus the dynamic loadability must always be given together with the time interval.

3.2 Limitations of Loadability

Having defined loadability, the physical limitations of power cables are to be investigated. By searching the literature, for instance [8], it is found that the loadability of underground cables basically is limited by the temperature of the insulating material. As it is discussed in the following, high temperatures on the dielectric will result in significant decreasing of the performance of the insulation. Cross-linked poly-ethylene (XLPE) insulation, which is the preferred material for cables in the Danish grid, is e.g. by most manufacturers limited to 90 °C as the dielectric strength, mechanical strength, etc. decreases rapidly at higher temperatures and, because the insulating material is in close contact with the conductor, the 90 °C limit is imposed on the conductor.
The loadability is thus defined as the calculated current which result in a conductor temperature of 90 °C.

The described limit is during normal dynamic operation of the Danish (as well as many other countries') transmission system determined not to be sufficient. When the jacket of the cable becomes hot, the moisture in the surrounding sand (see figure 2.2) will migrate away from the cable, resulting in a lower thermal conductivity (higher thermal resistivity). The higher thermal resistivity will result in an increased jacket (and conductor) temperature, and thus a vicious circle can arise. In the Danish transmission system the cable jacket is on this background limited to 50 °C, at which the moisture have been experienced not to migrate under normal conditions. The limit of 50 °C on the jacket generally automatically also limit the conductor temperature to be lower than 90 °C during normal operation.

3.2.1 Temperature Dependent Properties of XLPE

As stated, cable loadability is limited by the temperature of the insulation because some properties of the material are temperature dependent. This

clause describes in greater detail the changing properties and why these changes require the operating temperature to be limited.

There are two aspects of the temperature dependent changes of the material properties. Firstly, some material property changes are reversible. These changes most often occur instantaneously when the temperature varies. Secondly, some material property changes are non-reversible, why they are often denoted as thermal ageing. These changes will most commonly require longer time before they become noticeable. Examples of such reversible and non-reversible changes are given in the following.

In [11] experimental data shows that the thermal resistivity of tree-retardant XLPE (TRXLPE) is fairly constant for temperatures below 80 °C, however above 80 °C the thermal resistivity decreases and reaches a minima at approximately 100 °C, where after the thermal resistivity increases and seems to become steady for temperatures above 120 °C. It should be noted that similar materials may have significantly different properties, which is illustrated by the fact that the thermal resistivity of XLPE in [12] is reported to be steadily increasing, over the entire temperature range, with no local minima[1].

The specific heat is in [11] (as well as in [12]) found to increase steadily for temperatures up to 80 °C, where after the increase becomes steeper. At approximately 105 °C the specific heat peaks and at approximately 115 °C, the specific heat settles at a constant level in the same range as below 80 °C[2].

The immediate response of both the AC breakdown voltage and impulse voltages to elevated temperatures is discussed in [12, 13]. It is shown in [12] that at 90 °C the AC breakdown voltage is decreased by more than one third compared to the breakdown voltage at 25 °C, and the impulse withstand voltage is decreased to approximately half the value of 25 °C. At 130 °C the AC breakdown voltage is approximately half of the value at 25 °C and the impulse withstand voltage is less than one fourth. Again it should be noted that the data in [12] is 30 years old, but the data of e.g. [14] from 1994 and [15] from 2011 shows similar tendencies, though the decrease in breakdown strength are lower than the data reported in [12].

In [3] it is stated that the tensile strength of XLPE drops significantly for temperatures above approximately 100 °C, and in cases where the tensile strength of the insulation is a limiting property, the temperature may thus automatically also be a limiting property. The comprehensive study of [16]

[1] Note here that [12] is from a time where steam curing of XLPE was the dominating cross-linking method and [11] is based on dry cured XLPE. This difference can be an explanation to the variations in the results.

[2] According to [11] this behaviour is explained by the material's phase change: from highly crystalline to amorphous.

shows how the tensile strength is affected by long term exposure to elevated temperatures. It is shown that the tensile strength decreases fairly steady when the material is exposed to 80 °C and 100 °C for a period of 5000 hours, however when the temperature is increased to 120 °C, the tensile strength falls drastically with ageing times above 2000 hours. It becomes even worse when the temperature is increased to 140 °C, where the tensile strength decreases steadily, but with a steep slope, from the beginning of temperature exposure.

[16, 17] also investigates how the electrical resistivity evolves when the material is exposed to elevated temperatures for longer periods of time. It is seen that for temperatures up to 100 °C, the electrical resistivity decreases steadily as a function of exposure time, but for temperatures of 120 °C and above, the decrease as a function of exposure time is far steeper.

In [16], also the relative permittivity (ϵ_r, also denoted dielectric constant) is found to be affected by long term exposure to high temperatures. For temperatures up to 100 °C ϵ_r is constant throughout the 5000 hours test period, but at 120 °C it seems that ϵ_r increases significantly after approximately 2000 hours, and for 140 °C, ϵ_r increases significantly after 1500 hours.

Moreover, the dielectric loss factor ($\tan\delta$) is in [16] found to be slowly decreasing for temperatures below 100 °C, whereas it increases after some ageing time for temperatures above 120 °C.

The study presented in [18] shows that the electrical strength of XLPE is highly dependent on the temperature and the exposure time. Cable model samples are in the study exposed to temperatures ranging from 100 °C to 150 °C, and it is found that the electrical strength halves in approximately 400 hours, 2000 hours and 10000 hours for samples exposed to 150 °C, 130 °C and 110 °C respectively. For 100 °C the tested material does not show an unambiguous and simple characteristic, as the electric strength stays at 1 pu for approximately 5000 hours where a steep decrease occurs to 0.8 pu which seems to be a new fairly stable electric strength level for the remaining of the 20000 hours test period.

The comprehensive study of [19] is a laboratory study partly concerned with the long term effects of elevated temperatures on the electrical properties of XLPE, and it is directly focussed on power cable applications. By studying a significant amount of small scale power cable models [19] shows that the electrical breakdown strength of XLPE is affected by thermal ageing, however for temperatures below 100 °C it is shown that the breakdown strength converges towards static values, which means that the material ages to a certain degree where after it may be assumed that no further ageing will be experienced.

3.2.2 Discussion of Loadability Limitations

The above description shows that there are various concerns which must be addressed when designing a cable and determining it's thermal limits. It is stressed that both real time responses of the properties of XLPE to temperature changes and long term changes must be taken into account during the cable design phase.

Most obviously is perhaps the breakdown strength of the material. If the material is subjected to 130 °C for 2000 hours (less than one quarter of a year), the material may only retain one fourth of the initial breakdown strength at 25 °C, and, as a power cable is supposed to sustain for several decades, a continuous operating temperature of 130 °C seems unrealistic.

Where precisely the thermal operational limit is set is up to the individual cable manufacturer, however just looking at the data presented above, it does not look harmful to set the limit at 100 °C as the continuous operating temperature. As stated the typical limit is set to 90 °C which is probably enforced for allowing for uncertainties in the design calculations, the manufacturing process and during installation. Furthermore, the temperature margin allows for the cable to survive the specific tests which are to be performed at temperatures at least 5 °C higher than the maximum operational temperature, [20].
It should be noted that even though this section has shown that the XLPE material will sustain 90 °C continuously, the Danish TSO limits the loading on their cables for a maximum jacket temperature of 50 °C. In this way thermal runaway is avoided and it is thus always ensured that the insulation is kept below 90 °C.

It should furthermore be acknowledged that the normal operating conditions may not be the limiting case for the cable loadability. It is possible that the loadability of a cable may be limited by conditions which are experienced during emergencies and faults as these situations can result in very high currents and voltages. Even though such fault conditions vary for only around 100 ms, the magnitude of the current can cause severe heating and the insulation must be able to sustain the magnitude of the voltage pulse.

3.3 Energy Conservation and Heat Transfer Mechanisms

Having established that the temperature is the limiting parameter in cable loading, it is to be determined how to calculate this quantity.
Conservation of energy is a prerequisite in any discussion of thermal systems,

[21], and it implies that the energy entering the system (Q_{ent}) must leave again (Q_{out}) or is otherwise stored internally (ΔQ_{int}). In mathematical terms this can be described as shown in (3.1), [10].

$$Q_{ent} = Q_{out} + \Delta Q_{int} \tag{3.1}$$

In order to maintain a dimensionless terminology much research is concerned with energy (or heat) flux (in this study denoted with a q) instead of energy (which in this study are denoted with Q). The interdependency between the two quantities is simply the area (denoted with an A) over which the energy flows, (3.2).

$$Q = q \cdot A \tag{3.2}$$

Q_{int} is directly related to the temperature and the evolution of the thermal system can thus be determined if each of the quantities Q_{ent}, Q_{out} and ΔQ_{int} are known. Heat transfer problems have therefore been investigated by researchers for hundreds of years, and it has been found that three basic mechanisms are involved in the transfer of heat, each is explained in the following clauses.

3.3.1 Conduction

Conduction is the movement of energy through atomic vibrations. At high temperatures atoms vibrate more than at low temperatures and the highly vibrating atoms will hit the less vibrating atoms. In this way thermal energy is conducted through atom vibrations from high temperatures to low.

The ability to conduct thermal energy is material dependent, which leads to the definition of thermal resistivity ρ_{therm}, (3.3), [10].

$$q_{cond} = -\frac{1}{\rho_{therm}} \frac{d\theta}{dx} \tag{3.3}$$

where q_{cond} is the heat flux flowing through a material with the thermal resistivity ρ_{therm}, causing a temperature difference of $d\theta$ over the distance dx.
Equation (3.3) is known as Fourier's law.

3.3.2 Convection

When a fluid (gas or liquid) comes in contact with the surface of a hotter solid, energy is transferred to the atoms in the fluid and is transported away from the solid as internal atomic/molecular vibrations. Convection can either be natural (free) or forced. For natural convection the fluid is

transported away from the solid solely via gravitational forces (hot fluids are lighter than cold fluids, causing the hot fluid to rise). In forced convection the fluid is pushed passed the solid, which is e.g. the case for fan cooling.

In depth descriptions of convective heat transport theory can be found in e.g. [22, 23], where it is shown that the explanation of even introductory knowledge about the subject requires several hundreds of equations. In this thesis convection is therefore described in the simplified version which is generally accepted within the power cable industry.
It is assumed that the heat flux from a solid to a fluid can be described as linearly dependent on the temperature difference between the solid and the fluid, such as suggested in (3.4), [10].

$$q_{conv} = h_{conv} \cdot (\theta - \theta_{amb}) \tag{3.4}$$

where q_{conv} is the heat flux caused by convection and θ and θ_{amb} are the temperature of the solid and ambient (and thus also the fluid) respectively. The convection constant h_{conv} is generally difficult to quantify, as it is highly dependent on the properties of the fluid, the geometry of the interface between solid and fluid, the pressure, velocity of the fluid, etc. This means that the calculation of the convective cooling is significantly different for the horizontal flat surface of the earth than for the cylindrical surface of a vertical cable. It should be noted that even literature dedicated to convective cooling theory, [22, 23], describe the necessity to determine h_{conv} by empirical means, as there in many cases are no analytical methods.
Equation (3.4) is known as Newton's law of cooling, [10].

It should furthermore be recognised that the simplified approach in (3.4) implies that h_{conv} is constant. When digging into literature dedicated to convection theory, [22, 23], it is seen that this is not entirely accurate. In order to increase accuracy of thermal calculations h_{conv} should be considered variable with temperature, pressure, etc, making (3.4) non-linear with the temperature. However in order to simplify the approach to analysing thermal systems, the accuracy of (3.4) is generally accepted and if choosing a properly conservative h_{conv} the integrity of the power cables will be maintained.

3.3.3 Radiation

Radiation is the transfer of energy through electromagnetic waves. Through experimental studies as well as through theoretical derivations, [22], it has been determined that the maximum heat flux which can be radiated from an object with temperature θ is as given in (3.5), [22].

$$q_{rad} = \sigma\theta^4 \tag{3.5}$$

where σ is the Stefan-Boltzmann constant (approx. $5.67 \cdot 10^{-8}$ $\mathrm{W/m^2 \cdot K^4}$). Objects which behave according to (3.5) are called black bodies, which means that such object radiate the most amount of energy possible. Objects in the real world will not behave according to (3.5) as they do not radiate heat ideally. Therefore a material property, called the emissivity (ϵ), is used to describe the objects ability to radiate energy. ϵ is a material dependent property in the interval $0 \leq \epsilon \leq 1$ and radiation from an object will thus obey (3.6).

$$q_{rad} = \epsilon \sigma \theta^4 \tag{3.6}$$

However objects will not only radiate energy to the surroundings, they will also absorb energy which is radiated from the surroundings. In general it is the material specific absorption coefficient (a) which describe the ability of an object to absorb energy from the surroundings, in a similar manner to (3.6). However for materials used in the real world the approximation that $\epsilon = a$ can be made without compromising accuracy too much. The net heat flux out of the object, caused by radiation, can thus be evaluated as (3.7).

$$q_{rad} = \epsilon \sigma \left(\theta^4 - \theta_{air}^4 \right) \tag{3.7}$$

where θ_{air} is the ambient air temperature.

Similar to the convection part it should be noticed that the emissivity, in dedicated literature, [22], is considered temperature dependent. Furthermore electromagnetic waves may be radiated also from inside the body of a solid object and is thus not entirely a surface phenomenon. These properties increases the complexity of analysing the thermal behaviour of a system. However within the operational temperature range of power cables it is assumed that such phenomena are negligible and by choosing a properly conservative ϵ the integrity of the power cables is maintained, why (3.7) is a valid approach.

3.3.4 Storing Thermal Energy

The internal energy of an object, and thus also the temperature of the object, can only change when heat fluxes change. The interdependency between change in temperature and energy is known as the heat capacity (C_{therm}), as defined in (3.8).

$$\Delta \theta = \frac{1}{C_{therm}} \cdot \Delta Q_{int} \tag{3.8}$$

Where the heat capacity is dependent of the size of the object, the specific heat (c_{therm}) is only material dependent. The two are thus related as defined

in (3.9).

$$c_{therm} = \frac{C_{therm}}{V} \tag{3.9}$$

where V is the volume of the object.

3.3.5 Discussion of Energy Conservation and Heat Transfer Mechanisms

As shown in this section evaluating the temperature in a thermal system, such as a power cable, requires the solution of (3.1). Such solutions may be impossible to obtain analytically, because e.g. (3.7) is non-linear, [24], and numerical methods must thus be utilised. However, in order to limit the complexity of analysing the thermal behaviour of power cable systems, a number of simplifications are often introduced. Most cable systems are for instance installed underground and the analysis of heat transfer may therefore be limited to include only thermal conduction. For cables installed above ground, or in large cavities (such as tunnels), radiation and convection must though be included in the analysis, [10].

Because the limiting parameter of cable loading is the temperature, and because the temperature evolution in an undergrounded power cable can be found by solving (3.1), the remaining of this chapter is targeted at finding the solution to (3.1) under varying conditions and assumptions.

3.4 Standardised Equations

In order to ensure safe operation of transmission cables the International Electrotechnical Commission (IEC) has published a number of standards which facilitates the estimation of the loadability of power cables[3]. These standards are widely used and referenced, and also the Danish TSO relies on these standards when dimensioning new cables.

The standards are basically divided into two main technical areas, one concerned with steady state calculations and one concerned with dynamic loadability calculations. The following will briefly introduce both of these standardised areas.

[3]Institute of Electrical and Electronics Engineers (IEEE) has also published standards on the subject [25], but the most commonly referenced standards are from IEC and these will therefore be used in this study.

3.4.1 Steady State Rating

A series of standards (series IEC 60287), [8, 26–32], is concerned with steady state loadability calculations. The calculation of the steady state loadability is in the standards based on the concept of thermoelectric equivalents (TEEs), also denoted lumped parameters models. The concept utilises the resemblance between heat flowing in a thermal system and current flowing in an electric system. In the electric analogy of the thermal system, thermal resistances are modelled as electric resistances, thermal capacitances are modelled as electric capacitances, and when modelling a flowing heat with a current, the temperature will automatically be modelled as the voltage.

A complete thermoelectric circuit of the transmission cable design of figure 2.1 is shown in figure 3.1.

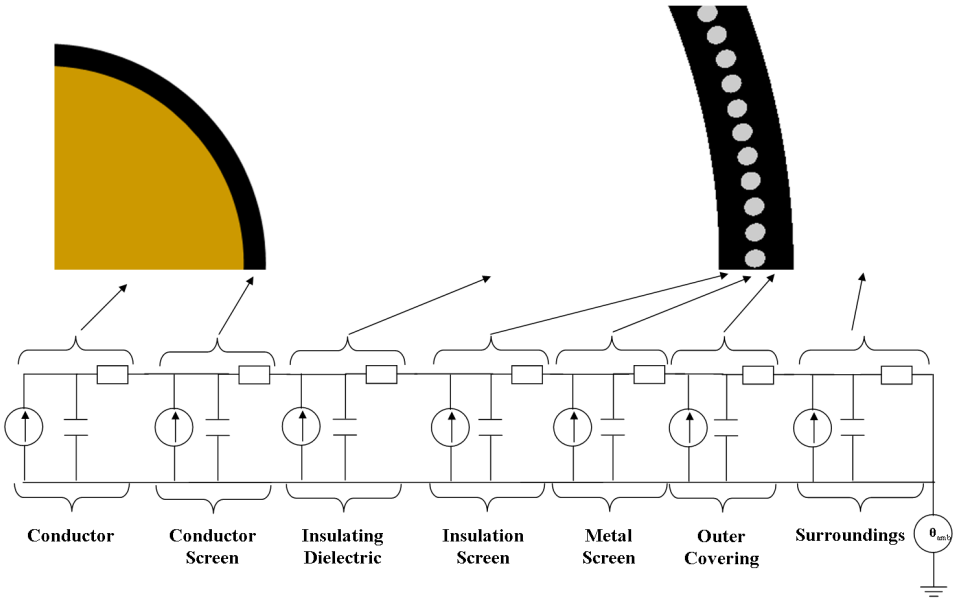

Figure 3.1: Thermoelectric equivalent of a single phase underground transmission cable.

It is seen in the figure that all subcomponents have both thermal resistances and thermal capacitances. Furthermore the figure shows that all subcomponents have the potential of being heat sources, where e.g. the conductor experiences joule losses and the insulation experiences dielectric losses.

As stated, the present clause discusses steady state loadability, which implies constant heat flows. The capacitances of figure 3.1 can thus be neglected, and if it is possible to determine the size of the heat sources, then the temperature at the interface between the different subcomponents is

easily calculated by summing up the voltage drops across these individual subcomponents.

In the analysis of the loadability, the standards allows for a number of simplifications. The first simplification becomes clear when comparing figures 3.1 and 2.2. As it is seen, the three dimensional aspect of the cable trench is simplified with a one dimensional thermoelectric analogy. This simplification can be made because the standards assume that the hottest spot along the cable route defines the loadability, and that no heat flows in the longitudinal direction from this hotspot. Thus the three dimensions can be limited to two. Furthermore, by adjusting the thermal resistances of the TEE to include the deviations from the two dimensions, it is argued that it is sufficient to consider loadability calculations as 1D studies.

Having argued for the validity of the 1D approach, the standard gives suggestions to calculating the size of the different thermal parameters. This is done by firstly simplifying the modelling by neglecting some of the parameters. The parameters which are assumed negligible are the thermal resistances of all metallic parts as these are several orders of magnitude smaller than what is typical for the other subcomponents. Furthermore, the only losses which are included in the analysis are losses in conductor, dielectric and screen[4]. In addition to these simplifications it is assumed that losses in the screen are directly related to the current in the conductor, and the screen losses are thus given as a fraction (denoted λ_1) of the conductor losses.

With all these simplifications it is determined that the loadability of a cable, where the limitation is determined by the conductor temperature, is given as stated in (3.10), [8].

$$I_{max,SS} = \left(\frac{\theta_c' - W_d \left(0.5 \cdot T_1 + T_3 + T_4\right)}{R_{AC} \left(T_1 + (1 + \lambda_1) \cdot (T_3 + T_4)\right)} \right)^{0.5} \tag{3.10}$$

Here $I_{max,SS}$ is the current which will lead to an increase in conductor temperature of θ_c' above ambient temperature, W_d is the dielectric losses in the insulation, T_1 is the thermal resistance between conductor and screen, T_3 is the thermal resistance of the outer covering, T_4 is the thermal resistance between the jacket and ground surface and R_{AC} is the AC resistance of the conductor[5]. (3.10) is seen to be directly related to the electric circuit in figure 3.1 as the conductor losses are given by $W_c = R_{AC} \cdot I^2$. It should furthermore be noticed that only half the dielectric losses passes through the insulation, which means that it is assumed that half the dielectric losses arises at the interface with the conductor and the other half at the interface

[4]For submarine cables, also armour losses must be considered.

[5]It is noted that T_2 is missing, however this quantity is only utilised for cables with armour.

with the screen. This approach has been verified as sufficiently accurate through years of service experience, [10].

When the limitation is given by the jacket temperature, instead of the conductor temperature, the loadability can be calculated as stated in (3.11), [8].

$$I_{max,SS} = \left(\frac{\theta'_e - W_d \cdot T_4}{R_{AC}\,(1+\lambda_1) \cdot T_4} \right)^{0.5} \tag{3.11}$$

Here $I_{max,SS}$ is the current which will result in an increase in the jacket temperature of θ'_e above the ambient temperature.

The calculation of the different thermal parameters of the equations (3.10) and (3.11) varies significantly with the cable design and installation method. For in depth descriptions the reader is referred to [8, 26–32], however (3.12), (3.13) and (3.14) gives the thermal parameters for three single phase cables which are directly buried in flat formation.

$$T_1 = \frac{\rho_{therm,i}}{2 \cdot \pi} \cdot \ln\left(\frac{d_i}{d_c}\right) \tag{3.12}$$

$$T_3 = \frac{\rho_{therm,j}}{2 \cdot \pi} \cdot \ln\left(\frac{D_e}{d_s}\right) \tag{3.13}$$

$$T_4 = \frac{\rho_{therm,soil}}{2 \cdot \pi} \cdot \ln\left(\ln\left(\frac{4 \cdot L}{D_e}\right) + \ln\left(1 + \left(\frac{2 \cdot L}{s_1}\right)^2\right)\right) \tag{3.14}$$

where $\rho_{therm,i}$ is the thermal resistivity of the insulation material, d_i is the outer diameter of the insulation, d_c is the diameter of the conductor, $\rho_{therm,j}$ is the thermal resistivity of the jacket material, D_e is the outer cable diameter, d_s is the outer screen diameter, $\rho_{therm,soil}$ is the soil thermal resistivity, L is the burial depth of the cables and s_1 is the axial distance between the cables.
It should especially be noticed that these standardised equations rely on Kennely's hypotheses, which assumes that the ground surface is an isothermal and that the losses of the cable flow towards a heat sink of equal size, located in a distance equal to the burial depth above ground. These simplifications significantly eases the definition of the external thermal resistance T_4.

3.4.2 Dynamic Loadability Models

Cables in for instance the Danish grid are normally not loaded at a constant current for long periods of time. This means that when cables occasionally are loaded up to the loadability calculated by (3.11) for a limited period of

time, the maximum allowed jacket temperature will never be reached due to the thermal inertia of the cable system, which again means that the cables are not fully utilised.

The series of standards [9, 33, 34] (series 60853) address this issue by giving suggestions to how the thermal inertia can be utilised, while ensuring that the temperature limits given in clause 3.2 are never exceeded. The standards are divided into two main subjects. Firstly, cyclic rating is the inclusion of a current profile for the cable, which typically varies in a cyclic manner on a daily basis. The cyclic rating will in general allow for a harder loading of the cable while ensuring that the temperatures are kept below their limits. Secondly, emergency rating denotes the calculation of a current which is acceptable for a specified period of time, where after the current must be lowered to the steady state limit.

3.4.2.1 Cyclic Rating

Many power cables are exposed to a load profile which is varying with time. For evaluation of the cyclic rating, thee standards [9, 33, 34] assume that the load profile varies in a known daily pattern, and that this daily pattern is repeated every 24 hours for an infinite period of time.
The cyclic rating is in the standards defined as the maximum current during the daily load cycle, which the cable system can sustain without ever exceeding the thermal limits. In practical application, the cyclic loadability is determined by calculation of a factor (M_c), based on the shape of the cyclic load, which can be multiplied to (3.10) and (3.11), as given in (3.15).

$$I_{max,c} = M_c \cdot I_{max,SS} \tag{3.15}$$

where $I_{max,c}$ is the cyclic rating.

For the specifics in calculating the cyclic load factor, the reader is referred to [9, 33, 34].

3.4.2.2 Emergency Rating

The emergency rating is defined as the current which the cable can conduct for a specified period of time (e.g. one hour) before the limiting temperatures are reached and the emergency rating is in the international standards determined by the calculation of the cable's thermal response to a load step. Note that calculation of the emergency rating requires knowledge about the real time temperature of the cable because a starting point for the thermal calculations is required.

The dynamic response to a load step can for directly buried cables be calculated by exponential integrals ($Ei(...)$) as seen in (3.16), [33]. Note that (3.16) obeys Kennely's hypothesis, i.e. that the ground surface is isothermal.

$$\theta'_e(t) = \frac{\rho_{therm,soil} \cdot W_T}{4\pi} \left(\left(-Ei\left(-\frac{D_e^2}{16t\delta_{soil}} \right) - \left(Ei\left(-\frac{L^2}{t\delta_{soil}} \right) \right) \right) + \sum_{k=1}^{k=N-1} \left(-Ei\left(-\frac{\left(d_{pk}\right)^2}{4t\delta_{soil}} \right) - \left(-Ei\left(-\frac{\left(d'_{pk}\right)^2}{4t\delta_{soil}} \right) \right) \right) \right) \quad (3.16)$$

where W_T is the sum of the loss changes inside the cable, t is the time from loss changes appeared, N is the number of cables affecting the cable temperature (including itself), d_{pk} is the distance from the cable under investigation p to cable k, d'_{pk} is the distance from the cable under investigation p to the mirror of cable k above ground and δ_{soil} is the thermal diffusivity of the cable surroundings defined as given in (3.17), [10].

$$\delta_{soil} = \frac{1}{\rho_{therm,soil} \cdot c_{therm,soil}} \quad (3.17)$$

It is seen that (3.16) determines the jacket temperature increase above ambient ($\theta'_e(t)$), caused by the loss change W_T, as a function of time. In order to determine the conductor temperature one must follow (3.18), [10].

$$\theta'_c(t) = \theta_{c-e}(t) + \alpha(t) \cdot \theta'_e(t) \quad (3.18)$$

where $\theta'_c(t)$ is the total temperature change of the conductor, above ambient temperature, caused by the loss change W_T, $\theta_{c-e}(t)$ is the temperature change of the conductor above the jacket temperature and $\alpha(t)$ is the attainment factor from jacket to conductor. The attainment factor is basically a variable in the interval $0-1$ which determines how much the jacket temperature influences the conductor temperature at any given time.
The attainment factor, $\alpha(t)$, is the time dependent ratio given in (3.19), [10].

$$\alpha(t) = \frac{\theta_{c-e}(t)}{\theta_{c-e}(\infty)} \quad (3.19)$$

The conductor temperature above jacket temperature, $\theta_{c-e}(t)$, is evaluated as shown in (3.20), [10].

$$\theta_{c-e}(t) = W_c \cdot (T_a(1 - \exp(-a \cdot t)) + T_b \cdot (1 - \exp(-b \cdot t))) \quad (3.20)$$

where T_a and T_b are apparent thermal resistances for the cable interior and a and b are coefficients dependent on thermal resistances and thermal capacitances for the cable interior.

The above described standardised method builds on a LaPlace transformation of the thermoelectric equivalent system shown in figure 3.1. The standardised method suggests that the thermal system is reduced such that the internal parts of the cable are represented by two loops only, and thus only two exponential terms are seen in (3.20). The evaluation of the parameters involved in the solution of the two loop representation, is shown in appendix A.

It should be noted that the size of the parameters T_a, T_b, a and b, in (3.20), is highly dependent on the investigated time scale. For short duration transients (where $t \leq 1/3 \cdot T \cdot C$, T and C being the total thermal resistance and capacitance of the cable respectively) one set of parameters is used and for long duration transients (where $t > 1/3 \cdot T \cdot C$) another set of parameters must be used.
Furthermore, if the temperature at another location inside or outside the cable is required to be modelled, e.g. the screen temperature, two new time dependent equations must be solved (for each location) and a corresponding number of parameters.

The calculation of cable temperatures via the above described use of exponential integrals and LaPlace transformation will in the remaining of this thesis be denoted the "Step Response" (SR) method.

3.5 Recent Research Studies

Throughout years of experience, the methodology of (3.11) and (3.16) has been shown to provide sufficiently accurate results for loadability calculation of simple power cable installations. However because the standardised methods assume static conditions, no longitudinal heat flow and require limited complexity of the thermal system, many research studies are still concerned with steady state and dynamic aspects of cable loadability evaluation. The following clauses will discuss the most important of these recent innovations.

3.5.1 Steady State Loadability

Many novel studies within steady state loadability focus on specific installation conditions as their task is to solve possible challenges for a specific cable system. As such installations can be very complex (3.11) will in many cases be difficult to apply and more comprehensive modelling techniques are therefore utilised. The following clauses provide a brief overview of such recent studies within the area of steady state loadability calculations.

3.5.1.1 Numerical Tools

With the introduction of high speed computers, researchers within the field of power cable loadability can now attack problems in a scale which previously was thought of as impossible. As seen in the following clauses the Finite Element Method (FEM) is the preferred when discussing such tools. As the name implies, FEM is a numerical method where the volume under investigation is divided into a finite number of elements with boundaries defined by the lines connecting the user generated internal nodes of the volume.
The continuous energy conservation equation (3.1), which for a thermally conductive element can be written as (3.21), is in the FEM approach assumed to be piecewise continuous between the nodes, and thus the temperature of the nodes can be seen as discrete values, [10, 35].

$$Q_{gen} - \left(\frac{\partial q^x_{cond}}{\partial x} + \frac{\partial q^y_{cond}}{\partial y} + \frac{\partial q^z_{cond}}{\partial z} \right) - c_{therm} \frac{\partial \theta}{\partial t} = 0 \tag{3.21}$$

where q^x_{cond}, q^y_{cond} and q^z_{cond} are the heat flows in the directions x, y and z respectively and Q_{gen} is the internally generated heat. Note that the last term on the left had side of (3.21) is negligible in the steady state case.
As stated, it is the temperature at the discrete nodes which is solved for, and the continuous representation of the temperature at the position (x, y) inside for instance a triangular element (with nodal temperatures θ_1, θ_2 and θ_3) is thus calculated with the aid of the interpolation (or shape) functions N_1, N_2 and N_3 as shown in (3.22).

$$\theta(x, y) = N_1(x, y) \cdot \theta_1 + N_2(x, y) \cdot \theta_2 + N_3(x, y) \cdot \theta_3 \tag{3.22}$$

where the shape functions are normally linear, quadratic or cubic.

There are a number of different solution strategies to the discretised heat balance equation, e.g. the Galerkin method, the Variational method, etc. which each have their individual strengths. In the Galerkin method for example, shape functions are multiplied onto the energy conservation equation, and the integration over the area[6] of the element is equalled to zero, (3.23).

$$\int_A \left(Q_{gen} - \left(\frac{\partial q^x_{cond}}{\partial x} + \frac{\partial q^y_{cond}}{\partial y} \right) - c_{therm} \frac{\partial \theta}{\partial t} \right) \begin{bmatrix} N_1 \\ N_2 \\ N_3 \end{bmatrix} \partial A = 0 \tag{3.23}$$

Because the heat flows (the q's) are related to the temperature via Fourier's law, i.e. $q^x_{cond} = -\frac{1}{\rho_{therm}} \frac{\partial \theta}{\partial x}$, it is with the Galerkin method possible to solve

[6] In a 2D simulation the integration is performed over the area, but in 3D the integration is of course performed over the volume.

the matrix equation of (3.23) by finding the parameters of the shape functions (N_1, N_2 and N_3), [35]. Note that (3.23) must be solved for all elements in the investigated area simultaneously.
It is seen that the solution to FEM requires a reference (boundary condition), which in cable temperature calculations for example can be the ground surface temperature, ground surface convection and/or ground surface radiation.

The above clause outlines the procedure for FEM simulations, but as it requires a thesis of its own to discuss FEM solution strategies in detail it was chosen not to give an exhaustive description. Instead the reader is referred to the extensive amount of dedicated literature on the subject, e.g. [35–37]. It should moreover be noted that several commercial softwares are available, such as Comsol Multiphysics, Quickfield, etc. providing easy setup of the physical system as well as easy definition of the thermal problem.

3.5.1.2 Cables under Unfavourable Thermal Conditions

The standardised loadability equations are based on the premise that the hottest spot of the cable is the limiting point. In order to predict the site of the hottest spot, researchers have investigated which external conditions should be given special considerations when dimensioning power cables.

The book by Dr. G. Anders, [38], is dedicated to the investigation of cable ampacity and temperature under unfavourable thermal conditions. It gives suggestions to a number of typical environments which can be defined as thermally unfavourable.
The hottest spot of a cable will, according to [38], typically be found when:

1. Cables crosses under obstacles
2. Trees are in proximity of the cables
3. External environment changes along cable route
4. Crossing of heat sources
5. Cables are exposed to solar radiation

Ad. 1: The external thermal resistance changes when cables are installed in pipes under roads, rivers, hills, etc., causing a possible hotspot.
It should though be noted that a possible deeper installation does not necessarily create a hotspot as the ambient soil temperature can decrease with increasing depth, [39].

Ad. 2: The roots of trees in proximity of the cables can cause the soil to dry out, resulting in higher thermal resistivity and thus higher cable temperatures.

Ad. 3: When the surrounding material changes characteristics, such as when the material changes from being a sand soil to a clay soil, the thermal properties may worsen and possibly causing a hotspot.

Ad. 4: Heat source crossing (or external heat sources in the vicinity of the cables) may be problematic as the cable temperature increases as a direct consequence.

Ad. 5: When cables are exposed to the sun, additional heating is experienced, and this must be included in the analysis.

Common for most of the above listed items is that the 1D approach may no longer be adequate. When cables crosses a thermally unfavourable region, heat may not only flow radially away from the cable, but some of the heat may flow in the longitudinal direction. [38] therefore suggests the use of two dimensional thermoelectric equivalents, such that the thermal system can be modelled with greater accuracy. In order to determine an ampacity value, [38] gives suggestions to the evaluation of derating factors, which can be multiplied to the standard loadability equations, for different environments.

An important conclusion from [38] is that the hotspot temperature will not increase with increased width of a thermally unfavourable region wider than three meters. Thus if a cable crosses a road or if the soil's thermal resistivity increases over a region of more than three meters, it should be possible to treat the thermal system via the one dimensional standardised equations.

3.5.1.3 Cable Joints

Another topic investigated by some researchers is the impact of joints on the loadability of power cables. Research such as [40–42] is however limited to looking at a single phase cable not influenced by other cables, and thus the research is of limited use to the common three phase AC based transmission system. The studies find, through two dimensional investigations, that cable joints in the steady state case are limiting the ampacity because the thermal resistance is higher at the joint than the rest of the cable.

Only sparse literature has been found to be concerned with joints in three phased systems, [43]. In the three phased case it is not adequate to perform the modelling in two dimensions, and [43] therefore utilise FEM to model the thermal system in three dimensions. It is found that the joints will not be the hotspot, under normal circumstances, for three single phased cables in flat formation. This is due to the normally increased spacing between

phases at joint bays.

3.5.1.4 Hotspot Mitigation

Because cable hotspots can be very localised it may be found acceptable to use some resources on mitigating the hotspot instead of upgrading the entire cable system.

One way of performing this mitigation is by including cooling pipes around the cable. The cooling can be performed either by natural or forced fluid (air or liquid) flow in the pipe, [38, 40, 41, 43, 44]. It should though be noted that forced cooling requires an active cooling system, which in itself has a risk of failure, and thus may decrease reliability.

[38] shows how a hotspot may be mitigated by inclusion of a backfill envelope around the cables, ensuring enhanced thermal properties of the cable surroundings. The size of the backfill envelope can be adjusted such that especially problematic sites along the cable route can be equipped with a larger envelope for ensuring proper thermal surroundings.

3.5.1.5 Other Steady State Issues

As mentioned, the research within cable ampacity calculations is very diverse and often directly related to solving problems to specific cable systems. Amongst others, topics within cables in tunnels [45], in trays [46, 47], deeply installed [48], in duct banks [49] and pipe type cables [50], are the most dominating at the present time. However as these topics are of limited relevance to the Danish transmission system the reader should address the references for further details.

3.5.1.6 Discussion of Steady State Loadability Calculations

It is seen from the above that the research within steady state loadability calculations is primarily focussed at installations which are special or have unfavourable surrounding conditions. This means that the scientific community has accepted the standardised equations as being sufficiently accurate for general purposes.
The standardised equations are relatively simple to use and can therefore easily be applied to the normal directly buried cable case. For more special situations it must be concluded from the above, that the FEM calculations is an acceptable way forward as it is capable of addressing even the most complex installations.

These conclusions mean that the present PhD project will not engage in enhancing the equations for steady state analysis because they, through experience, have been proven to calculate the temperature accurately. The remaining of this thesis can thus focus on the dynamic behaviour of cables and cable grids.

3.5.2 Dynamic Loadability

Dynamic loadability is, as mentioned, concerned with optimising the utilisation of cables while ensuring that their thermal limitations are never exceeded. As the conductor temperature is not a measurable quantity for operating cables, modelling the real time cable temperature is a prerequisite for dynamic loadability calculations and this research area has thus recently gained increased interest from the scientific community.
The following clauses summarises the most dominating research trends within dynamic loadability calculations and calculations of the dynamically varying temperature.

3.5.2.1 Dynamic Thermal Rating

In theory, optimising the utilisation of cables could mean that the power system operator would control the lines based on temperature instead of current values. A prerequisite for this change in the operation methodology is real time knowledge about cable temperatures.
Such a real time analysis and monitoring of the temperature, and a further online forecast of the dynamic cable loadability, is the definition of Dynamic Thermal Rating (DTR).

Much research has been concerned with DTR, however the amount of published methodologies is limited because the results in many cases are utilised in different commercial software, [51–59].

Some studies though show their developed DTR methodologies. [60, 61] shows how DTR can be performed for cables in tunnels by setting up thermoelectric equivalents. However the solution to the thermal system is suggested to be performed by setting up the full differential equation system instead of performing Laplace transformation, such as done in the SR method. In order to distinguish these two approaches this project uses the term ”TEE” when solving the full equation system and the term ”SR” when the Laplace approach i used.
As the focus of [60, 61] is dynamic studies, the thermal capacitances of the model are included in the analysis. The study suggests that cable subcomponents such as the insulation and jacket should be divided into multiple

thermal zones for increased accuracy of the modelling. This division is necessary when exponential integrals and attainment factors are not considered.

[62] shows how DTR can be performed with TEEs for cables installed in ducts. The soil thermal capacitance and thermal resistance are assumed to vary with time, and it is stressed that they are vital parameters to estimate accurately as the reliability of the models rely on them. In the TEE of the cable system, [62] divides the surroundings into two loops (two thermal resistances and two thermal capacitances) for increased accuracy. Based on a generic algorithm the size of the two thermal capacitances and two thermal resistances is given as the set of values which shows the least error between measured and modelled duct temperatures.
The solution to the TEE equations, which are setup in [60–62], are determined via numerical means. However there exist an analytical way of obtaining the solution of the TEE which the author prefers. The in depth explanation of the analytical procedure is given in section 3.6.

Instead of using the TEE method, studies such as [63, 64] utilises SR to dynamically evaluate the temperature and forecast the loadability in the cables under investigation. The dynamic thermal response is calculated on the basis of adding up a sequence of current steps, where the response to each current step is calculated by an exponential integral. The external thermal conditions in the thermal models are in [63, 64] not related to geometric parameters but are seen as apparent external thermal conditions, which means that the thermal resistance will take into account all influences, known and unknown, in vicinity of the cable. The studies show, via examples of real life cable systems, that the models are very accurate when comparing to measurements of the temperature.

[65, 66] uses a combination of TEEs to model the internal part of the cable and the SR method to model the external thermal conditions. Especially [66] provides proof of concept by comparing modelled temperatures to measurements.

Studies such as [67] uses the FEM methodology to get a comprehensive insight into the thermal behaviour of power cable systems. FEM models enable, in principle, the monitoring of the temperature of any point inside and in the vicinity of a cable, including the differences between adjacent phases, etc. The model is compared to measurements of both the conductor and jacket temperature, and very fine compliance is found.

3.5.2.2 Joints

As stated, joints should be seen as hotspots in the steady state case for single cables, but not as hotspots when three single phase cables are installed

in flat formation. However in the dynamic case, studies such as [42] determines that joints of single cables are not necessarily the hotspot as the thermal inertia may be significantly higher at the joint than the rest of the cable. It may therefore be important to model the temperature of both a normal cable cross section and a joint cross section in order to ensure that no part of the cable will be overheated.
It has not been possible to find any studies which are concerned with dynamic analysis of three single phased joints or joint bays.

3.6 Enhancement of the Thermoelectric Equivalent Method

Where equations for the FEM and SR method have been given previously in this thesis, the thermoelectric equivalent method has until now mainly been discussed in broad terms with references to [60–62]. As stated, the reason is that the solution methods of the studies are numerical and they are thus only sparsely explained. This PhD project has therefore investigated the TEE method in greater detail in order to establish a proper analytical mathematical solution strategy. The remaining of this section is on this background dedicated to the description of how these thermal models are defined and how they may be enhanced.

3.6.1 Setting Up Thermoelectric Equivalents

The thermoelectric equivalent for land cables, as seen in figure 3.1, can generally be simplified by assuming that the semiconductive layers have the same thermal properties as the insulating material, [8], which results in the TEE to look as shown in figure 3.2.

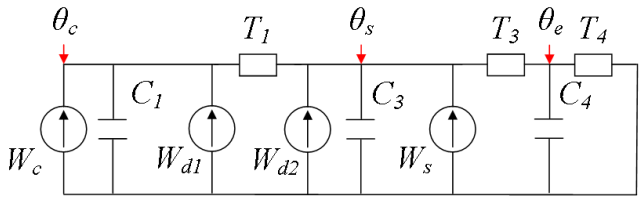

Figure 3.2: Simplified thermoelectric equivalent of a single phase underground transmission cable.

For the quantities of figure 3.2 the definitions of (3.12), (3.13) and (3.14) along with (3.24), (3.25) and (3.26) have generally been accepted to apply,

[10].

$$C_1 = C_c + p \cdot C_i \tag{3.24}$$
$$C_3 = (1-p) \cdot C_i + C_s + C_j \tag{3.25}$$
$$C_4 = C_{sur} \tag{3.26}$$

where p is denoted the Van Wörmer coefficient (see also appendix A). The subscript c relates to the conductor, i to the dielectric insulation, s to the screen, j to the jacket, e to the cable exterior (on the jacket surface) and *sur* to the cable surroundings. It is also generally accepted that the dielectric losses are evenly distributed on each side of the resistance, (3.27).

$$W_{d1} = W_{d2} = \tfrac{1}{2} \cdot W_d \tag{3.27}$$

3.6.2 Calculation of Dynamically Varying Temperatures

Solving for the voltages (i.e. temperatures) in the circuit of figure 3.2 is a well known mathematical problem. The differential equations to be solved are stated in (3.28).

$$\begin{aligned}
\dot{\theta}'_e(t) &= \frac{1}{C_4} \cdot \left(\frac{\theta'_s(t) - \theta'_e(t)}{T_3} - \frac{\theta'_e(t)}{T_4} \right) \\
\dot{\theta}'_s(t) &= \frac{1}{C_3} \cdot \left(W_s(t) + W_{d2}(t) + \frac{\theta'_c(t) - \theta'_s(t)}{T_1} - \frac{\theta'_s(t) - \theta'_e(t)}{T_3} \right) \\
\dot{\theta}'_c(t) &= \frac{1}{C_1} \cdot \left(W_c(t) + W_{d1}(t) - \frac{\theta'_c(t) - \theta'_s(t)}{T_1} \right)
\end{aligned} \tag{3.28}$$

where $\theta'_c(t)$, $\theta'_s(t)$ and $\theta'_e(t)$ are the conductor, screen and jacket temperature increase above ambient respectively and $\dot{\theta}'_c(t)$, $\dot{\theta}'_s(t)$ and $\dot{\theta}'_e(t)$ are their respective time derivatives.
Note that in order to obtain the total conductor ($\theta_c(t)$), screen ($\theta_s(t)$) and jacket ($\theta_e(t)$) temperature respectively, the TEE method uses the superposition principle, which means that the temperature increase caused by the cable losses is simply added to the ambient temperature, (3.29).

$$\begin{aligned}
\theta_e(t) &= \theta'_e(t) + \theta_{amb} \\
\theta_s(t) &= \theta'_s(t) + \theta_{amb} \\
\theta_c(t) &= \theta'_c(t) + \theta_{amb}
\end{aligned} \tag{3.29}$$

As previously discussed, different numerical methodologies have been developed for the solution of the interdependent equations, however [24, 68] show that linear differential equation systems, such as (3.28) can be solved by simply setting up the system as a matrix equation and finding eigenvalues

and eigenvectors of the system matrix. The equation system of (3.28) can be given as (3.30).

$$\begin{bmatrix} \dot{\theta}'_e(t) \\ \dot{\theta}'_s(t) \\ \dot{\theta}'_c(t) \end{bmatrix} = \begin{bmatrix} -\left(\frac{1}{C_4T_3}+\frac{1}{C_4T_4}\right) & \frac{1}{C_4T_3} & 0 \\ \frac{1}{C_3T_3} & -\left(\frac{1}{C_3T_1}+\frac{1}{C_3T_3}\right) & \frac{1}{C_3T_1} \\ 0 & \frac{1}{C_1T_1} & -\frac{1}{C_1T_1} \end{bmatrix} \cdot \begin{bmatrix} \theta'_e(t) \\ \theta'_s(t) \\ \theta'_c(t) \end{bmatrix} + \begin{bmatrix} 0 \\ \frac{1}{C_3}\left(W_s(t)+W_{d2}(t)\right) \\ \frac{1}{C_1}\left(W_c(t)+W_{d1}(t)\right) \end{bmatrix} \tag{3.30}$$

which in a compacted form can be represented as (3.31).

$$\underline{\dot{\theta}'}(t) = \underline{A} \cdot \underline{\theta'}(t) + \underline{u}(t) \tag{3.31}$$

By denoting the eigenvalues of $\underline{A}$ by λ_1, λ_2 and λ_3 and denoting the eigenvectors v_1, v_2 and v_3, the solution to (3.30) is as given in (3.32).

$$\underline{\theta'}(t) = c_1 \cdot v_1 \cdot e^{\lambda_1 \cdot t} + c_2 \cdot v_2 \cdot e^{\lambda_2 \cdot t} + c_3 \cdot v_3 \cdot e^{\lambda_3 \cdot t} + \underline{\theta'}(\infty) \tag{3.32}$$

where $\underline{\theta'}(\infty)$ is found by neglecting the capacitances in figure 3.2 (because steady state is achieved at $t \to \infty$), and evaluating the voltage distribution across the individual resistances of the TEE, (3.33).

$$\begin{bmatrix} \theta'_e(\infty) \\ \theta'_s(\infty) \\ \theta'_c(\infty) \end{bmatrix} = \begin{bmatrix} (W_c(0)+W_d(0)+W_s(0)) \cdot T_4 \\ \theta'_e(\infty) + (W_c(0)+W_d(0)+W_s(0)) \cdot T_3 \\ \theta'_s(\infty) + (W_c(0)+W_{d1}(0)) \cdot T_1 \end{bmatrix} \tag{3.33}$$

Here $t = 0$ has been used for the evaluation of the losses, as these are the losses which will result in $\underline{\theta'}(\infty)$ when they have been applied for an infinitely long time.

The constants c_1, c_2 and c_3 are evaluated by solving (3.34).

$$\begin{bmatrix} v_1 & v_2 & v_3 \end{bmatrix} \cdot \begin{bmatrix} c_1 \\ c_2 \\ c_3 \end{bmatrix} = \begin{bmatrix} \theta'_e(0) \\ \theta'_s(0) \\ \theta'_c(0) \end{bmatrix} - \begin{bmatrix} \theta'_e(\infty) \\ \theta'_s(\infty) \\ \theta'_c(\infty) \end{bmatrix} \tag{3.34}$$

Now the constants can be found by Gaussian elimination of the matrix shown in (3.35).

$$\left[\begin{array}{ccc|c} v_1 & v_2 & v_3 & \underline{\theta'}(0) - \underline{\theta'}(\infty) \end{array}\right] \tag{3.35}$$

It should be noted that the initial temperature distribution, $\theta'(0)$, is assumed known.

While (3.32) is a mathematically well known solution to stable differential equations, this easy and straight forward approach has, as previously discussed, not been found to have been applied in the evaluation of temperatures in power cables.

3.6.3 Defining the Thermal Parameters

The equation system for solving the thermal response to a load profile requires the evaluation of the thermal parameters (thermal resistances and thermal capacitances) for the cables and the surroundings. This can be done by following the guidelines of the international standards [8, 31], however the analysis in [69] showed that TEEs will be unacceptably inaccurate if lumping of the thermal components is as coarse as shown in figure 3.2.
In order to increase the accuracy, [69] proposes to divide the surroundings of the cables into 100 lumps and [70] further suggests that also the insulation and jacket should be divided into multiple zones for obtaining an even better accuracy. It is in [70] suggested that the insulation is divided into 10 lumps and the jacket into 3. The size of the system matrix of (3.30) will in this way be 113×113, as well as there will be 113 eigen vectors and eigen values. Note that the papers, [69, 70], were written as part of this PhD project and can be found in appendixes F.1 and F.2.

The division of the different subcomponents into multiple zones requires the definition of how the thermal parameters are to be calculated. The present thesis is only concerned with single phased cables, and the thermal resistance and capacitances of the different zones inside the cable can thus be seen individually as hollow cylinders. It should though be recognised that the method is also applicable to other cables, for instance three phased submarine cables, with similar definitions of the thermal parameters.
Figure 3.3 shows how the zones can be visualised for the internal part of the cable. The thermal capacitance per meter of zone $'x'$ is calculated based on the cross sectional area of the zone x, as given in (3.36).

$$\begin{aligned} C_{1,x} &= c_{therm,i} \cdot \pi \cdot \left(r_x^2 - r_{x-1}^2\right) \\ x &= 1, 2, ..., s \end{aligned} \tag{3.36}$$

where $c_{therm,i}$ is the specific heat of the insulating material, r_x is the outer radius of zone x, r_{x-1} is the inner radius of zone x (where r_0 is equal to the conductor radius) and s is the total number of zones in the insulation.
Note that the thermal capacitance of the conductor is added to the boundary element $C_{1,1}$.

The present study has calculated the thermal resistance, $T_{1,x}$, of zone x in the insulation as given in (3.37).

$$\begin{aligned} T_{1,x} &= \frac{\rho_{therm,i}}{2 \cdot \pi} \ln\left(\frac{r_x}{r_{x-1}}\right) \\ x &= 1, 2, ..., s \end{aligned} \tag{3.37}$$

where $\rho_{therm,i}$ is the thermal resistivity of the insulation material.

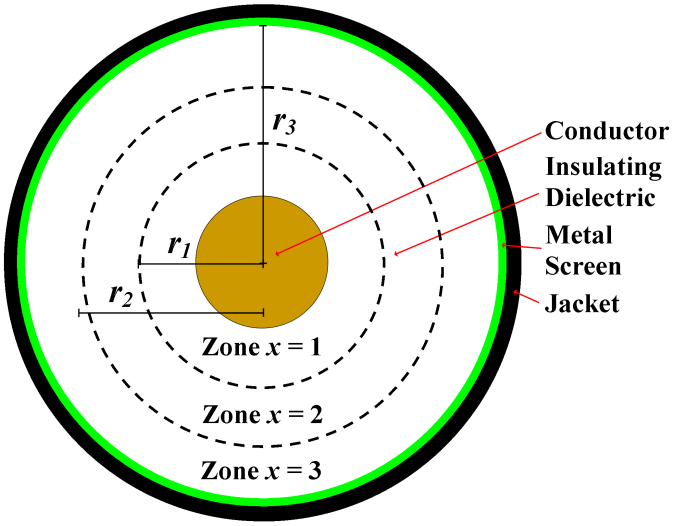

Figure 3.3: Division of the insulation into multiple zones allows increased accuracy of the thermal model. Here is for simplicity shown a division into three zones, however [70] suggest a division into ten zones.

Similarly, the thermal capacitance and thermal resistance of zone $'y'$ in the jacket is calculated as given in (3.38) and (3.39).

$$C_{3,y} = c_{therm,j} \cdot \pi \cdot \left(r_y^2 - r_{y-1}^2\right) \tag{3.38}$$

$$T_{3,y} = \frac{\rho_{therm,j}}{2 \cdot \pi} \ln\left(\frac{r_y}{r_{y-1}}\right) \tag{3.39}$$

$$y = 1, 2, ..., t$$

where $c_{therm,j}$ is the specific heat of the jacket material, r_y is the outer radius of zone y, r_{y-1} is the inner radius of zone y (where r_0 is equal to the screen outer radius) and t is the total number of zones in the jacket.
Note that the boundary element $C_{3,1}$ is added to the screens thermal capacitance.

The thermal resistance of zone $'z'$ is calculated as given in (3.40).

$$T_{4,z} = \frac{\rho_{therm,sur}}{2 \cdot \pi} \left(\ln\left(\frac{r'_{z-1}}{r_{z-1}}\right) - \ln\left(\frac{r'_z}{r_z}\right) + \frac{\sum_{k=1}^{n} \ln\left(\frac{d'_{pk}}{d_{pk}}\right)}{u} \right) \tag{3.40}$$

$$z = 1, 2, ..., u$$

where $\rho_{therm,sur}$ is the thermal resistivity of the surrounding material, r_z is the outer radius of the zone, r'_z is the distance from the outer radius of the zone to the mirror of the cable itself above ground, r_{z-1} is the inner radius

of the zone (r_0 the outer radius of the cable), r'_{z-1} is the distance from the inner radius of the zone to the image of the cable itself above ground, d_{pk} is the distance from the cable under investigation, p, to cable k, d'_{pk} is the distance from cable p to the image of cable k above ground and u the total number of zones.
The $\frac{r'_{z-1}}{r_{z-1}}$ term gives the external thermal resistance for the cable from inner radius of zone z to ground surface. However, in order not to account for the same resistance multiple times, subtraction of the term $\frac{r'_z}{r_z}$ is required. In addition, the term $\sum_{k=1}^{n} \ln\left(d'_{pk}/d_{pk}\right)$ takes into account any other cables (experiencing losses equal to those of cable p) in the vicinity.

The capability of the surroundings to store heat is in the present project assumed to be limited to an area around the cables equal to the cross section of a circle with a radius equal to the burial depth of the cable. This area is naturally divided into the defined amount of zones. For illustrative purposes, a division of the surroundings into three zones is shown in figure 3.4.

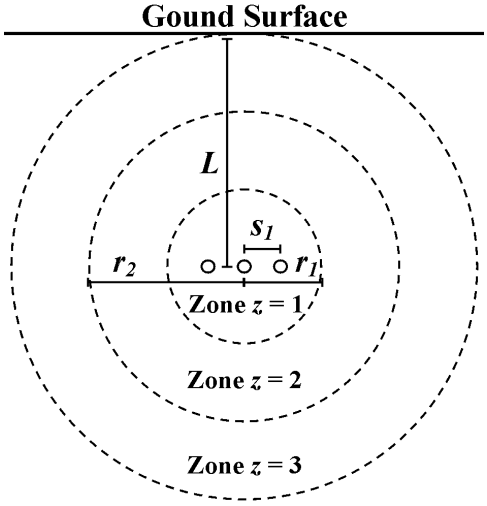

Figure 3.4: Division of cable surroundings increases accuracy of the thermoelectric equivalent methodology. In the present PhD project it has been chosen to divide the burial depth into equal lengths, such that the calculation of thermal resistances and capacitances is based on equal lengths. This figure shows, for illustrative purposes, a division into only three, however the recommendation is a division into one hundred.

The thermal capacitance of zone $'z'$ of the cable surroundings is thus approximated to (3.41).

$$C_{4,z} = c_{therm,sur} \cdot \pi \cdot \left(r_z^2 - r_{z-1}^2\right) \qquad (3.41)$$
$$z = 1, 2, ..., u$$

where $c_{therm,sur}$ is the specific heat of the surrounding material.

It should be noted that in trenches where the cables are surrounded by an envelope of sand, the first zone elements of $T_{4,z}$ and $C_{4,z}$ are to be calculated with the thermal properties of the sand and the last zone elements are to be calculated with the native soil's thermal properties.
Because the thermal model is one dimensional, the two dimensions (height and width) of the sand envelope have to be equivalated with a one dimensional radius. [10] suggests that the equivalent radius of the sand envelope ($r_{backfill,eq}$) is calculated as (3.42).

$$r_{backfill,eq} = \frac{2 \cdot L}{e^{G_b}} \tag{3.42}$$

where G_b is a geometric parameter dependent on the $L/h_{backfill}$ and the $w_{backfill}/h_{backfill}$ ratios. $w_{backfill}$ and $h_{backfill}$ are the width and height of the backfill envelope respectively. Tables of G_b suggestions are given in [10].

It should be acknowledged that the division of the thermal parameters, as shown in this clause, has not been found to have been previously discussed to this extend in any published research studies. Note also that summing up (3.37), (3.39) and (3.40) over all zones will equal the total thermal resistances as they are defined by the steady state equations (3.12), (3.13) and (3.14).

3.6.4 Loadability of Power Cables

In addition to simply calculating the dynamically varying temperature, the described enhanced TEE method also allows for a straight forward evaluation of the steady state as well as dynamic loadability, such as discussed in the following.

3.6.4.1 Steady State Loadability Calculation

As the sum of the thermal resistances of TEEs adds up to the thermal resistances of the standardised steady state loadability method, the steady state loadability is calculated via equation (3.10) or (3.11).

3.6.4.2 Development of Dynamic Loadability Algorithm

The dynamic loadability is, as mentioned, defined as the current which the cable system can carry for a given period of time.
Because of the different parameters temperature dependency (e.g. the electrical resistivity is temperature dependent), the evaluation of the dynamic

loadability must be performed in an iterative way such as suggested in the following. An illustration of the algorithm is given in figure 3.5.

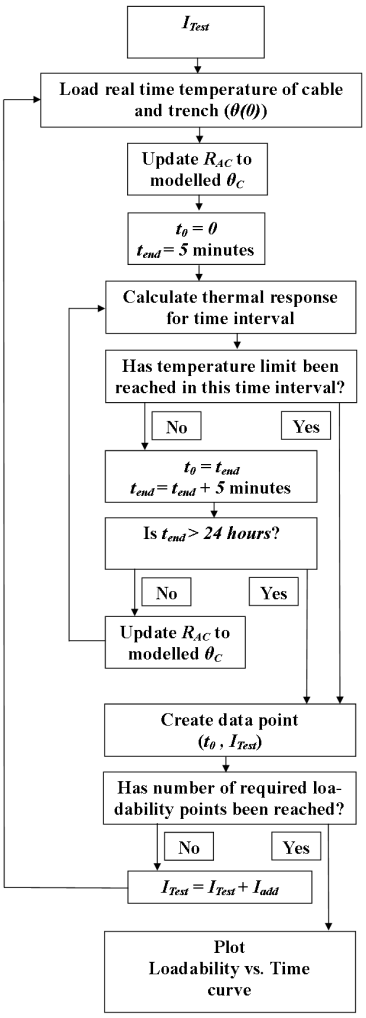

Figure 3.5: Illustration of the algorithm which is used to calculate the data points for the loadability vs. time graph.

The temperature distribution of the cable at the time of the loadability calculation ($\underline{\theta}(0)$) is given as input to the algorithm. A test current, I_{Test}, is assumed pushed through the cables, and the time dependent thermal response to this current is calculated via equation (3.32) until the time where the thermal limits are exceeded. It should be remembered that it is necessary to perform this calculation in an iterative way (each iteration covers for example 5 minutes) as the electric resistivity, and thus also the losses, of the conductor is dependent on the temperature.
Having determined how long it takes for I_{Test} to heat the cable to the thermal

limit, one point on the "Loadability vs. Time" curve (t_0, I_{Test}) has been obtained.
Thereafter a new I_{Test} is chosen ($I_{Test} = I_{Test} + I_{add}$) and the procedure is performed again and again until a satisfactory amount of data points for the "Loadability vs. Time" curve have been found.
It is chosen here that if the required time to heat up the cable is more than 24 hours, then the point will not appear on the Loadability vs. Time graph.

3.7 Other Loadability Concerns

There are different special concerns which must be included when discussing loadability calculations, however these are not easily categorised into any of the previously discussed subjects.

3.7.1 Thermal Conditions of the Ambience

Measurements and prediction of different quantities are often used in the evaluation of dynamic temperatures and dynamic loadabilities. As a cable's dynamic response to a load change is highly dependent on the thermal properties of the surroundings, accurate knowledge of these properties may enhance the accuracy of models significantly.

3.7.1.1 Ambient Temperature

The native soil temperature[7] at the cable burial depth is a very important parameter for studies which are concerned with dynamic temperature calculations and, as mentioned, dynamic temperature calculations are a prerequisite for DTR. The native soil temperature is important because studies such as [63–66] utilises the superposition principle when determining the temperature of cables (as it is also seen in figure 3.1). This means that the temperature of e.g. the cable conductor is the sum of the individual (and assumed decoupled) temperature influences within the vicinity of the cable, hereunder is the native soil temperature at the cable burial depth. [63] utilises direct measurements of the ambient soil temperatures for the dynamic simulations, however where measurements are not available modelling of the temperature is necessary.

[7] The native soil temperature is defined as the temperature which would be experienced if the soil had been left untouched.

[71] utilises a methodology similar to the TEEs to estimate the temperature dynamically at different depths over several years. The study includes both solar radiation, long wave irradiation and convection as heat sources and heat sinks in the model. It is shown that the model is very accurate for shallow soil depths. The methodology requires multiple input parameters in order to operate, hereunder measurements of solar intensity, wind speed and air temperature. However [71] also shows that obtaining these quantities within approximately 40 km gives a sufficiently accurate soil temperature modelling in a depth of 300-600 mm.

An older report on the subject of ambient soil temperature [72] introduced a simpler approach where only measurements of the air temperature above ground is necessary as input. [72] suggests that the temperature at a depth x in the ground, based on the average monthly temperature, at time t (beginning January 1st), can be estimated by using equation (3.43).

$$\theta(x,t) = A - B \cdot \exp\left(-\sqrt{\frac{\pi}{\delta_{soil} \cdot T}} \cdot x\right) \cdot \cos\left(\frac{2\pi t}{T} - \sqrt{\frac{\pi}{\delta_{soil} \cdot T}} \cdot x - P\right) \quad (3.43)$$

where A is the average temperature at ground surface, B being half the difference between yearly minimum and maximum temperature, T is the length of the temperature cycle (e.g. one year), P is the phase angle of the earth temperature cycle and δ_{soil} the thermal diffusivity of the soil. [72] compares the accuracy of their model with measurements from a number of sites, each carrying data from multiple depths. It is concluded that the model in general is fairly accurate, especially when x increases.

3.7.1.2 External Thermal Properties

As stated, the external thermal properties are of vital importance when modelling the thermal behaviour of power cables and performing DTR. In most research studies only the thermal resistivity is of special interest and the importance of the specific heat's variations are thus neglected (or included as a part of the thermal resistivity's variation).

There are basically three different approaches for handling the thermal resistivity of cable surroundings. Firstly, it is possible to measure the thermal resistivity prior to commissioning of the cable and utilise this value in the model, such as it is done in [65, 66]. Secondly, it is possible to adapt the thermal resistivity, by comparing modelled temperatures (at e.g. the jacket) with measured. If the modelled temperature is incorrect, it is assumed that the thermal resistivity in the model is wrong and must be updated. This updating is performed until the modelled temperature is within an acceptable range of the measured. This approach to handling the thermal resistivity is utilised in [62, 63]. Finally, the thermal resistivity can be measured online,

and the measured values can be utilised in the thermal models. This method is for instance utilised in [73].

3.7.1.3 Probabilistic Parameter Estimation

In order to utilise a larger part of the current carrying capacity of transmission cables for a larger part of the operation time, [74] uses a probabilistic parameters estimation (PPE) of soil temperature, load shape and temperature of water in cooling pipes. The method is proposed for use at places where online monitoring of the thermal properties is not possible and it is concluded in [74] that PPE can increase the ampacity significantly. A similar use of PPE, where the thermal resistivity of surroundings, the load shape and the ambient temperature are variables, is included in [38].

3.7.1.4 Moisture Migration

As stated, moisture migration should be considered when installing transmission cables, as thermal runaway can be experienced when the cable surroundings dry out.
Among others, [38, 75] gives curves that relate the thermal resistivity to the moisture content (M) of the surrounding material. The studies clearly shows that even a small change in M can have significant impact on the loadability of power cables.
It has not been possible to find literature describing accurate methods for determining the spatial distribution of the moisture content around cables as a function of time and temperature, however studies such as [76, 77] give suggestions to a possible method. The accuracy of the method is though shown not to be sufficient for implementation in the analysis of power cable rating.

3.7.2 Using Measured Temperatures in Thermal Modelling of Cables

Many studies concerned with dynamic loadability calculations utilises a measured temperature for increasing accuracy of their models. The place of the measurements varies from study to study, e.g. [56] utilises a measurement of the metallic screen temperature and [66] utilises a measurement of the ducts outer temperature. The temperature measurements are normally performed with Distributed Temperature Sensing (DTS) equipment, which enable the operator to get a picture of the temperature distribution in the longitudinal direction of the cable, see appendix B, however single point measurements

with thermocouples or PT100 sensors can also be utilised where optic fibres for DTS are not installed.

3.7.3 Lifetime Consumption

Instead of designing cables to be able to sustain a maximum temperature during the entire lifetime of the cable, suggestions have been given on designing cables using other methods. Due to the fact that cable design is under a never ending research progress, the author of [78] states that dimensioning cables for more than 20 years of service life is not beneficial, especially if the full current carrying capacity of the cables is not utilised. It is therefore in [78] suggested that the ampacity is determined on the basis of the temperature dependent lifetime consumption instead of the magnitude of the temperature. The lifetime consumption could in such cases e.g. be evaluated based on Arrhenius law.

3.7.4 Evaluation of Jacket Temperature as Limitation

As stated earlier, the thermal properties of the cable surroundings are vital for calculating the loadability of cables and modelling their real time thermal behaviour. Especially the thermal resistivity of the surroundings has been of great concern to cable designers and the dependency of the moisture content on the thermal resistivity has resulted in the general requirement of limiting the jacket temperature to 50 °C.
Recent research studies, such as presented in [79, 80], have questioned the validity of using 50 °C as a static maximum limit for the jacket temperature. [79] describes a laboratory study of moisture migration in sand samples of different compositions. It is shown that moisture does migrate away from the heat source, leaving a spatial gradient of the moisture content, however it is also seen that the thermal resistivity for most of the tested samples stays constant for at least an hour after application of the heat. After 1 hour, the thermal resistivity is found to increase near the heat source and after 24 hours the thermal resistivity remains at an almost static level for the rest of the 48 hours test period.
The above stated time periods for thermal resistivity increase are of course dependent on the size of the heat source, the type of material, the suction tension, etc, but [79] suggests that the critical temperature at which moisture migration may be expected is closer to 60 °C than 50 °C. Furthermore it may be concluded from [79] that for shorter periods of time high temperatures can be allowed without experiencing dry-band formation.

As suggested in [79] it is generally accepted that different soil compounds can have significantly different thermal resistivities, and Energinet.dk there-

fore subjected the sand of 40 sand pits in Jutland, Denmark, to tests in order to obtain knowledge about how to specify appropriate requirements for the sand to be used in cable trenches. The 5 sand samples with the lowest thermal resistivities were chosen for further analysis of their thermal properties.

In order to obtain conditions as close to what the sand will experience in a cable trench, it was decided to create a field experiment which was to determine:

- At what temperature dry-bands would occur for different sand materials
- The speed of the possible dry-band formation
- How fast moisture content can be restored during rainy weather

Because the experiment was performed outside as a field study, it was not the intent, neither was it possible, to control the environmental impact on the results. The knowledge gained from the experiment is thus to be used for more qualitative than quantitative discussions about moisture migration.

The main conclusion from the field experiment is that the sand around cables does not show sign of significant moisture migration when subjected to 50 °C. The sand may dry out at 60 °C under dry weather conditions, however it can take months for this to happen and it is dependent on the type of sand whether or not it dries out. Furthermore it is found that the moisture returns quickly under rainy conditions. This means that the static jacket temperature limit of 50 °C seems to be conservative for the Danish transmission system, and that temperatures of 60 °C may be allowed for many days without jeopardising system reliability.

The experimental setup and results are explained in greater detail in appendix C.

3.8 Loadability of Cables in the Danish Transmission Grid

This section describes how the Danish TSO calculates loadability and how temperature monitoring is utilised. These aspects are important for this PhD project as they show which tools are available when the concept for dynamic calculation of the transmission system is to be developed in part III of this thesis.

In Denmark, loadability calculations for cables are only performed during the design of new lines. This means that DTR calculations are not performed during operation of the transmission system. Furthermore cyclic ratings (or other dynamic ratings) are not considered during operation of the grid as well as it is normally not considered during the planning of new lines.

The loadability of new cables are calculated with the steady state equation (3.11) by allowing a maximum jacket temperature of 50 °C. Furthermore, during contingencies the load is allowed to increase to (and maintain for 40 hours) the value which will result in a jacket temperature increase to 60 °C after 40 hours. In addition to this, the load is allowed to increase to (and maintain for 1 hour) the value which results in a conductor temperature of 90 °C after 1 hour. Both of these dynamic loadabilities are calculated by assuming a 0.5 pu preloading and the dynamic calculations are carried out with the commercial program Cymcap, [51].
The thermal parameters for the loadability studies are determined by performing a survey of the thermal conditions of the proposed cable route, including a sampling of the thermal resistivity, estimation of burial depths and evaluation of the impact when drilling under roads, etc. and the worst case conditions would define the steady state loadability of the specific cable system[8]. For installations in ducts filled with bentonite the 50 °C temperature limitation is enforced on the outside of the duct, as this is where moisture migration could be experienced.

The Danish TSO Energinet.dk normally installs optic fibres for DTS monitoring with their new cables. The fibre is installed in a pipe taped to the centre phase, as seen in figure 2.2. After commissioning of the cables, the DTS system gathers data for approximately one year where after the data is utilised to find the exact hotspots and determine if initiatives should be taken for mitigating the hotspots. Thereafter the DTS system is moved to a new cable system.
In addition to the DTS measurements, single point PT100 sensors are installed, for further thermal monitoring, near the ends of the cables. The data from these sensors is, similar to the DTS system, not utilised in the daily operation of the transmission system.
It should be noted that many older cable systems are installed in Denmark, especially in urban areas, and such systems are not necessarily equipped with temperature monitoring.

Energinet.dk is aware that some cable manufacturers are able to provide optical fibres for DTS integrated into the metallic screen, however as problems with the sustainability during manufacturing, transport, installation and especially during jointing work, of such integrated fibres have been reported,

[8]The loadability of the cable system was calculated for a native part of the cable, and thus joints, termination, etc. were not considered in the analysis.

and the fact that the pipe taped to the centre phase would be installed for communication anyway, Energinet.dk has chosen to measure the temperature in the pipe.

3.9 Conclusion on Loadability Calculations of Power Cables

This part of the thesis has defined steady state loadability as the calculated current which can be pushed through a cable continuously for an infinite period of time without the thermal limits (conductor and/or jacket temperature) being exceeded. It is also defined in this study that dynamic loadability is the calculated current which the cable can carry for a specified period of time without the same thermal limits being exceeded, and it is stressed that the dynamic loadability value must be given along with the time period which this current is allowed.

A significant amount of literature has been studied, and it shows that the standardised equation for the steady state loadability in general is accepted, however for complex installations FEM may be used.
The studied literature also shows that there is a wide variety of areas within dynamic loadability, such as lifetime assessment, moisture migration, etc., which are still investigated by the scientific community.

The tools and thermal models which have been discussed in this chapter are now available and can be utilised in the remaining of this thesis when the point-to-point analysis of dynamic loadability (which is the subject investigated in this part) is changed to a transmission system analysis in part III. It should be recognised that while the SR and FEM models have been discussed mainly based on a literature review it has been a part of this PhD project to enhance the TEE method and it should thus be acknowledged that the definition of TEE as given in this chapter and the dynamic loadability algorithm are contributions of this PhD project.

On the background of the definition of dynamic loadability, Dynamic Thermal Rating (DTR) is defined as a system which is capable of calculating the real time temperature evolution in the cable and from this temperature calculate the dynamic loadability.

The models and methods to be developed in this PhD project will utilise the best of the standardised and state of art research within loadability of transmission cables, in order to provide proper DTR for the future Danish cable based transmission grid.
The DTR system to be developed should thus be able to evaluate the thermal state of a large transmission system with many cables, each potentially

having multiple hotspots. The developed DTR methodology should rely on thermal models requiring limited computational resources.
For ensuring accuracy, the DTR methodology should be able to take the measured pipe fibre temperature as input. However as some older cable systems in the Danish grid are without temperature monitoring, and in order to ensure operation during fallout of the measurement equipment, the DTR system should also be able to operate without the temperature input.
The developed models should be able to estimate the real time jacket and conductor temperature of the cables, as well as estimate the loadability given the real time thermal state of the cables and the surroundings.
It should be assumed that the loadability will be dictated by a regular part of the cable, and thus joints, terminations, etc. will not be necessary to model for the DTR.
In addition, it is to be assumed that unfavourable thermal regions will be wider than three meters, and thus longitudinal heat flows can be neglected at hotspots.

Chapter 4

Choice and Verification of Thermal Model for use in Large Transmission Grids

In this chapter a suitable method for performing DTR simulations on the future Danish cable based transmission system will be chosen.

It should be acknowledged that there are basically two requirements to such a model. Firstly, the model needs to be fast, as the temperature will have to be modelled for all cables in the transmission grid which potentially necessitates many simultaneous calculations. Secondly, the chosen model has to be accurate, as the reliability of the entire transmission system depends on the accuracy.

As seen from the previous chapter, mainly three modelling principles are utilised for DTR today, the thermoelectric equivalent method, the finite element method and the step response method. It was decided that the model to be used in this study was to be found among these three and a comparison of the methods was thus required in order to be able to choose the model that best suits the requirements of speed and accuracy.

4.1 Comparison and Choice of Thermal Models

A comparison of the TEE methodology to both FEM and SR models is given in the following sections such that the most suitable method for modelling

dynamic loadability of transmission systems can be chosen.

4.1.1 Comparing TEE and FEM Simulations

The following comparison of TEEs and FEM is based on the paper [69], given in appendix F.1, which has been produced as part of this PhD project.

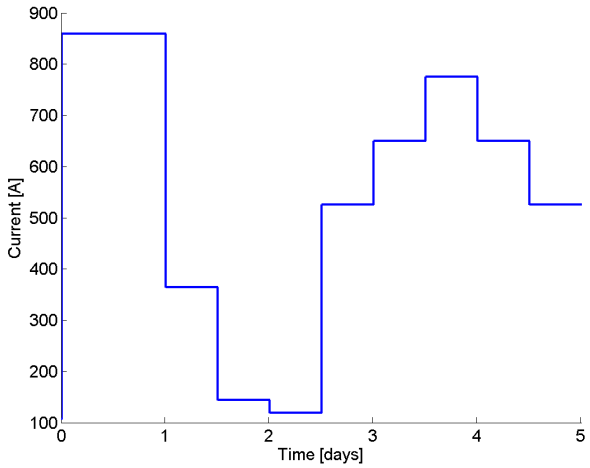

Figure 4.1: Load profile applied to 420 kV cables for comparing the accuracy of the finite element and thermoelectric equivalent methods.

The load profile of figure 4.1 is applied to three single phase 420 kV XLPE insulated cables in flat formation, with a 1000 mm^2 compacted aluminium conductor, 200 mm^2 copper wire screen and an aluminium water blocking foil. The cables are buried at a depth of 1.4 m with a separation of 300 mm. The specifications of the cable are taken from a cable manufacturer data sheet, [7], and is reproduced in tables 4.1 and 4.2.

U [kV]	S_c [mm^2]	S_s [mm^2]	d_c [mm]	d_i [mm]	d_s [mm]	D_e [mm]
420	1000	200	34	109.6	120.4	131.6
S_c are the conductor cross section S_s is the screen cross section						

Table 4.1: Dimensions of cable used for modelling the comparability of the FEM and TEE methodologies. The numbers have been taken from [7]. It is in the thermal model assumed that the semiconductive layers are parts of the insulation and that the metallic screen is a hollow cylinder with inner diameter equal to the outer diameter of the insulation. This is an approximation as the cable is equipped with a wire screen.

Material	$\tan(\delta)$ [ ]	ρ_{elec} $[\mu\Omega \cdot \mathrm{m}]$	α_{elec} $\left[\frac{\Omega}{\mathrm{K}}\right]$	c_{therm} $\left[\frac{J}{\mathrm{m}^3 \cdot \mathrm{K}}\right]$	ρ_{therm} $\left[\frac{\mathrm{K} \cdot \mathrm{m}}{\mathrm{W}}\right]$
XLPE	0.005*	-	-	$2.40 \cdot 10^{6}$***	3.5*
Aluminium	-	$2.83 \cdot 10^{-2}$*	$4.03 \cdot 10^{3}$*	$2.5 \cdot 10^{6}$***	0**
Copper	-	$1.72 \cdot 10^{-2}$*	$3.93 \cdot 10^{3}$*	$3.45 \cdot 10^{6}$***	0**
Soil	-	-	-	$2.0 \cdot 10^{6}$***	1*

* Numbers are taken directly from [8].
** The thermal resistivity of metals is several orders of magnitude lower than for most other materials and thus the thermal resistance is assumed negligible.
*** Numbers originate from [33].

Table 4.2: Material specifications used for modelling the comparability of the FEM and TEE methodologies.

All FEM simulations have been carried out in the commercially available Comsol Multiphysics, a software which is easy to setup and use, as it enables straight forward interaction between electrical and thermal calculations.

In order to prove that the thermal resistances for the TEE are calculated adequately accurate, the temperature distribution from the centre of the cable to the ground surface is evaluated and compared to the FEM model. The ground surface temperature is in both FEM and TEE simulations set to 15 °C. In the FEM model, the temperature at a depth of 10 m is, for simplicity also set to 15 °C. The sides of the 2D simulation are given as "infinite elements" (simulating a very large volume of soil) and the boundaries allow an outward flow if necessary. The FEM model, including mesh, is shown in figure 4.2.

Figure 4.3 shows the spatial temperature comparison between the FEM and TEE model when the load at $t = 0$, shown in figure 4.1, is assumed to have been applied for an infinite amount of time. The load is seen to be relatively low however in combination with the substantial dielectric losses, the result is a temperature increase significantly above the surrounding 15 °C[1]. The TEE model used in this simulation has divided the insulation into 10, the jacket into 3 and the surroundings into 100 zones. It is seen that the two simulation methods give very similar results, within ±0.2 °C over the entire modelled area from conductor centre to ground surface.

Having confirmed that the static models are comparable, the dynamic part of the model must be analysed as well. Figure 4.4 shows the dynamic response of the 420 kV cables, when subjected to the load profile of figure 4.1. The conductor temperature, calculated by TEE models of varying resolution, is

[1] It should be noticed that dielectric losses have been evenly distributed over the volume of the insulation.

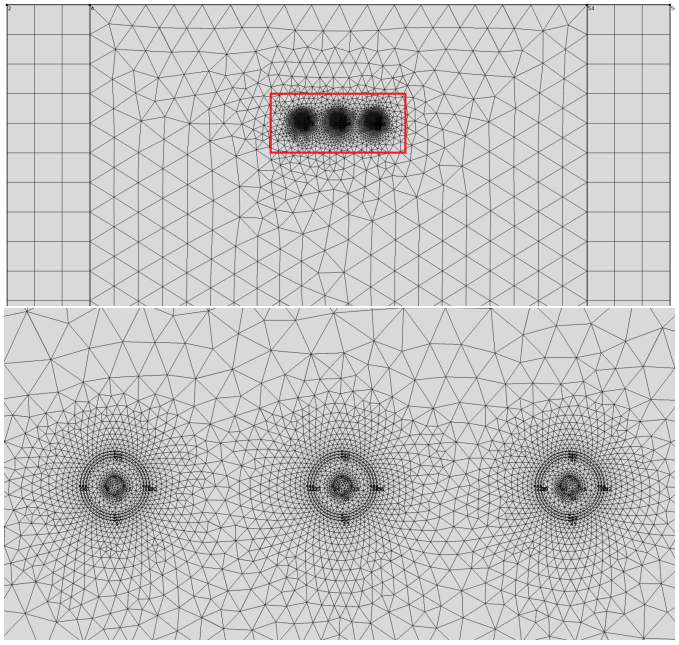

Figure 4.2: FEM of three single phase cables buried in flat formation in a depth of 1.4 m and with a horizontal spacing of 0.3 m. It is assumed that the ground surface is an isothermal with a temperature of 15 °C, as well as the temperature in a depth of 10 m is assumed to be 15 °C constantly. The lower figure is a zoom of the upper.

shown and compared to FEM calculations.

It is clearly seen that increasing the number of zones of the surroundings in the TEE model increases accuracy of the calculations when comparing to FEM, however it should be recognised that the calculation time also increases when the resolution is enhanced as it is shown in figure 4.5.
It is observed in figure 4.4 that only a minor differences appear between modelling the surroundings with 100 and 1000 zones, however the solution time for 100 zones was approximately 25 seconds and approximately 1300 seconds for 1000 zones. Therefore it is chosen to use 100 zones in the remaining of this thesis for cables buried at a normal depth (i.e. around 1.5 meters), as this provides the best compromise between accuracy and solution time.

In order to compare the solution times of TEE and FEM, the default mesh size, default solver, etc. chosen by Comsol, was found to give a FEM solution time of approximately 9 hours. It was attempted to decrease the mesh resolution, however also for FEM a poorer resolution yield a lower accuracy and it was found that the lowest computational time which could be obtained while ensuring that the solution converged towards the same results,

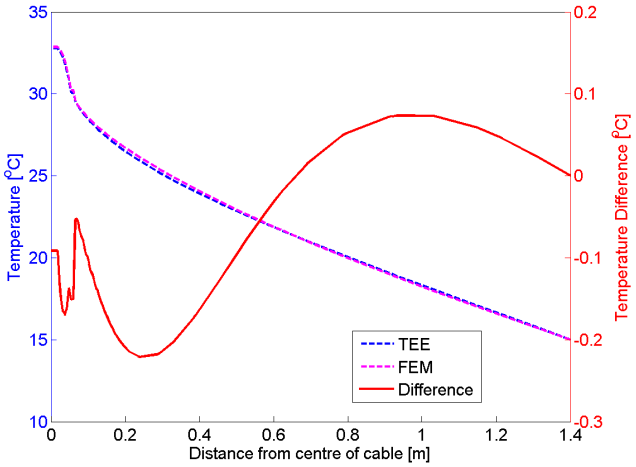

Figure 4.3: Temperature distribution from centre of cable to ground surface. Comparison of FEM and TEE methodologies. It is clearly seen that the results are very similar, which suggests that the TEE methodology is sufficiently accurate at least for static modelling.

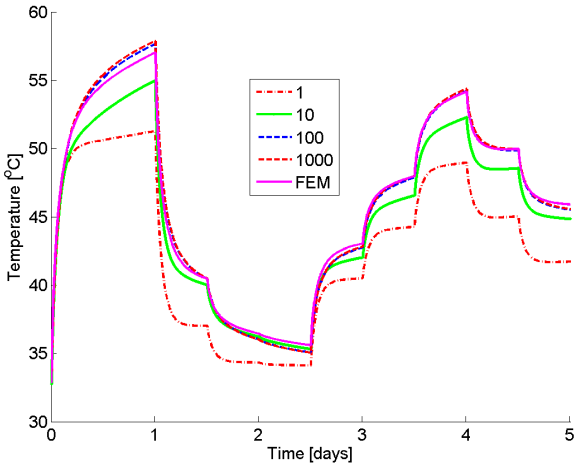

Figure 4.4: Calculated temperature profile for the conductor of the centre 420kV cable subjected to the load profile of figure 4.1. It is clearly seen that a higher resolution of the TEE results in a more accurate modelled temperature when comparing to the FEM model. However increasing the number of zones above 100 is seen to have only minor effect.

was approximately 4.5 hours. This is approximately 650 times the computational time of the 100 zones TEE model. It is of course possible to use 2D symmetry through the centre of the FEM model, however the simulation time only decreases by approximately half when this method is used, result-

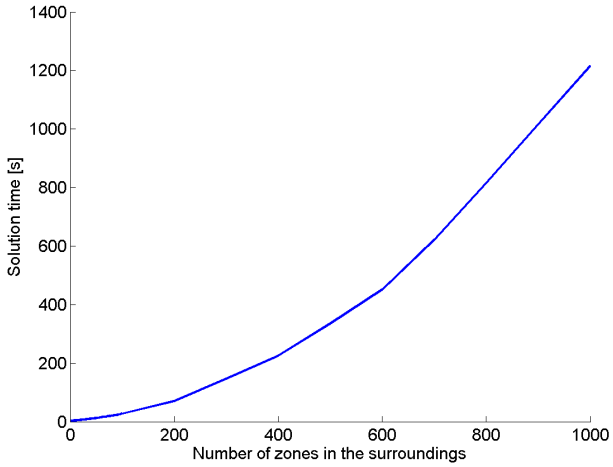

Figure 4.5: Required computational time for the five days dynamic temperature calculations, when varying the number of TEE-zones of the surroundings. The solution time is seen to increase for increased resolution. For comparison the default solution time for the FEM simulation is 9 hours.

ing in the FEM simulations being more than 300 times slower than the TEE method.

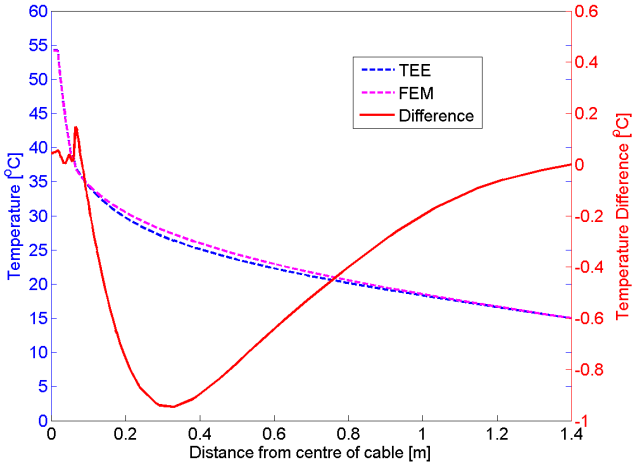

Figure 4.6: Temperature distribution from centre of cable to ground surface after four days of dynamically varying load. Comparison of FEM and TEE methodologies. It is seen that the results suggest that the TEE methodology provides similar results as FEM also in the dynamic modelling.

In order to ensure that the TEE-calculated temperature distribution from centre of the cable to ground surface remains accurate when performing dynamic calculations figure 4.6 has been produced. The figure shows the temperature distribution after exactly four days of modelling, which is at the second temperature peak of the load profile. The figure shows that the TEE and FEM models produce results which are within 1 °C throughout the entire modelled area. However inside and closely outside the cable (which are the most important sites), the results are within ±0.2 °C.

4.1.1.1 Discussion

The comparison of the TEE models with FEM has shown that TEEs are capable of performing temperature calculations which are within an acceptable range of the FEM simulations. The accuracy depends on the resolution of the TEE and it has been suggested to divide the cable insulation into 10, the jacket into 3 and the surroundings into 100 zones.
The time required to perform the simulation is significantly lower for the TEE than for the FEM and it must therefore be concluded that TEEs can be preferred for real time simulations over FEM as accuracy is sufficient and computational speed is significantly higher.

4.1.2 Comparing TEE and SR Simulations

The cable system of figure 4.2 was also used for comparing the results of the TEE and SR methodologies. The load profile of figure 4.1 is again used as the studied case. The SR results are obtained by assuming the thermal transients to be of long duration when calculating the parameters to be used in (3.18). The estimated conductor temperature determined by the three modelling tools, SR, FEM and TEE, are shown in figure 4.7.

It is seen in the figure that the three simulation tools provide very similar results and the choice of the model may thus be based on the modelling time.

4.1.2.1 Modelling Time

As seen in clause 3.4.2.2, the SR methodology requires the evaluation of a number of variables and the solution of several equations. The solution time for modelling the five days load profile with SR methodology was 150 seconds, which is approximately six times the required calculation time for the TEE methodology. Furthermore, if the spatial temperature distribution similar to figure 4.3 is wanted, the solution time for the SR method

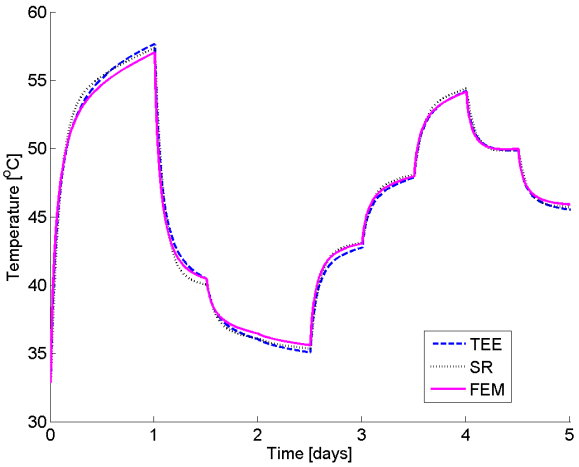

Figure 4.7: Comparison of TEE, FEM and SR methods. The modelled centre phase conductor temperature for the cable system presented in clause 4.1.1. It is seen that both the TEE and SR methodologies have good correlation with the FEM solution.

increases as it requires the solution of two new equations for solving the temperature in one new spatial point. This feature is inherent in the TEE methodology.

4.1.3 Choosing the Thermal Model

As previously stated the TEE method has the advantage over the SR method that it inherently models the temperature in multiple places inside and outside of the cables. In the SR methodology each new location requires the solution of two new time dependent equations. If for instance the screen temperature is wanted, the time dependent temperature increase, above the jacket temperature, must be found in addition to the screen's time dependent attainment factor. The comparison of the modelled temperature with measurements will thus be easier with TEE models as measurements can be taken all over the volume of the system without the need for further adaption of the model.

Furthermore the zone approach to thermal modelling allows in principle for each zone to have it's own distinct thermal and electric properties. Inside the cable this means that the dielectric constant may be varied over the insulation as a function of the temperature resulting in a more accurate distribution of the dielectric losses.
Outside the cables, the surroundings will benefit from the zone approach as each individual zone may have it's own thermal properties. This means that

it is possible to assign distributed thermal resistances and capacitances to the surroundings, which may increase the accuracy of the modelling during moisture migration, etc.

Moreover the TEE method requires only one model of the system where the standards suggests the use of two different models in the SR approach (one for short duration transients and one for long duration transients). This means that for TEE, the same model can be utilised to keep track of both the real time temperature and evaluation of the emergency rating.

The author acknowledges that it historically has made sense to utilise the Laplace transformation of the thermal system, however with modern technology the solution of (3.32) can be found for a long time interval within seconds and the TEE methodology is therefore straight forward to implement. The present study has further determined that the TEE method seems faster than the SR method, making TEEs a serious candidate for future thermal modelling.

In addition to this, the author finds the TEE methodology more easily comprehensible as it only requires setting up of one single equation, (3.30), in order for the user to follow the method.

The FEM simulation was in this section shown to be slower than both SR and TEE and for real time simulations it may thus not provide sufficiently fast results. Furthermore, creating algorithms for FEM simulations is a complex process, and the user friendliness of such a tool will thus not be high if implemented in the control room of a power system operator.
It should though be acknowledged that for complex systems with crossing cables, external heat sources, etc., the FEM method may provide accuracies that the TEE and SR method cannot resemble, but for single phase cables in flat formation, the TEE has in this section been found to be superior to the two other methods[2]. It should furthermore be noted that the author does not categorise cables installed in trefoil or three phase submarine cables as complex installations and these should thus also be possible to model with the TEE methodology.

By comparing SR, TEE and FEM it has been shown that the three tools provide similar results. The author therefore conclude that the choice of method should be based on speed, reliability and user friendliness of the tools.
The SR method may have been proven reliable through years of experience,

[2]The author is aware that it is difficult to create a long cable without the crossing of other heat sources but, as described previously in this report, such hotspots are most likely of limited length and it may thus be reasonable to use some resources on mitigating them. In this way the TEE models can still be seen as representative for the entire cable system.

however the present section has shown that the TEE method is just as capable of modelling cable temperatures over long periods of time. The remaining of this project will therefore utilise the TEE methodology for performing thermal modelling of power cables.

4.2 Experimental Verification of TEE Method

Comparing results of different simulation tools (e.g. TEE, SR and FEM) can only determine that the simulations are equally accurate or equally inaccurate.
In order to ensure that the TEE model is applicable to real operating cables, verification by measurements is required. As only sparse temperature monitoring is performed on power cables in the Danish transmission grid, and this monitoring only includes temperature measurements outside the cables, it was decided to perform the validation of the TEE method by comparison with experimentally obtained measurements. It was furthermore chosen that the experiment was to be performed inside a laboratory, such that the external conditions affecting the setup could be controlled and monitored closely. As the experimental setup is to model real installation conditions, the choice of performing the experiment inside required the construction of a box containing soil, in which the cables could be buried.

4.2.1 Design of Experimental Setup

The design of the experiment was a compromise between spatial limitations of the laboratory and the requirement of a large experimental volume to ensure realistic thermal time constants and boundary conditions.

It was possible to use three pieces of 245 kV XLPE cable, each having a length of approximately 4.75 m, which naturally set limitations on the length of the setup. Out of these 4.75 m, at least 0.5 m was required for electrical connections, etc., leaving approximately 4 m cable to be buried in soil.
The analysis of axial heat flow in power cables presented in [81] shows that when cables crosses a region longer than 3 m, the thermal analysis can be performed by assuming the longitudinal heat flow in the middle of the cable to be negligible. The 4 m of available cable should thus be sufficient for performing realistic thermal experiments.

As stated, many cables installed in Denmark are buried in flat formation in a depth of approximately 1.4 m, with a spacing of approximately 0.3-0.4 m. In order to resemble this installation in the laboratory, an experimental setup of at least 3 m high and 4 m wide would be required. In order to limit the volume of the experimental setup it was therefore chosen to install the cables

in a depth of 0.7 m with an axial spacing of 0.3 m, which are adequately realistic installation conditions (e.g. [7] uses a similar burial depth for their standard calculations).

In summary, the cables were thus to be installed in a box with the dimensions (L×W×H) 4 m×2 m×2.4 m. Just as for real installations, the cables were buried in an envelope of sand, and a pipe for optic fibres was installed next to the centre phase.

The setup was equipped with 60 type-K thermocouples, monitoring both conductor, screen and jacket temperatures as well as multiple places in the surrounding sand and soil, hereunder inside the optic fibre pipe. Furthermore the moisture content of the sand and soil was monitored with 5 sensors of the type Trime-Pico 64 from the company IMKO.
Finally, the current was monitored in real time as well.

For simplicity, the cables were electrically connected in series, see figure 4.8. This means that the phase angle between adjacent phases is 180 ° instead of

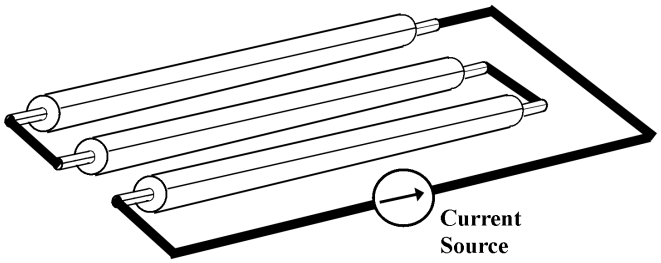

Figure 4.8: Electrical connection of cables in experimental setup. The cables are connected in parallel, meaning that the phase angle of currents and voltages of adjacent phases will be displaced by 180 ° instead of 120 ° which is the norm in transmission systems.

the 120 ° which is the norm in transmission systems.

This difference to the real transmission system affects the screen losses and the proximity effect of the conductor losses, and thus the standardised equations for calculating the losses may be inaccurate. This possible inaccuracy is analysed in clause 4.2.5.

A cross section of the setup is shown in figure 4.9 and a picture from the laboratury is seen in figure 4.10.

Details about design of the setup, measurement systems etc. can be found in appendix D.

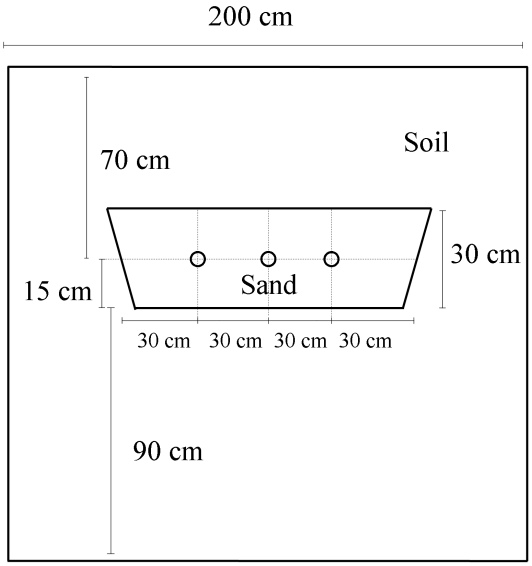

Figure 4.9: Cross section of the wooden box designed to create dynamic temperature data for verification of the thermal models.

Figure 4.10: Experimental setup under construction. Three 245 kV XLPE cables with conductor cross sections of 1600 mm^2 and lead screens are installed in an envelope of sand and surrounded by soil. In order to complete the setup, a layer of soil was installed on top.

4.2.2 Test Subjects

The cables installed in the experimental setup were 245 kV cables equipped with 1600 mm^2 solid aluminium conductor, XLPE insulation, semiconduc-

tive layers at the conductor and screen, lead screen and a polyethylene jacket. The dimensions of the cables are given in table 4.3.

U [kV]	S_c [mm^2]	S_s [mm^2]	d_c [mm^2]	d_{cs} [mm^2]	d_i [mm]	d_{is} [mm]	d_s [mm]	D_e [mm]
245	1600	737	45.0	50.0	99.0	102.0	106.5	112.0
d_{cs} is the outer diameter of the semiconductive conductor screen d_{is} is the outer diameter of the semiconductive insulation screen								

Table 4.3: Dimensions of cable used in the experimental setup. In the thermal simulations, the semiconductive conductor and screen layers are assumed to be a part of the insulation with identical thermal properties.

The thermal properties of the materials are determined in clause 4.2.6.

4.2.3 Load Curve

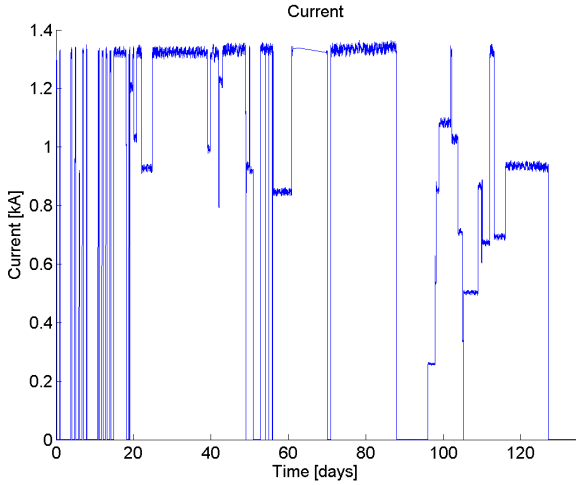

Figure 4.11: Load applied to the 245 kV power cables used as test subjects in the experimental setup. The load profile is seen to contain both fast and large variations as well as longer periods with static load.

The setup was subjected to a varying load over more than four months. The load curve was designed to include segments where the load changed on an hourly basis as well as segments where the load was kept constant over long periods of time. Figure 4.11 shows the alternating current applied at 50 Hz over the approximately four months test.

4.2.4 Precipitation

As previously discussed, the moisture content of the cable surroundings is dependent on a number of parameters. In the laboratory, precipitation has been included by adding water to the setup four times during the four months testing period.

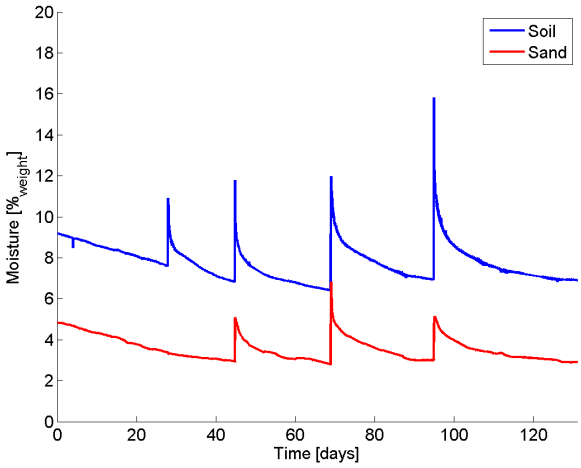

Figure 4.12: Moisture content of the sand and soil, in percentage of the total weight, in the experimental setup as a function of time. The moisture content of the soil is seen to always be higher than that of the sand even though the moisture contents vary fairly much over the entire test period.

These four simulated rain scenarios are seen as spikes, with almost immediate increase, in the measured soil moisture content, see figure 4.12. The soil moisture content shown in figure 4.12 has been measured in the centre of the setup, approximately 30 centimetres above the centre cable, and the sand moisture content has been measured between the centre phase and one of the outer phases. It may be noticed that the moisture spikes in the sand are smoothed compared to the soil and shifted slightly in time.

4.2.5 Analysis of Screen Losses

Electromagnetic FEM calculations (using Comsol Multiphysics) of the experimental setup were performed in order to establish the difference in the screen losses when the cables are loaded with a phase angle difference of 180 ° instead of 120 °. In the experiment, the screens were kept electrically floating, and thus only eddy currents would cause losses in the screens.

The ratio between screen and conductor losses is in the international standards, [8], denoted with the symbol λ_1. Table 4.4 shows values of λ_1 when calculated by the IEC method and when using the FEM software.

Calculation method	λ_1
IEC 60287	0.0291
FEM 120 ^{o}	0.0242
FEM 180 ^{o}	0.0004

Table 4.4: Values of the screen to conductor loss ratio for the centre phase of the experiment, calculated by the IEC standards [8] and by using FEM simulations.

It is clearly seen that the losses in the screen of the centre phase are much lower when the cables are configured as in figure 4.8 than when configured with the normal 120 ^{o} phase angle difference. Even for the leading and lacking phases, the FEM calculated screen losses are low in the 180 ^{o} configuration. It can thus be assumed that the screen losses are negligible for the performed experiment. Note also that loss calculations for the conductor have been performed and these losses are not significantly affected by the changed conditions, i.e. the proximity effect is relatively small.

It is noticed that the screen losses evaluated by FEM are 17 % lower than the IEC calculated losses in the 120 ^{o} phase angle difference case. However this difference should be seen in the light that there is an ongoing discussion in the scientific community about the accuracy of the standardised calculation procedure for λ_1, [82, 83].

4.2.6 Thermal Properties of Materials

In the presented experiment, measurements of the thermal resistivity and specific heat of the involved materials have been performed, see appendix D. Thermal properties of metallic subcomponents are though taken from standard values as they are assumed to be very well defined.

Table 4.5 gives the thermal properties for the internal parts of the cables. As the thermal properties of the surroundings are dependent on the moisture content, single point measurements of these may not be sufficient. Figure 4.13 shows the thermal properties of the sand and soil as a function of the moisture content. It is to be noticed here that the specific heat is only measured in dry state and extrapolated, [84], while the thermal resistivity is measured at a number of different moisture contents. The measuring procedure and fitting of the measurements are explained in detail in appendix D.

Material	c_{therm} $\left[\frac{J}{\mathrm{m}^3\cdot\mathrm{K}}\right]$	ρ_{therm} $\left[\frac{\mathrm{K}\cdot\mathrm{m}}{\mathrm{W}}\right]$
Aluminium	$2.5 \cdot 10^{6}$*	0**
XLPE	$2.40 \cdot 10^{6}$ ***	2.8***
Lead	$1.45 \cdot 10^{6}$*	0**
PE	$2.40 \cdot 10^{6}$ ****	2.8****

* Standardised numbers listed in [33].
** The thermal resistivity of metals is several orders of magnitude lower than for most other materials and thus the thermal resistance is assumed negligible.
*** Quantities obtained through experiments. Procedure is explained in appendix D.
**** The jacket material is assumed to have thermal properties identical to the insulation.

Table 4.5: Material specifications of the cable used in the experimental study for verification of the thermal models.

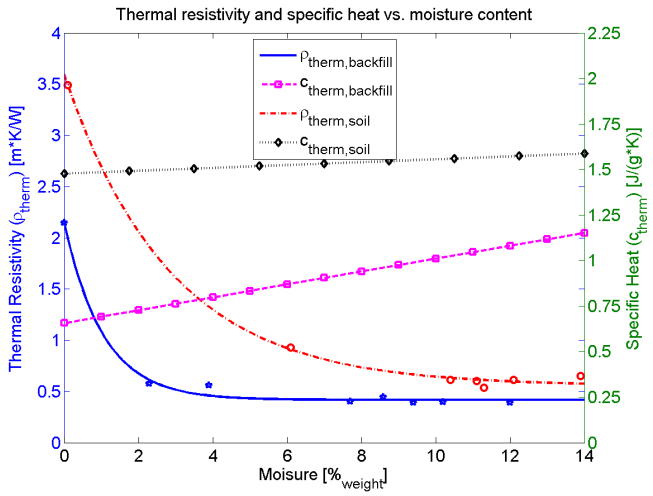

Figure 4.13: Experimentally determined thermal resistivity and specific heat as a function of the moisture content for the two materials surrounding the cables in the experiment. The moisture content is measured in percentage of the total sample weight. Details about measurement procedures, fitting, etc. is found in appendix D.3.

4.2.7 Thermal Modelling of Experimental Setup

There are basically three different ways in which the thermal evolution of the experimental setup can be modelled with the measurements available. Firstly it is possible to model the temperature assuming that all thermal

parameters are static. Secondly it is possible to model the temperature by adjusting the surrounding conditions to the measured moisture content. Finally it is possible to utilise the temperature measurements to compare with the modelled temperature data.

Each of the models, having their individual strengths, are described in the following clauses.

4.2.7.1 Static Thermal Parameters

Dynamic conditions, such as moisture migration, are neglected in this method. This means that the thermal resistivity and specific heat of the cable surroundings is assumed constant throughout the modelling period. The benefits of this methodology is that it only takes the current as input, and is therefore independent of other measurements. This method is typically necessary for older cable system where temperature measurements are not obtained. Furthermore if the measurement system fails, it is necessary to have a backup solution, and the static thermal parameters model is well suited for this.

4.2.7.2 Moisture Dependent Thermal Parameters

When measuring the moisture content of the cable surroundings, it is possible to determine the thermal properties of the material in real time. Having determined the thermal resistivity and specific heat, of the material surrounding the cables, as a function of the moisture content before installation, it is possible from measurements of the moisture content to directly obtain the necessary thermal parameters for a presumably more accurate modelling.
The moisture content is taken as an input to the model, which converts it to specific heat and thermal resistivity through the relation in figure 4.13. These quantities are inserted in equations (3.40) and (3.41) and the system matrix, eigen values, eigen vectors, etc. are reevaluated for the new moisture content, where after the temperature evolution can be calculated.

4.2.7.3 Thermal Parameters Dependent on Temperature Feedback

Having direct measurements of the temperature within the cables trench will allow for comparing the accuracy of the model. In the case that deviations between measured and modelled temperature arise, it must be assumed that the external thermal parameters used in the model are wrong due to a chang-

ing moisture content. It is suggests to utilise the temperature measurements in the following way; if the modelled temperature at 12:00 is equal to the measured, then it is assumed that the thermal parameters before 12:00 are modelled correct. If then the modelled temperature at 18:00 differs from the measured, then the thermal properties of the surrounding material must have changed since 12:00, and the period from 12:00-18:00 is re-modelled with adapted specific heat and thermal resistivity. This re-modelling process by updating the thermal parameters is performed until the modelled temperature is within an acceptable tolerance of the measured. Due to the fact that DTS systems typically have an accuracy of 1 °C, [85], it was decided that the present study accepts deviations between measurements and models of ±1 °C. This means that the thermal parameters will only be updated and the temperature re-modelled if the difference between modelled and measured temperature exceeds 1 °C.

A normal cable trench is only equipped with temperature monitoring in one place, e.g. in the pipe next to the centre phase. This excludes knowledge about the spatial distribution of the thermal parameters over the cross section of the cable trench, and the present project therefore has, as a basic case, assumed that the entire cross-section of the sand envelope has a uniform moisture content and the entire cross-section of the surrounding soil has a uniform moisture content. As seen in figure 4.12, the moisture contents of the sand and soil are though not necessarily equal, so knowledge about the relation between the two moisture contents is required.
Figure 4.14 shows the measured real time soil-to-sand moisture content (M_{weight}) ratio and the average value ($R_{M/M} = 2.24$) of this ratio. It is seen that the ratio varies around the average and significant deviations are brief. It is thus in this project assumed that the moisture content of the soil can be given as 2.24 times the moisture content of the sand[3]. It is acknowledged that the real time $R_{M/M}$ seems to have a slightly increasing tendency, however this is attributed to the fact that the experiment was performed inside and it is assumed that an equilibrium state will be obtained for cable trenches in the real transmission system.

The thermal properties of the soil and sand for the model, are determined by inserting the moisture contents into figure 4.13 and obtaining the four necessary parameters.

It is stressed that the inclusion of a varying specific heat in the analysis of power cable temperatures has not been seen before to the extend proposed here. [62] adapts both the thermal resistance and capacitance of their model as a function of time, but this adaption is not related to actual physical

[3]It should be acknowledged that this ratio is dependent on soil and sand material properties, as well as the ratio may be site specific. An experimental evaluation of the ratio is thus necessary for each specific cable installation.

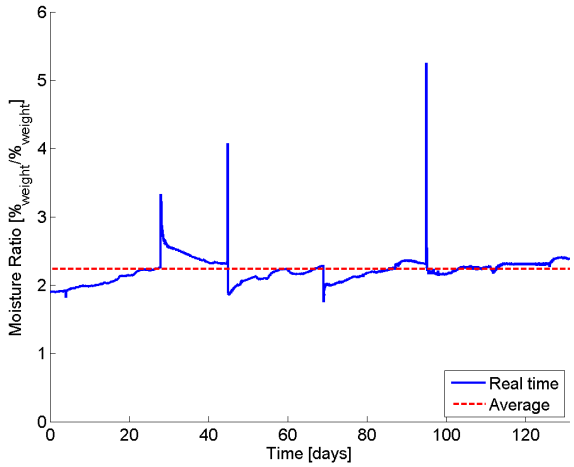

Figure 4.14: Relation between moisture content in the sand and soil as a function of time. Even though the moisture contents vary fairly much over time, it is seen that the ratio between the two is fairly constant (average 2.24) over the four months of testing.

changes which arises due to moisture content variations. Instead [62] defines a set of boundary conditions for the thermal resistance and capacitance[4] and guesses, via a generic algorithm, on the appropriate values for the thermal parameters.

4.2.8 Temperature Results

This clause presents the thermal modelling of the experimental setup over the four months load profile. The three different approaches to thermal modelling are applied and a discussion of the results can be found at the end.

4.2.8.1 Static Thermal Parameters

In case of utilising static parameters for dynamic thermal rating of power cables, it is obvious that the choice of appropriate values for the material properties is important. There may be different approaches to choose the thermal properties of the surroundings. Firstly, IEC has made suggestions which are given in [30] to different quantities for the thermal resistivity under varying conditions, where the resistivity ranges from 0.5 $^{\mathrm{K\cdot m}}/_{\mathrm{W}}$ to 3 $^{\mathrm{K\cdot m}}/_{\mathrm{W}}$.

[4] It is important to noticed that the thermal resistance and capacitance are geometry dependent quantities, which the thermal resistivity and specific heat is not.

These quantities may be seen as relatively arbitrary as they are not related to the specific materials used. Secondly, it is possible to measure the thermal resistivity prior to commissioning of the cable. This procedure means that it is quantities of the actual materials (for the given moisture contents) which are used in the thermal models. However the moisture content in a sample taken in a sand pit may be very different from the moisture content the sand will have in a cable trench as well as the compaction of the sand may be different. Thus the measured values might not be representative when installed in a cable trench.

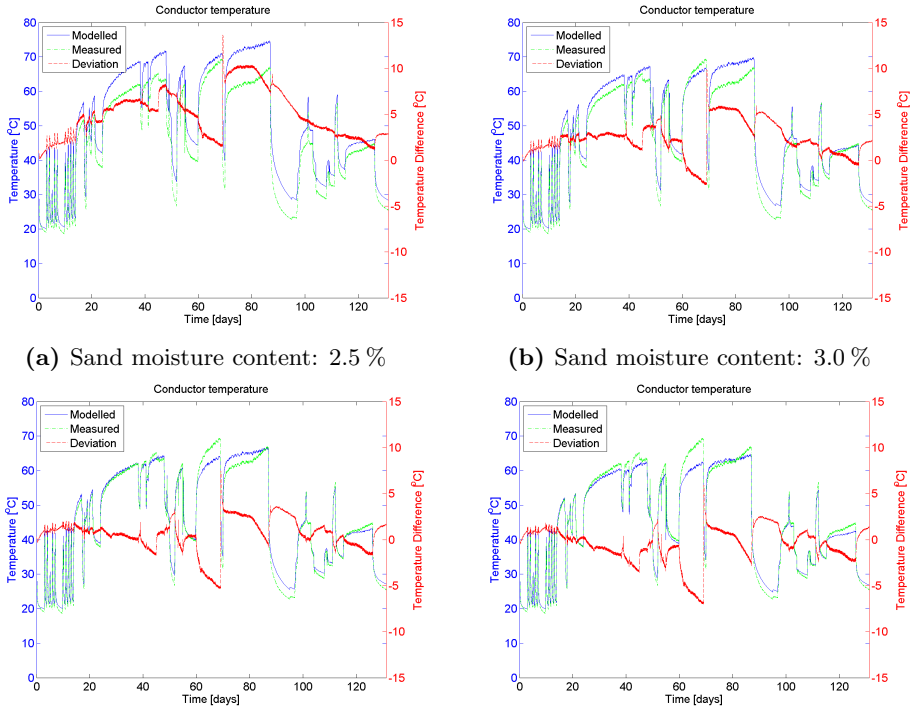

(a) Sand moisture content: 2.5 %

(b) Sand moisture content: 3.0 %

(c) Sand moisture content: 3.5 %

(d) Sand moisture content: 4.0 %

Figure 4.15: Results of TEE conductor temperature modelling, using static sand and soil moisture contents, compared to measured values. It is seen that the model deviates from the measurements in all cases. Using a sand moisture content of 2.5 % will ensure that the model is always on the safe side of the measurements, however this results in under estimating the loadability of the cable for the majority of the time.

Figure 4.15 shows the measured and modelled temperature over the four months of testing. The moisture content of the sand and soil is assumed to be constant throughout the test and figure 4.15 shows the measured conductor temperature compared to the modelled for a number of different moisture contents. It is assumed that the moisture content of the soil is 2.24 times the moisture content of the sand.

It is clearly seen from figure 4.15 that the thermal model has difficulties in producing accurate results when assuming static external thermal conditions.
The consequence must be to choose a conservatively low moisture content, in order to be sure that the modelled temperature is never lower than the one which could be measured. For the specific four months of data it is seen that this static moisture content for the sand should be 2.5 $\%_{weight}$ in order for the modelled temperature to always be on the safe side.

4.2.8.2 Moisture Dependent Thermal Parameters

Assuming that moisture content measurements are only available from one site in the cross section of the cable trench, it is necessary to make the assumption that moisture content in the sand is homogeneous and the moisture content in the soil is homogeneous. Having real time moisture content measurements obviously enables a dynamic adaption of the external thermal conditions and the results are seen in figure 4.16.

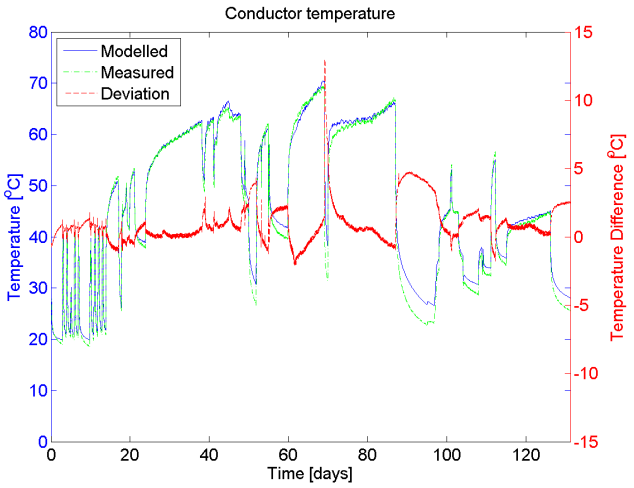

Figure 4.16: Results of modelling the conductor temperature of the experimental setup with the TEE method, compared to measured values, when adapting the thermal properties of the surroundings based on measurements of the moisture content in the sand. Accuracy of the model is seen to be far better than when modelling with static thermal properties.

The results of figure 4.16 shows better accuracy than the static parameters model when comparing over the entire four months testing period, however deviations between model and measurements are seen to occur. As stated, these deviations may be related to the fact that the moisture content is as-

sumed homogeneous, but as discussed later in this chapter, other parameters may have an equal influence on the accuracy of the model.

4.2.8.3 Thermal Parameters Dependent on Temperature Feedback

As mentioned, measuring the temperature enables a direct assessment of the accuracy of the thermal model. The temperature measurements within the fibre pipe have been used in this study, as it is such a temperature which will be available when the methodology is to be implemented in the Danish transmission system.

Under normal conditions, it is expected that the thermal parameters are only slowly varying. It may therefore be sufficient to perform a check of the modelled temperature four times each day. However during high loads, where the jacket temperature may exceed the 50 °C limit, the moisture could be expected to migrate away fast, and under high load conditions (e.g. above 0.7 pu) it may thus be reasonable to check if the modelled temperature is sufficiently accurate once every hour. Precipitation can cause an almost instant increase in the moisture content, but as seen in figure 4.12, the moisture content of the sand does not exceed 8 $\%_{weight}$, and a limit for the upper moisture content allowed in the model can thus be implemented without loosing validity.
The fact that the temperature is measured inside an air filled pipe laid next to centre phase can constitute a modelling issue as the pipe and the air inside are not necessarily an inherent part of the thermal model. Because the air in the pipe is a fluid it may be assumed that the temperature inside the pipe is homogeneous and the temperature measuring point in the pipe may thus have a different temperature than the temperature in the sand in an equal distance from the cable. Especially during sudden load increases, this may lead to deviations between measurements and model, causing the model to attempting to decrease the moisture content unrealistically fast. In order to prevent such an unrealistic moisture decrease, the present study has introduced a limit in the rate of decrease in the moisture content to $\frac{\mathrm{d}M_{weight}}{\mathrm{d}t} \leq 1 \frac{\%_{weight}}{\mathrm{h}}$, for further detail see appendix B.2.1. This also ensures that single errors in the measurements do not affect the model drastically.

The described temperature checks have been implemented in the methodology and the result of the four months load cycle is seen in figure 4.17.

It is noticed that the modelled conductor temperature is within ±2 °C of the measured for most of the time, and this accuracy is better than what the static and the moisture dependent methods were capable of delivering.

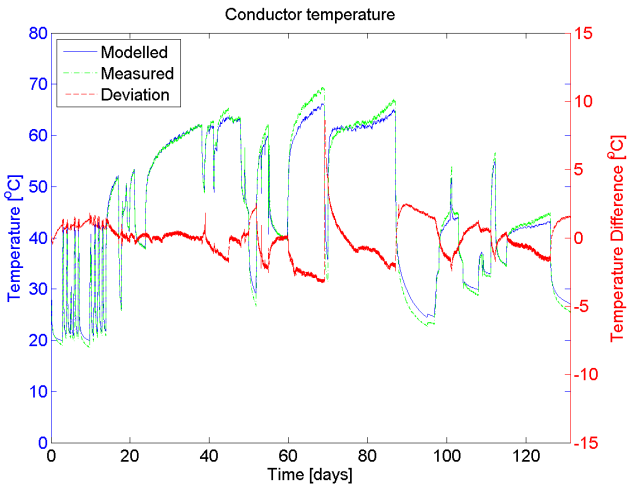

Figure 4.17: Results of conductor temperature modelling, compared to measured values, with implemented feedback from temperature measurements obtained by the fibre in the pipe installed next to the centre phase. The accuracy is seen to be even better than when moisture measurements are utilised.

4.2.8.4 Heavy Precipitation

As stated, comparing the three methods of modelling, will rank the temperature feedback method as the most accurate, followed by the moisture content and lastly the static parameters methods.
Figures 4.15, 4.16 and 4.17, show that all three modelling methods have difficulties in following the measured decreasing temperature which is experienced at approximately day 69, resulting in inaccuracies in the range of 10-15 °C. This implies that there are parameters which have yet to be accounted for.

Figure 4.18 shows where the problem arises. The figure shows the measured and modelled fibre temperature when modelling with temperature feedback for the two days around the major modelled deviation.

In the temperature feedback modelling 'mode' the modelled temperature was required to be within 1 °C of the measured or otherwise the thermal properties of the surroundings should be adapted until the modelled fibre temperature was acceptable. However as seen in figure 4.18, the model is not capable of following the measured temperature decrease at day 69 even when the sand moisture content is lowered to 8 $\%_{weight}$. This means, that even though the moisture content has been adapted to the upper limit, the model is still inaccurate, and other parameters than the specific heat and thermal resistivity must be taken into account.

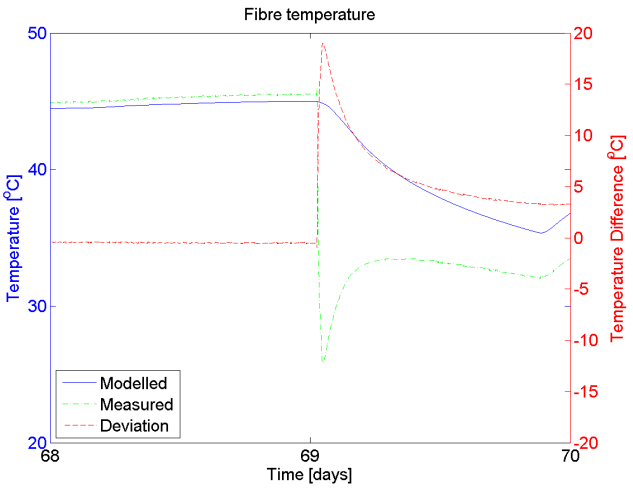

Figure 4.18: Measured and modelled temperature inside the fibre pipe. Focus around the 69th day the experiment where the model is seen to deviate significantly from the measurements. The deviation is caused by heavy precipitation which causes an instant temperature decrease in the fibre pipe.

By analysing the measured moisture content of figure 4.12 at approximately day 69, it becomes clear that the moisture contents peak almost at the exact same time as the temperature begins to decrease in figure 4.18. This results in two things. Firstly, as already mentioned, the thermal resistivity and specific heat changes, but secondly a large amount of water runs down through the soil and sand, and causes an instantaneous temperature decrease of the fibre pipe and cable, see also the publication written as art of this PhD project enclosed in appendix F.2, [70]. Such a temperature decrease cannot be implemented in an algorithm as a simple heat sink because it is instantaneous, and it is therefore necessary to simply lower the modelled temperature until it is within the accepted accuracy of the measured. It should be acknowledged that heavy precipitation implies that the sand and soil will be saturated with water, and the model will thus try to adapt the moisture content until the upper limit before direct lowering of the temperature is enforced.
At the end of the described temperature decrease a slight increase in the measured temperature is seen, even though no losses are experienced in the cable. It must thus be concluded that the large amount of water, which caused the instantaneous temperature decrease, has passed by the cables so fast that the surroundings were unable to release all the internally stored energy, and the temperature of the fibre reflects this increase. In such situations it may be required to add some of the previously subtracted temperature.

A sketch of the development in the soil subjected to heavy precipitation is seen in figure 4.19.

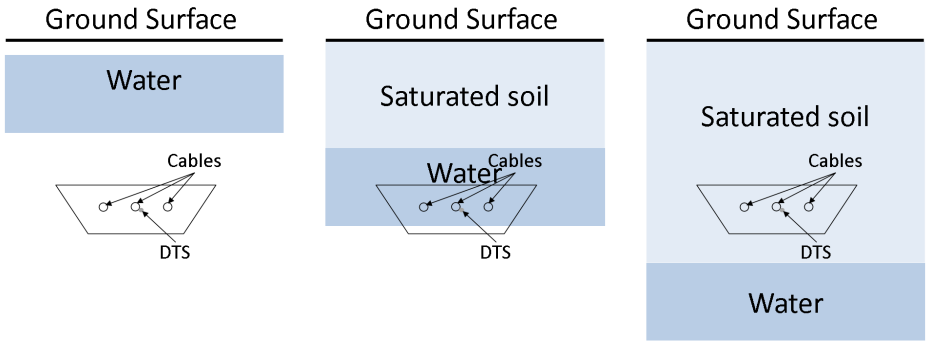

(a) Beginning of precipitation. **(b)** During precipitation. **(c)** After precipitation.

Figure 4.19: Development of the water flow during heavy precipitation. A wave of water is seen to flow down through the soil causing an instantaneous temperature decrease in the fibre pipe.

By implementing these conditions in the temperature feedback mode, the resulting modelled conductor temperature develops as shown in figure 4.20.

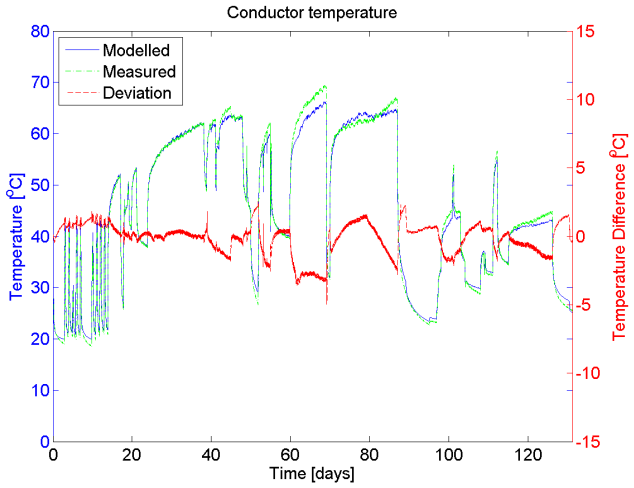

Figure 4.20: Modelled conductor temperature in the experimental setup when correcting for heavy precipitation, compared to measured values. It is seen that the modelled conductor temperature is within $\pm 2\,^{\circ}\mathrm{C}$ of the measured for far the majority of the four months testing period.

The figure clearly shows that the model, including the necessary adaptions, is very accurate for modelling the conductor temperature even when the temperature feedback is obtained by a fibre in a pipe.

It is emphasised that the implementation of heavy precipitation in thermal modelling is a novelty which have not been considered in any previous studies.

4.2.8.5 Thermal Parameters Dependent on Screen Temperature Feedback

In the case that the temperature is measured at the screen, the thermal modelling of the temperature becomes even more accurate as seen in figure 4.21.

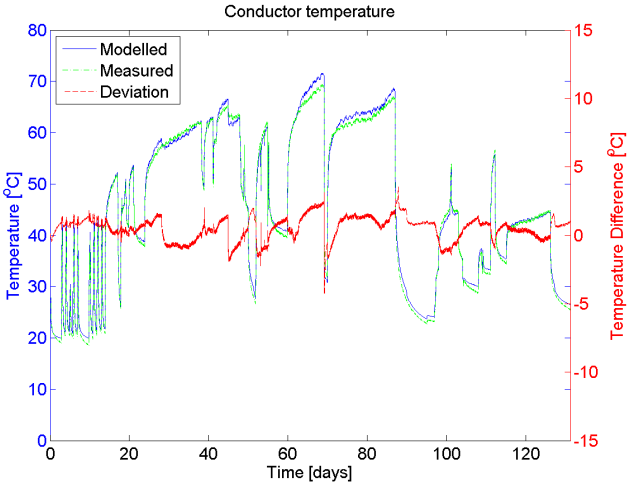

Figure 4.21: Results of modelling the conductor temperature in the experimental setup when utilising measurements of the screen temperature as a feedback for the simulations, compared to the measured conductor temperature. The conductor temperature is seen to be modelled slightly more accurate than when using measurements of the fibre pipe temperature as feedback. Measurements of the screen temperature will though not be available for cables in the Danish grid.

These measurements are possible to perform on cables in operation, but as explained in appendix B the measurements will not be available from the Danish transmission system due to higher costs and increased possibility of mechanical failure of the fibre.

4.2.9 Thermal Resistivity

In order to evaluate the validity and applicability of the discussed results, it is useful to compare the modelled resistivity and the resistivity which can be directly extracted from the experiment via the moisture content sensors.

Figure 4.22 shows that the modelling procedure allows for the modelled thermal resistivity to follow fairly well the measured value. It should be

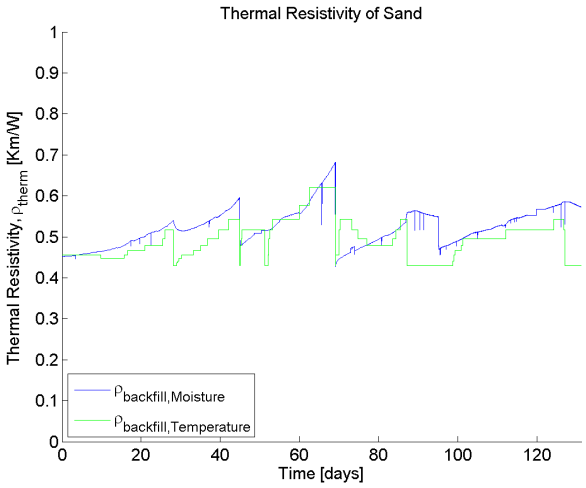

Figure 4.22: Comparison of the modelled and measured thermal resistivity in the sand of the experimental setup. The thermal resistivity obtained by modelling the temperature, with a screen temperature feedback, is seen to follow fairly well the thermal resistivity which is obtained via the moisture content sensors and figure 4.13.

acknowledged that the modelled thermal resistivity evolves with only few changes over the four months of modelling, even during significant load changes. This means that the model is reliable also for predicting the future evolution of the temperature and trustworthy loadability values can thus be evaluated and displayed to the cables operator.

4.2.10 Loadability of Power Cables

For the experimental setup the steady state loadability as well as dynamic loadability (i.e. the algorithm of figure 3.5) have been calculated at midnight on day 69 and midnight on day 70, where the thermal limit has been defined as 90 °C on the conductor. The "Loadability vs. Time" curves are shown in figure 4.23.
It is seen that the steady state loadability increases slightly due to the lower thermal resistivity observed after the heavy precipitation. The load which it is possible to apply for the coming hours though increases significantly, as this dynamic loadability both takes into account the lower thermal resistivity, the higher specific heat and the lower initial temperature.

It should be noted that the loadability levels of figure 4.23 are evaluated with no dielectric losses, such as is the case in the experimental setup, and

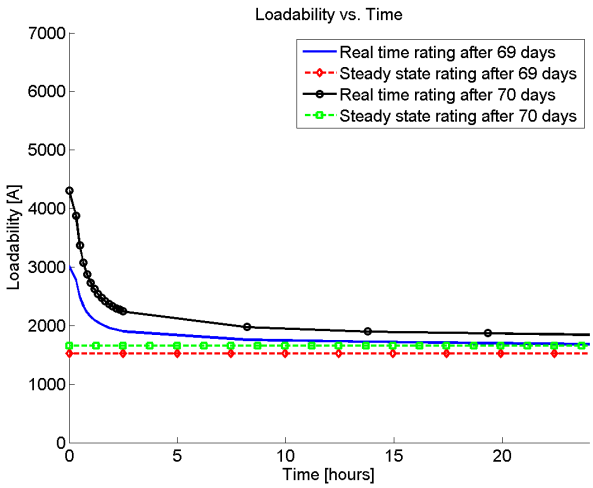

Figure 4.23: Steady state and real time rating at midnight of the 69th and 70th day. It is seen that the steady state loadability increases slightly due to decreased thermal resistivity after the heavy precipitation. Furthermore the real time loadability increases to a greater extend because it takes into account both the decreased thermal resistivity and the lower initial temperature.

the loadability levels might therefore seem high. Including dielectric losses in the evaluation of the loadability levels is though, as previously described, not a limitation in the modelling procedure.

Note furthermore that the developed algorithm takes the increased resistivity of the conductor into account, and thus gives a more accurate estimation of the dynamic loadability.

4.3 Hotspot Location

As previously discussed, the thermal properties of the cable surroundings are not only time dependent but also dependent on the site. A long cable line of several tens of kilometres may pass through different thermal environments and it can thus be difficult to setup a thermal model which covers the entire cable. It should though be remembered that it in general is only necessary to model the hottest spot of the cable as this will be the bottleneck for the line.
Setting up a trustworthy thermal model for the cable therefore requires locating the hotspot which can be done in at least two different ways. Firstly, it is possible to measure the thermal conditions along the cable route before installation, and secondly, DTS measurements, which allows for direct mea-

surement of the hotspot location.
When utilising the first of these methods it must be assumed that the thermal properties do not vary with time and that the hotspot location therefore does not change.
The second of the methods, the DTS monitoring of the system, gives information about the hotspot location and how the thermal properties develop with time. This also means that DTS provides full awareness in cases where the hotspot location changes with time.

It is on this background recognised that the thermal model for DTS monitored cables will be more accurate and trustworthy than for other systems as both the location of, and the thermal properties at, the hotspot can be followed in real time.
It may thus be seen as problematic when transmission cables are not equipped with DTS systems as the hotspot cannot be followed. However it should be recognised that defining properly conservative values, for the model which uses static thermal properties, may enhance cable utilisation without jeopardising reliability when comparing to the steady state loadability calculations. The use of single point temperature measurements will not enable the possibility of determining if a hotspot location changes with time, however they may increase awareness about the general thermal state of the system which can also be beneficial for the TSO. Furthermore, if the temperature sensors have been installed at locations which have been pointed out by experts to be possible hotspots, the safety margin on the thermal modelling may be decreased and single point temperature monitoring is therefore better than no monitoring.

4.4 Soil Temperature Modelling

As stated, thermal modelling of power cables is performed by calculating the thermal response to the load profile, and adding this to the native soil temperature at cable burial depth. This section is dedicated to evaluating the accuracy of the thermal models in order to assess if measurements of the native soil temperature are necessary in the future Danish cable based transmission system, or if the soil temperature can be modelled with sufficient accuracy.

As discussed in clause 3.7.1, a number of different methods are available for modelling the ambient temperature at cable depth. In order to be certain to always have a methodology which can make an estimate of the soil temperature without being dependent on many input parameters, this study has chosen to utilise the best of [71] and [72] respectively.
[72] takes, as stated, only measurements of the above ground temperature

as input. The above ground temperature is easily measurable and data is even available for uncountably many weather stations around the globe. It is thus assumed that such data is always available and the soil temperature model can therefore take this as input.
[71] divides the soil into horizontal planes, each having a thermal resistance and thermal capacitance, which are calculated as given in equations (4.1) and (4.2) respectively.

$$T_{ground,v} = \rho_{therm,soil} \cdot (x_v - x_{v-1}) \tag{4.1}$$
$$C_{ground,v} = c_{therm,soil} \cdot (x_v - x_{v-1}) \tag{4.2}$$
$$v = 1, 2, ..., w$$

where v is the layer number increasing from ground surface and down, w is the total number of layers, x_v is the depth to bottom of layer v and $x_0 = 0$.
When the temperature at ground surface varies, the temperature throughout the layers in the soil changes with a time lag. Varying the ground surface temperature, and utilising the method for solving differential equations of clause 3.6.2, enables an easy estimation of the temperature throughout the soil.
By performing the modelling in this way it must be assumed that the temperature deep in the ground is constant throughout the year. In [71] the temperature is assumed constant in a depth of 7 metres, however in [72] measurements show that the temperature may vary up to 3 °C over the year in a depth of 9 metres. Based on these differences the present study has assumed that the temperature remains constant in depth of 15 metres.
Comparing the results of the TEE methodology with the data of [72], shows that the method is capable of estimating the temperature at a depth of 1 metre with equal accuracy as the model given in equation (3.43)[5]. However equation (3.43) requires the soil temperature to follow a sine curve throughout the year in order to be accurate, where the TEE method can take any temperature shape as input. This means that equation (3.43) will make inaccurate estimations during irregular weather patterns, resulting in possible under utilisation of the cables during long/cold winters and overheating during long/hot summers. As stated this is not a problem when using the TEE methodology as the actual real time measured air temperature is used as input.
The deviations which are experienced between measurements and model are attributed to the fact that only the air temperature is used for modelling, why parameters such as convection, solar radiation and long wave radiation are not included in the analysis. In order to improve accuracy of the model, these parameters are suggested to be measured and utilised according to the procedure suggested in [71].

[5] In this study, the measurements from Argonne, Illinois [72], has been used for showing the accuracy of the model.

Because the accuracy of the model is within ±3 °C at a burial depth of 1 metre, it is concluded that the TEE model is sufficiently accurate to be utilised in cases where measurements of the temperature in cable depth are not available.

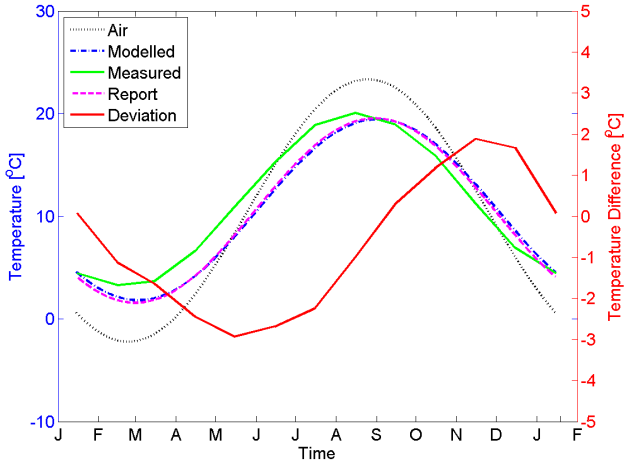

Figure 4.24: Native soil temperature in a depth of 1 metre according to simulations based on thermoelectric equivalents and the method of (3.43). The TEE-model is seen to be just as accurate as the one given in [72] (in the figure denoted 'Report'), however it enables the use of the actual weather conditions where [72] can only make predictions based on historical monthly averages. The deviation between TEE-model and measurements is seen to be within ±3 °C over the entire year.

4.5 Discussion of Thermal Modelling of Power Cables

This chapter has compared and discussed different methods for modelling the thermal evolution of power cables. It was shown that the step response (SR) method, finite element method (FEM) and thermoelectric equivalent (TEE) method provides similar results, but with significant differences in the required computational time. The FEM is the slowest of the three, followed by SR and with the TEE methods as the fastest. Furthermore, the TEE method is easier to comprehend which is a strong argument if the tool is to be implemented at transmission system operators.
As the results from the three modelling methods were similar, the TEE was chosen as the method to be used for the remaining of this thesis.

It was, through application of a laboratory experiment, shown in this chap-

ter that TEEs can model the thermal behaviour of real power cables with an accuracy of approximately $\pm 2\,^{o}$C, and that the thermal modelling can be performed in different ways.
Firstly the thermal analysis can be performed by assuming the surrounding conditions to be static. Using static values for the external thermal resistivity and specific heat was shown to result in deviations between modelled and measured conductor temperature.
Secondly, in order to improve the method, the temperature of the cables were modelled by adapting the thermal properties according to the measured moisture content of the sand, this resulted in greater accuracy of the modelled temperature.
Finally measured temperatures were utilised as a feedback mechanisms to the model. If the modelled temperature deviates more than $\pm\,1^{o}$C from the measured, it is assumed that the moisture content of the surrounding material must have changed. The model adapts the moisture content, and thus also the specific heat and thermal resistivity, and reevaluates the temperature. This adaption is performed until the modelled temperature is within the acceptable $\pm 1\,^{o}$C of the measured. This feedback method results in the most accurate estimation of the conductor temperature. The temperature feedback has in this chapter been the screen temperature and the temperature measured in a fibre laid next to the centre phase, where the most accurate model was obtained with the screen temperature because it is measured closer to the conductor.

Based on this discussion of the different approaches the following must be concluded.
In order to obtain the most reliable and accurate temperature estimations of power cables, measuring the temperature inside, or close to, the cable is required. However in case of breakdown of the temperature measuring equipment, and for older cable systems without temperature measurements installed, it is required to have a model which is independent of measured temperature data. This model can e.g. be the static parameters method or it may be possible to assume that the soil zones which have a modelled temperature higher than $60\,^{o}$C, are dried out, and the zones below $60\,^{o}$C are moist. This means that one will obtain a quasi dynamic development of the thermal surroundings which may be more accurate than a model with simple static thermal parameters.
The moisture dependent parameters model may be of limited use in real transmission systems as the measuring equipment is expensive and only single point measurements are possible. However in the academic perspective the moisture dependent parameters model is very interesting as it is shown that the measurements increases accuracy significantly when compared to the static parameters model.

The final part of this chapter discussed the modelling of the native ground

temperature at cable burial depth and it was found that the TEE methodology allows for modelling the native ground temperature at cable burial depth with an accuracy of $\pm 3\,^{\circ}\mathrm{C}$ when comparing to measurements. This means that the modelled ground temperature can be used for cable systems where measurements are not available.

PART III

Electrothermal Coordination for Cable Based Transmission Systems - Developing the Concept

---

Loadability of power systems has traditionally been addressed only on component level with limited discussion about the impact of, and on, the rest of the transmission system. This means that transformers, cables, overhead lines, etc. are each dimensioned individually in order to fulfil the requirements given by the grid designer. Once the design criteria for the grid has been determined, the components are considered as individuals and the benefits which may be gained because they are a part of a grid can be lost.
This part of the thesis will aim at defining the loadability of transmission systems when including the grid in the analysis.
As shown in part II all components in the grid have their individual limitations and are exposed to different environments. Loadability calculations of transmission systems should therefore be based on the physics of the individual components.

On this background an extensive investigation is performed on how loadability calculations of cables can be combined with knowledge of the grid topology and behaviour for optimising the utilisation and performance of the transmission system.

Chapter 5

Defining Loadability of Transmission Systems

Having discussed loadability of individual transmission cables, with its inherent point-to-point focus, the present chapter will widen the perspective and discuss state of the art research within loadability of transmission systems.

The first issue to address in this matter is what loadability of a cable based transmission system means. Is it the sum of the loadabilities of all lines in the grid? Is it the average, minimum or maximum of the lines? Or is it something completely different?

The present study has used the latter option to define loadability of a transmission system. It is not a single value that can be easily given, neither is it a simple dynamic variable which changes with time. Instead the present study uses the following definition:

> *Loadability of electric power systems is a concept which enables utilisation of the synergies, related to loadability, that arise when having more than one power line in the system.*

It is seen that the above definition is very broad and that many different research activities could fit within it's boundaries. The following sections discusses such recent research activities.

5.1 Load Flow Studies

Some of the most basic tools for analysing the behaviour of power systems are the load flow algorithms. Load flow studies take as input the electrical parameters of the components in the system, the site and amount of generated power and the site and amount of consumed power. The result of a load flow calculation is, on this background, how the power (active and reactive) is distributed in the different transmission lines, bus voltage levels, etc.

Throughout the years, a number of different methodologies for solving the load flow problem have been developed, each having their own strengths and weaknesses. Among the most common are the Gauss-Seidel, Newton-Raphson and Fast Decoupled, [86–88].
Load flow studies of transmission grids are commonly solved by assuming completely balanced AC systems, however for fast solutions or when requiring the solution of many different system configurations, approximating the AC load flow with a DC approach has been proven sufficiently accurate for many applications. Results of DC load flow studies should though be used with caution due to the assumptions made, [89, 90].

For load flow studies, a substantial amount of different software is commercially available. However literature such as [88] also describes in greater detail different algorithms ready for implementation in order for the user to create a customised tool.
In depth analysis and development of load flow algorithms has not been a topic of major concern in the present PhD project as reliable and fast tools are already available. The remaining of this thesis will thus rely on thoroughly proven numerical load flow algorithms.

5.2 Optimal Power Flow

Another very common topic found when searching for literature dealing with loadability of transmission systems is "Optimal Power Flow" (OPF). OPF deals with optimising the configuration of power systems, such that the operation of the entire system becomes as optimal as possible, [91]. The operation of a transmission system can be optimised according to a number of parameters such as economic issues, congestion management, location of Flexible AC Transmission System (FACTS) devices, etc., [92].
In the daily operation of transmission systems, economy is the most commonly discussed objective function to be optimised, whereas location of FACTS devices may be investigated more by grid planners.

Performing for instance economic optimisation of a power system requires the optimisation of a significant amount of variables, including:

- Active power generation
- Reactive power generation/consumption
- Transmission losses

And all of this optimisation must be done while keeping all variables within the appropriate limits, including:

- Bus voltage limits
- Transmission line power limits
- Generation unit limitations

The result of such an optimisation is a suggestion to the optimal, steady state, system operating point.
Taking as example the optimisation of transmission losses (P_L), the objective function would look as (5.1), [91].

$$\min\left(P_L\right) = \min\left(\sum P_{L,k}\right) \tag{5.1}$$

where $P_{L,k}$ are the losses in component k.
It is seen from (5.1) that the optimal solution requires finding the minimum possible value of the total transmission loss function P_L.
In order to ensure an acceptable operation of the transmission system, the solution to (5.1) is subjected to some equality constraints, such as power conservation (5.2), and some inequality constraints, such as operational space for bus voltages (5.3), [91].

$$\sum P_{G,i} - \sum P_{D,i} - P_L = 0 \tag{5.2}$$

$$U_{i,min} \leq U_i \leq U_{i,max} \tag{5.3}$$

where $P_{G,i}$ is the generated power, $P_{D,i}$ is the demanded power and U_i is the voltage at bus i respectively.
It should be noticed that (5.2) and (5.3) are only excerpts of the total constraints and a significant amount of similar equations (such as loadability limits for the individual lines) have to be set up in order to obtain valid solutions. For in depth descriptions the reader is referred to literature dedicated to OPF studies, [91–94].

Considerations about the dynamic behaviour of power system components may be included in the analysis i.e. as limitations for the generating units. Such dynamic behaviour is included in the restrictions for the allowed operational state space of the system and, almost exclusively, dynamic limitations are concerned with voltage stability of generating units. In reality the dynamic limitations are implemented in the optimisation studies as narrower limitations of the static operational space of the individual generating units, [95, 96], and thus the dynamic aspect of OPF may appear as being static.

The backbone of OPF algorithms are the load flow calculations, [87]. Depending on the chosen optimisation algorithm, OPF firstly defines a transmission system scenario. Secondly, a load flow calculation is performed on the specified transmission system scenario. Thirdly, the result of the load flow is evaluated, i.e. it is determined if all limitations are respected for the given scenario. Thereafter a new scenario is defined. Having performed a sufficient amount of transmission system scenarios OPF determines which is the most optimal.

OPF has been a topic of interest since the 1960's, and now most OPF-research is concerned with optimisation of algorithms to enhance the computational time. Traditionally, conventional optimisation tools have been applied to OPF such as Linear Programming (LP), Newton-Raphson (NR) methods, etc., however modern OPF software utilise "intelligent" algorithms such Artificial Neural Networks (ANN), Genetic Algorithm (GA) and Fuzzy Logic (FL), [91, 92]. An in depth description of these tools is outside the scope of the present study and the reader is thus referred to the excessive amount of literature concerned with OPF.

Benefits obtained by implementing OPF in real power systems is also of increased interest to the researching community. A number of studies are concerned with implementing different algorithms on subsets of large power systems, [97, 98].
Reference [97] shows a methodology for implementing OPF in the grid of British Columbia, Canada. The OPF is to suggest control action that the operator can perform in order to make the transmission system more reliable. Similarly, [98] utilises OPF as the tool for making decisions in smart grids. The concept is proven applicable to real distribution systems by studying a case from Argentina.

It should on this background be recognised that OPF solutions are thoroughly investigated and conceived by many researchers as the path forward for optimising the utilisation of transmission systems.

5.3 Total Transmission Capability

The term Total Transmission Capability (TTC) covers the evaluation of the active power which it is possible to transfer from one area to another, where the areas can be different power markets, distribution systems, sub transmission systems, nodes, etc, [99].

Instead of TTC, much research is concerned with evaluating how much power it is possible to send into the system on top of the real time scenario, i.e. the Available Transmission Capability (ATC), [99–102]. ATC is defined as shown in (5.4).

$$\text{ATC} = \text{TTC-TRM-Existing Transmission Commitments} \tag{5.4}$$

where TRM is the Transfer Reliability Margin which is the quantity allowing e.g. for small variations in generation patterns etc. Existing transmission commitments is the amount of transfer capacity which has already been sold on the market, e.g. for regulation purposes etc.

When transporting power from Area A to D via Area B and C, the ATC is the maximum amount of extra power which can be transported from Area A to D without any limits (including thermal, voltage and stability limits) of any component being violated, [99].

The evaluation of ATC thus requires a definition of the interacting areas, as well as the physical limitations of the individual components.

ATC is sometimes discussed in a dynamic perspective. Similar to OPF, dynamic ATC is evaluated by frequently updating the static limits for the power transfer (e.g. the loadability values of overhead lines), [103], and thus the dynamic aspect of ATC seems to disappear.

5.4 Electrothermal Coordination

A novel concept within loadability of transmission systems, only discussed in a sparse number of publication, is denoted Electrothermal Coordination (ETC).
ETC, which was introduced in [104, 105] in 2005, is concerned with optimising transmission systems similarly to OPF, but with the addition of including the dynamic loadability of transmission lines.
In the OPF studies, the dynamic loadability of transmission lines would substitute the static loadability limits of OPF by (5.5).

$$\theta(t) \leq \theta_{max} \tag{5.5}$$

where the time dependent temperature $\theta(t)$ is evaluated via the heat balance equations and θ_{max} is the maximum allowable operating temperature for the power line.
In order to enable implementation of these thermal limits in OPF studies, [104] suggests a number of simplifications. This means e.g. that heat dissipated by convection and radiation is assumed to be linear with the temperature and that the temperature develops over time in discretized steps.

References [104, 105] only discuss dynamic loadability of overhead transmission lines as it is argued that these are the most common causes for congestion of transmission systems, and a higher utilisation of overhead lines will thus increase efficiency of the entire transmission system in general.
This hypothesis is maintained also in studies such as presented in [106, 107], and it is proven that significant economic benefits can be obtained if utilising ETC.

Reference [104] defines ETC as a method enabling the optimal utilisation of the thermal inertia of power lines on the day-ahead market. This means that ETC is an enhanced OPF methodology wherein the thermal limits are included in a true dynamic way.
Based on expectations to the future load consumption and prices of generation at different grid nodes in a simple system, [104] shows that ETC can determine the optimal economic solution. This solution is found by allowing line power flows to exceed the traditional loadabilities for a limited period of time while ensuring that all transmission lines are kept below their individual temperature limit.

ETC enables the implementation of all the stability limits utilised to define OPF studies, and ETC can thus be seen as a more extensive optimisation of transmission system operation.

5.5 Discussion of Transmission System Loadability

It is seen from the above sections that a substantial amount of research has been conducted within the evaluation of loadability of transmission systems. Load flow calculations are vital for all studies of the loadability of transmission systems, and different algorithms are available. It is noticed that most research concerned with loadability of transmission systems is limited to time independent scenarios (OPF and TTC), which are fairly simple to solve but may lack the potential of utilising the entire current carrying capacity of transmission lines. Electrothermal Coordination is a concept attempting to include the dynamically evolving temperature in the prediction of the opti-

mal power flow and the sparse literature available within ETC proves that enhancing the economic state of transmission systems is possible when allowing overhead transmission lines to exceed their normal steady state current ratings.

Utilising the ETC methodology is more complicated than OPF, as the temperature couples the otherwise time independent equations. ETC thus also requires larger computational resources than OPF and it must therefore be decided if the extra simulation time is acceptable or not.

As it will be described in chapter 6, the above given methods for calculating and optimising loadability of transmission systems may not be directly implementable in the Danish transmission system. However the discussion of the different methods has provided the PhD study with background knowledge and tools. In this way the issue of optimising utilisation of the future Danish cable based transmission grid can be addressed and a proper concept developed.

Chapter 6

Dynamic Loadability of the Danish Transmission System

The present study is aimed at finding a methodology enabling the utilisation of the thermal limits of power cables embedded in large grids, in stead of the static current limits.
Moreover, the developed methodology should respect the regulations which apply to the Danish transmission system operator and some of the aspects discussed in chapter 5 may thus not be possible to utilise. The following section is therefore dedicated to sketch the limitations and boundaries for the methodology which is to be developed in this PhD study.

6.1 Operation of the Danish Transmission Grid and the Energy Market

Electric energy is in Denmark sold and bought on market conditions. This means that the energy from the cheapest production unit is sold first where after more and more expensive energy is sold until the generation balances the consumer requested power. This trading is performed every day at 12:00 (noon) for each hour of the coming day of operation (00:00-24:00).
It should be noted that there are some deviations to the given market procedure, including the political decision of increasing the amount of renewable energy in the power system. This means that wind turbines and solar panels have been given unlimited access to the transmission system, possibly resulting in otherwise cheaper energy being pushed out of the production

scheme.

After the market has settled all energy trades for the 24 time intervals, it is up to the TSOs to transport the energy from the sites of generation to the sites of consumption. The TSO therefore performs load flow simulations on each of the 24 time intervals in order to ensure that the loading of the transmission lines does not exceed their individual steady state loadability. If the loadability limits are exceeded and the system is in complete 'N' state (no component outages) two things must be concluded. Firstly, the system is too weak and must be strengthened, for instance by purchasing of new transmission lines, and secondly the settled market cannot be allowed, why the TSO must interfere by rescheduling of power production.
In addition to the N state load flow simulations, the TSO furthermore performs N-1 load flow simulations on each of the hourly intervals. N-1 are simulations where all components one-by-one are assumed out of service. If the steady state loadability is exceeded in any component for any of these N-1 simulations, the operator is obliged to take actions which lower the power flow in the over loaded lines.
It should be noted that cases where the TSO has to interfere in the settled market are allowed e.g. during maintenance and contingencies but not during normal operation. If there is a risk of overloading during normal operation the grid has to be reinforced.

It should on this background be clear that, because all stakeholders are to have equal access to the grid on the day-ahead market, the TSO is not allowed to perform rescheduling of the power production in order to carry out socioeconomic optimisation. The basic concepts from TTC, OPF and ETC can thus not be directly implemented in the Danish transmission system.

In addition to the day-ahead market planning, the TSO is also responsible for ensuring the real time (i.e. during the day of operation) flow of power in the system. If the day-ahead market is accurate and unforeseen events are not experienced, then the real time operation should be an easy task as the flow of energy has already been modelled and reliability of the grid been proven through the load flow studies.
However during unexpected events, such as contingencies, unpredictable wind power production, etc. the flow of power in the system might be significantly different from the flow modelled on the day-ahead market. In this case, the real time operator may require to change the flow of energy by rescheduling of generation or load shedding. Such actions are allowed during contingencies as system integrity and reliability of power supply overrule the market conditions which the system is otherwise subjected to.

Given the described design of the power market and the way the load flow calculations are utilised in the assessment of the settled market, it must be concluded that if the TSO can increase the allowed loading on the individual

lines, both grid reinforcements and interference in the market can be avoided. On this background it is determined that the concept of "dynamic loadability of the Danish transmission system" is to utilise temperature modelling with load flow calculations of the day ahead market such that grid investments and interference in the market can be minimised.
Furthermore, given that the TSO may have to perform control actions in the real time system operation during contingencies and other unexpected events, the TSO might also benefit from using load flow calculations and dynamic temperature modelling in the real time system operation in order to predict the consequences of different possible control actions.

As the dynamic loadability concept to be developed in this way is a combination of electric (load flow) and thermal calculations, it is found that the term "Electrothermal Coordination" (ETC) covers the exact content of the platform to be developed, and ETC will thus be used for this platform in the remainder of the thesis.

It is acknowledged that ETC was defined differently in [104] than how dynamic loadability will be suggested implemented in the Danish grid, however given how accurate the term "ETC" covers the concept to be developed it is justifiable to utilise the ETC in the new context.

6.2 Development of Electrothermal Coordination for Cable based Transmission Grids Operated under Market Based Conditions

As stated, both the real time operator and the day-ahead planner will be able to utilise ETC in their daily work.

The real time operator will utilise measurements of the currents in the system to estimate the temperature evolution in each cable and this temperature can be utilised as background knowledge for making decisions on which control actions should be taken, e.g. during contingencies.
Furthermore, the day-ahead planner may use the thermal models to estimate the temperature evolution in the grid for the coming day of operation and based on these predicted temperatures it can be concluded if the settle market can be allowed or if remedial actions must be taken.

As a bonus it is noted that estimation of the temperature evolution in cables may also be utilised when analysing different possible grid enhancements. This means that also the grid planner may be able to benefit from including thermal models in the evaluation of optimising the grid.

It is thus evident that three different areas of expertise within the TSO may

be able to benefit from ETC, each covering a different timescale:

- Real Time Operation (minutes)
- Day-Ahead Planning (hours)
- Grid Planning (years)

In order to limit the amount of customised tools and thus ensure that enhancements to the tools made within one area could benefit all three areas, it was set as a prerequisite that all of the above three areas of expertise should be able to utilise the same ETC software package. Furthermore, it was chosen that the ETC tool should be developed such that it could fit into the portfolio of software which is already used at the Danish TSO.
On this background it was chosen to use the power system analysis software DigSilent PowerFactory (DSPF) as the centre for the ETC platform to be developed. It is recognised that other power system software might be better suited for the ETC concept, however in order to ease the integration into the TSO, it was a necessity that the developed algorithms were capable of interacting with the tools already in use.
The choice of creating ETC around DSPF also creates the possibility of spreading the tool to many other potential users, as DSPF is used in a wide range of distribution and transmission companies as well as at universities and many other research institutions throughout the world.

DSPF has a graphical user interface giving a nice and easy overview of the grid. In addition DSPF enables adapting all grid parameters through two different scripting environments, the DigSilent Simulation Language (DSL) and the DigSilent Programming Language (DPL).
DSL is designed, and well suited, for studies of stability and transient/dynamic modelling of power system components. This tool might therefore seem as an obvious choice as the temperature is a dynamically varying component property, however DSL is designed for fast varying quantities (such as voltage levels, etc.) and the simulations are comprehensive but slow because of the many time steps (which are difficult to eliminate). As the temperature is a slow varying quantity compared to e.g. voltage levels, it was on this background chosen to utilise the DPL scripting environment in stead. DPL calculations are in basic time independent so in order to include the time domain in the simulations, a discretisation of the time is necessary.

Having established that DSPF is the tool for performing load flow simulations and that the DPL scripting environment is the tool for controlling these load flow simulations, it is to be emphasised that there are two interdependencies between load flow simulations and the thermal models.
Firstly, the temperature in the power cable is directly related to the current,

and thus the current in the cables must be extracted from the load flow studies and inserted into the thermal models. Secondly, the temperature of the individual lines also has an impact on the load flow, because of the temperature dependency of the resistivity of the conductors. The conductor temperature must therefore be extracted from the thermal models and inserted into the load flow simulations.

As DSPF is not well suited to handle and perform calculations on large matrices, the thermal modelling by TEEs becomes difficult. It is therefore chosen to create the ETC software package by performing the power system calculations in DSPF and the thermal calculations in the mathematical software Matlab. It should be noted that it is possible to create executable files of the developed Matlab scripts and it is thus not necessary for the user to have Matlab installed on the computer.

The ETC package is to be developed such that it can be utilised by the three identified areas of expertise at the Danish TSO. However in order to ease explanations, the ETC platform will, in the following clause, be developed around an example from the real time operation. In the clauses thereafter the ETC software package is applied to examples for both the day-ahead market and the grid planning, proving the possibility of applying ETC to a wide variety of problems and analysis purposes.

6.2.1 Real Time Operation

Real time operation of the non-faulted transmission system (the N situation) should, as stated, not experience any power flow problems as thorough analysis were performed on the settled day-ahead market. However in case of failures in the system, ETC can be used to quickly predict the temperature evolution in the coming minutes and determine for how long the power flow can be maintained without any components being overheated. In this way, the operator will gain increased knowledge of the grid and know exactly which parts of the system to focus on to restore N-1 integrity of the system.

A case study of how ETC can benefit the real time operation of a cable based transmission system was presented in [108], which was produced as part of this PhD project (see also appendix F.3), and is outlined in the following. The case study investigates the two-line system of figure 6.1 (which was also used in [104]) to study ETC because it is easily comprehensible and makes it easy to investigate the principle of ETC.

The two lines are defined as cables of 100 km in length and the reactive power generated in the cables is compensated by half at each end. The base voltage is set to 132 kV and the cable screens are assumed to be perfectly cross-

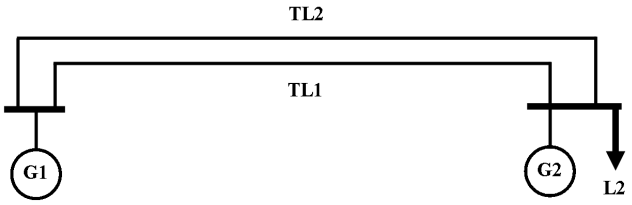

Figure 6.1: Two line system, with two generators and one load, used in the case study of ETC during real time operation of transmission systems.

bonded which, together with low eddy currents[1], will result in negligible screen losses. The two cable systems are laid far from each other, such that they can be seen as thermally independent.

The cable design is taken from [109], and the most important parameters are given in table 6.1. The material properties of the cables and surrounding were listed in table 4.2. The cables are installed in flat formation in a depth of 1.3 m with a spacing of 300 mm. In the presented case the cables are for simplicity assumed to be directly buried in soil and the native soil temperature at burial depth is assumed to be constant 15 °C.

U [kV]	S_c [mm^2]	S_s [mm^2]	d_c [mm]	d_i [mm]	d_s [mm]	D_e [mm]
132	1600 *	110	48.5	88.5 **	89.3 ***	101

Notes:
* Segmental aluminium conductor
** The cable is equipped with semiconductive layers, which have been assumed to be 2.5 mm thick. In the thermal studies these layers are assumed to have the same thermal properties as the XLPE insulation and the insulation thus has an effective thickness of 20 mm.
*** The thickness of the screen is calculated on the basis of the screen area and the effective outer diameter of the insulation. In the electrical calculations the screen is a copper wire screen, however in the thermal calculations it is assumed that the screen is a solid cylinder

Table 6.1: Cable design parameters of cables used in case study for ETC of real time operation of power systems. The parameters are found in [109] in the cable type '(A)2XS(FL)2Y 1x1600 RMS/50'.

[1] By choosing a proper screen design eddy currents can be minimised.

The load 'L2' has the active an reactive power consumption as shown in figure 6.2. The figure also shows the active power production of generator 'G2', which is seen to mostly assist the power production during peak hours. The remaining power production is provided by 'G1'. The load pattern is in this case, for simplicity, assumed to be repeated unchanged every day.

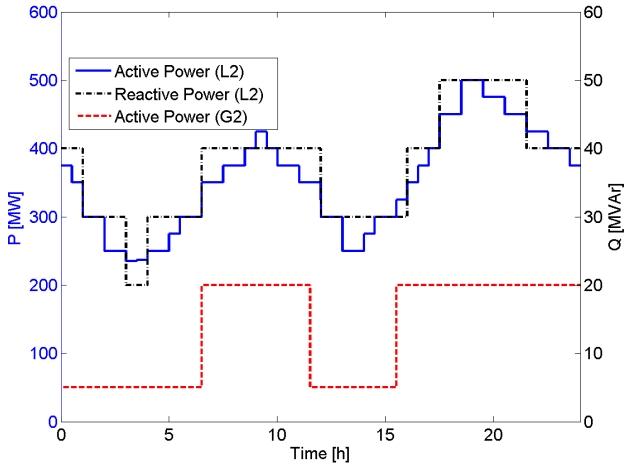

Figure 6.2: Active and reactive power consumption of the load 'L2' and the active power production of 'G2'. G2 is seen to assist with power production during peak hours. This load pattern is assumed to be repeated every day.

As this is a fabricated case study there are no DTS measurements to be used as feedback to the TEE models. This case study will thus calculate the temperature by using the static thermal parameters method as described in clause 4.2.8.1. Furthermore, the thermal history of the power system is not known and because the thermal evolution of cable systems is highly dependent on the load history, it is necessary to create this thermal history. In the present case, the thermal history is created by assuming a constant load of 0.5 pu for an infinitely long time, where after the load scheme of figure 6.2 is applied for 29 days. By doing this, the temperature in the cable system is assumed to be in dynamic equilibrium. At the 30th day, at 17:00, transmission line 2 (TL2) fails, and the load is immediately taken over by TL1. The simulation of the temperature thus requires four main steps:

1. Initialisation of system and calculations
2. Evaluate the dynamic equilibrium thermal state after 29 days
3. Disturb the system by letting TL2 fail
4. Evaluate temperature after failure

These four main steps have been elaborated in an algorithm, which is displayed as a flow chart in figure 6.3. Figure 6.3 shows which software handles the individual tasks, and the roman numbers in the text boxes refers to the explanations given in the following.

i In order to be able to adapt component parameters via DPL it is necessary to initialise the grid by running a load flow calculation.

ii Load names, line names and generator names are written to text files, such that DSPF and Matlab both knows exactly how the system looks.

iii Every parameter in the system can be changed via DPL-scripts, including the size of loads, lengths of cables, sizes of cables, sizes of generators, etc. These parameters are loaded into DSPF from text files, which defines the different parameters.
This approach has been chosen such that simulations with copper conductor cables can be easily compared to simulations with aluminium conductor cables.

iv Given the specific cable parameters, the eigenvalues and eigenvectors for the TEEs for all cables in the system are calculated. The initial temperature in the cables is obtained by assuming that the load has been static for a long time. The temperatures are exported to text files.

v The temperatures are loaded into DSPF from text-files.

vi The resistance of the conductors is updated according to the individual conductor temperatures and a load flow simulation i performed.

vii The currents running in the individual cables are exported to text files.

viii The currents are loaded in Matlab where the conductor losses (W_c) and the steady state temperatures are calculated for all lines.

ix The calculated temperatures ares stored for later analysis. The temperatures which are important for DSPF (conductor, screen and jacket temperatures) are exported to text-files.

x In order to obtain a sufficiently accurate starting point for the dynamic simulations, it has to be verified that the calculated steady state temperatures and load flow calculations are correct. This verification is performed by analysing if the result of the load flow simulations, or the results of the thermal calculations, have changed from one iteration to the next. If the conductor temperature difference between two iterations is below 0.01 °C and the current below 1 A for all cables, then the simulation is allowed to proceed to the dynamic calculations.

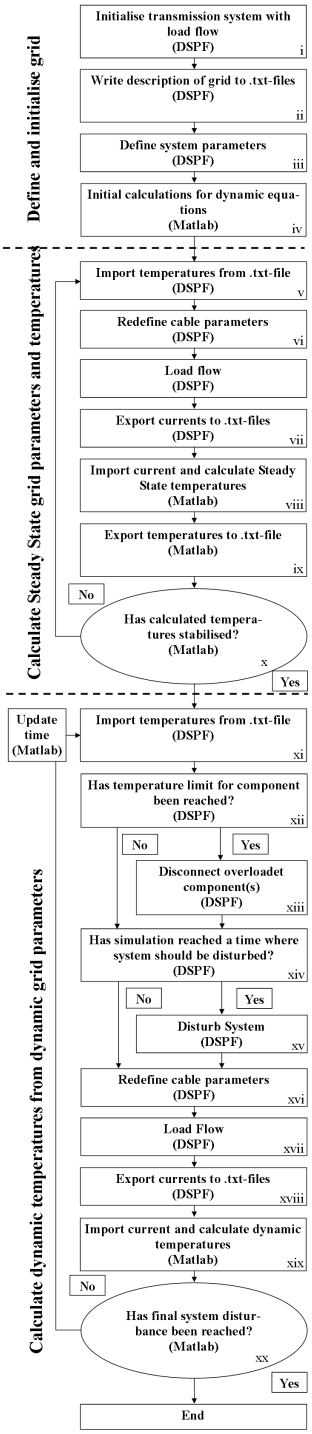

Figure 6.3: Flow chart of the algorithm performing the ETC analysis of the two-line case study.

xi The dynamic simulation starts by loading the lastly calculated temperatures into DSPF.

xii As previously discussed, cables are subjected to limitations on the conductor and/or jacket temperature. It is evaluated if these temperature limits are exceeded for any cables.

xiii If the temperature limit has been exceeded for one or more cables, the relevant lines are disconnected from the grid.

xiv It is evaluated if disturbances, e.g. contingencies, has been experienced in the system.

xv If the system has been disturbed, the disturbance is implemented in DSPF.

xvi The cable impedances are adapted to the real time temperature.

xvii Including all disturbances, disconnected lines, etc. DSPF runs a load flow simulation.

xviii The currents in all lines are exported to text-files for thermal analysis.

xix These currents are imported in Matlab and the dynamic thermal evolution in all lines is evaluated by using the TEE methodology.

xx Finally, test whether or not the end time has been reached. If not, the algorithm runs the steps from xi to xix again.

Figure 6.4 shows how the current and jacket temperatures evolve in TL1 on the 29th day of operation. It should be remembered that the 29th day of operation is a day without faults and the jacket temperature is therefore assumed to be the limiting property.

In order to show the potential of implementing ETC in the operation of the transmission system, the current and temperature of figure 6.4 are normalised in relation to their maximum values and the normalised quantities over the day are displayed in figure 6.5. The loadability of the cable is calculated with (3.11) to be 839 A, based on a maximum allowed jacket temperature of 50 °C[2].

Figure 6.5 clearly shows that while the current fluctuates between 0.35-0.85 pu, the jacket temperature lies almost static around 0.57 pu. This proves that the operator has a large freedom in operating the system as such high load variations shows almost no variation in the temperature. It may therefore be allowed to increase the loading on the line above rated on a daily basis.

[2]Note that 0 pu for the temperature is here set to 0 °C and for the current 0 A.

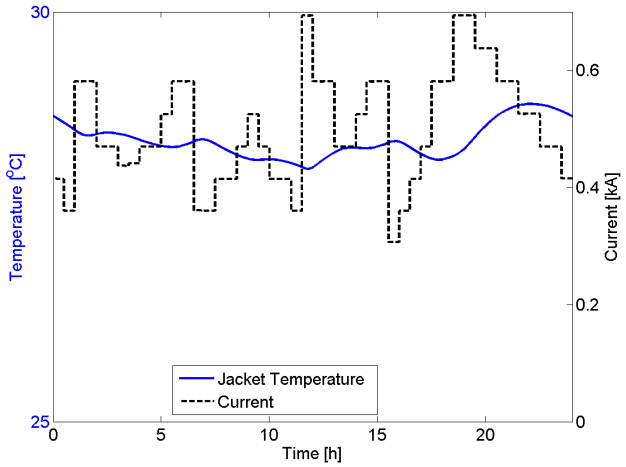

Figure 6.4: Jacket temperature and conductor current in TL1 of the two-line case study, on the 29th day of simulation. The dynamic temperature evolution is the result of the load pattern given in figure 6.2.

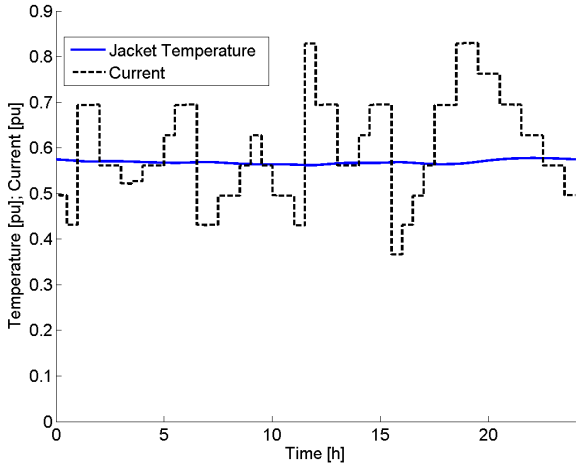

Figure 6.5: Normalised jacket temperature and conductor current. The temperature is normalised according to the maximally allowed jacket temperature, 50 °C, and the current is normalised according to the steady state loadability of 839 A. It is seen that while the current varies significantly the temperature is almost constant throughout the entire day. This shows that it is possible to increase the loading above rated on a daily basis.

Figure 6.6 shows the current and conductor temperature in TL1 from the beginning of day 30, where TL2 fails at 17:00, to the end of day 33. In this case, the conductor temperature is shown as it is the limiting parameter

during emergency operation.

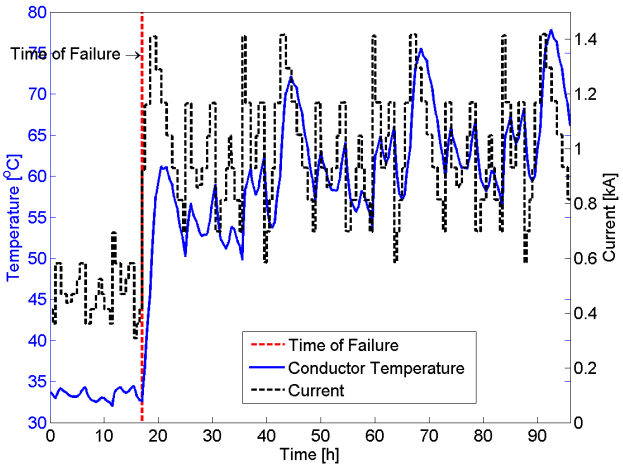

Figure 6.6: Current and conductor temperature evolution in TL1 in the days following the failure of TL2. It is clearly seen that even though the current exceeds the steady state loadability significantly for several hours each day, the temperature will not reach the limiting 90 °C. An extension of the time scale would show that the conductor will not reach 90 °C within the first 20 days after the failure.

Figure 6.6 gives a clear picture of how ETC can be very beneficial for the TSO.
When controlling the system based on static loadability values, the operator is forced to disconnect TL1 at 18:00 as the current is still above 1 pu after 1 hour. This means that load has to be shed if 'G2' is unable to produce sufficient power.
However when operating based on ETC, it can be foreseen that the conductor temperature will not reach the limit of 90 °C within the first 20 days after the failure, and the system can thus be allowed to run uninterrupted. This prediction of the temperature can only be performed via the close connection between load flow and thermal calculations, and thus the ETC application will enable the operator to make choices which increases flexibility while maintaining integrity of all components.

6.2.1.1 Implementation of ETC in Real Time Operation of the Danish Transmission Grid

Having determined that there is a significant potential in using ETC for real time operation it is important to focus also on how the algorithm can be implemented in practise.

It is obvious that the thermal history of the real transmission system will be based on measurements of the current of all transmission lines instead of an assumed load history. By having access to real time measurements (e.g. every 15 minutes) of the current, the temperature in all cables can be followed equally in real time. This real time monitoring means that the operator will always know the exact thermal state of the system and be able to operate based on temperature limits instead of currents.
In case of failures in the grid, the ETC algorithm will predict the load flow in the hours (or days) to come, and it can be predicted if/when the operator has to make control actions.

The implementation of ETC in real time operation requires that the thermal modelling is performed on one centralised computer.
As stated, different companies deliver stand alone software which can calculate the temperature in individual cable lines and determine for how long each line is capable of carrying specific loads. However such stand alone software does not enable implementation of ETC as the prediction of the future load flow scenario where much of the increased flexibility lies.

The implementation of ETC in real time operation can on this background be summarised in three main steps:

1. Evaluate the real time temperature of all cables based on current measurements. Possibly take as feedback also temperature measurements for increasing the accuracy of the temperature modelling.

2. Predict the future load flow scenario based on the settled market and projected load and generation patterns

3. Predict the future temperature evolution in all cables and determine when the thermal limits will be reached

6.2.2 Day-Ahead Planning

In a similar way to the real time operation, the day-ahead planning can utilise ETC to predict the evolution of the temperature in all cables in the grid. However because the day-ahead planning is required to be N-1 secure, it is not sufficient to simply evaluate the temperature of the system in the 'N' state. Furthermore, in order to ensure an easy implementation of ETC in the Danish transmission system it must be acknowledged that the developed methodology should follow similar principles as the present day-ahead market operation. It was therefore chosen to use the thermal calculations in the system to calculate a pseudo-continuous loadability as well as an emergency loadability.
The pseudo-continuous loadability will in this study be defined as the current

which the cable can carry for 40 hours without exceeding the steady state jacket temperature limit, given the real time thermal conditions (denoted "40 hours loadability"). The 40 hours loadability is suggested calculated with the algorithm presented in figure 3.5. A 40 hours loadability is suggested as the market is settled at 12:00 and predicts the power flow from 00:00-24:00 on the coming day, i.e. up to 36 hours into the future. Because it is easier and cheaper to control the system on the day-ahead market than during real time operation, the TSO wishes to be able to postpone interfering until the next day-ahead settling. As the market is settled 36 hours before the last delivery of energy, a 40 hours loadability will ensure that the TSO can control the system by interfering on market based conditions while at the same time increase the allowed loading of the individual cables[3].
Similarly the emergency loadability is defined as the current which the cable system will be able to carry for 1 hour without exceeding the limiting conductor temperature (denoted "1 hour loadability"). These two quantities are suggested to be evaluated and used as discussed in the following.

When the day-ahead market has settled at 12:00, the Danish TSO evaluates the expected load flow for the coming day of operation. This means that the temperature in all cables can be predicted for a period of 36 hours into the future. Having determined the thermal evolution of all cables, the maximum predicted temperature, during the 36 hours, for each cable is determined. This maximum temperature is utilised to evaluate the 40 hours loadability and the 1 hour loadability.
Thereafter 'N-1' simulations are performed and if any of these 'N-1' situations result in the current being higher than the 40 hour loadability, actions must be taken to ensure that the current keeps below the limit.

By integrating ETC in this way, it is seen that only limited effort is required as the only changes made, when comparing to the present operational procedure, is that the loadabilities change once every day instead of being static values.
The downside of choosing this implementation strategy in the day-ahead market is that the full potential of ETC is not utilised. In a complete change of operational procedure to ETC, the temperature in all cables during all N-1 conditions should be evaluated, and the operator would only have to interfere if the N-1 simulation would result in the limiting temperatures being exceeded.

The suggested ETC implementation is illustrated in the following by studying a case from the Danish transmission system. The case was presented in [110] which was produced as part of this PhD project, see also appendix F.4.

[3] 40 hours loadability is suggested in this study instead of a 36 hours loadability in order to obtain an inherent safety margin.

The island of Funen is connected to the Jutlandic transmission system via three transmission lines. System 1 and 2 are 400 kV and system 3 is 150 kV, see figure 6.7.

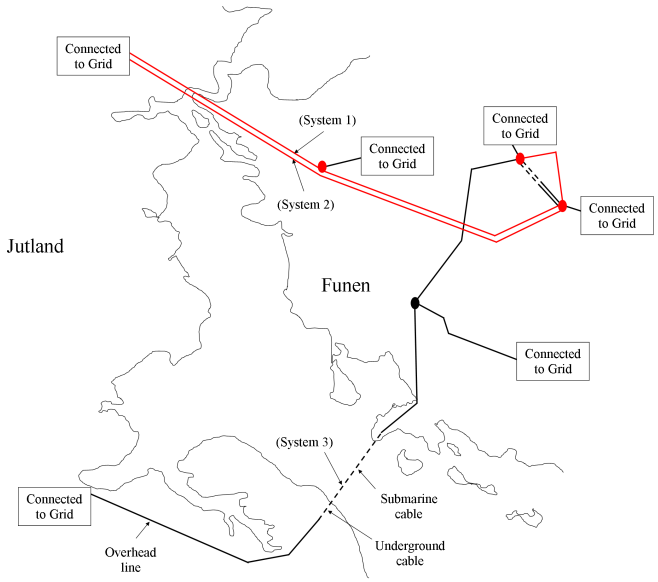

Figure 6.7: The island of Funen is seen to be electrically connected to Jutland through three transmission lines. Two on the 400kV level (red) and one on the 150kV level (black). Dashed lines are cables and solid lines are overhead transmission lines.

The TSO is interested in determining whether it can be allowed to take system 1 out for maintenance at 7:00 the next day, while maintaining N-1 integrity of the settled day-ahead market. At 12:00 the market is settled and the projected power flow from Jutland to Funen is as seen in figure 6.8[4].

In this case, the N situation before 7:00 includes all three transmission lines in operation, while after 7:00 only system 2 and 3 are included in the N situation. This gives the load flow scenario in the three lines as presented in figure 6.9.

Based on the situation of figure 6.9, the temperature evolution in all lines can be determined. As this thesis aims at underground cables, only the temperature evolution for the underground part of system 3 is shown in figure 6.10. The temperature is modelled based on the assumption that system 3 is a 150 kV underground cable with the design specifications as given in table 6.2 and material properties of table 4.2. Again the screens are assumed perfectly cross-bonded, which together with a proper wire screen may result in negligible losses. The cables are assumed buried in a depth of

[4]Notice that this is real life (historic) data taken from the Danish transmission system.

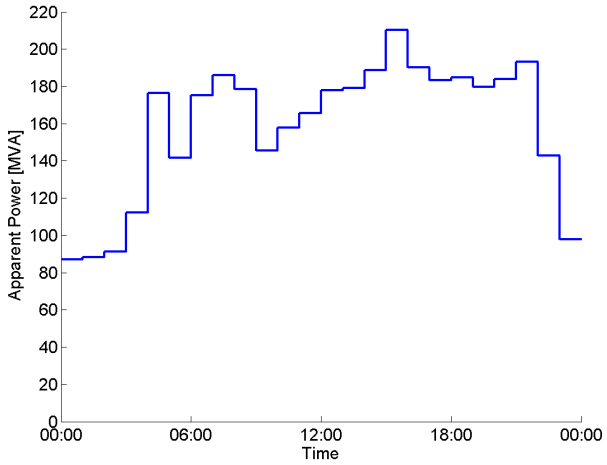

Figure 6.8: At 12:00, the load flow simulation of the settled day-ahead market predicts the apparent power flow from Jutland to Funen to be as seen in this figure.

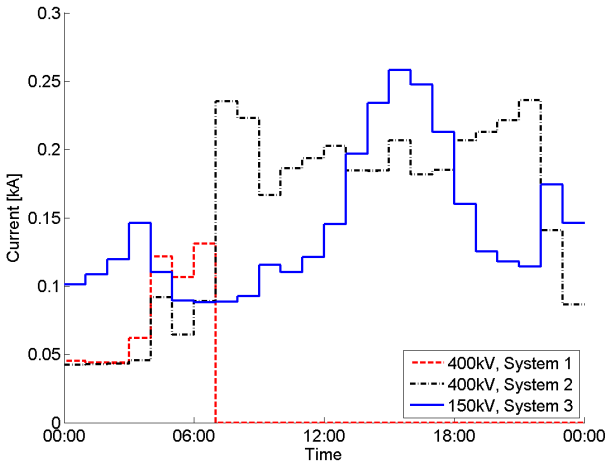

Figure 6.9: The predicted current running in each of the three lines (load flow simulation) is as given here.

1.4 m with a conductor spacing of 0.3 m. The soil temperature is assumed to be 20 °C, which is the yearly highest normal in Southern Denmark, and the cables are assumed to be buried in an envelope of sand of 0.3 m times 1.2 m, where the sand has a specific heat of 1.2 $\mathrm{J/m^3 \cdot K}$ and a thermal resistivity of 0.5 $\mathrm{K \cdot m/W}$.

The steady state loadability is calculated based on (3.11) to be 621 A and the 40 hour loadability is calculated based on the temperature of figure 6.10

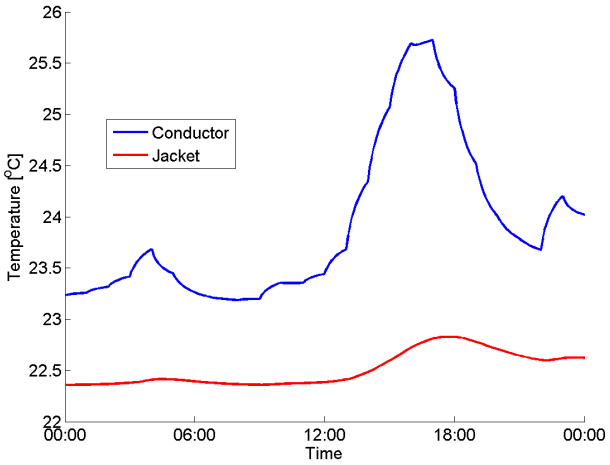

Figure 6.10: The predicted conductor and jacket temperatures of the 150kV underground cable denoted 'system 3'.

S_c [mm^2]	S_s [mm^2]	d_c [mm]	d_i [mm]	d_s [mm]	D_e [mm]
300	95	20.4	60.4	61.4	76.7
Notes: The quantities in this table are taken from [52].					

Table 6.2: Cable design parameters of cables used in case study for ETC on the day-ahead market. The parameters are found in [52].

to be 929 A. As seen in figure 6.9 the N situation does not violate either of the quantities, however as the dimensioning case is the N-1 situation further analyses are required.
If system 2 fails before 7:00, it is assumed that maintenance of system 1 will be possible to postpone, however if system 2 fails after 7:00 it is assumed that the maintenance of system 1 cannot be stopped. The worst N-1 situation that can be experienced is therefore that system 2 fails immediately after system 1 is taken out of operation. The load flow in this N-1 case is shown in figure 6.11.

It is seen that the current under these N-1 conditions is higher than the steady state loadability but lower than the 40 hours loadability. The operator would thus have to interfere in the settled day-ahead market when controlling the system based on current values but if the system control is based on ETC the settled day-ahead market would be allowed because the maximum current does not exceed the 40 hours loadability.

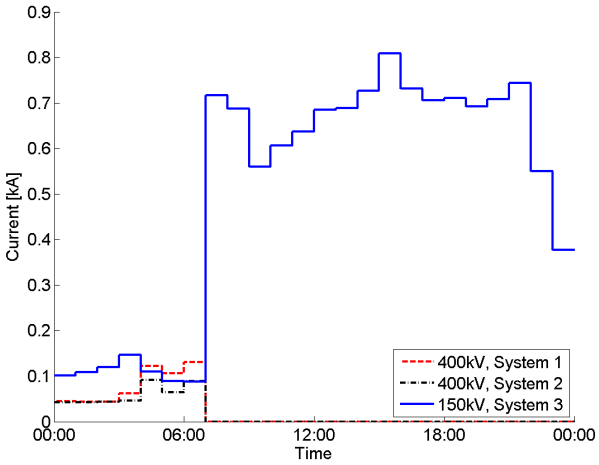

Figure 6.11: The predicted current running in the 150 kV underground cable denoted 'system 3' when system 1 is out for maintenance and system 2 fails at 7:00.

6.2.2.1 Implementation of ETC in Day-Ahead Planning of the Danish Transmission System

As seen from the above case, ETC can be implemented with clear benefits in the day-ahead planning of the transmission system. In summary it is suggested to implement ETC in the following main steps:

1. Predict load flow for the system during the coming day, based on the settled market
2. Calculate the temperature in all cables during the N situation
3. Determine the maximum temperature for each cable and calculate the current which, from this temperature, will result in the limiting jacket temperature after 40 hours
4. Perform N-1 simulations
5. If any of the N-1 simulation result in power flows being higher than the 40 hours loadability interference in the market-settled load production and consumption is necessary, otherwise no interference is necessary

6.2.3 Grid Planning

Planning of the Danish transmission grid is to ensure that electric power, also in the future, can be transported to the sites of consumption. The grid

is to be designed such that all components (one at the time) can be taken out of service for maintenance while maintaining a reliable system operation. As it is further required that one additional components must be able to fail without interrupted service (the N-1-1 situation), the transmission grid planner (TGP) must perform load flow calculations where up to two components are out at the same time. In the following these concerns are addressed through a case study presenting how the TGP can benefit from ETC in designing the future transmission grid. It should be noted that the presented case is a real life scenario from the planning of the future Danish transmission grid[5].

A section of the Northern Zealandic transmission system is shown in figure 6.12.

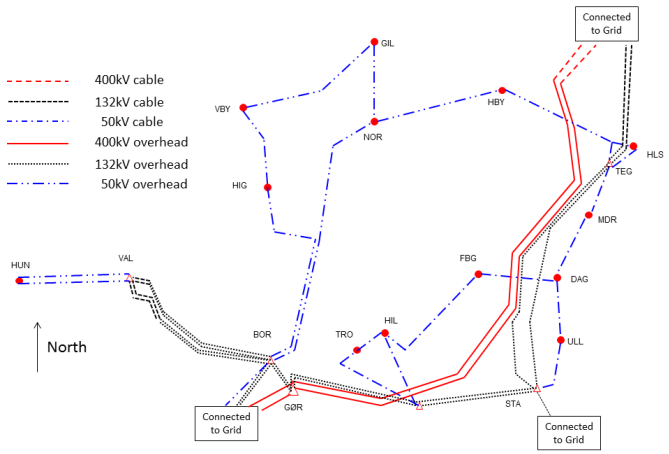

Figure 6.12: The transmission system in Northern Zealand as it looked in 2009, from 50 kV and up. It is seen that the transmission system to a high degree is radial and consists mostly of overhead lines. The radial topology requires several lines in parallel to ensure redundancy especially to the VAL-node which, besides normal residential and commercial users, has large scale industry connected.

Given Energinet.dk's Cable Action Plan [1], the TGP is requested to change the Danish grid by undergrounding many of the overhead transmission lines. However instead of simply changing overhead lines with cables 1:1, the TGP seeks to optimise the design of the transmission system to the future load flow scenario. Figure 6.13 shows the proposed topology of the grid in 2025.

It is clearly seen that the grid is proposed to consist mainly of cables and

[5]Note also that the given case is presented in [110] which was produced as part of this PhD project, see also appendix F.4.

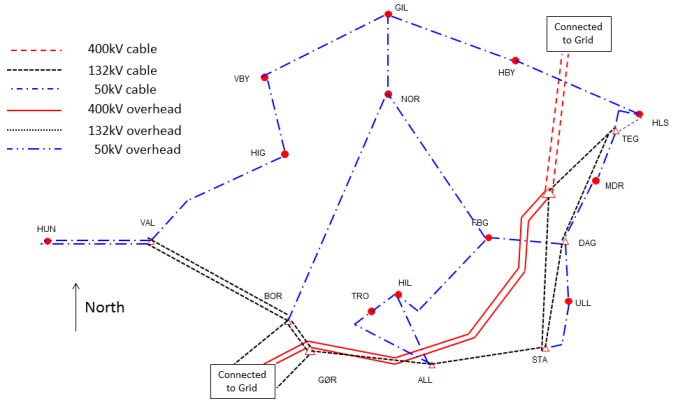

Figure 6.13: The transmission system in Northern Zealand as it is suggested to be designed in 2025, from 50 kV and up. The transmission system is seen to consist mainly of underground cables and the radial topology has changed to a more meshed structure.

that a more meshed topology has been chosen in order to limit the number of required parallel lines. The question is now whether the proposed design will be able to handle the predicted load flow scenario or if additional lines are required.
In the following it is specifically to be investigated if the large industrial load at the VAL node can be supplied in the case of the two 132 kV lines from BOR to VAL are out of service. In this case all power is to be delivered via the 50 kV network which results in the cable from GIL to VBY being the hardest loaded. The current is assumed constant until the N-1-1 situation arises where after it varies in the daily load pattern between 600-1200 A as shown in figure 6.14.

By modelling the temperature caused by this load profile, it can be determined whether or not a third 132 kV line from BOR to VAL is needed.
In order to determine the required size of the 50 kV cable, the temperature modelling is performed on four different conductor sizes. The cable design parameters are shown in table 6.3 and the material specific properties are as given in table 4.2. The cables are assumed buried in a depth of 1.4 m with a conductor spacing of 0.3 m. The soil temperature is assumed to be 20 °C, which is the yearly highest normal in Northern Zealand, and the cables are assumed to be buried in an envelope of sand of 0.3 m times 1.2 m, where the sand has a specific heat of 1.2 $^{J}/_{m^3 \cdot K}$ and a thermal resistivity of 0.5 $^{K \cdot m}/_{W}$.

These properties result in a steady state loadability of the four cables as given in table 6.4.

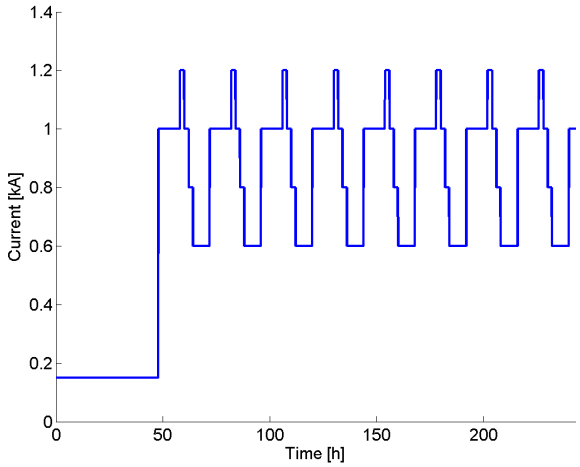

Figure 6.14: Projected current in the cable from GIL to VBY, during an N-2 situation where both 132 kV cable systems to VAL are out of operation.

S_c [mm^2]	S_s [mm^2]	d_c [mm]	d_i [mm]	d_s [mm]	D_e [mm]
400	50	21.3	45.3	50.5	57.5
500	50	24.3	47.7	52.9	59.9
630	50	28.3	50.1	55.3	62.3
800	50	31.5	52.9	58.1	65.3
Notes: The quantities in this table are taken from [52].					

Table 6.3: Design parameters of cables used in case study for ETC on the grid planning. Thermal modelling of the individual conductor sizes will allow for determining which cable size is required to be installed such that a third 132 kV cable line can be avoided. The parameters are found in [7].

S_c [mm^2]	400	500	630	800
$I_{max,SS}$ [A]	523	594	684	753

Table 6.4: Steady state loadability of the four different cables.

By comparing these loadability levels with the expected current of figure 6.14, it becomes evident that the TGP either has to use multiple cables per phase, even a 800 mm^2 cable requires two cables per phase, or build the extra 132 kV system. However when modelling the temperature evolution in the cables new information is obtained as seen in figure 6.15.

By looking at the temperature it becomes clear that the load curve can

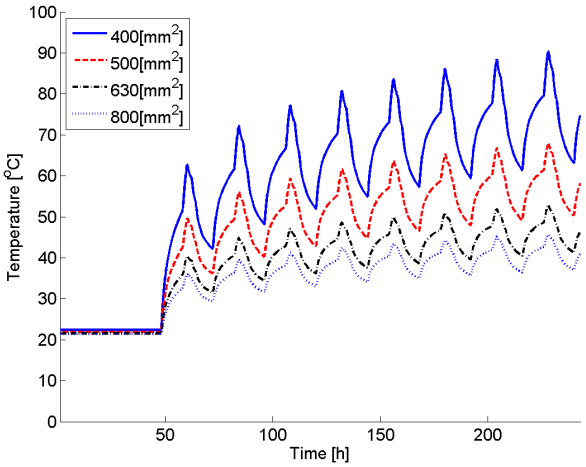

Figure 6.15: Jacket temperature evolution of the cable from GIL to VBY during the N-2 situation. The temperature for four different conductor sizes is presented.

be carried by the 500 mm^2 cable for more than one day before the jacket temperature reaches 50 °C, and increasing the cross sectional area of the conductor to 800 mm^2 means that the TSO will have significantly longer than the eight days presented here before the temperature reaches critical temperatures. It is up to the TGP to evaluate how long time is required to decrease the loading of the line, and on this background choose the proper cable size.

Based on this case study it should be clear that also the transmission grid planner at the TSO will be able to benefit significantly from implementing ETC.

6.2.3.1 Implementation of ETC in Designing the Future Danish Transmission System

As seen from the above example, this PhD study proposes ETC to be introduced in grid expansion planning (and reshaping) by using the following steps:

1. Suggest a grid topology
2. Run ETC simulation according to the flow chart of figure 6.3
3. Evaluate if the dynamically varying temperature exceeds limitations

6.2.4 Discussion of ETC in the Danish Transmission System

This section has shown the technical potential for implementing Electrothermal Coordination in the Danish transmission system.
It is shown that both the real time operation, day-ahead planning as well as planning of the future grid design can utilise ETC in similar approaches, which makes it possible to build the ETC tool on one single platform. This condition is assumed to make the integration, as well as the maintenance, of ETC simpler.

As discussed along the way, the utilisation of the theoretical thermal limits of the transmission system can be increased even further than with the proposed implementation methods. However in order to obtain these enhancements other subjects, e.g. the design of the day-ahead market, should be included in the discussion and such analyses are out of the scope of the present study.

6.3 ETC Applied to IEEE 14-Bus Test Network

In section 6.2, a number of case studies showed the potential of implementing ETC in the operation and planning of the Danish transmission system. The different cases presented different grid aspects and investigated the thermal responses for cables of varying size and manufacturer. This proves the inherent flexibility of ETC, and it shows that many different transmission grid aspects can be investigated with the same tool.
However the cases presented until now has been of rather small scales, and it is now time to prove that ETC can be utilised on a larger transmission system.

For this purpose, the ETC system is to be tested on the well known IEEE 14-bus test network as seen in figure 6.16, [111].

In figure 6.16 C's are synchronous compensators, G's are generators and triangles are loads. In the remaining, the generator at bus one will be denoted 'G1', and similarly with the compensators and loads.

As this 14-bus network, both in [111] and all investigated other references, is assumed to consist of overhead lines, adaptions to the system are required. Furthermore, the 14-bus network is most often used to test the accuracy of time independent load flow algorithms, and a variable load flow scenario is thus also to be developed.

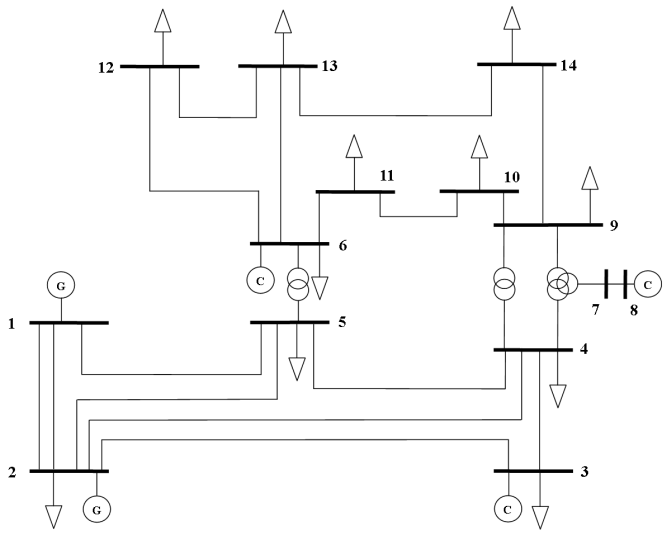

Figure 6.16: IEEE 14-bus test network. C's are synchronous compensators, G's are generators and triangles are loads. The generator at bus number one will be denoted G1 and so forth.

6.3.1 Design of the Adapted 14-Bus Test Network

The higher voltage grid, bus 1 to 5, is defined as 400kV and the lower voltage grid, bus 6 to 14, is defined as 132 kV. The synchronous condensers in figure 6.16 are exchanged with generators. Furthermore, it was chosen to introduce parallel lines between bus 6 to 11, between bus 9 to 10 and between bus 10 to 11. The length of the individual cable lines is shown in table 6.5.

The number in the column denoted "parallel path number" is used to distinguish between two cables running between the same busses. Furthermore, the letter in the column denoted "cable type" is related to the cable types listed in table 6.6.

The cables are assumed to be directly buried in soil with thermal properties as defined in table 4.2 in a depth of 1.4 m with an axial spacing of 0.3 m. Cable systems running in parallel are for simplicity assumed to be so widely spaced that they do not affect each other electrically or thermally.

This adapted version of the IEEE 14-bus test system has been designed in DSPF as shown in figure 6.17 (note also that a larger version of this figure is found in appendix E). For simplicity, the reactive power of all cables is compensated by half at both ends with reactors, and the reactive power produced by the generators is thus only to supply the loads. The current used in the thermal calculations does in this way include both the reactive part of the power as well as the active, however the phase angle of the

Start bus	End bus	Voltage level [kV]	Length [km]	Parallel path number	Cable Type	$I_{max,SS}$ [A]
1	2	400	56.23	1	A	682
1	2	400	56.23	2	A	682
1	5	400	49.31	1	A	682
2	3	400	42.89	1	A	682
2	4	400	29.90	1	A	682
2	5	400	11.42	1	B	761
3	4	400	13.69	1	A	682
4	5	400	7.56	1	A	682
6	11	132	43.35	1	C	820
6	11	132	43.35	2	C	820
6	12	132	56.09	1	C	820
6	13	132	47.98	1	C	820
7	8	132	0.10	1	C	820
9	10	132	14.52	1	C	820
9	10	132	14.52	2	C	820
9	14	132	32.70	1	C	820
10	11	132	37.44	1	D	992
10	11	132	37.44	2	D	992
12	13	132	56.84	1	C	820
13	14	132	43.98	1	C	820

Table 6.5: Lengths of cables in the IEEE 14-bus test network. In case of two cable systems being installed in parallel, they are distinguished by different numbers in the "Parallel path number" column. Design parameters for the "cable type" column are given in table 6.6 and the steady state loadability is evaluated based on (3.11).

Cable Type	U [kV]	S_c [mm^2]	S_s [mm^2]	d_c [mm]	d_i [mm]	d_s [mm]	D_e [mm]
A	400	1000	200	36.0	104.0	120.4	131.6
B	400	2000	200	50.6	108.6	125.0	136.5
C	132	1000	95	36.0	70.0	81.7	90.2
D	132	1600	95	45.0	77.0	88.7	97.9
Notes: All conductors are compacted aluminium conductors All screens are copper wires with an equalising tape The quantities in this table are taken from [7].							

Table 6.6: Cable design parameters of cables used in case study for ETC on the grid planning. The parameters are found in [7].

generators will be limited.

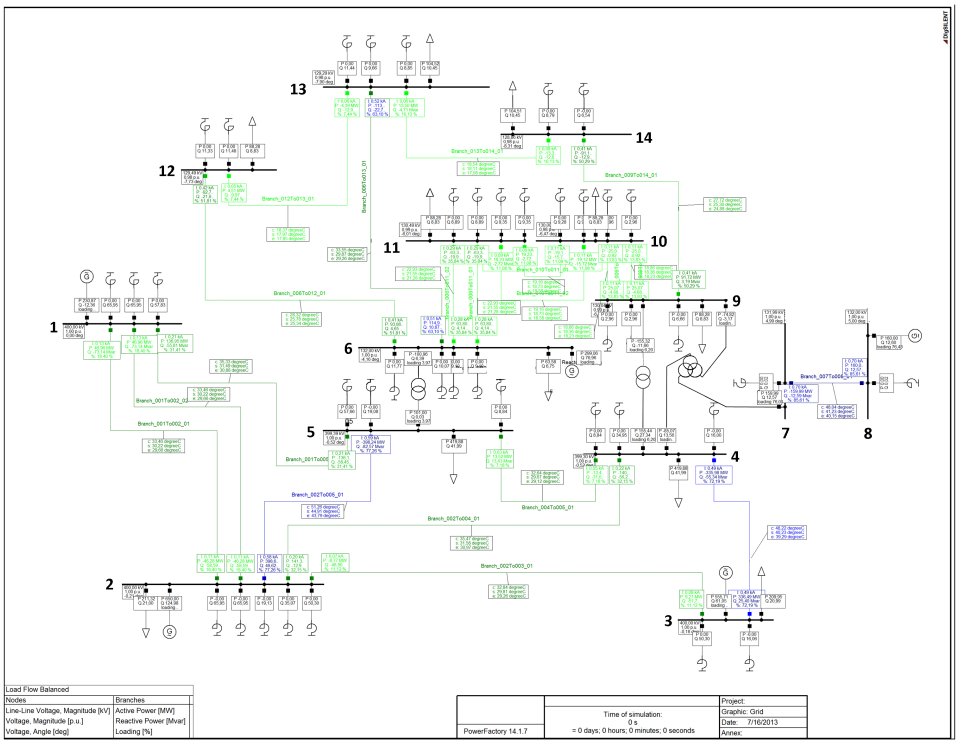

Figure 6.17: IEEE 14-bus test network as designed in DSPF. A larger version of the figures can be found in appendix E.

It should be acknowledged that a significant amount of customised tools had to be created to give this DSPF user interface. Amongst many others, the dynamically varying temperatures in conductor (c), screen (s) and at the jacket (e) are shown directly on each line in the system, such that the operator can evaluate the thermal performance of the system directly on the basis of the overview of the grid. The lines are coloured according to their thermal state from light green lines with low temperatures, over blue, to dark red lines which are too hot (over 50 °C on the jacket). Similarly, the electrical values are presented in different colours dependent on the loading of the line, i.e. dark red means that the current is above the steady state loadability.

The operator is thus shown, in a very visual way, the parts of the transmission system which he should focus on. This is believed to be helpful in cases of contingencies where the operator is required to keep an overview and act where it is necessary.

6.3.2 Load Flow and Failure Scenario

For simplicity it is assumed that all loads and generators vary in a daily pattern for the entire studied period. The loads are given in table 6.7 and the production is given in table 6.8.

Time [h]	L2-L3 [MW]/ [MVAr]	L4-L5 [MW]/ [MVAr]	L6 [MW]/ [MVAr]	L9-L12 [MW]/ [MVAr]	L13 - L14 [MW]/ [MVAr]
0	160 / 16	320 / 32	40 / 4	40 / 4	40 / 4
1	160 / 16	320 / 32	40 / 4	40 / 4	40 / 4
2	160 / 16	320 / 32	40 / 4	40 / 4	40 / 4
3	160 / 16	320 / 32	40 / 4	40 / 4	40 / 4
4	160 / 16	320 / 32	40 / 4	40 / 4	40 / 4
5	160 / 16	320 / 32	40 / 4	40 / 4	40 / 4
6	160 / 16	320 / 32	60 / 6	60 / 6	60 / 6
7	200 / 20	400 / 40	80 / 8	120 / 12	150 / 15
8	240 / 24	480 / 48	80 / 8	120 / 12	150 / 15
9	240 / 24	480 / 48	80 / 8	120 / 12	150 / 15
10	240 / 24	480 / 48	80 / 8	120 / 12	150 / 15
11	240 / 24	480 / 48	80 / 8	120 / 12	150 / 15
12	240 / 24	480 / 48	60 / 6	60 / 6	60 / 6
13	240 / 24	480 / 48	60 / 6	60 / 6	60 / 6
14	240 / 24	480 / 48	60 / 6	60 / 6	60 / 6
15	240 / 24	480 / 48	60 / 6	60 / 6	60 / 6
16	240 / 24	480 / 48	60 / 6	60 / 6	60 / 6
17	240 / 24	480 / 48	80 / 8	120 / 12	150 / 15
18	240 / 24	480 / 48	100 / 10	120 / 12	150 / 15
19	240 / 24	480 / 48	80 / 8	120 / 12	150 / 15
20	240 / 24	480 / 48	80 / 8	120 / 12	150 / 15
21	240 / 24	480 / 48	80 / 8	120 / 12	150 / 15
22	200 / 20	400 / 40	80 / 8	120 / 12	150 / 15
23	160 / 16	320 / 32	80 / 8	120 / 12	150 / 15

Table 6.7: Daily load pattern for loads in the IEEE 14-bus test system. The load pattern is assumed to be repeated indefinitely.

For the initialisation of the temperatures, the average of the load pattern is assumed to have been applied for a long time. Thereafter, in order to obtain a dynamic equilibrium, the thermal response of all cables, to the load pattern given in table 6.7, is modelled for 29 consecutive days.

On the 30th day at 7:00 two simultaneous contingencies happen, the cable from bus 2 to 5 and the cable from 3 to 4 fails.

Time [h]	G1 [MW]	G2 [MW]	G3 [MW]	G6 [MW]	G8 [MW]
0	Slack	650	320	160	160
1	Slack	650	320	160	160
2	Slack	650	350	160	160
3	Slack	650	400	200	160
4	Slack	650	550	200	160
5	Slack	650	500	240	160
6	Slack	650	550	280	160
7	Slack	650	600	320	160
8	Slack	650	600	360	160
9	Slack	650	650	400	160
10	Slack	650	650	400	160
11	Slack	650	600	360	160
12	Slack	650	600	360	160
13	Slack	650	550	320	160
14	Slack	650	550	280	160
15	Slack	650	600	320	160
16	Slack	650	600	320	160
17	Slack	650	650	360	160
18	Slack	650	650	400	160
19	Slack	650	650	400	160
20	Slack	650	600	400	160
21	Slack	650	600	400	160
22	Slack	650	550	320	160
23	Slack	650	550	240	160
24	Slack	650	350	200	160

Table 6.8: Daily production pattern for generators in the IEEE 14-bus test system. The production pattern is assumed to be repeated indefinitely. The reactive power production is calculated by DSPF such that the generator buses are kept at nominal voltage level.

The following clause describes the scenario which follows these failures when controlling the system based on steady state loadabilities (the current based control strategy) and when controlling the system based on maximum allowed temperatures (the ETC based control strategy).
The two operating procedures are in the following allowed to disconnect lines when they are overloaded as well as disconnect loads in order to avoid total system failure.

6.3.3 Results

The transmission system evolution in the first three hours after the failures is shown in figure 6.18. The figure is a comparison of the current based control strategy (left column of figures) and the ETC based control strategy (right column of figures), larger versions of the figures are shown in appendix E.

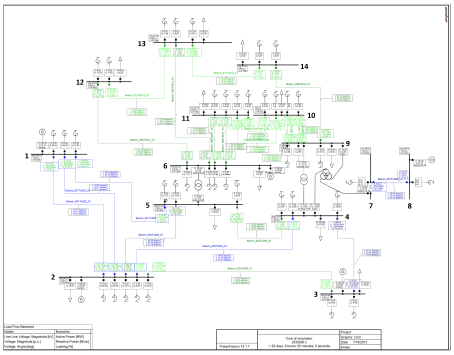

(a) 6:50 at the 30th day

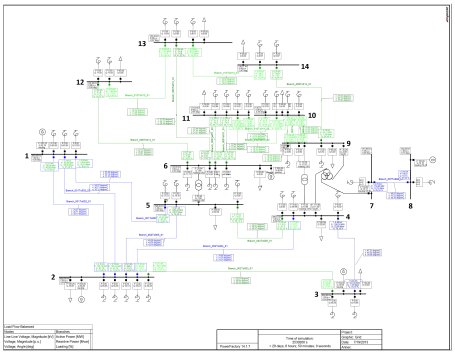

(b) 6:50 at the 30th day

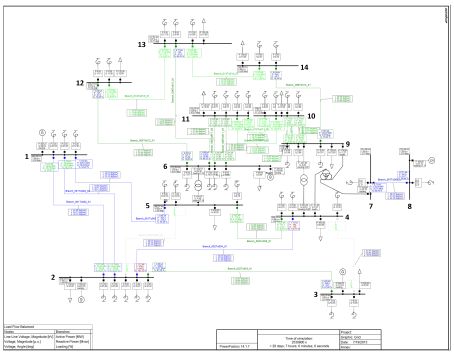

(c) 7:00 at the 30th day

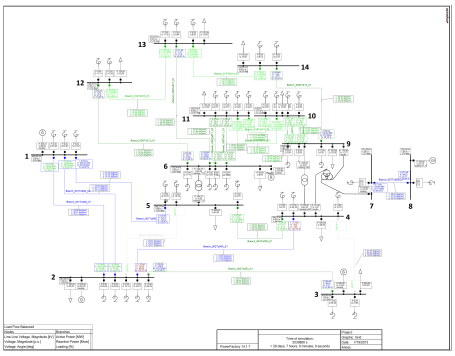

(d) 7:00 at the 30th day

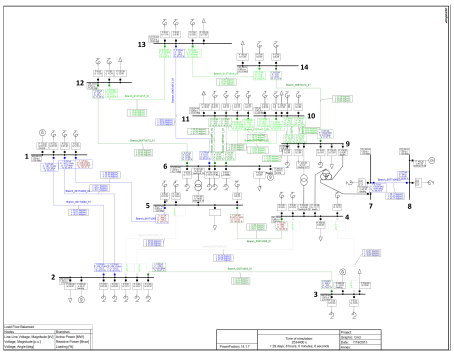

(e) 8:00 at the 30th day

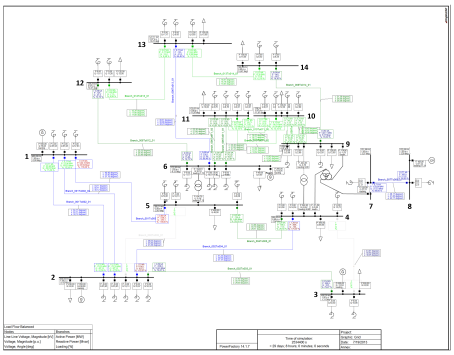

(f) 8:00 at the 30th day

Figure 6.18: *A larger version of these figures can be found in appendix E. Continued on next page.*

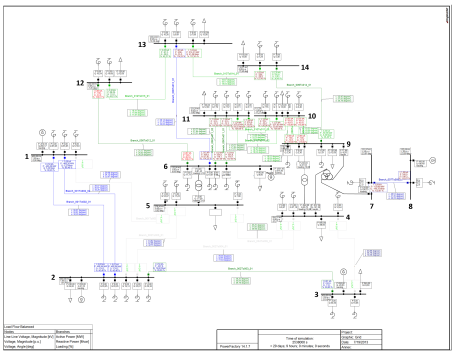

(g) 9:00 at the 30th day

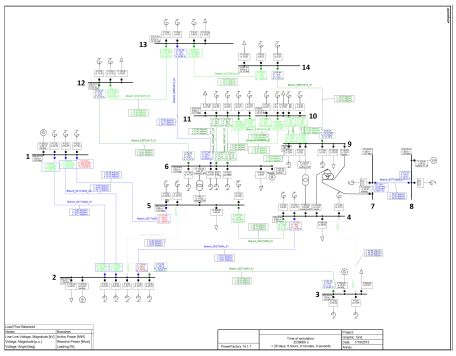

(h) 9:00 at the 30th day

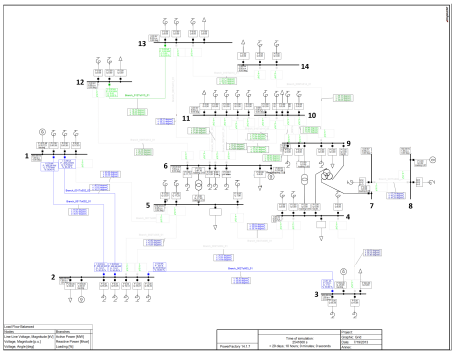

(i) 10:00 at the 30th day

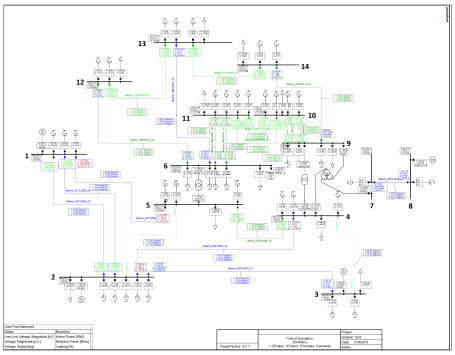

(j) 10:00 at the 30th day

Figure 6.18: Transmission system evolution when the cables from bus 3 to 4 and 2 to 5 both fails at 7:00. The left column of figures show the evolution when the system is operated with steady state loadability limits and the right column shows ETC based operation. It is seen that the current based operation requires the operator to make several control action, leading almost to total system collapse whereas the ETC based operation continues without the need for operator interference. A larger version of these figures can be found in appendix E.

It is seen that the current in cable 2 to 4 exceeds the steady state loadability immediately after the failures, figure 6.18c. As this cable is still overloaded after one hour, the current based operation procedure dictates disconnection. In order to avoid the system from an immediate collapse, the load at bus 5 is also shed at this time.

These disconnections causes the cables from 1 to 5 and 4 to 5 to be overloaded, which after one hour (at 9:00) prescribes disconnection of the two lines, figure 6.18g.

This leads immediately to the cables from 6 to 12, 6 to 13, 6 to 11, 7 to 8, 9 to 10, 10 to 11 and 13 to 14 to be loaded above their steady state rating. As the cables are still overloaded after one additional hour they are disconnected. Furthermore, in order to avoid total system failure, the operator has to disconnect the cable from bus 9 to 14, figure 6.18i.

It is seen that the system, when operated based on the static loadability limits, may evolve dramatically towards an unacceptable state where most loads are shed and the system has to operate in separated islands.

If on the other hand the system is operated based on ETC, the operator has easy access to the real time temperature in all cables in the system. In the right column of figure 6.18 it is seen that even with the two failures, the temperature will not exceed the critical 90 °C on the conductor in any of the cables within the shown first three hours. Instead of forcing unnecessary disconnections, ETC allows the transmission system to continue with the scheduled load pattern without the need for interference. Even the most critical line, the cable from bus 2 to 4, will not exceed the specified temperature limit and, as it is shown in figure 6.19, the temperature in this cable will not exceed the limit within the first two days of operation after the failure.

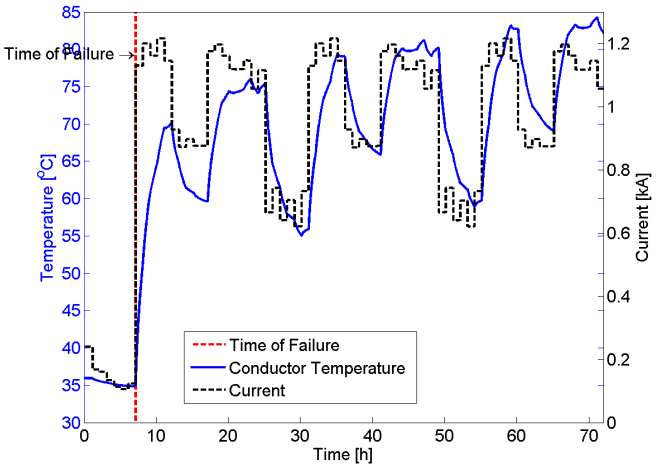

Figure 6.19: Development of temperature and current in the cable from bus 2 to 4 when the system is operated based on ETC. It is seen that even though the current exceeds the steady state loadability of 682 A significantly, ETC based control allows for several days of operation without the need for interference.

6.3.4 Discussion of ETC in Large, Meshed, Cable Based Transmission Systems

Even though the above example is fabricated, it illustrates again clearly the possible benefits of implementing the ETC concept as the operational strategy for the transmission system.
In the current based approach, the operator may be able to perform other

control actions than the ones described above, however no matter which control action are performed they will always leave the system in a less flexible/optimal state than if no actions are performed.

It should be noted that the snapshots of the transmission system evolution presented in figure 6.18, represent a significant amount of the work performed in this PhD project. First of all the figure shows, in a simple manner, the real time electrical and thermal state of the transmission system. The figure is the result of the DSPF-ETC software package which includes all of the knowledge about thermal models of individual cables obtained in Part II of this thesis, the interdependencies between these thermal models and load flow studies, as well as the integration of the combined models into DSPF. Furthermore, while it may seem simple to have the temperature presented on the individual lines, along with a colour representation of how critical the temperature is, their creation has required an in depth understanding of DPL algorithms and stretching the purpose of DSPF to the limit.

6.4 Discussion of Loadability of the Danish Transmission System

This chapter has given suggestions to how thermal models can be imbedded in operation and planning of large, meshed, cable based transmission grids. It was discussed that traditional optimisation tools such as optimal power flow (OPF) algorithms are not applicable to the Danish transmission grid due to the design of the electric power market. This part therefore suggested that thermal models of power cables can be combined with load flow simulations in a concept denoted Electrothermal Coordination (ETC). ETC is suggested to be utilised in the assessment of the settled day-ahead market by the calculation of 40 hours loadabilities for the cables. It was shown through a case study that this approach can give an increased flexibility in the transmission system operation.
It was furthermore shown that the developed ETC methodology can also be applied to both the real time operation of transmission systems as well as long term grid planning.

The ETC algorithms have been developed around the power systems analysis software DigSilent PowerFactory (DSPF) as this is already extensively used at the Danish TSO. The ETC software package has been created such that DSPF handles the load flow analyses and Matlab takes care of the thermal simulations.

The developed software package has been shown to be efficient, as large systems can be analysed, and flexible, as a number of different cable designs

(from different cable manufacturers) have been tested.

It should be noted that the present PhD project has only dealt with the limitations and thermal modelling of power cables. Equipment such as breakers, and transformers, etc. have thus been assumed not to be limitations for the flow of power. However as the developed ETC tool is flexible, it will allow for the implementation of thermal modelling of all necessary components, including transformers, breakers, etc.

It is the believe of the author that the developed ETC concept is the best compromise between system reliability, user friendliness and simplicity which will allow for the smoothest possible implementation into the control room of the Danish TSO. The tools have been developed in close collaboration with the different stakeholders at Energinet.dk in order to ensure that the outcome of this PhD project could become more than a scientific/theoretical contribution. The analysis of both real life power system data, the modelling of the IEEE 14-bus test network, etc. show that ETC can be of both scientific interest as well as of practical importance.

PART IV

Advantages of Implementing Electrothermal Coordination in Cable Based Transmission Systems

---

From a technical point of view, the previous chapters have shown, that electrothermal coordination is capable of enhancing the utilisation of cable based transmission systems. However in order for such a system to be implemented at a modern transmission system operator, advantages must not only be technically proven but also come with measurable economical benefits.

This part of the thesis is on this background dedicated to clarify the advantages of ETC related to both reliability of the grid as well as the economical aspects.

Chapter 7

Reliability of Power Systems Operated with Electrothermal Coordination

This chapter is dedicated to the analysis of reliability of power systems when operating the system based on the static current limitation and when operating the system based on ETC.

Textbooks, [112–115], as well other scientific contributions, [116–119], give a comprehensive overview of transmission system reliability assessment.
The majority of literature within this subject is concerned with evaluating the reliability of radial power systems, parallel systems or power systems where a redundant system can be connected in case of a contingency. When it comes to the analysis of meshed power systems, the literature is sparse and most often give a statement similar to: "For meshed transmission systems, the brute force Monte-Carlo simulations must be used", with little to no further explanation.

It is not within the scope of this PhD project to develop new methods for evaluating the reliability of power systems and thus the remaining of this chapter will be concerned with discussing different existing possibilities for assessing reliability as well as explaining Monte-Carlo simulations of meshed transmission systems.
These analyses are performed such that it can be evaluated how large an impact the implementation of ETC has on power systems reliability.

7.1 Definition of Transmission System Reliability

As seen from the preceding chapters, many different stakeholders are concerned with transmission system reliability, hereunder consumers, production units, operators, etc. Each of the stakeholders will though consider different aspect of grid operation more important than others and it is thus difficult to determine the reliability of transmission systems with one single value. In order to cover as many interests as possible, the literature has therefore proposed the use of a number of different reliability indexes. These indexes are used to assess historic system performance, compare different grid topologies and evaluating the impact of possible grid enhancements. The most commonly used reliability indexes are listed in the following clauses, [112, 113].

7.1.1 SAIFI

The System Average Interruption Frequency Index (SAIFI) is the annual number of interruptions which each customer can expect. It is evaluated as given in (7.1).

$$\text{SAIFA} = \frac{\sum_i N_i}{N_T} \tag{7.1}$$

where N_i is the number of interrupted customers per event, i is the interrupting event number and N_T is the total number of customers.

This index is thus concerned with the consumers and it is obvious that consumers experiencing many outages per year may be annoyed. But it should be noted that the index does not include the size of the consumers or how long the outages last, and thus an outage of a big consumer lasting for several months will, in principle, count just as much as an outage of a single household for ten minutes.

7.1.2 SAIDI

The System Average Interruption Duration Index (SAIDI) is the average time (e.g. in hours per year) which the consumers are without power. The SAIDI is calculated as given in (7.2).

$$\text{SAIDI} = \frac{\sum_i N_i \cdot t_i}{N_T} \tag{7.2}$$

where t_i is the restoration time for event number i.

This index is seen to take care of one of the weaknesses of the SAIFI as it includes the time aspect. However by including this time aspect the number of interruptions obviously disappears and ten outages of one hour will thus affect the index equally to one outage lasting ten hours.

7.1.3 CAIDI

The Customer Average Interruption Duration Index (CAIDA) is the average time each interruption lasts. It is evaluated as given in (7.3).

$$\text{CAIDI} = \frac{\sum_i N_i \cdot t_i}{\sum_i N_i} \tag{7.3}$$

This index is seen to weigh the time aspect of each duration of each outage, however it is also seen that the index is indifferent to whether the system experiences one outage of ten minutes or ten outages of ten minutes.

7.1.4 ASAI

The Average System Availability Index (ASAI) is the fraction of the time which the system is operating without interrupted customers.

$$\text{ASAI} = 1 - \frac{\sum_i t_i}{T} \tag{7.4}$$

where T is the total time span on which the index is based, typically a year.

This index is seen to be evaluated with a different perspective than the previous three. Where SAIFI, SAIDI and CAIDI were concerned more with the individual consumer, the ASAI is concerned with the system. The interruption of any consumer will affect the index and in a similar way as the SAIDI small consumers and large consumers are thus weighed equally.

7.1.5 AENS

The Average Energy Not Supplied (AENS) is the average energy which was not supplied (even though demanded) to customers, as defined in (7.5).

$$\text{AENS} = 1 - \frac{\sum_i P_i t_i}{\sum_i N_i} \tag{7.5}$$

where P_i is the energy not delivered during interrupting event number i.

This index is seen to include both duration of outages as well as size of unsupplied customers, but the frequency of outages is not included.

7.1.6 Choosing the Proper Reliability Index

As seen from the above, different indexes shows different aspects of grid operation and it is thus in general not possible to state system reliability with just one single number. TSOs therefore commonly calculate several of the above indexes on a yearly basis to be able follow the evolution of the different aspects of system reliability.

Even though it is difficult to assess system reliability with just one single number, the ASAI is, by the author, seen as a good indicator for comparing current based operation and ETC based operation because it shows the fraction of time where the system is fully functioning.
The remaining of this chapter will thus focus on the ASAI for comparing ETC and current based operation of transmission systems.

7.2 Prediction of Reliability Indexes

Transmission systems are in ever development and it is thus difficult to use last years data to estimate this years reliability indexes. In order to evaluate up to date indexes, the TSO can utilise average failure rates for the individual components and determine the different reliability indexes through simulations. Failure rates for different components are estimated based on historical data.

7.2.1 Failure Rates and Repair Times

The failure statistics of electrotechnical components are most often assumed to follow the so called bathtub curve, which means that the probability of failure falls drastically within the first time after commissioning. Thereafter follows many years with a static probability of failure. Finally, towards the end of the lifetime, the components typically experiences an increase in failure rate. The failure rate as function of time appears therefore as a bathtub shape.

Because components typically have many years where the failure rate is constant, and because it is significantly easier to perform statistical mathematics on constant failure rates than on time dependent, components are typically assigned a static failure rate over their entire lifetime.

The present study has used the failure rates of cables which has been published by Cigré in [120].

For 132-150 kV systems, the total failure rate per 100km cable per year is:

$$\lambda = 0.103 \, {}^{\text{failures}}/_{\text{100km·year}} \tag{7.6}$$

For 400 kV systems, the total failure rate per 100km cable per year is:

$$\lambda = 0.231 \, {}^{\text{failures}}/_{\text{100km·year}} \tag{7.7}$$

When failures happens in the transmission system, the TSO will initiate a repair of the component as quickly as possible. For cables, the time from a failure appears until the cable can be reinstated into normal operation includes a number of different tasks. Firstly the failure site has to be located which is not necessarily an easy task on cable systems because they can be several tens of kilometres long. Thereafter the cable has to be excavated, the jointing has to be performed, where after the cable system has to be tested. Cigré has in [120] determined that this process takes on average 15 days (which equals 0.04 year) for cables on the 132-150 kV level and 45 days (which equals 0.12 year) for cables on the 400 kV level. The repair rate, μ, i.e. the number of repairs it is possible to make during a year, is thus for 132-150 kV cables:

$$\mu = \frac{1}{0.04 \, {}^{\text{year}}/_{\text{repair}}} = 24 \, {}^{\text{repair}}/_{\text{year}} \tag{7.8}$$

and for 400 kV cables:

$$\mu = \frac{1}{0.12 \, {}^{\text{year}}/_{\text{repair}}} = 8 \, {}^{\text{repair}}/_{\text{year}} \tag{7.9}$$

7.2.2 Monte-Carlo Simulations

As previously mentioned, the analysis of the reliability of meshed transmission systems is suggested to be performed by using Monte-Carlo simulations. The Monte-Carlo method covers a wide area of numerical simulations of physicals problems which are impossible to solve deterministically, e.g. because the number of possible inputs is incomprehensible.

In Monte-Carlo simulations a numerical representation of the physical system is created and randomly selected (but realistic) values are given as input. For these inputs, the response of the system is calculated deterministically, and the results are analysed. Thereafter a new set of randomly chosen input values are given, and the physical response is calculated, etc. This process is repeated so many times such that it is assumed that the performed calculations are representative for all possible inputs.

In the analysis of meshed power systems, the reliability is dependent on the transmission system's capability of transporting the produced energy

to where it is consumed. Monte-Carlo simulations on meshed transmission systems may thus be divided into two categories.
Firstly, it is possible to investigate the reliability of different load scenarios. In the IEEE 14-bus test network, this will e.g. mean that each load and production unit is assigned a value within it's realistic operational space, where after a load flow calculation is performed. If all loadability constraints, voltage constraints, etc. are respected, the input system values are said to represent a reliable operational state.
This procedure is repeated for many other load and production unit values and when a sufficient amount of simulations have been performed, the reliability indexes of the transmission system can be evaluated.
This way of performing Monte-Carlo simulations does though not necessarily include the possibility of component failure. Why the reliability is only determined for a complete system (i.e. in the 'N' situation).

Secondly, Monte-Carlo simulations can be used for constant load scenarios, such that it is the possibility of component failure which is the modelled parameter. This means that the input parameters to the Monte-Carlo simulation are whether or not each component is in operation (the so called 'system state').
Given this system state, a load flow simulation is performed and it is evaluated if the given operational state of the system is capable of handling the load scenario, i.e. if all loadability limits, voltage limitation, etc. are respected.
Thereafter a new set of input parameters (a new system state) is defined and given as input to the load flow simulation and the procedure is repeated until a sufficient amount of system states have been tested. Given the results of the Monte-Carlo simulation it is possible to evaluate the different reliability indexes.

As this PhD project is not concerned with exhausting the different possibilities of calculating the reliability of power systems, but merely to show that ETC may enhance system performance, the remaining of this chapter will focus only on the analysis of the reliability of the transmission system when taking the failure of components into account. The procedure is discussed in greater detail in the following.

7.2.3 Power System States

In the state space approach to system reliability cables may be seen as being either in operation, 'O', or being in failed state, 'F'. The probability of the cable to go from O to F is equal to the failure rate λ, and in the opposite direction the repair rate, μ.

Because each cable can be in two states, a system such as the two line system (which was discussed in clause 6.2.1) can exist in four different states: *OO* where both cables are operational, *FO* where the first cable is failed, *OF* where the second cable is failed and *FF* where both cables are failed. By assuming that it is possible to move between these state by only changing the state of one component at the time, a so called Markov process, the state space for the two line system looks as shown in figure 7.1, [119].

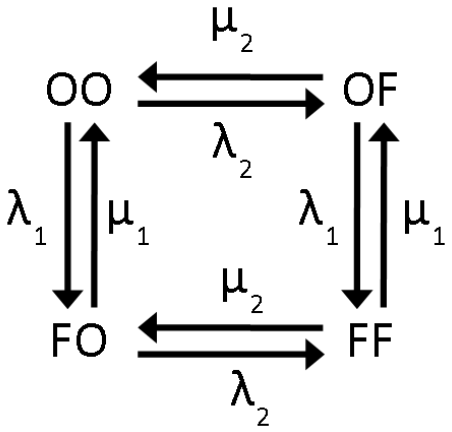

Figure 7.1: State space of a system with two components. It is assumed that each component can be in either operating mode '*O*' or failed mode '*F*', and that the probability of changing from the *O* to the *F* state is equal to the failure rate, λ, and in the opposite direction the repair rate, μ.

The probability that the system is in the different states is, [119], as given in (7.10).

$$\begin{aligned} P_{OO} &= \frac{\mu_1 \cdot \mu_2}{(\lambda_1 + \mu_1) \cdot (\lambda_2 + \mu_2)} \\ P_{OF} &= \frac{\mu_1 \cdot \lambda_2}{(\lambda_1 + \mu_1) \cdot (\lambda_2 + \mu_2)} \\ P_{FO} &= \frac{\lambda_1 \cdot \mu_2}{(\lambda_1 + \mu_1) \cdot (\lambda_2 + \mu_2)} \\ P_{FF} &= \frac{\lambda_1 \cdot \lambda_2}{(\lambda_1 + \mu_1) \cdot (\lambda_2 + \mu_2)} \end{aligned} \tag{7.10}$$

This evaluation can be extended to any amount of components, and it should be noticed that $\sum P = 1$, meaning that the system will always be in one of the defined states.

7.2.3.1 Assessing Reliability of Power Systems

As shown above, calculations of the probability of the different system states can be made easily when failure rates and repair rates are known. However the calculated probabilities will in themselves not give any indication to whether or not the states are acceptable to the TSO and it is therefore necessary to define the criteria for when the system is in an acceptable state.
In the present study, an acceptable system state is defined as a state where all loads are provided with the power they require, all generators are kept below their production limit and lines must not be loaded above their maximum capacity.
In this third criterion the reliability of ETC controlled systems can be distinguished from the current based controlled system, because the maximum allowable load on the individual lines may be different. In the ETC based approach the 40 hours loadability can be calculated and used as the loadability limit, whereas in the current based control the steady state loadability has to be utilised.

Having defined the allowable states, through the evaluation of the results from the load flow calculation, the ASAI of the system can be calculated by summing up the probability of the allowable states.

If e.g. both cables have to be in operation, then:

$$\text{ASAI} = P_{OO} \tag{7.11}$$

But if only one of the cables have to be operational for the system to be in an allowed state, then:

$$\text{ASAI} = P_{OO} + P_{OF} + P_{FO} \tag{7.12}$$

7.3 Reliability of IEEE 14-Bus Test System

In this study, the reliability of the IEEE 14-bus test network will be investigated and the load scenario at 7:00 (before cable failures), as defined in clause 6.3, will be analysed by using static loadability limits and the 40 hours loadability. The system will be considered acceptable if the loading of the individual transmission lines is kept below the limits of table 7.1, if all loads are supplied wit the required power and if the required generation for the individual production units is kept below the limits of table 7.2.

It is seen from the above sections that adding one extra component to the system doubles the amount of possible states. It was therefore chosen to simulate cable failures only and the failure of other components (such as

Start bus	End bus	Steady State Loadability [A]	40 Hours Loadability [A]
1	2	682	1150
1	2	682	1150
1	5	682	1122
2	3	682	1165
2	4	682	1132
2	5	761	997
3	4	682	955
4	5	682	1163
6	11	820	1304
6	11	820	1304
6	12	820	1239
6	13	820	1172
7	8	820	1013
9	10	820	1345
9	10	820	1345
9	14	820	1235
10	11	992	1635
10	11	992	1635
12	13	820	1353
13	14	820	1351

Table 7.1: Steady state and 40 hours loadabilities of cables at 17:00.

Generator	Active Power Limit [MW]
1	1000
2	800
3	750
6	600
8	200

Table 7.2: Defined maximum active power production capacity for the different generators of the IEEE 14-bus test network.

breakers, transformers, etc) is not included in the analysis. As this reliability study is an analysis of the impact of implementing ETC more than an in depth study of specific reliability values, this simplification of the simulations is acceptable.
The 14-bus test network, which consists of 20 cables, will on this background have $2^{20} = 1,048,576$ different possible operational states. In order to calculate the ASAI, this means that more than one million load flow simulations have to be set up, carried out and for each simulation it has to be evaluated if any of the defined limitations has been exceeded.
Such an enormous amount of loadflow calculations are normally not well suited to be carried out in DSPF because of relatively long computational times. However as one of the requirements for the developed ETC package was to use software already available at the TSO it was attempted to simplify the calculations as shown in the following. The described simplifications made it possible to perform the calculation in DSPF, which will enable the TSO to perform reliability assessment of systems which has already been built in DSPF.

The first simplification utilises that the paths from bus 1 to 2, 6 to 11, 9 to 10 and 10 to 11 each consists of two identical parallel lines. The result of a simulation where the first parallel line is operational and the second is failed is on this background assumed to be identical to the situation where the second line is operational and the first is failed.
Secondly, if a simulation with a failed cable is determined to be unacceptable, then it is assumed that all situations where that cable is failed are unacceptable.
In the two-line system these simplifications would e.g. mean that if the state OF is determined unacceptable, then the state FO is also unacceptable because the two lines are parallel and identical. Furthermore, the state FF is also determined to be unacceptable because the cable is also failed in this state. Similarly it is assumed that if state OF is determined to be acceptable, then also FO is acceptable as well as OO.
With these simplifications it is seen that the simple two line system may only require two load flow simulations instead of four, and when summing up the number of lines in the 14-bus test network this will give significant computational time reductions.
In the case of the 14-bus test system, the individual analysis of all 1,048,576 possible states would require more than 1.5 months of simulation time, however by implementing the simplifications, the analysis took less than 10 hours.

It is acknowledged that there may be very specific situations where e.g. two failed lines will result in an acceptable state even when just one of those lines being failed will result in unacceptable system performance. However in order to be able to perform the simulations it was decided that such inaccuracies are acceptable, especially since this chapter is to compare current

based operation with ETC based operation which means that some of these inaccuracies will be evened out.

7.3.1 Results

Performing the load flow analysis for all 2^{20} system states[1], given the simplifications of section 7.3, followed by a reliability assessment of the individual states, results in two simple ASAI values.

The ASAI of the system, when having static loadability limits for the cables, is:

$$\mathrm{ASAI}_{\mathrm{Current}} = 0.864 \tag{7.13}$$

And the ASAI when using the ETC approach (40 hours loadability):

$$\mathrm{ASAI}_{\mathrm{ETC}} = 0.897 \tag{7.14}$$

In basic (7.13) and (7.14) mean that the fraction of time where the system is fully functioning increases from 86.4 % to 89.7 % when shifting from current based operation to ETC based operation, which is an increase in operational time of almost 4 %. If such an increased reliability should come through grid enhancements it would cost a substantial amount of money but, as shown, ETC can give this increase by simply monitoring the system properly.

It is acknowledged that the ASAIs of the investigated test scenario are low. This probably means that the system is harder loaded than what would be the Danish standard, but again it is emphasised that the reliability study is performed to compare current based operation with ETC based operation and in this respect the test case clearly shows the possible benefits of ETC as it increases the ASAI significantly.

7.4 Discussion of Reliability of Meshed Transmission Systems

This chapter has shown that the TSO will experience increased reliability of the transmission system when operating the system based on ETC as

[1] It should be noted that having performed the analysis for all possible states means that the performed calculations are not Monte-Carlo simulations. This is because Monte-Carlo simulations inherently only performs the calculations on a sample of the total number of states and provides results based on this sample. However it should be recognised that Monte-Carlo simulations may be used for systems which are too large for the suggested, exhaustive, procedure to be carried out, and reliability indexes may thus be estimated for systems of all sizes.

compared to the presently used current based operation. As it has also been shown in this chapter, reliability can be expressed by many different indexes. The present study has focussed on the evaluation of the Average System Availability Index (ASAI), which is a measure for how much of the time the system performs to an acceptable level.

As discussed, the ASAI does not show the full picture of the system reliability which would require other reliability indexes to be calculated as well. However the ASAI shows clearly the potential of ETC and the results can be utilised in a number of ways. Firstly, it can be used in the argumentation for implementing ETC as it increases flexibility in system operation. Secondly, it can be used for postponing, or mitigating the need for, grid enhancements. The latter can be of significant importance as TSOs have goals for system performance, e.g. goals for the value of the ASAI, and by implementing ETC this goal may be maintained even if the $\text{ASAI}_{\text{Current}}$ is lower than required.

Chapter 8

Economic Benefits by Implementing Electrothermal Coordination

The final analysis of this project is an assessment of the possible economical benefits by implementing ETC in the decision processes at the TSO.

Because the economical aspects of real time operation, day-ahead planning and system expansion planning are very different, the present chapter has been divided into three sections each explaining the possible economic benefits of the different areas of expertise.

8.1 Real Time Operation

As stated, the real time control of the transmission system is, in case of contingencies, more concerned with system performance than costs. Discarding the market during real time operation may therefore become very costly and the economic potential in ETC may therefore be significant.

In the example of clause 6.2.1 transmission line TL2 fails, where after the operator is forced to disconnect transmission line TL1 after 1 hour when controlling the system based on the static current limitations. This means that the operator will have to increase the production of G2, however as this is a smaller scale production unit it may be limited to the maximum of 200 MW and the operator will thus have to perform load shedding to the extend where the loading of TL1 decreases to the steady state loadability.

As the contingency happens after the market is settled, it is not possible to purchase voluntary loads to be shed, and the operator must thus force some load shedding.
By assuming that the generator G2 can produce 200 MW constantly over the day and that the loading of the line TL1 is kept constantly at the loadability of 839 A, the operator needs to shed load as shown in figure 8.1.

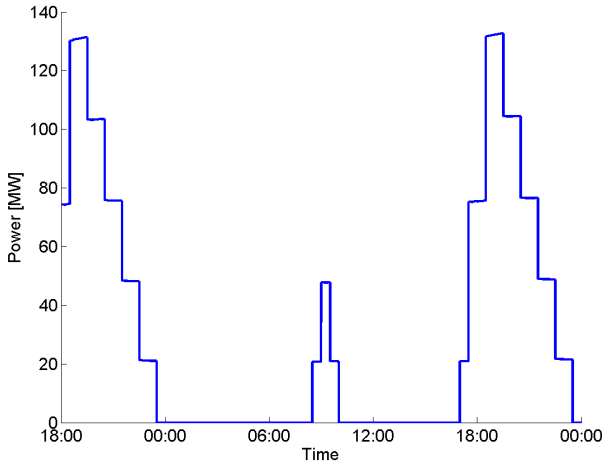

Figure 8.1: Required load shedding in the two line case study of clause 6.2.1 when the system control is based on static current limits.

Integrating this over the day with an assumed prices of 300 DKK/MWh, [121][1], the shed load costs 279157 DKK over the first 30 hours where the operator must act out of the market.
Each additional 24 hours, the operator needs to find 509 MWh to be shed, and these will obviously also contribute to the total cost of the contingency.

In addition to these costs, production unit G2 must be more expensive than G1 as it otherwise would produce at full capacity constantly. This means that the added costs of moving the production can be found by multiplying the price difference between G1 and G2 to the increased production of G2.

8.2 Day-Ahead Planning

In the day-ahead market planning, the economical benefits of ETC can be measured by the lower required production reserves.

[1] As seen in the reference there are significant variations in the price of power and in order to give conservative estimations of the benefits of ETC, a low power price of 300 DKK/MWh has been used in this chapter.

In the case study of clause 6.2.2, the present current based operation of transmission systems would require forcing (against the market) an increased power production on the Funen side in order to maintain N-1 reliability. This forced production is to be bought on the day-ahead market and the extra power required to be produced on the Funen side is calculated based on the steady state loadability of the 150 kV underground cable.
Given the steady state loadability of 645 A, the underground cable system is capable of handling 168 MVA, which means that the predicted lack of power on the Funen side looks as shown in figure 8.2.

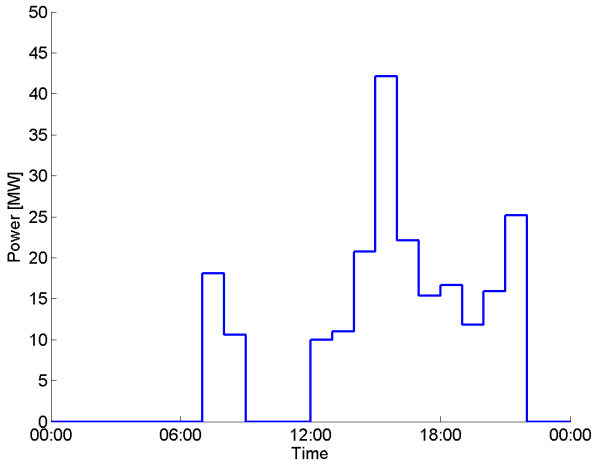

Figure 8.2: Required extra power to be produced on the Funen side when the transmission system operation is based on static current limits. This extra power must be produced in order to maintain N-1 reliability during maintenance of one of the 400 kV lines.

At an assumed regulating price of 300 DKK/MWh, [122], this required increased power generation on the Funen side costs 65831 DKK per day.

8.3 Future Grid Planning

The calculation of the economical benefits from this area is straight forward. In the example shown in clause 6.2.3 ETC enables the TGP to avoid investing in an additional 132 kV cable line. The costs associated with purchasing and installing a high voltage cable is not well defined as it may vary significantly over time. Furthermore, high voltage cables are not given in price lists as each cable is designed specifically for the individual projects. However making the rough assumption that a 132 kV cable installation costs around 3-4 million DKK pr. km including everything, [123], the savings on the BOR-VAL line, which is approximately 15 km, is 45-60 million DKK.

It is recognised that the savings become smaller when including the lower losses of transporting power from BOR to VAL, however such losses will only account for thousands of DKK each year and never add up to millions of DKK even over a 30-50 years period which may be the lifetime of such cables.

In addition to determining if new transmission lines are necessary, ETC might be utilised to minimise the conductor cross section of the lines which have to be build. In [123] it is suggested that the installation of (including everything) a 1200 mm^2 and 2000 mm^2 cable system costs approximately 3 million DKK/km and 4 million DKK/km respectively.
Assuming that the utilisation of ETC enables just 10 % of the planned 723.4 km cables of 2000 mm^2 to be build as 1200 mm^2 instead, a cost reduction of more than 72 million DKK can be obtained without jeopardising the reliability of the grid. Again it should be noted that lowering the cross section of a transmission line will increase the losses which will lead to a lower economic gain.

8.4 Discussion of Economical Benefits of ETC

As it has been shown in this chapter, a substantial amount of money can be saved by implementing ETC in the real time operation, day-ahead planning and in the planning of the future grid design. This chapter presents rough estimations of possible cost savings when utilising ETC on a number of cases, however it should be recognised that, just as all other benefits, ETC will not come totally cost free.
The system has to be implemented into the Danish TSO, and the quality of the algorithms tested, which both has a certain price. In addition ETC has to be maintained after installation which will also require resources. Furthermore, utilising ETC will most probably cause a harder loading of the individual transmission lines which will lead to higher losses. Such losses can be capitalised, and these costs must be included in the decision process. However given that ETC will give a much clearer overview, as well as deeper insight, into the state of the transmission system, the TSO should be able to utilise ETC in an asset management perspective as part of the total lifetime cost assessment.

It should be noted that the goal of the present PhD project was not to give accurate predictions of the cost savings when implementing ETC, but first of all to develop the tools which makes ETC possible. Thereafter this chapter has proven that not only will the engineers benefit from ETC by an increased operational flexibility of the transmission system, also the economists will now be able to justify ETC as the concept for the future operation of the

Danish transmission system.

PART V

Concluding Remarks

This part concludes the thesis by summarising and discussing the findings, analysing the limitations in the developed methodologies and giving proposals to further work to be performed within the area of dynamic loadability of cable based transmission systems.

Chapter 9

Conclusion

In the effort to enhance utilisation of the future almost entirely undergrounded transmission grid, the Danish TSO, Energinet.dk, initiated this PhD project with the main focus of developing a concept for using dynamic calculations of temperature and loadability of transmission cables in different decision processes within the company.

The project was divided into three main subjects. Firstly, an investigation of how loadability and temperature of individual transmission cables can be evaluated dynamically, i.e. a point-to-point perspective. Secondly, the knowledge about the thermal behaviour of individual power cables was utilised to define and develop a concept for dynamic loadability of transmission grids. Finally, it was shown that the developed concept enables a higher utilisation of the grid without jeopardising reliability as well as it was shown that there might be significant economic incentives to implement the tools.

9.1 Summary of PhD Project

The project has investigated the design and material limitations of high voltage power cables, searching for the possibility of enhancing utilisation of the individual cable lines. It is found that cable loading is limited by the insulation temperature and as the insulation is in close contact with the conductor, this limitation, which for XLPE insulation is 90 °C, is enforced on the conductor as well. However as a high jacket temperature has been

experienced to create a dry band around the cables, the jacket temperature is normally defined as the load limiting property. It is found in this study that the standardised suggested jacket temperature limit of 50 °C may be too conservative for some installations and it can thus possibly be increased to 60 °C instead.

The analysis of cable materials as well as design and installation of transmission cables furthermore lead to the conclusion that a significant amount of thermal inertia is available for power cables and that this thermal inertia may be utilised to load the cables in a more dynamic way than presently done. In order to obtain knowledge about the available dynamic current carrying capacity it is necessary to model the cable temperature and this study therefore has investigated and compared several different thermal models. It was after due considerations decided to use the thermoelectric equivalent (TEE) model for the calculation of the temperature as well as for the calculation of the cables' loadability. This choice was made as TEEs showed the best compromise between speed and accuracy of the investigated models.
The accuracy of the thermal model is verified by a large scale laboratory experiment, where three 245 kV cables in flat formation were exposed to a varying load profile over more than four months. Through the experiment it was shown that when having measurements of the temperature in close proximity to the cable available, it is possible to model the conductor temperature with an accuracy of ± 2 °C. It is also shown that measurements of the temperature are not a necessity but they will allow for increased accuracy of the model.

The chosen thermal model is in this project integrated with the power systems analysis software DigSilent PowerFactory (DSPF) such that the TSO becomes capable of following the dynamic thermal state of the system in real time as well as capable of predicting the future thermal evolution. The electrical calculation of the grid (load flow calculations) combined with thermal modelling (TEE) performs the backbone of the proposed concept for utilising the dynamic loadability and it is thus denoted electrothermal coordination (ETC).

Through the close integration of load flow calculations and thermal modelling, the real time operator of the transmission system gains an in depth knowledge of the state of the system and, in case of contingencies, this knowledge can be utilised in deciding whether the system can be allowed to run or if interfering actions are necessary.
Furthermore, the day-ahead planning of the transmission system may also benefit from ETC. In Denmark, the electric energy market is settled at 12:00 (noon), for the power which is to be delivered from 0:00 to 24:00 on the next day. It is proposed that load flow studies are carried out on each of the hourly intervals from 0:00 to 24:00. By extracting the flow of power in the

system from these load flow studies it is possible to predict the temperature evolution in all cables for the coming day of operation. Today the settled power market is allowed to run without interference if the loading is kept below the steady state loadability in case of a contingency (the N-1 condition). However in this thesis it is suggested that ETC is used to calculate, for each individual cable, the current which the cable is capable of carrying continuously for 40 hours without exceeding the maximum jacket temperature. This 40 hours loadability is suggested to be used when assessing if the N-1 condition is respected instead of the steady state loadability.
In addition to this, it is also suggested in this PhD project that the TSO can use ETC in the planning of future grid enhancements. Today cables are dimensioned such that they are capable of carrying the current which the cable will subjected to when the grid experiences two simultaneous component outages. However with ETC it is shown that the TSO can utilise the dynamic capabilities of the power cables to minimise the cross section of the conductor or possibly even avoid such investments.

Case studies of several different fabricated and real life grids shows that significant technical benefits may be obtained when implementing ETC. Amongst others an adapted version of the IEEE 14-bus test system is shown to be capable of sustaining several outages without the need to interfere when operating the system based on ETC. On the other hand it is shown that if the system is operated based on static current limitations the TSO might experience a blackout.
The present study also shows, that ETC is capable of increasing the reliability of transmission systems. In specific it is shown that the fraction of time where the transmission system will be fully functioning can be increased significantly when using the 40 hours loadability as the operational limit, instead of the steady state loadability.

As it is acknowledged that technical benefits are not necessarily sufficient to ensure the decision of implementing ETC, this thesis briefly shows that significant cost savings can be obtained, simply because of the increased awareness of the state of the system which ETC enables.

9.2 Scientific Contributions

It should be recognised that this thesis has presented a number of novel scientific contributions where the most pronounced are given in the following.

- The proposed mathematical approach to solving the differential equation systems (the TEE method), has been enhanced such that it has become straight forward to use. As the TEE solution method has

shown good characteristics compared to other solution strategies it is worth considering in future applications. The zone based approach of TEEs furthermore creates the possibility of assigning different thermal properties to each zone and thereby possibly giving a more accurate thermal model.

- Furthermore, the moisture dependence of the specific heat of sand and soil is implemented in a way which has not previously been seen.

- The present project has also raised the awareness that heavy precipitation can cause cooling of the cables which cannot be modelled with conventional methods.

- Moreover an algorithm for the calculation of the dynamic loadability has been proposed such that an assessment of how long the real time loading of a cable may be allowed, can easily be made.

- The most significant contribution of this PhD project is though the integration of the thermal models with the load flow simulations which in this project is denoted electrothermal coordination (ETC). This includes the definition of the 40 hours loadability which enables a significant increased utilisation of the transmission grid. Furthermore, the way of using thermal models in the design of new grid components may also be considered a novelty.

9.3 Limitations of Project and Further Work

It has been the goal of this PhD project to develop the ETC concept and in this way show how calculations of the dynamic thermal behaviour of power cables can be utilised in transmission grid operation. The study has therefore not been concerned with transformers, breakers, etc. and as these components are connected in series with the cables they may, also in the dynamic perspective, set further restrictions to the loadability. Further work within this field is thus required, which would include analysis and development of dynamic thermal models for such components.

The above limitation also applies to joints, cables in air, as well as other cable hotspots, which cannot be analysed easily with the TEE method. For such installations FEM modelling may be necessary, however as FEM simulations have only been briefly mentioned in this thesis, further work is required.

The concepts and algorithms presented in this thesis have been developed with the scope of implementation in the Danish TSO which e.g. means that only cables in flat formation have been investigated. Further verification

of the accuracy of the models, when subjected to trefoil formation, etc., is suggested before direct application to such installation.

Moreover, in the analysis of the thermal behaviour of power cables, the proposed TEE method assumes a constant ratio between the moisture contents of the surrounding sand and soil. Further work within the analysis of this topic is required. It is proposed that moisture content data from real cable trenches is obtained in order to increase the knowledge within this area, as well as an investigation of the possibility of developing a dynamic moisture content model for the surroundings would be of significant interest.

Furthermore, when implementing the ETC concept it must be considered how to adjust the protection relays. If these relays are set such that they will trip even when ETC shows that the line temperature is still low, the ETC concept cannot be utilised fully. The development of a plan for the implementation is thus necessary, such that these practical concerns can be addressed.

In relation to the implementation of ETC, it should also be considered how to perform dynamic thermal modelling of cables which do not have DTS monitoring. As stated in this thesis a model with static thermal properties can be utilised, however the uncertainties related to the hotspot location, thermal properties of the environment, etc. must be considered when using this method.

In addition, the reliability assessment has, as described, been based on the assumption that if the system is in an unacceptable state when line 'x' is failed, then all states where that line is failed are defined as unacceptable. This assumption may not be entirely accurate, and further work in the analysis of reliability assessment of meshed power systems is required.

This PhD project has shown a way for using thermal calculations in the design and operation of transmission systems and the author suggests that this topic in general is further investigated in the future. It would e.g. be beneficial to gain hands on experience with the integration of ETC in the Danish transmission system, hereunder an evaluation of the practical issues will be of significant interest to both the scientific community as well as TSOs.

Bibliography

[1] Energinet.dk, "Cable action plan," Energinet.dk, Tech. Rep., March 2009.

[2] ——, "Forskønnelse af 400 kv-nettet," Energinet.dk, Tonne Kjærsvej 65, 7000 Fredericia, Denmark, Tech. Rep., March 2009, in collaboration with: Århus, Odense and Roskilde Miljøcentre and By- og Landskabsstyrelsen. ISBN: 978-87-90707-64-4. Only in danish.

[3] E. F. Peschke and R. v. Olshausen, *Cable Systems for High and Extra-High Voltage*. Pirelli, 1999.

[4] G. F. Moore, *Electric Cables Handbook*, 3rd ed. Kurfürstendamm 57, 10707 Berlin, Germany: Blackwell Science KK, 1997.

[5] W. A. Thue, *Electrical Power Cable Engineering*. Hutgasse 4, Postfach 812, CH-4001 Basel, Switzerland: Marcel Dekker, Inc., 1999.

[6] T. Worzyk, *Submarine Power Cables - Design, Installation, Repair, Environmental Aspects*, ser. Power Systems. Springer, 2009.

[7] nkt cables, "Produktkatalog elforsyning 2010," nkt cables, Tech. Rep., 2010, from: http://www.nktcables.dk/Downloads/GetMaterial.aspx.

[8] International Electrotechnical Commission - IEC, "Publication 60287-1-1. electric cables - calculation of the current rating - current rating equations (100 % load factor) and calculation of losses - general," International Electrotechnical Commission - IEC, Tech. Rep., 2006.

[9] ——, "Publication 60853-1. calculation of the cyclic and emergency current rating of cables - cyclic rating factor for cables up to and including 18/30 (36) kv," International Electrotechnical Commission - IEC, Tech. Rep., 1985.

[10] G. J. Anders, *Rating of Electric Power Cables - Ampacity Computations for Transmission, Distribution and Industrial Applications*, 1st ed. IEEE Press, 1997.

[11] X. Qi and S. Boggs, "Thermal and mechanical properties of epr and xlpe cable compounds," *IEEE Electrical Insulation Magazine*, vol. 22, no. 3, pp. 19–24, May/June 2006.

[12] R. Eiichhorn, "A critical comparison of xlpe-and epr for use as electrical insulation on underground power cables," *IEEE Transactions on Electrical Insulation*, vol. EI-16, no. 6, pp. 469–482, December 1981.

[13] H. St-Onge, "Research to determine the acceptable emergency operating temperatures for extruded dielectric cables," EPRI, Tech. Rep., 1978.

[14] T. De-min, L. Yongkang, and L. Xuezhong, "Dielectric behaviours of cross-linked polyethylene (xlpe) impregnation with compressed sf_6," in *Proceedings of the 4th International Conference on Properties and Applications of Dielectric Materials*, July 1994, pp. 355–358.

[15] C. Green, A. Vaughan, G. Stevens, S. Sutton, T. Geussens, and M. Fairhurst, "On the temperature dependence of electrical and mechanical properties of recyclable cable insulation materials based upon polyethylene blends," in *Annual report - Conference on Electrical Insulation and Dielectric Phenomena*, 2011, pp. 36–39.

[16] M. Nedjar, "Effect of thermal aging on the electrical properties of crosslinked polyethylene," *Journal of Applied Polymer Science*, vol. 111, pp. 1985–1990, 2009.

[17] Y. Mecheri, L. Boukezzi, A. Boubakeur, and M. Lallouani, "Dielectric and mechanical behavior of cross-linked polyethylene under thermal ageing," in *2000 Conference on Electrical Insulation and Dielectric Phenomena*. IEEE, 2000, pp. 560–563.

[18] G. Montanari and A. Motori, "Thermal endurance evaluation of xlpe insulated cables," *Journal of Physics D: Applied Physics*, vol. 24, no. 7, pp. 1172–1181, 1991.

[19] G. Mazzanti and G. C. Montanari, "A comparison belween xlpe and epr as insulating materials for hv cables," *IEEE Transactions on Power Delivery*, vol. 23, no. 1, pp. 15–28, January 1997.

[20] International Electrotechnical Commission - IEC, "Publication 60840 - power cables with extruded insulation and their accessories for rated voltages above 30 kv (u_m=36 kv) up to 150 kv (u_m=170 kv) - test

methods and requirements," International Electrotechnical Commission - IEC, Tech. Rep., 2011.

[21] C. Kittel and H. Kroemer, *Thermal Physics*, 2nd ed. Freeman, 1980.

[22] H. D. Baehr and K. Stephan, *Heat and Mass Transfer*, 2nd ed. Springer, 2006.

[23] O. G. M. P. P. Khramtsov, *Free-Convective Heat Transfer*. Springer, 2005.

[24] O. Christensen, *Differentialligninger og uendelige rækker*. Polyteknisk Boghandel og Forlag, 2006, in Danish.

[25] Institute of Electrical and Electronics Engineers - IEEE, "Ieee standard power cable ampacity tables," IEEE - Institute of Electrical and Electronics Engineers, 3 Park Avenue, New York, NY 10016-5997, USA, Tech. Rep., June 2006.

[26] International Electrotechnical Commission - IEC, "Publication 60287-1-2. current rating equations (100 %load factor) and calculation of losses - sheat eddy current loss factors for two circuits in flat formation," International Electrotechnical Commission - IEC, Tech. Rep., 1993.

[27] ——, "Publication 60287-1-3. current rating equations (100 % load factor) and calculation of losses - current sharing between parallel single-core cables and calculation of circulating current losses," International Electrotechnical Commission - IEC, Tech. Rep., 2002.

[28] ——, "Publication 60287-2-1. electric cables - calculation of the current rating - thermal resistance - calculation of thermal resistance," International Electrotechnical Commission - IEC, Tech. Rep., 2006.

[29] ——, "Publication 60287-2-2. thermal resistance - a method for calculating reduction factors for groups of cables in free air, protected from solar radiation," International Electrotechnical Commission - IEC, Tech. Rep., 2006.

[30] ——, "Publication 60287-3-1. electric cables - calculation of the current rating - sections on operating conditions - reference operating conditions and selection of cable type," International Electrotechnical Commission - IEC, Tech. Rep., 2006.

[31] ——, "Publication 60287-3-2. electric cables - calculation of the current rating - sections on operating conditions - economic optimization of power cable size," International Electrotechnical Commission - IEC, Tech. Rep., 2006.

[32] ——, "Publication 60287-3-3. electric cables - calculation of the current rating - sections on operating conditions - cables crossing external heat sources," International Electrotechnical Commission - IEC, Tech. Rep., 2006.

[33] ——, "Publication 60853-2. calculation of the cyclic and emergency current rating of cables - cyclic rating of cables greater than 18/30 (36) kv and emergency ratings for cables of all voltages," International Electrotechnical Commission - IEC, Tech. Rep., 1989.

[34] ——, "Publication 60853-2. calculation of the cyclic and emergency current rating of cables - cyclic rating factor for cables of all voltages, with partial drying of the soil," International Electrotechnical Commission - IEC, Tech. Rep., 2002.

[35] G. Nikishkov, *Introduction to the Finite Element Method*, UCLA, 2001, lecture Notes, UCLA.

[36] A. Öchsner and M. Merkel, *One-Dimensional Finite Elements An Introduction to the FE Method*. Springer, 2013.

[37] J. Chaskalovic, *Finite Element Methods for Engineering Sciences - Theoretical Approach and Problem Solving Techniques*. Springer, 2008.

[38] G. J. Anders, *Rating Of Electric Power Cables In Unfavourable Thermal Environment*, 1st ed. 111 River Street, Hoboken, NJ 07030: John Wiley & Sons, Inc, 2005.

[39] G. Williams and L. Gold, "Ground temperatures," National Research Council Canada, Tech. Rep., July 1976.

[40] B. M. Weedy and J. P. Perkins, "Steady-state thermal analysis of a 400 kv-cable through joint," in *Proceedings of the Institution of Electrical Engineers*. IEE, January 1967, pp. 109–115, vol. 114, No. 1.

[41] J. Ruiter and A. Thus, "Cooling of oil-filled cable joints using heat pipes," in *IEE Proceedings Generation, Transmission and Distribution*. IEE, 1984, pp. 340–348, vol. 131, No. 7.

[42] S. Nakamura, S. Morooka, and K. Kawasaki, "Conductor temperature monitoring system in underground power transmission xlpe cable joints," *IEEE Transactions on Power Delivery*, vol. 7, no. 4, pp. 1688–1697, October 1992.

[43] J. A. Pilgrim, D. J. Swaffield, P. L. Lewin, S. T. Larsen, and D. Payne, "Assessment of the impact of joint bays on the ampacity of high-voltage cable circuits," *IEEE Transactions on Power Delivery*, vol. 24, no. 3, pp. 1029–1036, July 2009.

[44] M. Chaaban and J. Leduc, "Reduction in current carrying capacity due to cables crossing," in *8th International Conference on Insulated Power Cables*, July 2011, paper id: C.8.4.

[45] Éric Dorison and G. Anders, "Current rating of cables installed in deep or ventilated tunnels," in *8th International Conference on Insulated Power Cables*, 2011.

[46] G. J. Anders, M. Coates, and M. Chaaban, "Ampacity calculations for cables in shallow troughs," *IEEE Transactions on Power Delivery*, 2010.

[47] J. A. Pilgrim, P. L. Lewin, S. T. Larsen, F. Waite, and D. Payne, "Rating of cables in unfilled surface troughs," *IEEE Transactions on Power Delivery*, vol. 27, no. 2, pp. 993–1001, April 2012.

[48] E. Dorison, G. J. Anders, and F. Lesur, "Ampacity calculations for deeply installed cables," *IEEE Transactions on Power Delivery*, vol. 25, no. 2, pp. 524–533, April 2010.

[49] W. Moutassem and G. J. Anders, "Configuration optimization of underground cables for best ampacity," *IEEE Transactions on Power Delivery*, vol. 25, no. 4, pp. 2037–2045, 2010.

[50] M. Zubert, G. J. Anders, A. Napieralski, and A. Skorek, "Rating of pipe-type cables with slow circulation of dielectric fluid," *IEEE Transactions on Industry Applications*, vol. 43, no. 5, pp. 1164–1171, 2007.

[51] Cymcap, http://www.electrical-powersystems.com/product_5_cymcap.htm, November 2010.

[52] ABB, "Network manager scada/dms," ABB, SE-721 82 Västerås, Sweden, Tech. Rep., 2009, www.abb.com/networkmanagement.

[53] Areva T&D, "e-terraplatform - the power to adapt!" http://www.areva-td.com/solutions/liblocal/docs/1025787446713-ePlatform_1042.pdf, 2005.

[54] General Cable, "High- and extra-high-voltage global cable system solutions," http://www.generalcable.com/NR/rdonlyres/77BB059A-77D9-4EAE-BE55-B7C3661DB89F/0/GEN37727SilecBrochure_FA.pdf, 4 Tesseneer Drive, Highland Heights, Kentucky 41076-9753, USA, 2010.

[55] Nexans, "Nexans norway offers cablesense - a versatile cable monitoring system," Nexans Norway AS, Innspurten 9, P.O. Box 6450 Etterstad, 0663 Oslo, Norway, 2010.

[56] E. Jacobsen, J. F. Nielsen, S. B. Nielsen, S. T. Salwin, A. S. Jensen, W. Nolden, K.-H. Cohnen, A. Mohrs, and S. Seier, "Dynamic rating of transmission cables," in *2010 Cigre Session Papers´*. 21, rue d'Artois, F-75008 Paris: Cigre, 2010, b1-101-2010.

[57] Siemens Energy, November 2010, http://www.energy.siemens.com/us/en/automation/power-transmission-distribution/control-center-and-energy-management-solutions/spectrum-power-3.htm.

[58] Top Cable, http://www.topcable.es/topmatic.php, November 2010.

[59] USAmp+, http://www.usi-power.com/Products\%20&\%20Services/USAmp/USAmp.htm, November 2010.

[60] W. G. . of Study Commitee 21, "Calculation of temperatures in ventilated cable tunnels," *Eltra*, vol. 143, no. 5, 1992.

[61] ——, "Calculation of temperatures in ventilated cable tunnels - appendices i-iv," *Eltra*, vol. 144, no. 6, 1992.

[62] M. Sakata and S. Iwamoto, "Genetic algorithm based real-time rating for short-time thermal capacity of duct installed power cables," in *Proceedings of the International Conference on Intelligent Systems Applications to Power Systems, ISAP*, 1996, pp. 85–90.

[63] G. Anders, A. Napieralski, M. Zubert, and M. Orlikowski, "Advanced modeling techniques for dynamic feeder rating systems," *IEEE Transactions on Industry Applicaitons*, vol. 39, no. 3, pp. 619–626, 2003.

[64] G. J. Anders and H. Brakelmann, "Improvement in cable rating calculations by consideration of dependence of losses on temperature," *IEEE Transactions on Power Delivery*, vol. 19, no. 3, pp. 919–925, July 2004.

[65] S.-H. Huang, W.-J. Lee, and M.-T. Kuo, "An online dynamic cable rating system for an industrial power plant in the restructured electric market," *IEEE Transactions in Industry Applications*, vol. 43, no. 6, pp. 1449–1458, November/December 2007.

[66] T. Igi, H. Komeda, and S. Mashio, "Study of the dynamic rating of a 138kv xlpe cable system by optical fiber monitoring," in *8th International Conference on Insulated Power Cables*, July 2011, paper id: C.9.4.

[67] H. Li, "Assessment of underground cable ratings based on distributed temperature sensing," *IEEE Transactions on Power Delivery*, vol. 21, no. 4, pp. 1763–1769, 2006.

[68] Z. S. Tseng, "Systems of first order linear differential equations," http://www.math.psu.edu/tseng/class/Math251/Notes-LinearSystems.pdf, March 2013.

[69] R. Olsen, J. Holboll, and U. Gudmunddóttir, "Dynamic temperature estimation and real time emergency rating of transmission cables," in *IEEE Power & Energy Society General Meeting*. IEEE, July 2012.

[70] R. Olsen, G. Anders, J. Holboell, and U. Gudmundsdottir, "Modelling of dynamic transmission cable temperature considering soil specific heat, thermal resistivity and precipitation," *IEEE Transactions on Power Delivery*, vol. 28, no. 3, pp. 1909–1917, 2013.

[71] P.L.Lewin, J.E.Theed, A.E.Davies, and S.T.Larsen, "Method for rating power cables buried in surface troughs," in *IEE Proceedings Generation, Transmission and Distribution*, 1999, pp. 360–364, vol. 146, No. 4.

[72] T. Kusuda and P. Achenbach, "Earth temperature and thermal diffusivity at selected stations in the united states," National Bureau of Standards, Tech. Rep., June 1965.

[73] J. Lyall, G. Nourbakhsh, and H. Zhao, "Underground power cable environment on-line monitoring & analysis," *Proceedings of the IEEE Power Engineering Society Transmission and Distribution Conference*, vol. 1, pp. 457–462, 2000.

[74] A. Blackwell, A. Davics, and C. Ong-Hall, "Forecasting cable ratings using a probabilistic method and real time parameter values," *AC and DC Power Transmission*, pp. 81–85, April 1996.

[75] D. Parmar and J. Steinmanis, "Underground cables need a proper burial," *Transmission & Distribution World*, vol. 55, no. 4, pp. 44–51, 2003.

[76] G. Groenveld, A. Snijders, G. Koopmans, and J. Vermeer, "Improved method to calculate the critical conditions for drying out sandy soils around power cables," in *IEE Proceeding Generation, Transmission and Distribution*, 1984, pp. 42–53.

[77] D. D. Vries, "The theory of heat and moisture transfer in porous media revisited," *International Journal of Heat and Mass Transfer*, vol. 30, no. 7, pp. 1343–1350, 1987.

[78] G. Parise and L. Martirano, "Circuits operation control and overloads protection: Power cables equivalent ampacities," *IEEE Transactions on Industry Applications*, vol. 30, no. 1, pp. 22–29, February 2000.

[79] O. E. Gouda, G. M. Amer, and A. Z. E. Dein, "Effect of dry zone formation around underground power cables on their ratings," *International Journal of Emerging Electric Power Systems*, vol. 10, no. 3, 2009.

[80] O. Gouda, A. E. Dein, and G. Amer, "Effect of the formation of the dry zone around underground power cables on their ratings," *IEEE Transactions on Power Delivery*, vol. 26, no. 2, pp. 972–978, April 2011.

[81] H. Brakelmann and G. Anders, "Ampacity reduction factors for cables crossing unfavourable regions," *IEEE Transactions on Power Delivery*, vol. 16, no. 4, pp. 444–448, October 2001.

[82] K. Ferkal, M. Poloujadoff, and E. Dorison, "Proximity effect and eddy current losses in insulated cables," *IEEE Transactions on Power Delivery*, vol. 11, no. 3, pp. 1171–1178, July 1996.

[83] B. Novák and L. Koller, "Current distribution and losses of grouped underground cables," *IEEE Transactions on Power Delivery*, vol. 26, no. 3, pp. 1514–1521, July 2011.

[84] J. Basinger, G. Kluitenberg, J. Frank, P. Barnes, and M. Kirkham, "Laboratory evaluation of the dual-probe heat pulse method for measuring soil water content," *Vadosa Zone Journal*, vol. 2, no. 3, pp. 389–399, 2003.

[85] S. a Schlumberger company, "Ultra," http://www.sensa.org/cat_view/3-ultra?ascdesc=DESC&orderby=dmdatecounter, April 2013, ultra DTS-system Data Sheet.

[86] J. Glover, M. Sarma, and T. Overbye, *Power System - Analysis and Design*, 4th ed. Nelson Engineering, 2007.

[87] A. von Meier, *Electric Power Systems - A Conceptual Introduction*. John Wiley & Sons, Inc., 2006.

[88] P. Kundur, *Power System Stability and Control*. McGraw-Hill, 1994.

[89] K. Purchala, L. Meeus, D. V. Dommelen, and R. Belmans, "Usefulness of dc power flow for active power flow analysis," in *2005 IEEE Power Engineering Society General Meeting*. IEEE PES, 2005, pp. 454–459.

[90] D. V. Hertern, J. Verboornen, K. Purchala, R. Belmans, and W. L. Kling, "Usefulness of dc power flow for active power flow analysis with flow controlling devices," in *The 8th IEE International Conference on AC and DC Power Transmission*, 2006, pp. 58–62.

[91] R. V. Amarnath, "Design and development of cluster algorithms for power system problems," Ph.D. dissertation, Jawaharlal Nehru Technological University of Hyderabad, March 2012.

[92] K.S.Pandya and S.K.Joshi, "A survey of optimal power flow methods," *Journal of Theoretical and Applied Information Technology*, vol. 4, no. 5, pp. 450–458, 2005.

[93] A. Mohapatra, P. Bijwe, and B. Panigrahi, "Optimal power flow with multiple data uncertainties," *Electric Power Systems Research*, vol. 95, pp. 160–167, 2013.

[94] J. Carpentier, "Optimal power flows," *International Journal of Electrical Power and Energy Systems*, vol. 1, no. 1, pp. 3–15, 1979.

[95] B. H. Chowdhury, "Toward the concept of integrated security: optimal dispatch under static and dynamic security constraints," *Electric Power Systems Research*, vol. 25, pp. 213–225, 1992.

[96] E. Vaahedi, Y. Mansour, C. Fuch, S. Granville, M. de Lujan Lator, and H. Hamadanizade, "Dynamic security constrained optimal power flow/var planning," *IEEE Transactions on Power Systems*, vol. 16, no. 1, pp. 38–43, February 2001.

[97] V. R. Vinnakota, B. Brewer, D. Atanackovic, A. Steed, G. Dwernychuk, and D. Cave, "Implementation of opf as a supportive system voltage control tool in real-time for british columbia transmission network," in *IEEE Power & Energy Society General Meeting*, 2010.

[98] A. Vargas and M. E. Samper, "Real-time monitoring and economic dispatch of smart distribution grids: High performance algorithms for dms applications," *IEEE Transactions on Smart Grid*, vol. 3, no. 2, pp. 866–877, June 2012.

[99] NERC, "Available transfer capability definitions and determination," North American Electric Reliability Council, Tech. Rep., June 1996.

[100] G. Luo, D. Shi, J. Chen, J. Xi, M. Jiang, Y. Xu, and J. Dang, "Fast calculation of available transfer capability in bulk interconnected grid," in *IEEE Power & Energy Society General Meeting 2012*. IEEE, 2012.

[101] X. Tong, F. F. Wu, and L. Qi, "Available transfer capability calculation using a smoothing pointwise maximum function," *IEEE Transactions on Circuit and Systems - I: Regular Papers*, vol. 55, no. 1, pp. 462–474, February 2008.

[102] A. Kumar and J. Kumar, "Atc determination with facts devices using ptdfs approach for multi-transactions in competitive electricity markets," *Electrical Power and Energy Systems*, vol. 44, pp. 308–317, 2013.

[103] M. Mahmoudian and G. R. Yousefi, "Atc improvement and losses estimation considering dynamic transmission line ratings," in *20th Iranian Conference on Electrical Engineering*, 2012.

[104] H. Banakar, N. Alguacil, and F. D. Galiana, "Electrothermal coordination part i: Theory and implementation schemes," *IEEE Transactions on Power Systems*, vol. 20, no. 2, pp. 798–805, May 2005.

[105] N. Alguacil, H. Banakar, and F. D. Galiana, "Electrothermal coordination part ii: Case studies," *IEEE Transactions on Power Systems*, vol. 20, no. 4, pp. 1738–1745, November 2005.

[106] M. Khaki, P. Musilek, J. Heckenbergerova, and D. Koval, "Electric power system cost/loss optimization using dynamic thermal rating and linear programming," in *IEEE Electrical Power and Energy Conference: Sustainable Energy for an Intelligent Grid*, 2010.

[107] M.-X. Wang and X.-S. Han, "Study on electro-thermal coupling optimal power flow model and its simplification," in *IEEE Power & Energy Society General Meeting 2010*, 2010.

[108] R. Olsen, J. Holboell, and U. Gudmundsdottir, "Electrothermal coordination in cable based transmission grids," *IEEE Transaction on Power Systems*, 2013, accepted for publication.

[109] nkt cables, "High voltage cable systems - cables and accessories up to 550 kv," NKT cables, Schanzenstrasse 6 - 20, 51063 Cologne (Germany), Product Catalogue, 2009.

[110] R. Olsen, J. Holboell, U. Gudmundsdottir, and C. Rasmussen, "Electrothermal coordination in cable based transmission grids operated under market based conditions," *IEEE Transaction on Power Systems*, 2013, in review.

[111] U. of Washington Electrical Engineering, "Ieee 14-bus test network," http://www.ee.washington.edu/research/pstca/, July 2013.

[112] M. Čepin, *Assessment of Power System Reliability - Methods and Applications.* Springer, 2011, e-ISBN 978-0-85729-688-7.

[113] A. A. Chowdhury and D. O. Koval, *Power Distribution System Reliability - Practical Methods and Applications.* IEEE Press, 2009, iSBN 978-0470-29228-0.

[114] D. E. (Ed.), *New Computational Methods in Power System Reliability.* Springer, 2008, e-ISBN 978-3-540-77812-7.

[115] T. A. Short, *Distribution reliability and power quality.* CRC Press, 2006, iSBN 0-8493-9575-5.

[116] A. Basu, A.Bhattacharya, S. Chowhuty, S. Chowdhury, and P. Crossley, "Reliability study of a micro grid with optimal sizing and placement of der," in *CIRED Seminar 2008: Smart Grids for Distribution*, June 2008, paper 127.

[117] S. Blumsack, L. B. Lave, and M. Ilic, "A quantitative analysis of the relationship between congestion and reliability in electric power networks," *The Energy Journal*, vol. 28, no. 4, 2007.

[118] V. Dumbrava, C. Lazaroiu, C. Roscia, and D. Zaninelli, "Expansion planning and reliability evaluation of distribution networks by heuristic algorithms," in *2011 10TH International Conference on Environment and Electrical Engineering*, 2011.

[119] T. K. Vrana and E. Johansson, "Overview of power system reliability assessment techniques," in *CIGRE International Symposium Recife 2011 on Assessing and Improvin Power System Security, Reliability and Performance in Light of Changing Energy Sources*, 2011.

[120] C. W. B1.10, "Update of service experience of hv underground and submarine cable systems," Cigre, Technical Brochure 379, 2009.

[121] N. Spot, "Regulating prices," http://www.nordpoolspot.com/Market-data1/Regulating-Power1/Regulating-Prices1/ALL/Hourly/, July 2013.

[122] ——, "Elspot prices," http://www.nordpoolspot.com/Market-data1/Elspot/Area-Prices/ALL1/Hourly/, July 2013.

[123] Energinet.dk, "Kabelhandlingsplan - bilagsrapport," Energinet.dk, Tech. Rep., March 2009.

[124] G. Agrawal, *Nonlinear Fiber Optics*, 4th ed. Academic Press, 2006.

[125] R. Boyd, *Nonlinear Optics*, 2nd ed. Academic Press, 2003.

[126] W. W. Parson, *Modern Optical Spectroscopy*, 1st ed. Springer, 2009.

[127] International Electrotechnical Commission - IEC, "Publication 60840 - power cables with extruded insulation and their accessories for rated voltages above 30 kv (u_m=36 kv) up to 150 kv (u_m=170 kv) - test methods and requirements," International Electrotechnical Commission - IEC, Tech. Rep., 2004.

[128] ——, "Publication 62067. power cables with extruded insulation and their accessories for rated voltages above 150 kv (u_m=170 kv) up to 500 kv (u_m=550 kv) - test methods and requirements," International Electrotechnical Commission - IEC, Tech. Rep., 1993.

[129] A. Jahromi, Z. Li, J. Kuffel, M. Fenger, and J. Levine, "Load-cycling test of high-voltage cables and accessories," *IEEE Electrical Insulation Magazine*, vol. 27, no. 5, pp. 14–28, September/October 2011.

[130] K. Noborio, "Measurement of soil water content and electrical conductivity by time domain reflectometry: a review," *Computers and Electronics in Agriculture*, vol. 31, pp. 213–237, 2001.

[131] G. Topp, J. Davis, and A. Annan, "Electromagnetic determination of soil water content: Measurements in coaxial transmission lines," *Water Resources Research*, vol. 16, no. 3, pp. 574–582, June 1980.

[132] N. Abu-Hamdeh, "Thermal properties of soils as affected by density and water content," *Biosystems Engineering*, vol. 86, no. 1, pp. 97–102, 2003.

[133] T. Ren, T. Ochsner, R. Horton, and Z. Ju, "Heat-pulse method for soil water content measurement: Influence of the specific heat of the soil solids," *Soil Science Society of America Journal*, vol. 67, no. 6, pp. 1631–1634, November/December 2003.

[134] J. Toman and R. Černý, "Temperature specific heat of high performance concrete," *Acta Polytechnica*, vol. 41, no. 1, pp. 5–7, 2001.

PART VI

Appendices

This part is dedicated to describing selected topics to a depth which has not been possible to fit into the main content of this thesis. Especially is given a description of the experimental setups which were designed during the course of the three years. Furthermore, a list of publications is given along with a selection of the written publications.

Appendix A

Definition of Variables for Evaluation of Standardised Step Response Method

The following shows the evaluation of the necessary variables suggested in the international standards [33].

$$T_a = \frac{1}{a-b} \cdot \left(\frac{1}{C_A} - b\,(T_A + T_B) \right) \tag{A.1}$$

$$T_b = T_A + T_B - T_a \tag{A.2}$$

$$a = \frac{M_0 + \sqrt{M_0^2 - N_0}}{N_0} \tag{A.3}$$

$$b = \frac{M_0 - \sqrt{M_0^2 - N_0}}{N_0} \tag{A.4}$$

$$M_0 = \frac{1}{2}\,(T_A \cdot C_A + T_B \cdot C_B + T_B \cdot C_A) \tag{A.5}$$

$$N_0 = T_A \cdot C_A \cdot T_B \cdot C_B \tag{A.6}$$

For short transients ($t \leq \frac{1}{3} T \cdot C$, C being the total thermal capacitance of the cable and T being the total thermal resistance of the cable) the following

definitions apply:

$$T_A = \frac{1}{2} \cdot T_1 \tag{A.7}$$

$$T_B = \frac{1}{2} \cdot T_1 + q_s \cdot T_3 \tag{A.8}$$

$$q_s = \frac{W_c + W_s}{W_c} \tag{A.9}$$

$$C_A = C_c + p^* C_{i1} \tag{A.10}$$

$$p^* = \frac{1}{\ln\left(\frac{d_i}{d_c}\right)} - \frac{1}{\ln\left(\frac{d_i}{d_c} - 1\right)} \tag{A.11}$$

$$C_{i1} = c_{therm,i} \cdot \frac{\pi}{4} \cdot d_c \cdot (d_i - d_c) \tag{A.12}$$

$$C_B = p^* \cdot C_{i2} + (1 - p^*) \cdot C_{i1} + \left((1 - p^*) \cdot C_{i2} + \frac{C_s + p' \cdot C_j}{q_s}\right) \cdot \left(\frac{q_s \cdot T_3}{\frac{1}{2} \cdot T_1 + q_s \cdot T_3}\right)^2 \tag{A.13}$$

$$C_{i2} = c_{therm,i} \cdot \frac{\pi}{4} \cdot d_i \cdot (d_i - d_c) \tag{A.14}$$

$$p' = \frac{1}{2 \cdot \ln\left(\frac{D_e}{d_s}\right)} - \frac{1}{\ln\left(\frac{D_e}{d_s}\right)^2 - 1} \tag{A.15}$$

where T_1 is the thermal resistance from conductor to screen, T_3 is the thermal resistance from screen to (and including) the jacket, W_c is the joule losses in the conductor, W_s is the losses in the screen, C_c is the thermal capacitance of the conductor, C_s is the thermal capacitance of the screen, C_j is the thermal capacitance of the jacket, d_c is the conductor diameter, d_i the outer diameter of the insulation, $c_{therm,i}$ the specific heat of the insulating material, d_s the outer diameter of the screen and D_e the outer diameter of the jacket.

For long duration transients ($t > \frac{1}{3} T \cdot C$) the following definitions are recommended to be used instead:

$$T_A = T_1 \tag{A.16}$$

$$T_B = q_s \cdot T_3 \tag{A.17}$$

$$C_A = C_c + p \cdot C_i \tag{A.18}$$

$$p = \frac{1}{2 \cdot \ln\left(\frac{d_i}{d_c}\right)} - \frac{1}{\ln\left(\frac{d_i}{d_c}\right)^2 - 1} \tag{A.19}$$

$$C_B = (1 - p) \cdot C_i + \frac{C_s + p' \cdot C_j}{q_s} \tag{A.20}$$

$$\tag{A.21}$$

where C_i is the thermal capacitance of the insulation.

Appendix B

Temperature Measurements and DTS Systems

Many cable manufacturers and utilities have installed temperature monitoring equipment on their power cables in order to obtain knowledge about their real time thermal state. Mainly two different approaches have been developed for monitoring the temperature of power cables, firstly through single point measurements and secondly through distributed temperature measurements.

B.1 Single Point Temperature Measurements

Probes for single point measurements are capable of measuring the temperature in a single point. The measurements are typically performed by attaching PT100 sensors or thermocouples to the cable jacket and connecting them to data logging equipment.
The benefits of using single point measurements is that the technology is reliable, sensors are durable and the measuring system is relatively cheap.
The downside is that the temperature is known only for the specific site where the sensor is installed. Even though the installation site is carefully chosen by experts, it is still not certain that the site of installation is where the highest temperatures will be experienced and potentially harmful temperatures can thus arise in parts of the cables which the operator has no knowledge about. An additional issue with single point measurements is that power has to be available on site for the measurement equipment as

well as communication needs to be established between measurement device and the place where data is to be utilised. This means that either wired or wireless communication systems must be created which increases the costs.

B.2 Distributed Temperature Sensing Measurements

Distributed temperature sensing (DTS) measurements are capable of obtaining temperature data in multiple sites with one piece of equipment.
The basic concept of state of the art DTS systems is that temperature measurements are obtained by sending a light impulse into a fibre and analysing the light which is reflected in the fibre.
The main benefit is that temperatures can be monitored over tens of kilometres with a spatial resolution of down to one metre and an accuracy of $\pm 1\,^{o}$C.
The main downside of DTS monitoring of cables is that the equipment is expensive.

For underground cable systems there are two main alternatives for the installation of DTS fibres. Firstly, the fibre can be installed in a pipe which is laid next to the cables and secondly, the fibre can be installed in the cable screen.

B.2.1 DTS Fibres in Pipes

When power lines are installed in transmission systems today a lot of communication is often required between the two ends of the line. Optical fibres are therefore installed alongside the power lines such that protection systems, power monitoring systems, control systems, etc. can perform reliably. By installing these fibres in an air filled pipe in the cable trench the fibres are mechanically protected but they can also be easily replaced in case of damage.
Figure B.1 shows how the installation of the fibre pipe is usually performed for cables in flat formation.

There are a number of concerns which must be recognised when performing DTS measurements on a fibre in such a pipe. Firstly, the pipe is not necessarily attached to the cable. The distance between cable and measurement point can therefore vary and the exact reference point in the thermal model is thus not necessarily known. In the dynamic analysis of the temperature of power cables the reference point must therefore be chosen only after due consideration.

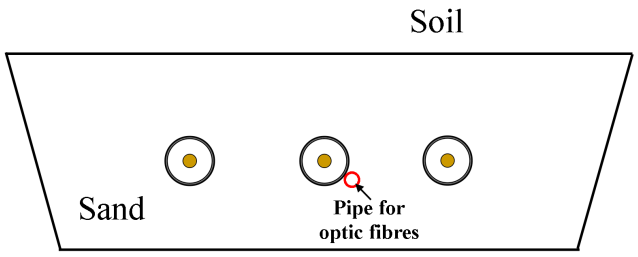

Figure B.1: Cross section of a typical cable trench where the cables are installed in flat formation. It is especially noticed that the pipe for the optical fibre is installed next to the centre phase.

A second concern is that the fibre pipe is filled with air. This means that the thermal environment, in which the temperature measurements are obtained, is different from the surrounding sand. In the TEE model the measurements of the temperature are proposed to be utilised by assuming that the measurement is obtained in the sand in a distance equal to the diameter of the pipe. The difference in the thermal properties of air and sand can therefore have an impact on the accuracy of the model.
As the air in the pipe is a fluid it may be assumed that the temperature inside the pipe is homogeneous and the temperature which is measured by the fibre may thus be higher than the temperature in the sand in an equal distance from the cable. This is especially problematic during sudden high load increases as the temperature measured by the fibre may increase much faster than the thermal model. The model will therefore, as described in chapter 4, attempt to decrease the moisture content, even though this should not be the case. In the present PhD study this shortcoming in the algorithm-measurement interface has been addressed by limiting the rate at which the moisture content of the sand can decrease, that is $\frac{\mathrm{d}M_{weight}}{\mathrm{d}t} \leq 1 \frac{\%_{weight}}{\mathrm{h}}$.

B.2.2 DTS Fibres Embedded in Screen

Some cable manufacturers offers the opportunity to implement the optic fibre for DTS in the screen. The fibre is typically installed inside a metallic pipe which is wound around the insulation screen together with the other metallic screen wires. The obvious benefit, when bearing the discussion above in mind, is that the measurement point is directly modelled in the thermal simulations, and thus the thermal properties of the fibre surroundings are the same in the model as they are in the measurements. In case the DTS fibre is installed in the screen it is thus not necessary to include a $\frac{\mathrm{d}M_{weigth}}{\mathrm{d}t}$ limit.

There are though also downsides of installing the fibre in the screen. Firstly, at cable joints, extra components are required because splicing of the fibre is also needed. These extra components are necessary because the fibre will either have to exit the cable on one side of the joint and enter the cable on the other, or the splicing will have to be made inside the joint with increased complexity of the joint as a result.
Secondly, in case of fibre failure, it is not possible to simply replace the fibre. Thus, in case of fibre failure, the possibility of performing temperature measurements on the cable is lost for the remaining of the cable lifetime.

B.2.3 DTS Monitoring of Three Phased Submarine Cables

In three phased submarine transmission cables, a bundle of fibres for communications etc. can be installed in the filling material underneath the armour, see figure B.2. This also enables the possibility of performing DTS measurements inside the cable. The number of joints on submarine cables is generally low, and the fibres embedded underneath the armour will thus not increase the jointing costs and complexity as much as if embedding the fibre in the screen.

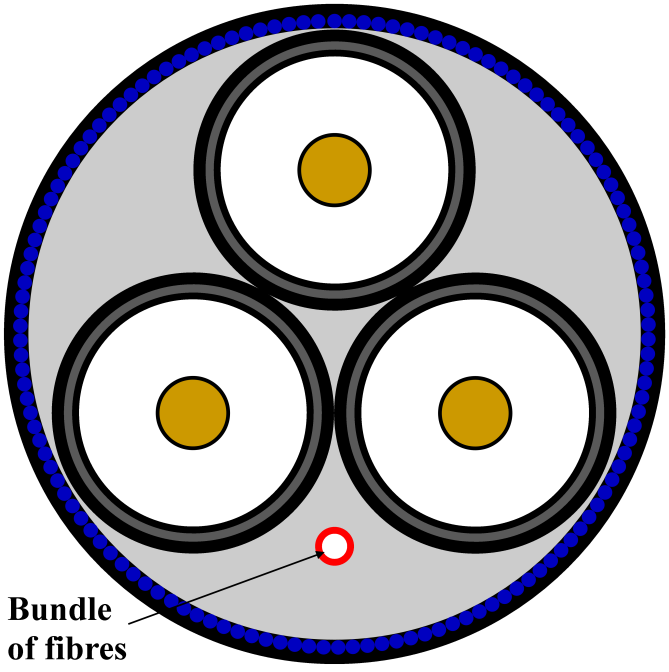

Figure B.2: Cross section of a typical three phase submarine power cable. Especially it is noticed that the optical fibres are installed in the filling under the armour.

B.2.4 The DTS Measuring Unit

The DTS fibre in itself is a passive component not capable of performing anything else than carrying an electromagnetic wave. Therefore an active measuring unit is required to be connected at the end of the fibre. The DTS measuring unit consist in basic of three things. Firstly, a laser sends out a wave through the fibre. The fibre carries the wave, however some of the energy from this light pulse is scattered by the molecules (denoted Raman scattering) in the fibre and passes back to the origin. Here, the second part of the DTS unit collects the scattered part of the laser pulse. Thirdly, the DTS unit includes a data analyser. The scattered pulses which are collected are compared to the emitted laser pulse. The difference in intensity, between emitted and collected pulses, at different wavelengths can then be converted to the temperature at the molecule site where the scattering occurred. The described conversion, of the intensity of the back scattered waves, to temperature requires deep insight into quantum mechanical which is outside the scope of the present report. Instead the reader is referred to textbooks such as [124–126] which describe Raman scattering in detail.
The distance to the site where the scattering occurred can be determined by measuring the time from emitting the laser pulse to collecting the back scattering and multiplying by the speed of light inside the fibre.

Appendix C

Field Experiment for Assessment of Moisture Migration

In order to determine if the standardised static jacket temperature limit of 50 °C is appropriate when designing and dimensioning cables for grids where the temperature is modelled in real time, it was decided to conduct a field experiment to investigate the severity of moisture migration in sand at 50 °C.

C.1 Design of Experimental Setup

A 1.5 m deep and 15 m long cable trench was dug in the native soil of the field outside of Energinet.dk's main office in Erritsø. The length of the trench was divided into 7 sections. The 5 centre sections contained different sand types and 1 at each end was simulating infinite boundary conditions for the trench. The 5 types of sand were delivered from different sand pits in Denmark and were installed in an envelope around two water pipes (simulating hot cables), in a similar way as done when installing real cable systems, see figure C.1. On top of the envelope of sand the native soil was installed to fill up the trench.

As indicated, the heat in the trench is released from two pipes circulating hot water. The pipes were connected to a water heating system capable of maintaining a very static temperature in the pipe. The temperature

Figure C.1: Experimental setup under construction. Temperature and moisture content sensors were installed such that the moisture migration, caused by the hot water circulating the pipes, could be monitored.

was monitored by type-k thermocouples in 32 different places in the cable trench. These measurements covered both the outer temperature of the pipe in numerous places and in a number of sites in different distances from the pipe. The 32 thermocouples were connected to 4 USB TC-08 Temperature Loggers from Pico Technology, and the data was gathered on a computer installed on site. The moisture content was measured by 5 Trime-Pico 64 sensors from the company IMKO and the data was collected on a computer. The experiment ran for a year, thus obtaining data from all four weather seasons.

A sketch of the experiment can be seen in figure C.2.

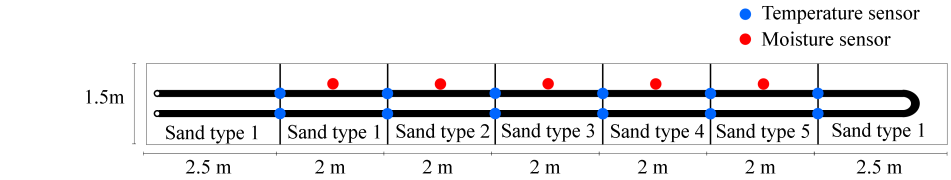

(a) Design of experiment seen from the top.

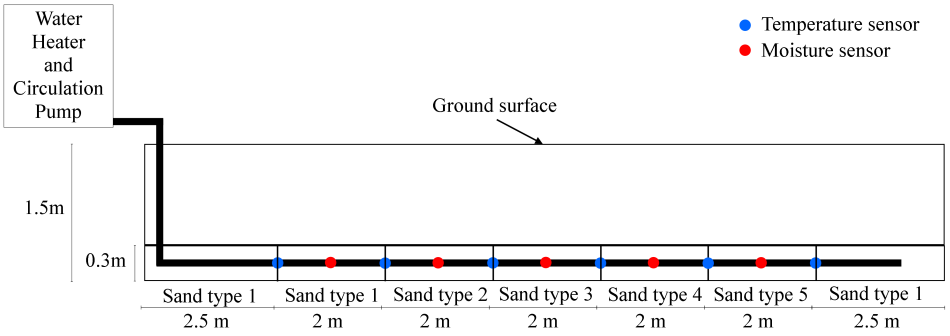

(b) Design of experiment seen from the side.

Figure C.2: Experimental setup of field experiment. The water heating system was capable of maintaining a very static temperature in the pipe. Temperature and moisture sensors are seen to cover the experiment in order to maintain a comprehensive overview of the thermal conditions of the trench. It should be noted that this is a field experiment and the outside environmental conditions (which are not controllable) thus have a high impact on the results.

C.2 Measurements of Moisture Migration and Temperature

As the experiment was conducted outside, the surrounding conditions were not controllable and they were ever changing. The results of the experiment will thus in the present project be used for qualitative discussions rather than quantitative comparisons.

The measured moisture contents of the five sand types are seen in figure C.3 along with the temperature measured on the outside of the pipes. Data is seen to cover a year worth of measurements.

The moisture is seen not to migrate away from the heat source in any significant amount as long as the temperature is kept below 60 °C. As the temperature is increased to 60 °C, dry-out occur at least in one of the sand types. However it is noticed that it takes more than one month before the sand dries out. Note that November of 2011 was very dry with only 19mm precipitation spread over the entire month. When rain fall is experienced

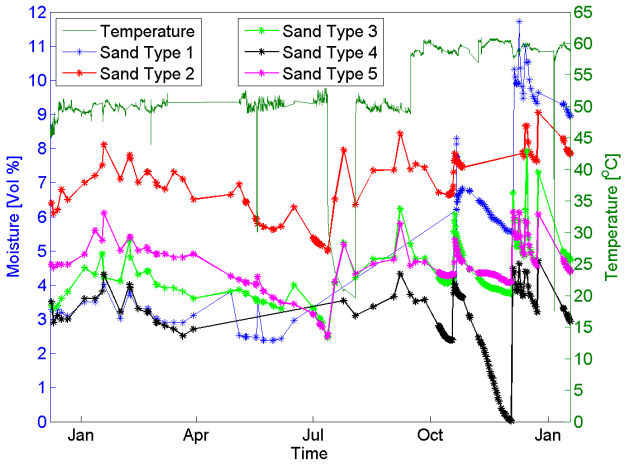

Figure C.3: Measured moisture content of the five types of sand and the outer temperature of the pipes. Data is seen to cover a year worth of measurements. It is noticed that severe moisture migration is only found in one type of sand and with a pipe surface temperature of 60 °C. It is seen that there are periods of time where the moisture content has not been measured. These periods are caused by faulted measurement equipment which had to be replaced.

after such a dry month the moisture content is seen to increases almost instantaneously. On this background it may be argued that 50 °C as a static jacket temperature limit is too conservative, and that 60 °C may be allowed for a long time without jeopardising the reliability of the system.

C.3 Discussion Moisture Migration and Critical Temperatures

It must be concluded from the experimental study that dry-band formation around power cables will not necessarily be experienced even when the jacket temperature increases to 60 °C. The moisture was in the study found to migrate slowly away from the heat source, even at 60 °C, and high jacket temperatures may thus be allowed for many consecutive days.
It should be acknowledged that the described study was performed in one specific location, and the results are thus not necessarily directly applicable to all cables in the Danish grid. It must though also be noted that even though the experimental site is not comparable to all cable installations, conditions such as the ground water level was determined not to be especially beneficial at the discussed site, and the site may therefore be assumed to have average thermal properties.

Appendix D

Laboratory Setup for Verification of Thermal Models

This appendix describes the experiment performed in the high voltage lab at the Technical University of Denmark in the spring of 2012.

D.1 Design of Experimental Setup

The purpose of performing the experiment was to analyse the accuracy of the thermoelectric equivalent (TEE) model for estimating the dynamically varying conductor temperature of power cables.
Bearing this purpose in mind a wooden box 2 metres high, 2.4 metres wide and 4 metres long was designed, in which soil, sand, cables and measurement equipment was installed.
In order to create as realistic a scenario as possible, it was attempted to create a trench with a cross sectional profile similar to cable trenches in the field, including the envelope of sand around the cables. A cross section of the experimental setup looks as shown in figure D.1.

A picture, taken during construction, of the experiment is given in figure D.2.

Before the current was applied, a layer of soil was installed on top for completion of the setup.

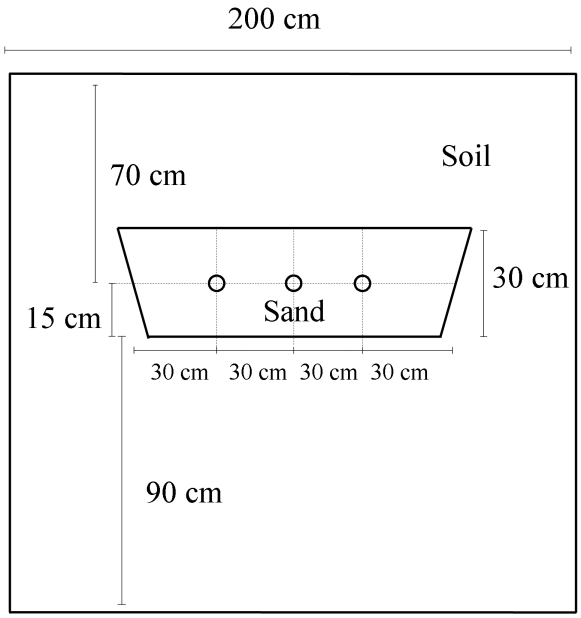

Figure D.1: Cross section of the wooden box designed to create dynamic temperature data for verification of the thermal models.

Figure D.2: Experimental setup under construction. Cables, sand and most measurement equipment is installed. A layer of soil was installed on top for completion of the setup.

D.1.1 Test Subjects

The cables used in the experiment were equipped with solid aluminium conductors, XLPE insulation, semiconductive layers at the conductor and

V [kV]	S_c [mm^2]	S_s [mm^2]	d_c [mm^2]	d_{cs} [mm^2]	d_i [mm]	d_{is} [mm]	d_s [mm]	D_e [mm]
245	1600	737	45.0	50.0	99.0	102.0	106.5	112.0

Table D.1: Dimensions of cable used in the experimental setup. In the thermal simulations, the semiconductive conductor and screen layers are assumed to be a part of the insulation with identical thermal properties.

Material	c_{therm} $\left[\frac{J}{m^3 \cdot K}\right]$	ρ_{therm} $\left[\frac{K \cdot m}{W}\right]$
Aluminium	$2.5 \cdot 10^{6}$*	0**
XLPE	$2.40 \cdot 10^{6}$ ***	2.8***
Lead	$1.45 \cdot 10^{6}$*	0**
PE	$2.40 \cdot 10^{6}$ ****	2.8****
* Standardised numbers listed in [33]. ** The thermal resistivity of metals is several orders of magnitude lower than for most other materials and thus the thermal resistance is assumed negligible. *** Quantities obtained through experiments. Procedure is explained in appendix D. **** The jacket material is assumed to have thermal properties identical to the insulation.		

Table D.2: Material specifications of the cable used in the experimental study for verification of the thermal models.

screen, lead screens and jackets of polyethylene. The cable specifications are given in tables D.1 and D.2.

D.2 Measurement Equipment

D.2.1 Current Measurements

The alternating current was applied to the setup with a current transformer, and it was measured through a Rogowski transducer, giving an output of $0.02\,\mathrm{mV/A_{RMS}}$. This voltage was then logged with the Benchlink software on a computer, through a Hewlett Packard 34970A Data Acquisition/Switch Unit.
As the current was applied in series, see figure 4.8, the current was only measured in one place.

D.2.2 Temperature Measurements

The temperature in the setup was closely monitored by 60 type-k thermocouples obtaining data every minute. Additionally, approximately 30 thermocouples were installed for redundancy purposes.
The 60 thermocouples were connected to a Hioki LR8401-20 data logger, which directly exported the measurements to a computer.
The following clauses describes the procedure for installing the temperature sensors in the cables and in the surroundings.

D.2.2.1 Conductor Temperature

Different procedures have been suggested for measuring the conductor temperature with single point probes.
Firstly, IEC [127, 128] suggests the insertion of a metallic cylinder into the cable, containing a thermocouple. The cylinder is to create good thermal contact between conductor and probe. In order to ensure good contact is remained over time it is suggested that a spring is used to keep mechanical pressure on the probe.
Secondly, [129] suggests that the layers above the conductor (meaning semiconductive layers, insulation, screen, jacket, etc.) are carefully stripped, over e.g. 30 cm, from the conductor in one piece. The thermocouples are placed at the conductor in the middle of stripped area and the stripped layers are reapplied to the conductor in order to restore the thermal properties of the cable. The advantage of this approach should be that the thermal properties directly above the temperature probes resembles the real cable better than the IEC approach which may be seen as a heat sink.
The present study finds the two described approaches to be very invasive to the thermal environment in the cable and thus the measured temperatures may differ from what would be experienced in the real cable case. In order to minimise the impact on the thermal characteristics of the cable, the conductor temperature in the experimental setup was measured by drilling a narrow (approx. 2 mm in diameter) hole through the jacket, screen and insulation to the conductor. The sensor and wire was covered with glue in order to fill the gap between wire and dielectric, see figure D.3. At the cable surface, a fast drying glue was applied to ensure the position of the probe. It is assumed that the temperature measurements disturbs the thermal environment to a limited extend when using this procedure.

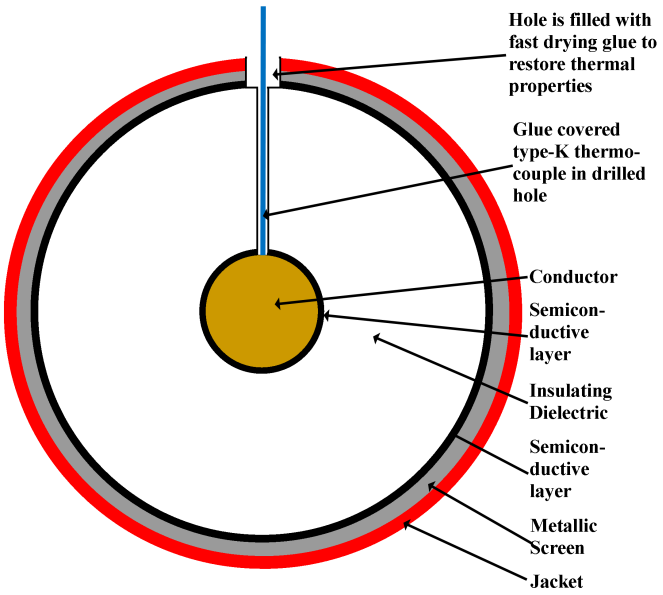

Figure D.3: Sketch of the installation procedure for thermocouples monitoring the conductor temperature. This method has been chosen instead of other suggested methods, [129], in order to minimise the impact on the thermal properties of the cable.

D.2.2.2 Screen Temperature

Probes for monitoring the screen temperature are inserted in a similar way as the conductor probes. A small hole is drilled in the jacket, the jacket is lifted a little such that a probe can be pushed in between the screen and jacket. The hole is then covered with a fast drying glue.

D.2.2.3 Jacket Temperature

Probes for measuring the jacket temperature are attached to the outside of the cable by gluing the probe wire to the cable.

Figure D.4 shows a set of installed probes. Such a set of probes were installed five places along the centre phase, five places along one of the outer phases, and three places along the second outer phase.

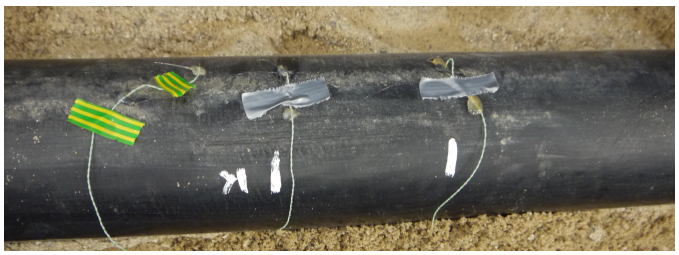

Figure D.4: Installed temperature sensors for monitoring the conductor (right wire), screen (centre wire) and jacket temperatures (left wire).

D.2.2.4 Fibre Temperature

As seen in figure D.2, a pipe was installed next to the centre phase. 2 thermocouples were installed in this pipe, approximately in the centre of the setup, for delivering feedback to the thermal models. The pipe was closed at both ends in order to limit the possible air flow.

D.2.2.5 Surrounding Temperature

The temperature of the cable surroundings was monitored in multiple places. The present study has not used these measurements but they are stored for possible future utilisation.

D.2.3 Moisture Content Measurements

The moisture content was measured with Time Domain Reflectometry (TDR) probes of the type Trime-Pico 64 from the manufacturer IMKO Micromodultecknik GMBH, see figure D.5.

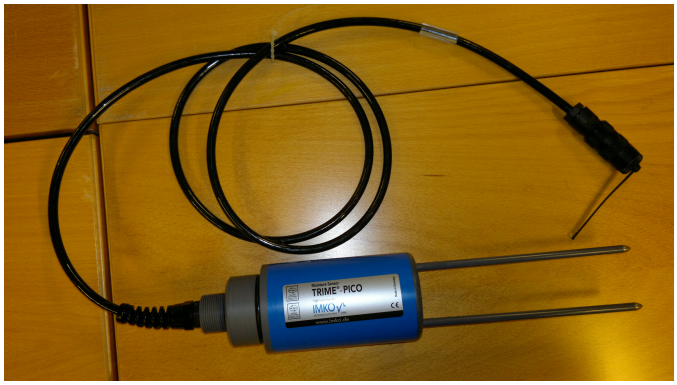

Figure D.5: Time domain reflectometry probe for measuring the moisture content of the cable surroundings.

D.2.3.1 Time Domain Reflectometry

The operational principle of TDR is that the probe sends a high frequency (up to the GHz range) wave into the rods of the probe. The time it takes this wave to propagate through the rods and return when reflected is directly related to the dielectric constant of the material surrounding the rod [130]. The dielectric constant can then be converted to a moisture content via an empirically determined relation which is applicable to mineral soils with an accuracy of approximately 1.3 %, according to [131].

D.2.3.2 Installation of Sensors

The experiment was equipped with five sensors monitoring the moisture content four places in the sand and one in the soil as shown in figure D.6.

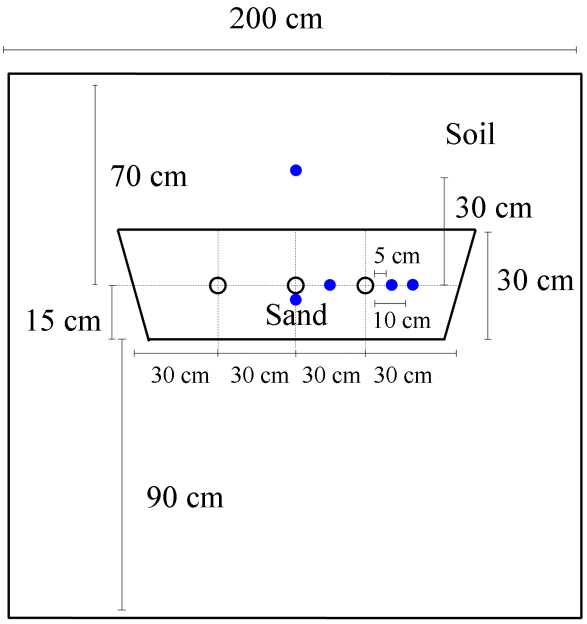

Figure D.6: Cross section of the experimental setup. It is noticed how four of the moisture content sensors are installed in the sand and one in the soil.

D.2.3.3 Data Collection

One of the advantages of using the Trime-Pico 64 sensors is the inherent RS232 communication feature which enables easy and automatic gathering of data. The five sensors were connected to a computer with the data logging software "Trime WinMonitor" which is provided with the probes.

D.3 Determination of Thermal Resistivity and Specific Heat

Before the start up of the above described experiment, a small scale laboratory experiment was performed, investigating the thermal properties of the involved materials.

The thermal resistivity and specific heat are the properties which are required for performing thermal modelling, and thus these were attempted to be empirically estimated as explained below.

It should be noted that the present study has used the standardised values

for the thermal properties of metallic component, [28, 33].

D.3.1 Specific Heat

The specific heat was difficult to determine accurately with the tools available in the present study. However an attempt was made to measure the specific heat of the insulation, the sand and the soil.

The measurements were performed by heating a sample of a specific amount of the material to a known temperature and mixing it into a known amount of de-mineralised water in an insulated container. When the temperature of the water reaches a maximum steady state, it is assumed that the material has exchanged all the stored energy with the water. Because water has a fairly well known specific heat, it is possible to relate the temperature increase in the water to a specific heat of the material under investigation, (D.1).

$$c_{therm,material} = \frac{c_{therm,water} \cdot \Delta\theta_{water} \cdot V_{water}}{V_{material} \cdot \Delta\theta_{material}} \tag{D.1}$$

where $V_{material}$ is the volume of the material. For porous materials such as sand and soil it is inevitably easier to measure the weight than the volume when performing specific heat experiments, and the volume must thus be determined via the density which is found by measuring the volume and mass simultaneously.

D.3.1.1 Insulation

The standardised specific heat for XLPE is $2.4 \cdot 10^6$ J/m³·K, [33].
This value was attempted verified by the described experimental procedure. The specific heat was measured six times and was found to be $2.57 \cdot 10^6$ J/m³·K. It may on this background be concluded that the specific heat can be estimated fairly accurate with the tools available to the project.
As the measured value was so close to the standardised value, and taking the uncertainties of the experiment[1] into account it was chosen to use $2.4 \cdot 10^6$ J/m³·K in the thermal models.

D.3.1.2 Sand and Soil

The estimation of the specific heat for the sand and soil was performed in the same way, and the experiment gave $0.66 \cdot 10^6$J/m³·K as the specific heat

[1] Inaccuracies are for instance: measured weights, measured temperature, specific heat of water, leaking energy to the surroundings, etc.

of dry sand and $1.48 \cdot 10^6 \mathrm{J/m^3 \cdot K}$ for the dry soil.
The specific heat of sand and soil is dependent on the moisture contents, [84, 132–134]. As the cavities between the sand (or soil) grains fills with water, thus pressing out the air, the specific heat increases. [84] states that because the specific heat of air is negligible compared to water, the specific heat may be considered linearly dependent on the moisture content. It is therefore assumed sufficient to measure the specific heat for the dry material and creating a linear relation based on the well documented specific heat of water such as given in (D.2).

$$c_{therm,sand}\left(M_{weight}\right) = c_{therm,water} \cdot \frac{M_{weight}}{100} + c_{therm,sand}\left(0\%\right) \cdot \left(1 - \frac{M_{weight}}{100}\right) \quad \text{(D.2)}$$

The results of the measurements performed in the present study can be seen in figure D.7.

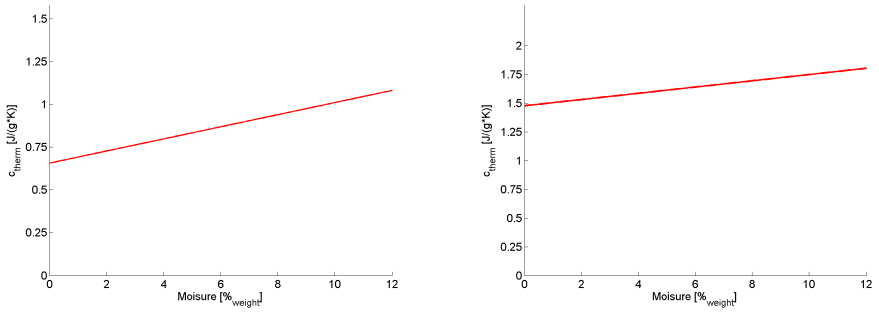

(a) Sand **(b)** Soil

Figure D.7: Specific of the sand and soil used in the experiment. Only the specific heat of dry material has been measured and the remaining data points are thus extrapolated based on the specific heat of water. This is a valid approach as [84] states that specific heat is linearly dependent on the moisture content.

D.3.2 Thermal Resistivity

The thermal resistivity has been measured for the insulating XLPE material, the sand and the soil, using temperature probes and equipment from the company Hukseflux. The Hukseflux equipment uses the Non Steady State Probe approach, which applies a heat loss to a needle and thus creating a temperature increase. The probe is also equipped with a temperature sensor which measures the dynamic temperature response to the heat input. By

analysing this temperature response over a period of 300-600 seconds, the equipment is capable of determining the thermal resistivity of the material. The equipment used for measuring the thermal resistivity uses a needle probe 6.35 mm in diameter and 17 cm long. It therefore requires a sample size of at least 20 cm in height and 10 cm in radius.

D.3.2.1 Insulation

As the insulation thickness was only 2.3 cm it was not possible to create a sufficiently large sample for measuring the thermal resistivity with the Hukseflux equipment. It was therefore decided to perform the measurement in the following way. A constant current was applied to the setup seen in figure D.1, and the temperature difference between conductor and screen was monitored.
When the temperature difference become stable for a constant applied load it is assumed that the thermal capacitance of the material between the conductor and screen does not affect the thermal behaviour anymore. The thermal resistivity can therefore be calculated by using equation (3.37) as shown in (D.4).

$$T_1 = \frac{(\theta_c - \theta_s)}{R_{AC} \cdot I^2} \Rightarrow \tag{D.3}$$

$$\rho_{therm,i} = \frac{(\theta_c - \theta_s)}{R_{AC} \cdot I^2} \cdot \frac{2 \cdot \pi}{\ln\left(\frac{d_i}{d_c}\right)} \tag{D.4}$$

where d_i is the outer diameter of the insulation and d_c is the conductor diameter.

By utilising this relation, and data where the temperature difference between conductor and screen had been stable for 7 days, a thermal resistivity of 2.8 $^{\mathrm{K \cdot m}}/_{\mathrm{W}}$ was obtained.
It should be noted that (D.4) is based on the assumption that the losses are well defined according to the standards ($W_c = R_{AC} \cdot I^2$). If the actual losses are different from the calculated, errors in the calculation of the thermal resistivity will also be encountered. Further investigation in this topic was not performed in this study and a thermal resistivity of 2.8 $^{\mathrm{K \cdot m}}/_{\mathrm{W}}$ has therefore been used in the modelling of the experimental setup.

D.3.2.2 Jacket

Because of the requirements to the sample size, it is not possible to measure the thermal resistivity of the jacket with the Hukseflux equipment.
Furthermore as the jacket nominally is only 3 mm thick, large variations in

results obtained by (D.4) will arise with only the smallest deviations in the jacket thickness at measuring site.
Because of the practical difficulties in measuring the thermal resistivity of the jacket material, it is instead chosen to assume that the thermal properties of the jacket are identical to those of the insulation.
The assumption that the PE jacket has the same thermal properties as the XLPE insulation is somewhat verified by the standards, [28], which assumes that the thermal properties of the two materials are identical.

D.3.2.3 Sand and Soil

The sand and soil thermal resistivity is, as stated, dependent on the moisture content. Measurements were therefore performed on samples with different moisture contents. This was done by adding water such that 12 % of the sample weight was water. In this sample the thermal resistivity was measured five times with the Hukseflux equipment. Thereafter the sample was slowly dried for several hours. The weight of the drying sample was measured, such that the moisture content could be determined, and the thermal resistivity was measured. This procedure with drying the sample was performed several times until a suitable amount of data points had been obtained.
Besides the moisture content, the thermal resistivity is also dependent on the compaction of the sand and soil samples. Sand and soil in a cable trench will over time become more and more compacted, and it was therefore attempted to compact the sand and soil samples in order to obtain as realistic thermal resistivity values as possible. The thermal resistivity data obtained from the two materials were fitted with an exponentially decaying function, and the results are shown in figure D.8.

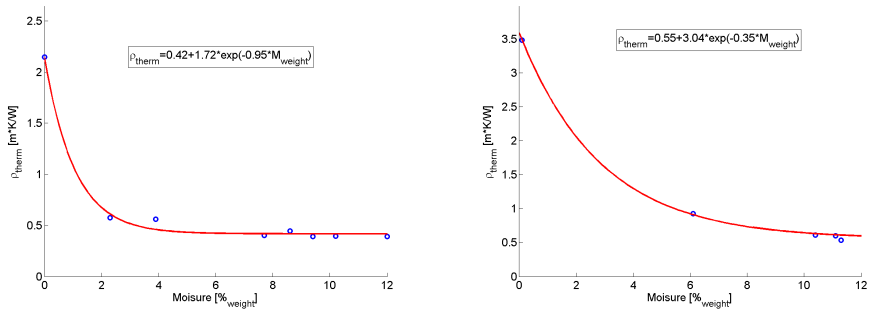

(a) Sand **(b)** Soil

Figure D.8: Thermal resistivity of the sand and soil used in the experiment. Measured data points are fitted to an exponentially decreasing function.

Appendix E

Case Study of IEEE 14-Bus Tests Network

This appendix shows larger versions of the figures presented in clause 6.3.1 and 6.3.3.

E.1 Design of the Adapted 14-Bus Test Network

See following page.

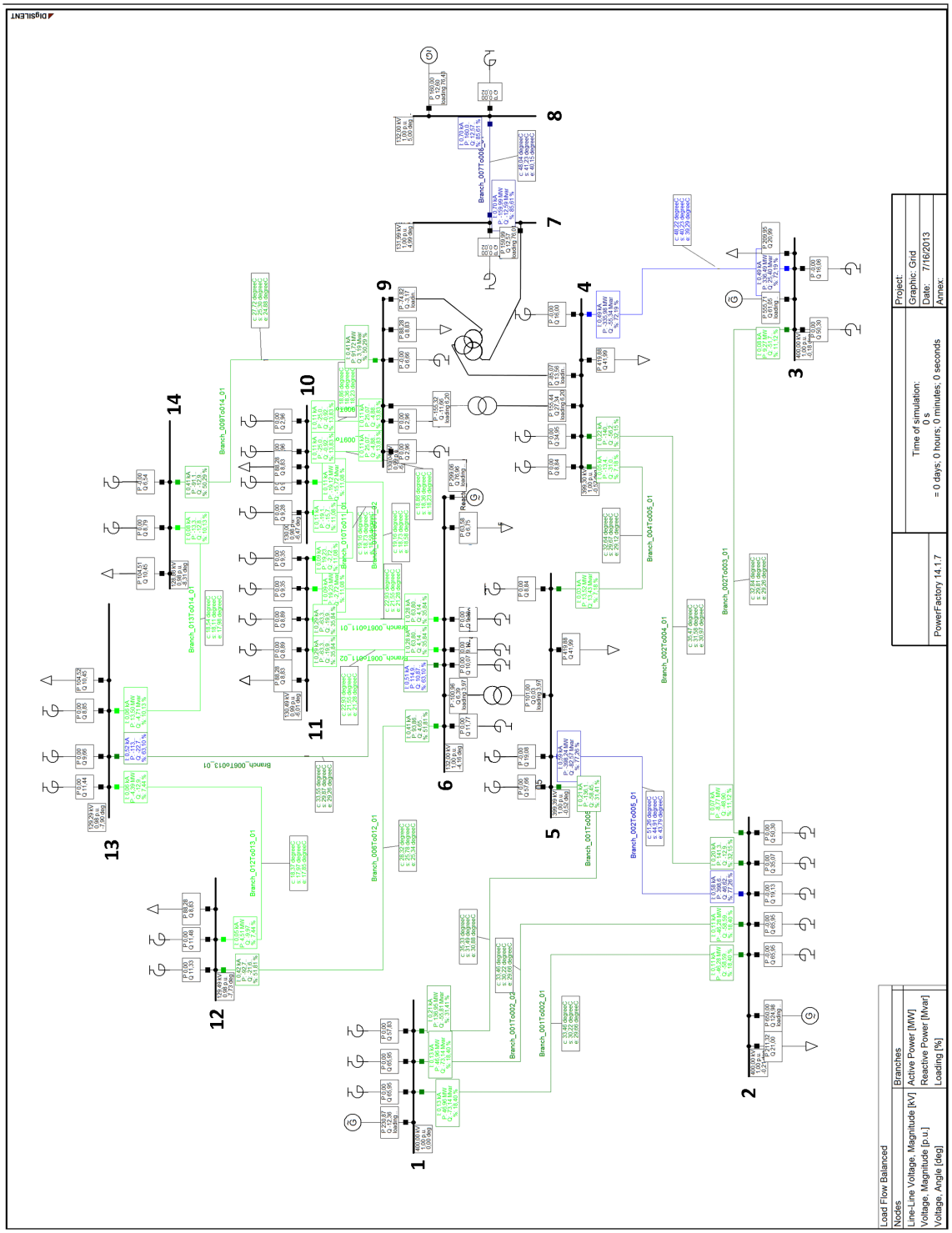

Figure E.1: IEEE 14-bus test network as designed in DSPF.

E.2 Load Flow and Failure Scenario

In the following, the current based operation and ETC based operation, presented in figure 6.18, is divided into separate figures for increased readability.

E.2.1 Current Based Operation

See following pages.

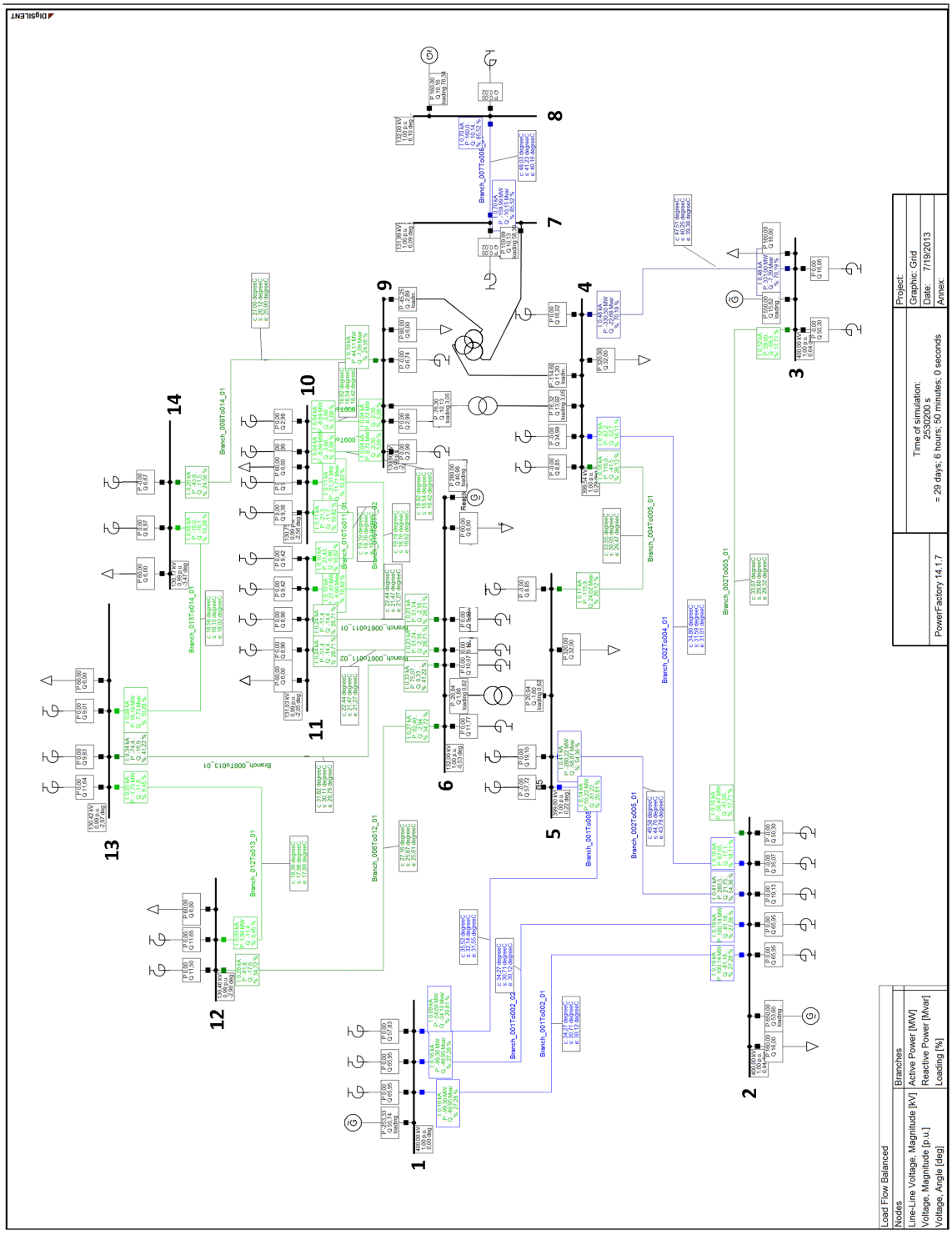

(a) 6:50 at the 30th day

Figure E.2: *Continued on next page.*

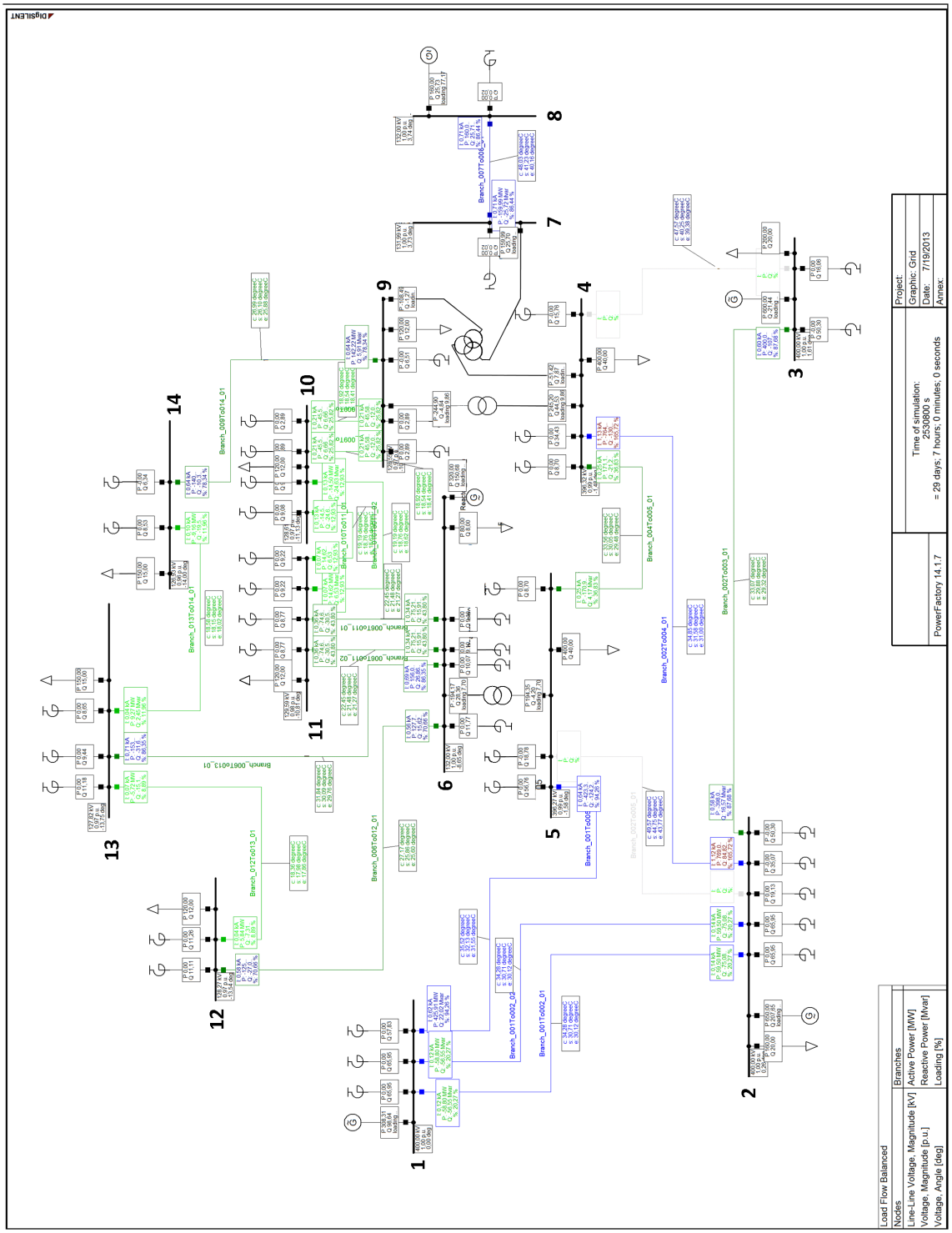

(b) 7:00 at the 30th day

Figure E.2: *Continued on next page.*

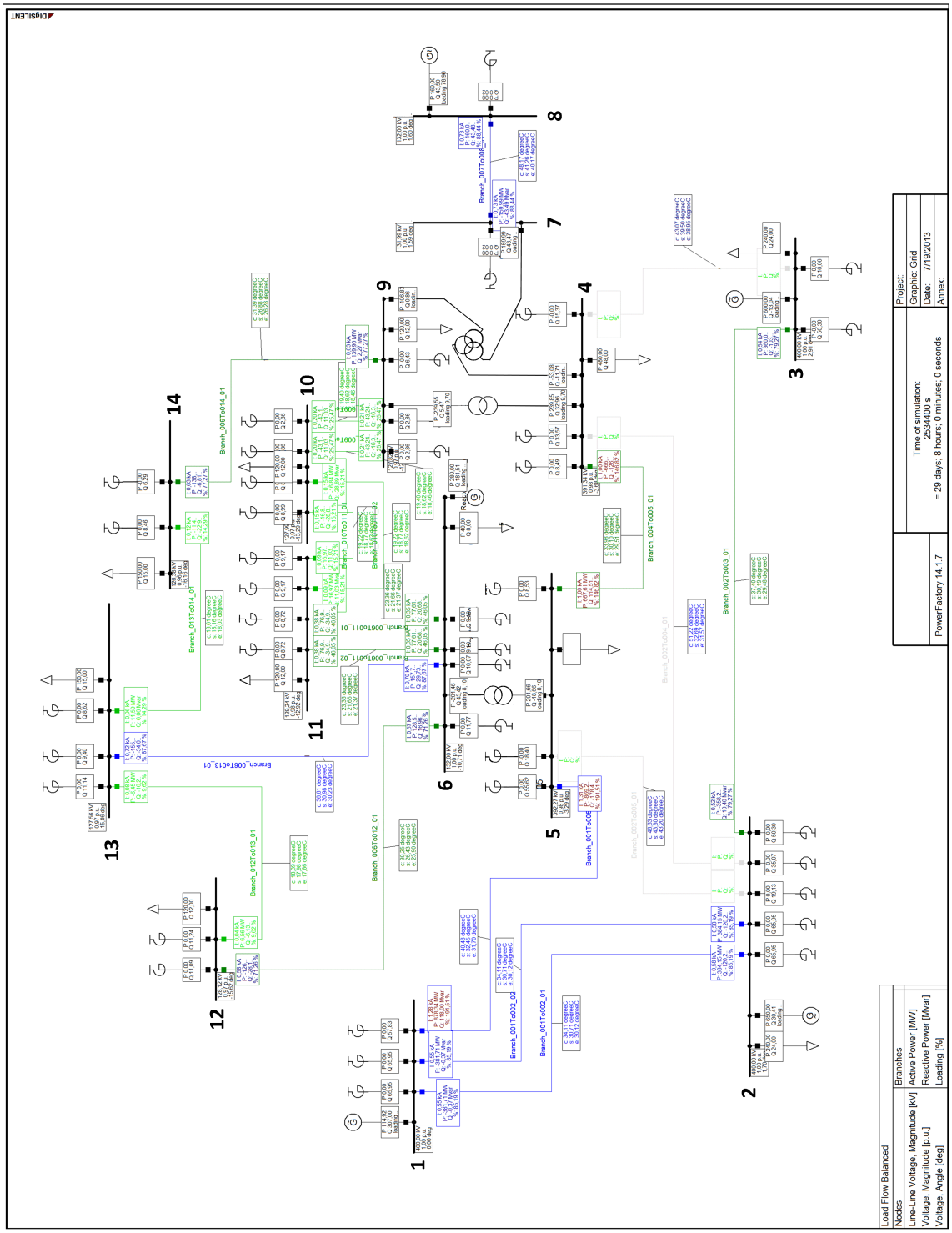

(c) 8:00 at the 30th day

Figure E.2: *Continued on next page.*

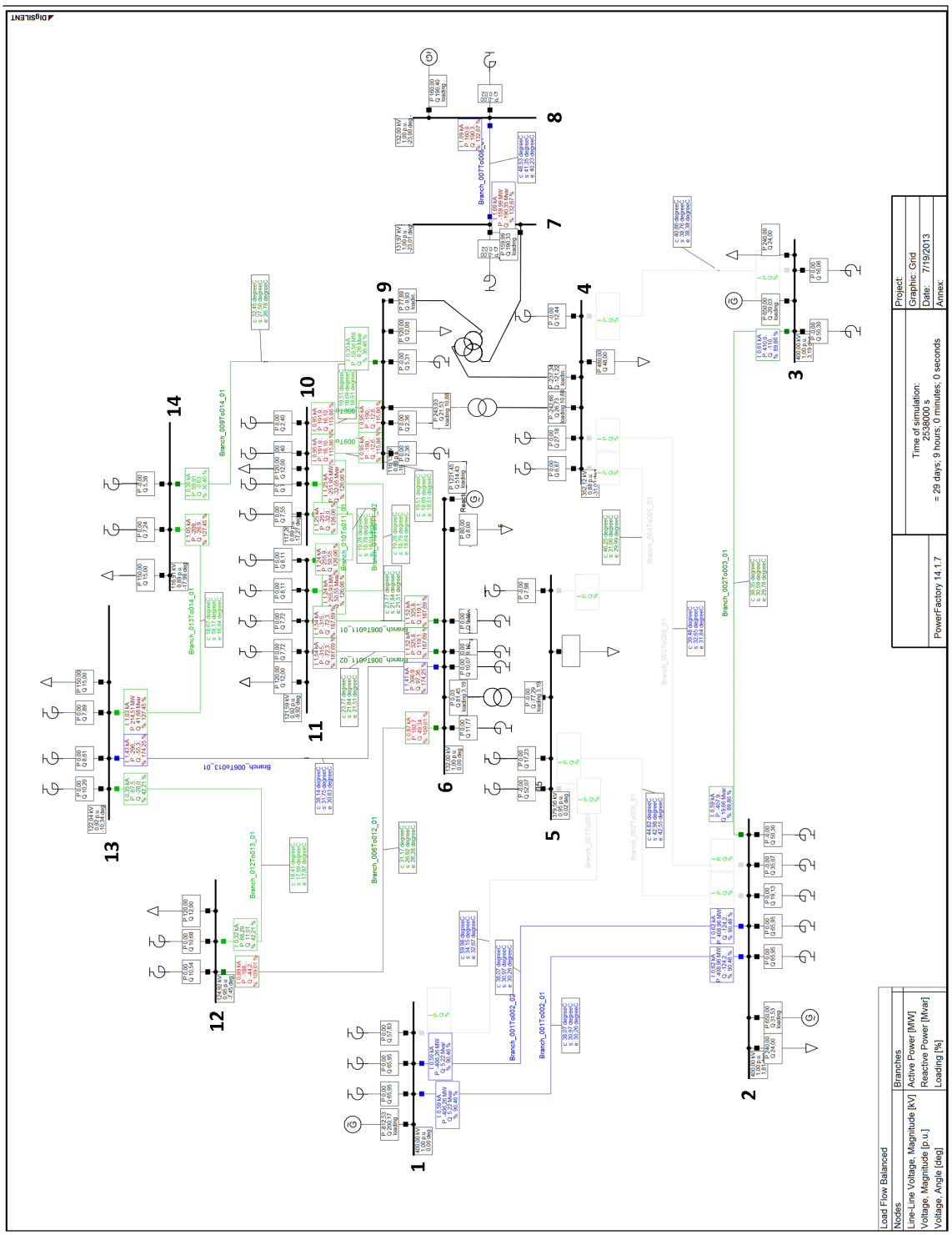

(d) 9:00 at the 30th day

Figure E.2: *Continued on next page.*

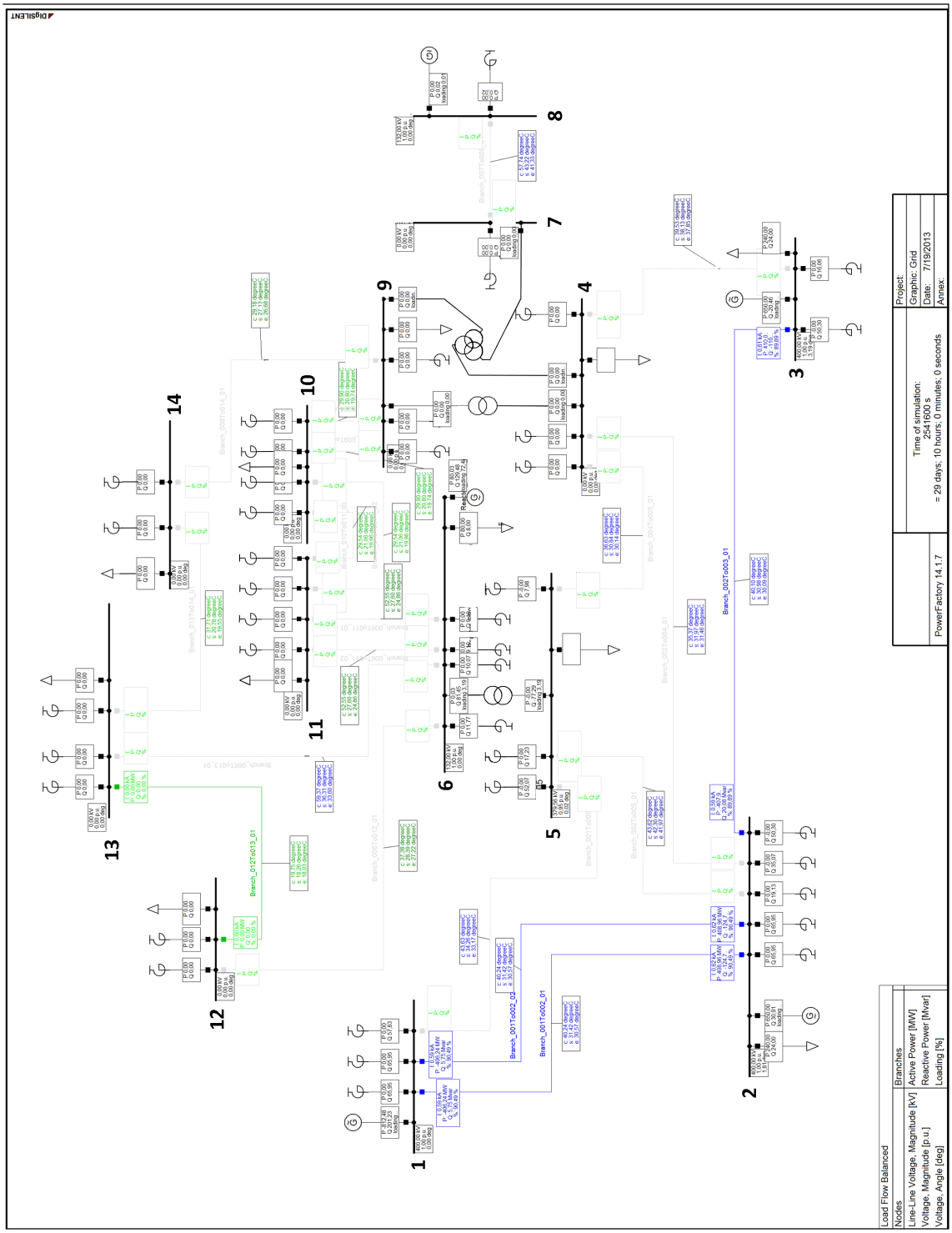

(e) 10:00 at the 30th day

Figure E.2: Thermal evolution of transmission system operated based on currents.

E.2.2 ETC Based Operation

See following pages.

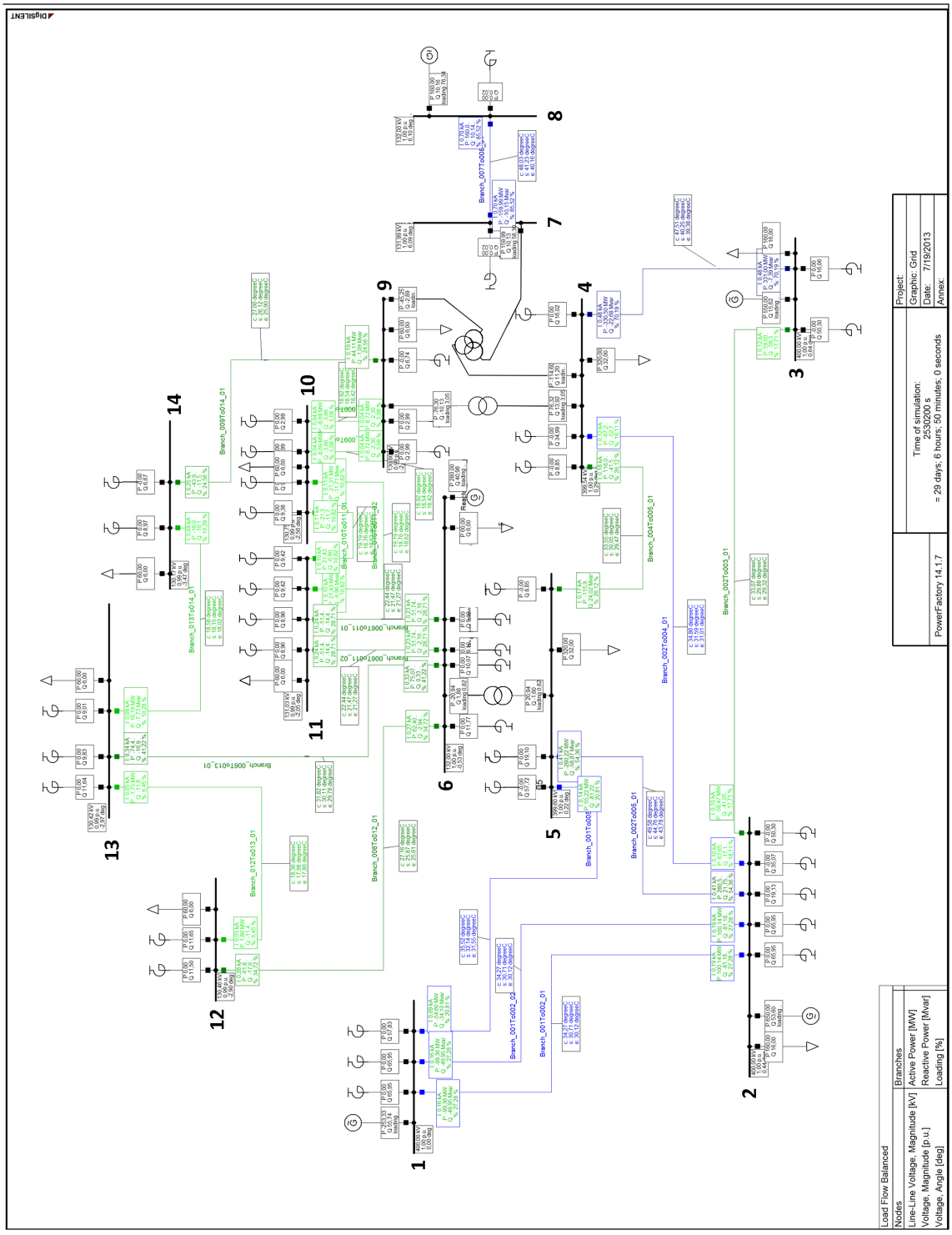

(a) 6:50 at the 30th day

Figure E.3: *Continued on next page.*

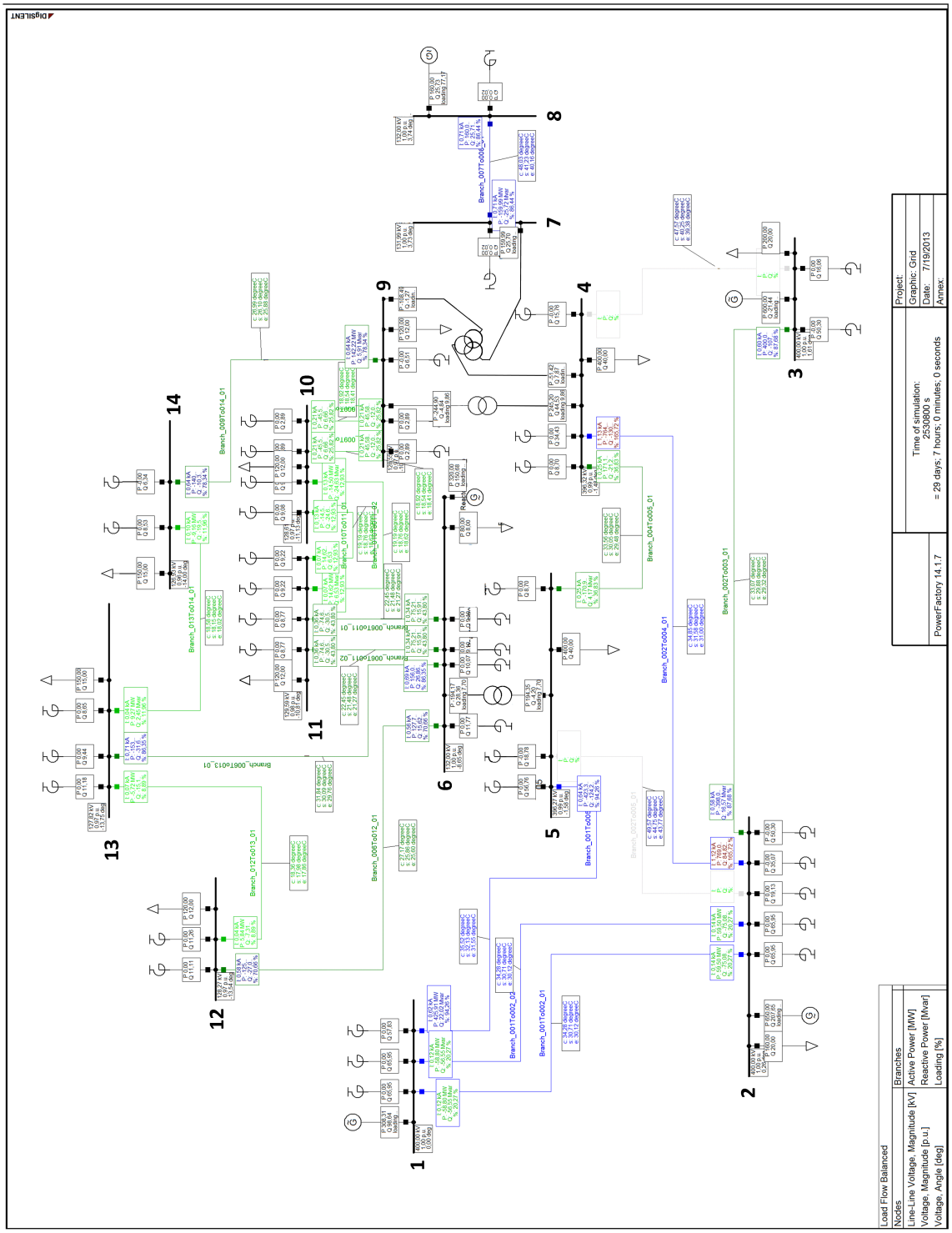

(b) 7:00 at the 30th day

Figure E.3: *Continued on next page.*

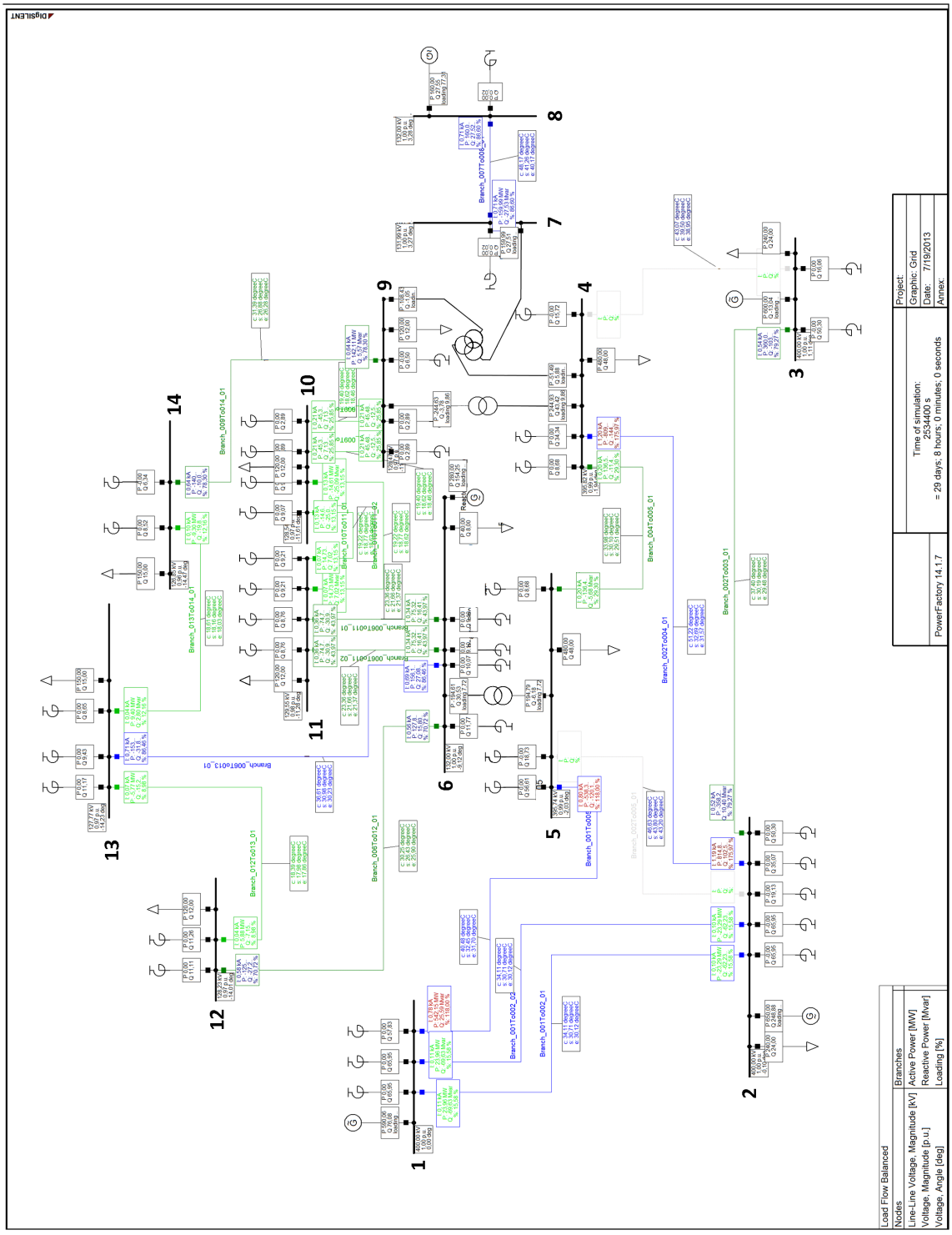

(c) 8:00 at the 30th day

Figure E.3: *Continued on next page.*

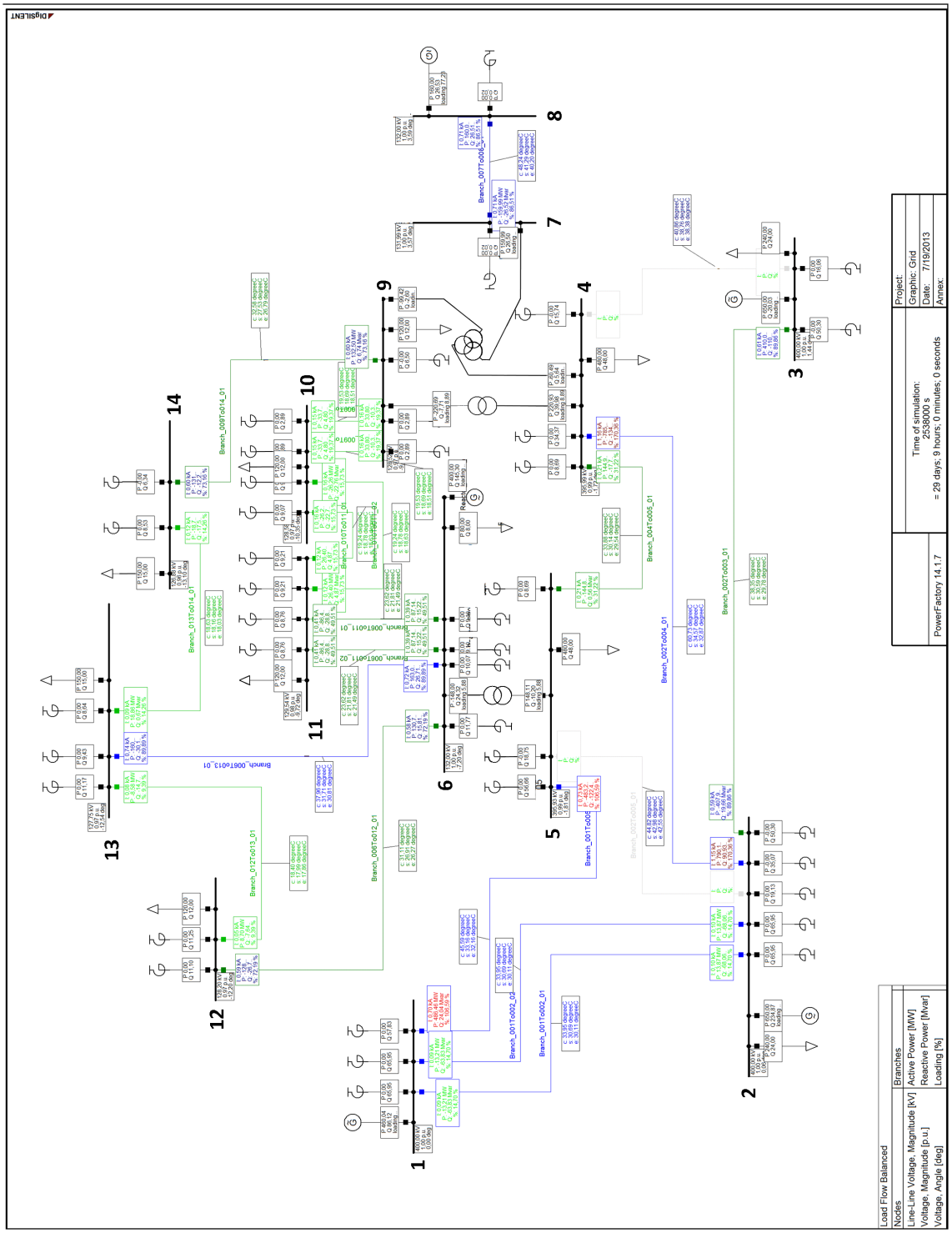

(d) 9:00 at the 30th day

Figure E.3: *Continued on next page.*

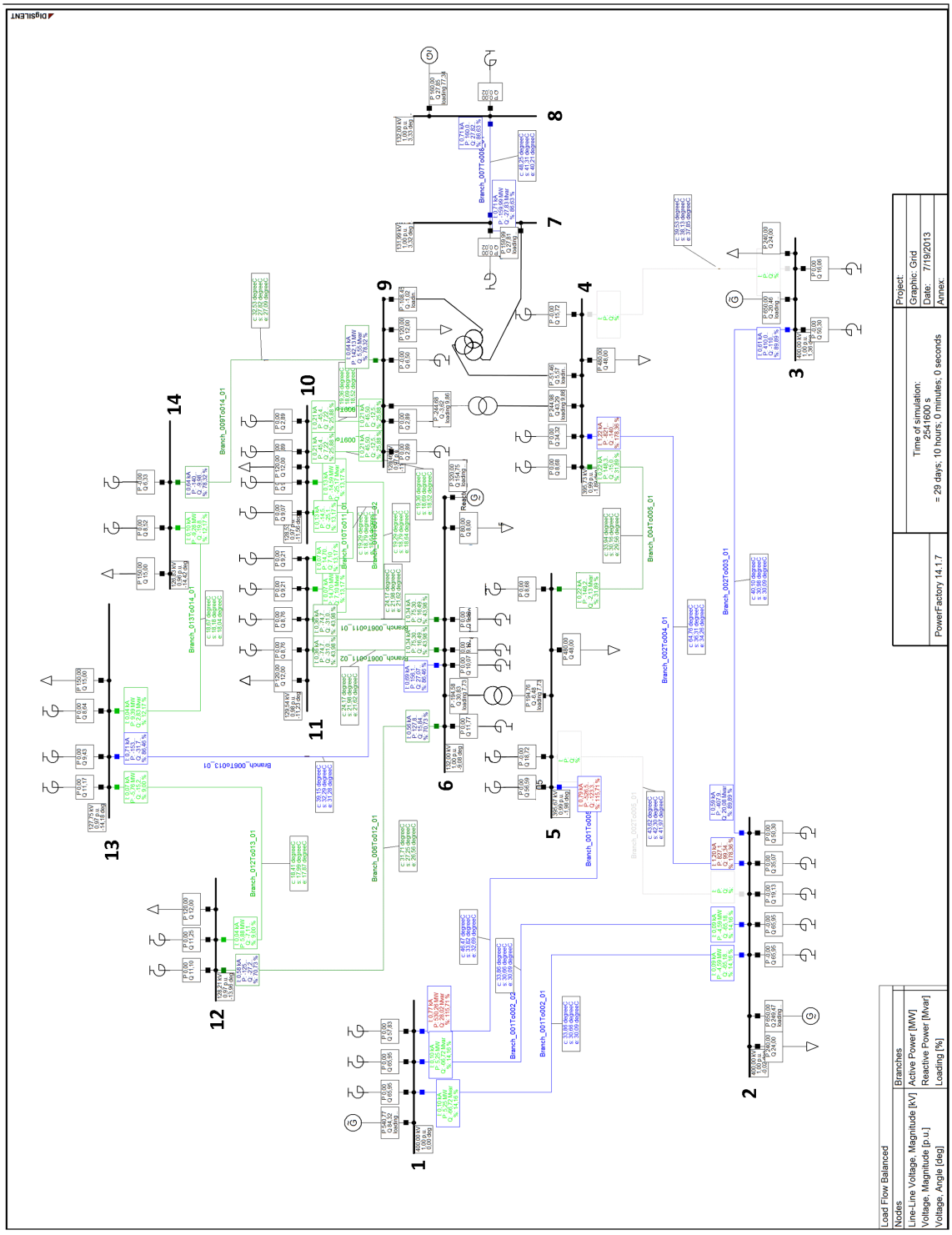

(e) 10:00 at the 30th day

Figure E.3: Thermal evolution of transmission system operated based on ETC.

Appendix F

Publications

The results of the present PhD project has been presented in a number of written scientific contributions, 4 papers presented at various conferences and 1 paper printed in a scientific journal. In addition, 1 paper has been accepted for publication in a scientific journal as well as 1 paper is currently under review for publication. The following pages shows a list of the publications in chronological order as they can be found in the different conference proceedings and journals. Furthermore, selected papers are printed in the following in their most recent version.

Conference	Title of Contribution	Authors
NordIS 2011 June 2011	Frequency Dependent Losses in Transmission Cable Conductors	R. Olsen J. Holbøll U.S. Guðmundsdóttir
JiCablé 2011 July 2011	Real Time Load Optimisation of Cable Based Transmission Grids	R. Olsen J. Holbøll U.S. Guðmundsdóttir
IEEE PES General Meeting 2012 July 2012	Dynamic Temperature Estimation and Real Time Emergency Rating of Transmission Cables	R. Olsen J. Holbøll U.S. Guðmundsdóttir
NordIS 2013 June 2013	Thermal aging of XLPE cable insulation under operational temperatures - Does it exist?	R. Olsen J. Holbøll J.Z. Hansen M. Henriksen

Journal	Title of Contribution	Authors
Published IEEE Transactions on Power Delivery, Vol. 28, No. 3, July 2013	Modelling of Dynamic Transmission Cable Temperature Considering Soil Specific Heat, Thermal Resistivity and Precipitation	R. Olsen G. Anders J. Holbøll U.S. Guðmundsdóttir
Accepted IEEE Transactions on Power Systems	Electrothermal Coordination in Cable Based Transmission Grids	R. Olsen J. Holbøll U.S. Guðmundsdóttir
Submitted IEEE Transactions on Power Systems, In 1st Review	Implementation of Electrothermal Coordination in Cable Based Transmission Grids Operated under Market Based Conditions	R. Olsen J. Holbøll U.S. Guðmundsdóttir C. Rasmussen

F.1 IEEE PES General Meeting 2012

Dynamic Temperature Estimation and Real Time Emergency Rating of Transmission Cables

R. S. Olsen, J. Holboll and U. S. Gudmundsdóttir

Abstract-- **This paper is concerned with the development of a fast computational methodology for dynamical estimation of the temperature in transmission cables solely based on current measurements and an enhanced version of the lumped parameters model, also denoted thermo electric equivalents (TEE). It is found that the calculated temperature estimations are fairly accurate - within 1.5°C of the finite element method (FEM) simulation to which it is compared - both when looking at the temperature profile (time dependent) and the temperature distribution (geometric dependent). The methodology moreover enables real time emergency ratings, such that the transmission system operator can make well-founded decisions during faults. Hereunder is included the capability of producing high resolution loadability vs. time schedules within few minutes, such that the TSO can safely control the system.**

Index Terms--**Cables, transmission lines, dynamic temperature control, finite element methods, temperature prediction methods.**

I. Introduction

THE present paper will introduce a methodology for fast estimation of dynamic temperatures in transmission cables, as well as enabling online dynamic temperature predictions.

The generally accepted method for rating of transmission cables follows the IEC 60287 standard [1], which is used to calculate the ampacity/loadability under steady state and worst case conditions. The limiting parameter for loadability of cables is the temperature, either at the conductor or at the jacket; however transmission systems are operated on the basis of power and voltage, and the loadability of a cable is therefore not given as a temperature but as a current.

It is implied by the term steady state rating that the thermal inertia is neglected in the equations and the temperature will thus, most of the time, be well below the steady state rating. Furthermore, the steady state current rating includes, as stated, the worst case conditions. These worst case conditions will only rarely, if ever, be fulfilled, and the cable will therefore for the largest part of its lifetime be underutilised. These facts are well acknowledged and researchers have therefore tried to develop dynamic thermal rating (DTR) methods for cable systems. Some of these methods utilise finite element methods (FEM) (e.g. [2]), some are concerned with online temperature measurements (e.g. [3]) and yet again some utilise analytical methods (e.g. [4]).

The standards focus mainly on steady state calculations; however some dynamics are included [5], as they are concerned with both cyclic and emergency ratings. Again, these ratings are given as currents.

For doing these rating calculations, the standards utilise the resemblance between current flowing in an electric circuit, and heat flowing in a thermal circuit, the so called thermo electric equivalents (TEEs), based on electrical lumped parameter models. In [5] the TEEs are developed to consist of two loops, one for the internal part of the cable and one for the cable surroundings. This simplification allows for distinguishing between slow and fast temperature changes.

It is the intention of the present study to develop a general methodology which can be used for estimating the temperature in transmission cables dynamically, without distinguishing between slow and fast temperature changes.

Moreover, the study should develop tools for calculation of real time emergency ratings, which can help the operator of the transmission system to make fast choices during faults.

It is furthermore the aim that the model should be independent of temperature measurements, the computational time should be low and the method should be able to predict the temperature in the transmission cable solely based on estimated loading profiles.

Unless otherwise stated, the authors have used Matlab for calculations and production of graphical elements.

All Matlab simulations have been run on a 3.1GHz four processor, 64-bit Windows server 2008 with 4GB of ram.

All finite element simulations have been run on a 2.7GHz quad-core, 64-bit Windows 7 PC with 8GB of ram.

II. Methodology

As mentioned, there are a number of different approaches to take when the goal is to estimate temperatures in cable systems.

Firstly, FEM can in principle give results almost as accurate as one wishes, the size of the elements in the simulation can simply be made 'infinitely' small and all subcomponents can be included to a very detailed level. However the computational time is highly dependent on the number of

R. S. Olsen is with Section of Transmission Lines, Energinet.dk, Fredericia 7000, Denmark (e-mail: rso@energinet.dk).

J. Holboell is with the Department of Electrical Engineering, Technical University of Denmark, Kgs. Lyngby 2800, Denmark (e-mail: jh@elektro.dtu.dk).

U. S. Guðmundsdóttir is with Section of Transmission Lines, Energinet.dk, Fredericia 7000, Denmark (e-mail: usg@energinet.dk).

978-1-4673-2729-9/12/$31.00

elements in the model, and the simulation can therefore become very long, even for relatively simple systems.

The second option is to use the semi-analytical approaches as done in [4]. This approach is capable of calculating the continuous thermal field in the insulation by assuming simple boundary conditions. According to [4], the method is fast but some inaccuracies must be accepted. There is a risk that the simplifications, which are necessarily made with respect to boundary conditions, will result in accumulated errors, which will especially arise when a continuously varying load is imposed on the cable and not just a single current step.

A number of other methods have been investigated, such as e.g. the Finite Difference Method (FDM), time series analysis, etc. However the only serious competitor to the previously two described methods, as it is seen by the authors, is to enhance the models proposed by IEC in e.g. [5]. The computational time is expected to be low compared to FEM, but the drawback is a possible less accurate calculation. One can argue that TEEs are simplified equivalents of FEM models; however FEM models are capable of easily implementing unsymmetrical parts, which is difficult in TEEs. The implementation of multiple cables is necessarily very simplified in the TEEs, whereas the FEM approach enables highly accurate implementation.

The lumped parameters model has proven sufficiently accurate for steady state analysis and to some degree it is possible to extend this accuracy to dynamic models also. As compared to the time demanding FEM simulations, the expected low computational time, required by TEE, introduces the perspective of including and utilising thermal calculations into entirely new applications in transmission system operation. In the following, FEM will only be used for parameter estimation and model verification.

TEEs are used e.g. in [1] for determination of the steady state ampacity and in e.g. [5] for cyclic and emergency ratings. However, the present study is not concerned with cyclic or emergency ratings, but true dynamic temperature estimations. It is therefore not sufficient to use the two loop TEEs which are suggested in [5].

As described, the concept of TEE is built on the resemblance between heat flowing in a thermal circuit and current flowing in an electric circuit. This means that thermal capacitances will be implemented as electrical capacitances in the TEE, and the thermal resistances will be inserted as electrical resistances. The heat sources in the different subcomponents of the cable will be implemented into the TEE as current sources. In the present study heat sources have been implemented at the conductor (W_c), in the dielectric (the dielectric losses are split into two: W_{d1} and W_{d2}) and in the screen (W_s).

Creating the dynamic TEE in this way makes it possible to follow the temperatures at the different subcomponent interfaces. The temperatures will appear in the TEE as voltages at the different nodes.

In Fig. 1 the simplest of such a TEE is shown for an unarmoured single phase cable.

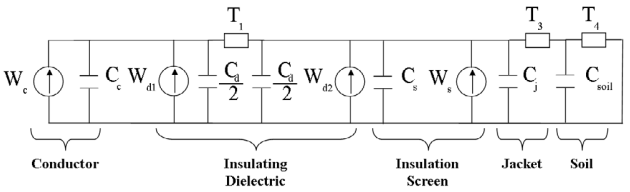

Fig. 1: The simplest thermo electric equivalent (TEE) of an unarmoured cable.

As it is seen from the figure, the thermal resistances of the metallic parts of the cable are neglected. This is assumed valid as the thermal resistivity of metals is usually two orders of magnitude smaller than the thermal resistivity of other parts of the cable.

It can be noticed from the above description and Fig. 1, that smaller subcomponents, such as semi conducting layers, are not included in the model. This is not due to restrictions in the methodology, but merely for easing the explanation of the proposed procedure.

The circuit in Fig. 1 is suitable for steady state and dynamic temperature estimation under constant and varying currents leaving the sources.

The proposed methodology has the inherent property of increasing the accuracy of the model with the cost of increased calculation time. By dividing the different subcomponents into several π-sections, a more accurate estimation of the temperature profile becomes available. This is an important feature, as the user of the model can choose the accuracy which is sufficient, and still have the benefit of high computational speed.

In clause III. it is shown why it can be important to utilise the possibility of increasing the accuracy of the model.

Considering simulation of the behaviour of a TEE circuit, it was chosen to solve the differential equations of the TEE at all nodes analytically [6], which means that the solution time can become very low.

The differential equations defining the 3-node system of Fig. 1 have for clarity been reduced to the matrix form as seen in (1).

An analytical solution requires the calculation of the Eigen values and Eigen vectors for the system matrix of (1).

$$\begin{bmatrix} \dot{\theta}_e \\ \dot{\theta}_s \\ \dot{\theta}_c \end{bmatrix} = \begin{bmatrix} -\left(\frac{1}{C_4T_3}+\frac{1}{C_4T_4}\right) & \frac{1}{C_4T_3} & 0 \\ \frac{1}{C_3T_3} & -\left(\frac{1}{C_3T_1}+\frac{1}{C_3T_3}\right) & \frac{1}{C_3T_1} \\ 0 & \frac{1}{C_1T_1} & -\frac{1}{C_1T_1} \end{bmatrix} \cdot \begin{bmatrix} \theta_e \\ \theta_s \\ \theta_c \end{bmatrix} + \begin{bmatrix} \frac{1}{C_4T_4}\cdot\theta_{amb} \\ \frac{1}{C_3}\cdot\left(W_{d2}+W_s\right) \\ \frac{1}{C_1}\cdot\left(W_c+W_{d1}\right) \end{bmatrix} \quad (1)$$

Here θ_{amb}, θ_e, θ_s and θ_c are the ambient (above ground), jacket, screen and conductor temperatures respectively, and we define three capacitances:

$C_1=C_c+C_d/2$

$C_3=C_d/2+C_s+C_j$

$C_4=C_{soil}$

The indices of these capacitances are: Conductor (*c*), dielectric (*d*), screen (*s*), jacket (*j*) and surrounding soil (*soil*).

The thermal resistances (*T*) are defined according to their physical position in the cable as it is seen in Fig. 1 and given in [7].

The solution to (1) is found by calculating the proper Eigen values (λ_1, λ_2 and λ_3) and Eigen vectors (v_1, v_2 and v_3). According to e.g. [6], the solution to such an equation system is as given in (2).

$$\begin{bmatrix}\theta_e(t)\\ \theta_s(t)\\ \theta_c(t)\end{bmatrix} = c_1\bar{v}_1\cdot e^{\lambda_1 t} + c_2\bar{v}_2\cdot e^{\lambda_2 t} + c_3\bar{v}_3\cdot e^{\lambda_3 t} + \begin{bmatrix}\theta_e(\infty)\\ \theta_s(\infty)\\ \theta_c(\infty)\end{bmatrix} \quad (2)$$

The steady state temperatures at infinite time can be easily calculated by using the circuit of Fig. 1 and discarding the thermal capacitances.

The three constants (c_1, c_2 and c_3) are determined by using the initial temperatures, which can be assumed to be equal to the ambient temperature if no previous load has been applied to the cable.

It should be noted that by increasing the accuracy of the model by splitting the subcomponents into more π-sections, the number of nodes will increase, thus the size of the system matrix of (1) and the computational time will also increase.

A. Parameter Sizes

In the present study, the thermal resistances (T_i) are calculated according to the suggestions of [7]. The thermal resistivities ($\rho_{i,thermal}$) of the individual layers are in this reference multiplied by a factor (G_i) depending on the geometry of the cable. The thermal resistance is therefore calculated as it is rephrased in (3), where i is the layer (e.g. dielectric, jacket, etc).

$$T_i = \frac{\rho_{i,thermal}}{2\pi}\cdot G_i \quad (3)$$

The losses in the conductor and dielectric are simply given by:

$$W_c = R_{\theta,AC}\cdot I^2 \quad (4)$$

$$W_d = 2\cdot\pi\cdot f\cdot C_{el}\cdot U_0^2\cdot\tan(\delta) \quad (5)$$

$R_{\theta,AC}$ being the temperature dependant AC resistance, I is the current, f is the system frequency, C_{el} is the electrical capacitance of the cable, U_0 is the phase to ground voltage and tan(δ) is the dielectric loss factor.

It is in [1] assumed that the screen losses can be assessed directly as a fraction of the conductor losses. This approach is therefore also used in the present study. However the formulae used for the calculation of this quantity is highly dependent on the screen type, laying condition and bonding configuration. It is also recognised in [1] that the losses, under certain conditions, can become very small or even negligible.

The thermal capacitances are calculated by using the geometric parameters of the cable, given by the manufacturers, and utilising specific heat capacities typical for the materials involved.

The thermal capacitance and thermal resistance of the surrounding soil are usually the difficult quantities to determine due to their size and unsymmetrical heat flow.

Models are available for the thermal resistance of cable surroundings, but the authors have found only limited literature within the area of thermal capacitance. Furthermore, the models for thermal resistance are mainly aiming at steady state conditions. For that reason models on how to divide the soil equivalent into more π-sections is not thoroughly described in the literature.

On that background, it was chosen here to model the thermal capacitance of the soil with a cylinder centred at the centre cable and with a radius equal to the laying depth. The assumption is that such a cylinder will overestimate the thermal capacitance, compared to what will be experienced in real life. The heat will, in real life, seek mainly to the surface of the ground, whereas in the thermo electric equivalent, the heat is approximated to be distributed symmetrically away from the cable. This difference will result in the cylindrical approximation of the thermal capacitance of the soil being an overestimation, when comparing to what will be seen in real life experiments. The quantification of this overestimation and more suitable soil equivalents are left for future research.

The thermal resistance of the soil is known as varying a lot and being dependent on a number of parameters, e.g. moisture content. Also some laying configurations promote better thermal conditions than other. However the publications describing the thermal resistance of the soil are, as stated, almost solely concerned with steady state conditions (see e.g. [7] and [8] for extensive descriptions). On the basis of these steady state quantities, the present study uses some approximations in order to calculate the thermal conditions. For three single phase cables with an outer diameter of D_e, laid in flat formation with axial spacing of s_1, installed in a depth of L and in soil with a thermal resistivity of $\rho_{soil,therm}$, the thermal resistance T_4 can, according to [7], be calculated as follows.

$$T_4 = \frac{\rho_{soil,therm}}{2\cdot\pi}\cdot\left(\ln\left(u+\sqrt{u^2-1}\right)+\ln\left(1+\left(\frac{2\cdot L}{s_1}\right)^2\right)\right) \quad (6)$$

Where:

$u=2L/D_e$

Equation (6) reduces to (7) when u is much larger than unity, which is a normal condition.

$$T_4 = \frac{\rho_{soil,therm}}{2\cdot\pi}\cdot\left(\ln(2\cdot u)+\ln\left(1+\left(\frac{2\cdot L}{s_1}\right)^2\right)\right) \quad (7)$$

In the present study, the material specific parameters of Table 1 have been used.

TABLE 1
MATERIAL SPECIFIC PARAMETERS USED IN THE PRESENT STUDY

Material:	tanδ [ ]	$\rho_{electrical}$ [μΩ·m]	$\alpha_{electrical}$ [Ω/K]	$c_{thermal}$ [J/(m³·K)]	$\rho_{thermal}$ [K·m/W]
XLPE	0.005	-	-	$2.40\cdot10^6$	3.5
Aluminium	-	$2.83\cdot10^{-2}$	$4.03\cdot10^3$	$2.43\cdot10^6$	0
Copper	-	$1.72\cdot10^{-2}$	$3.93\cdot10^3$	$3.35\cdot10^6$	0
Soil	-	-	-	$1.92\cdot10^6$	1

III. RESULTS

Results achieved by means of the analytical TEE approach were verified by comparison with a finite element model created in the commercial software Comsol Multiphysics version 4.2. Later, dynamic temperature measurements performed on real cables will be used for further verification.

The cable type modelled in the present paper is: single phase, 1000mm^2 compacted aluminium conductor, XLPE

420kV insulation, copper wire screen with a total cross sectional area of 200mm^2 and aluminium water blocking foil. The geometric quantities of the cable have been obtained from the NKT product catalogue [9]. The manufacturer's reference for this cable type is '1-leder PEX-AL-LRT 420 kV'. The important cable geometries are given in Table 2.

TABLE 2
GEOMETRIC PARAMETERS OF CABLE UNDER INVESTIGATION.

Component	Conductor	Insulation	Screen	Jacket
Outer diameter [mm]	34	109.6	120.4	131.6

The cables are laid in flat formation with 70 mm of spacing in between neighbouring cables and laid in a depth of 700 mm.

A. Models

1) Finite Element Model

The FEM model is designed in 2D as seen in Fig. 2.

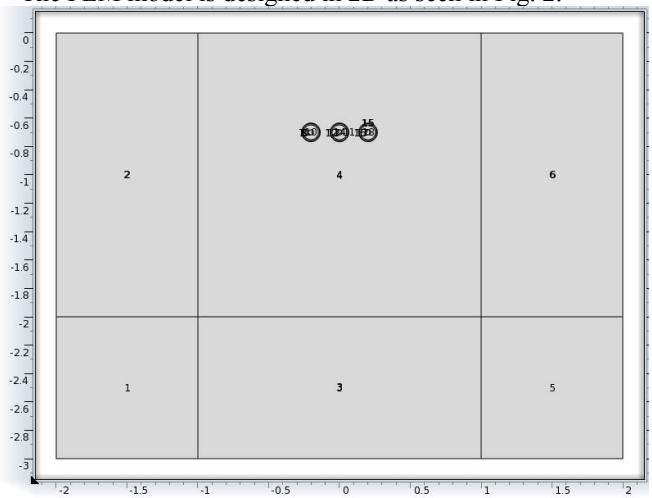

Fig. 2: Finite element model as designed in Comsol Multiphysics 4.2. The axes show the size in meters. The soil is an assembly of a normal rectangular part and infinite elements. The infinite elements limit the effects of the boundary conditions very much. The surface of the soil is assumed to be at 15ºC at all sides.

The cables are modelled as four subcomponents, a solid aluminium conductor, XLPE insulation, solid copper screen and XLPE jacket. Conductor and screen are modelled as solids, which is done for simplicity and it is assumed that only limited errors will be introduced when only thermal equations are to be solved. Comsol is capable of combining the electric and thermal physics, however in the present study, focus is on validating the thermal models, and therefore only the thermal physics in Comsol are utilised. The size of the heat inputs are therefore calculated based on the equations given in [1].

The soil is in Comsol modelled as a large square part (denoted 4 on the figure) in combination with the infinite elements (1, 2, 3, 5 and 6), which limit the boundary effects.

It may appear that the model is small, so in order to confirm the sufficiency of it, a larger version was modelled as well, which gave identical results.

2) Thermo Electric Equivalents

The thermo electric equivalents of this study are designed according to the description of the preceding sections.

It is known that the thermal properties of the insulating material have a large impact during fast load changes (see e.g. the discussion on Van Wormer coefficients in [8]), why a division of the dielectric into multiple π-sections is reasonable. However for longer lasting load changes, the surrounding material will also have a large impact, why it is equally reasonable to divide the soil into multiple π-sections.

As this study is primarily concerned with dynamic load conditions the authors have focused on the long time scale. The remaining of this paper therefore deals with π-sectioning of the surrounding material, but it is to be noted that in order for the model to become more accurate, especially for fast load changes, π-sectioning of the dielectric may be highly necessary.

Regarding the division in π-sections, the laying depth was divided into k equally large intervals as shown in Fig. 3. In Fig. 3 k is equal to three. It is seen that the thermal capacitances in this case must be calculated via the specific heat and the volume of hollow cylinders. In the figure is, for simplicity, shown the single cable case.

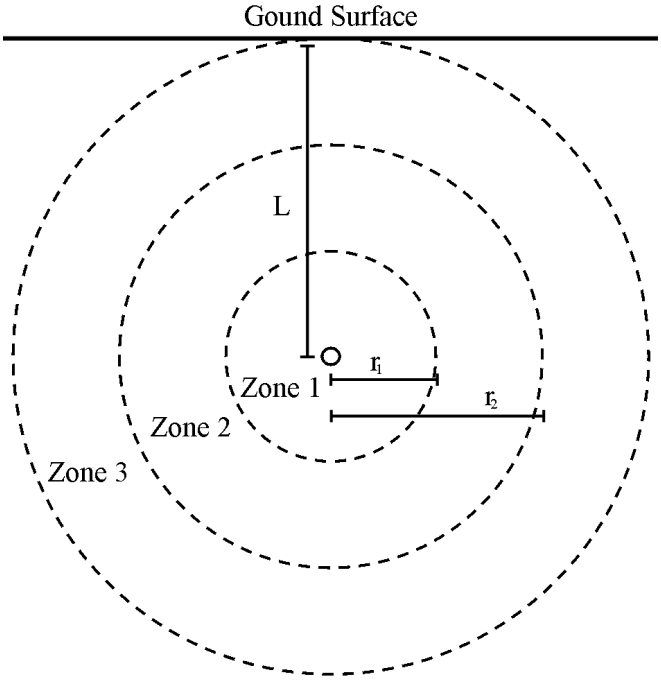

Fig. 3: The thermal resistance of the cable surroundings is divided into zones. In this figure a single cable is shown for simplicity. The soil is seen to be divided into three resistance parts.

The thermal resistance of the individual π-sections has been calculated based on adapted versions of the steady state equations of e.g. [8]. It should be noticed that the thermal resistance of Zone 3 is not equal to that of Zone 1 because the ratio of the radii is smaller. It is thus not sufficient simply to divide the thermal resistance T_4, as calculated by (7), with the number of intervals, k.

Equation (7) is therefore used in an adapted version to calculate the thermal resistance of the individual zones. The thermal resistance of Zone *'x'* (for the simple model of Fig. 3, *x* can be the numbers 1, 2 or 3) has in the present study been calculated as seen in (8).

$$T_{4,x} = \frac{\rho_{soil,therm}}{2 \cdot \pi} \cdot \left(\ln\left(\frac{r_x}{r_{x-1}} \right) + \frac{\ln(2) + \ln\left(1 + \left(\frac{2 \cdot L}{s_1}\right)^2\right)}{k} \right) \qquad (8)$$

It is seen from (8) that the thermal resistance is broken into two parts. The first part, related to the first logarithmic term, is concerned with the thermal resistance caused by the size of the zone. The second part, related to the second and third logarithmic terms, is concerned with the influence of the neighbouring cables.

It is seen from (8) that the first part of the formulae takes care of the difference in thermal resistance for the different zones. On the other hand, the second part of (8) shows that the present study assigns an equal quantity of the influence of the neighbouring cables for all zones. The latter is an approximation, however for simplicity, this approach has been chosen.

It should moreover be noted that the thermal parameters are assumed constant throughout the modelled timeframe. This means e.g. that no dry out of the soil is assumed. Again it is emphasized that this is not a limit enforced by the methodology, as $\rho_{soil,therm}$ can easily be made dependent on the distance from the cable (r_x), but that the assumption is included for simplifying the explanation of the model.

In the following clauses, the sensitivity of the above described π-section division is tested.

The internal parts of the cable are, for simplicity, modelled as seen in Fig. 1. This means that no additional π-section division is performed for the cable subcomponents. It was considered to include Van Wormer coefficients as they are given in e.g. [8], however these coefficients change according to whether the transient is short or long lasting, and an inclusion in a dynamic study, such as the present, is therefore not meaningful.

To increase accuracy of the modelled thermal behaviour, the authors suggest that the thermal parameters, of the internal parts of the cable, can be divided into more π-sections in a similar way as it is done for the soil in (8). In this way it will also be possible to distribute the dielectric losses more evenly throughout the insulation. However, as mentioned, for simplicity, π-sectioning is used on the surrounding soil only.

B. Load Profile

The cables have in the present study been subjected to the load profile seen in Fig. 4. It has been chosen to vary the load in steps; however this is not a limitation in the methodology of TEE.

It is assumed in the present study that the screen losses can be neglected. This may be a valid assumption, when proper bonding, etc. is performed, see [1] for confirmation.

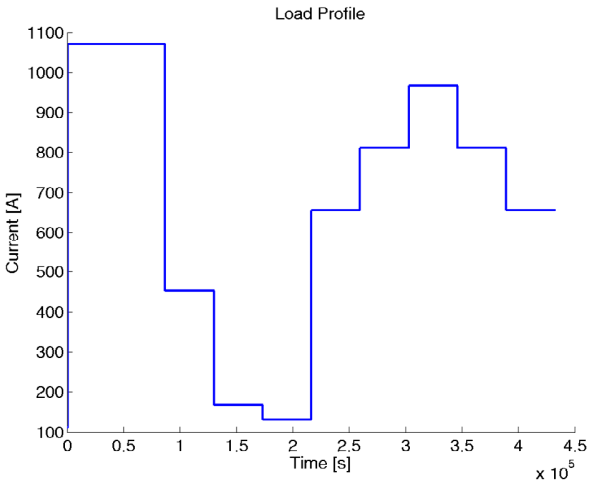

Fig. 4: Load profile of the cable. The cable is seen to be subjected to five days of varying load. Both small and large steps are included in the load profile as well as increases and decreases in the load current are analysed.

On the other hand, for cables operated at voltages at transmission level, dielectric losses cannot be neglected. The present study therefore includes dielectric losses (W_d), and the size is determined by (5) as suggested in [1].

The dielectric losses are estimated to be 11.7 W/m for the given cable.

C. Temperature Profiles

In this paper a clear distinction is made between temperature distribution and temperature profile. A temperature distribution (dealt with in clause III. D.) is the geometrical description of the temperature, which means the temperature at different locations in the cable. On the other hand, the temperature profile is concerned with time variations of the temperature at the different sites of the cable.

In Fig. 5 the temperature profile as calculated by the TEE methodology for 1, 10 and 100 π-sections is shown. Fig. 5 furthermore shows the same temperature profile calculated by FEM as it can be designed in Comsol.

Fig. 5 shows how sensitive the TEE methodology is to the number of π-sections which the soil is divided into. It is clear from the figure that a single π-section is not sufficient for modelling the dynamic thermal behaviour. Modelling with ten π-sections also seems to deviate from the FEM simulation, although for certain purposes it might be sufficient. One hundred π-sections are seen to follow the FEM simulation very accurately for the given load profile, and in case of a need for high accuracy, this is the obvious choice among the three shown simulations. Furthermore the method was tested with five hundred π-sections. However no significant improvement can be seen as compared to one hundred π-sections.

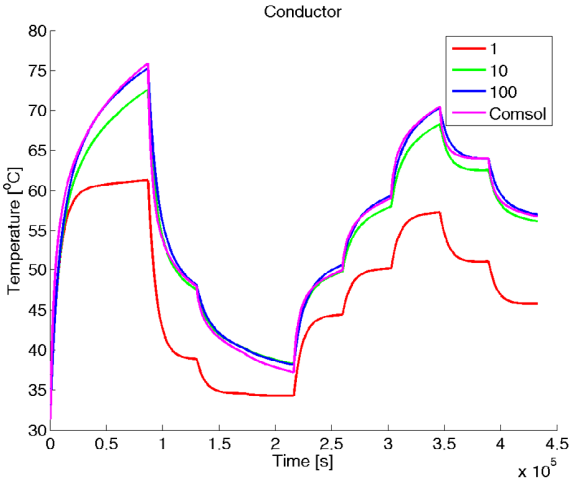

Fig. 5: Temperature profile at the conductor of the 420 kV cable under test. It is seen that the number of π-sections (1, 10 and 100) in the thermo electric equivalent has a high impact on the accuracy of the results. The results of the TEEs are here compared with results obtained from the FEM model of Fig. 2.

The drawback of a comparable high number of π-sections is, as previously discussed, the increased computational time. Fig. 6 shows the computational time as a function of the number of π-sections. It is seen from the figure that the relation is not linear; however the computational time is only increased approximately two and a half times when the number of π-sections is doubled.

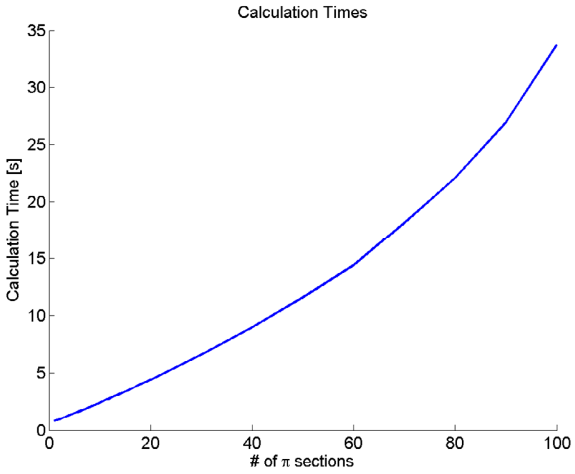

Fig. 6: Computational time for the TEE as a function of the number of π-sections in the model.

It should be noted that the FEM simulation performed in Comsol Multiphysics took more than 11 minutes of computational time to solve the problem defined in Fig. 2, while, as shown in Fig. 6, the TEE simulations with 100 π-sections only took 35 seconds. Increased speed of the FEM simulations can be obtained by utilising the vertical symmetry around the centre cable, but it is expected that such a symmetrical analysis will only halve the computational time.

Based on the above observations it was decided to model the soil by using one hundred π-sections. In case of a need for fast calculations, Fig. 5 shows that ten π-sections can give fairly accurate results.

D. Temperature Distribution

The temperature distribution is, as mentioned, a measure of the temperature at different sites in the cable system. Fig. 7 shows the temperature distribution at time *t = 0* s for the cable modelled in Fig. 5.

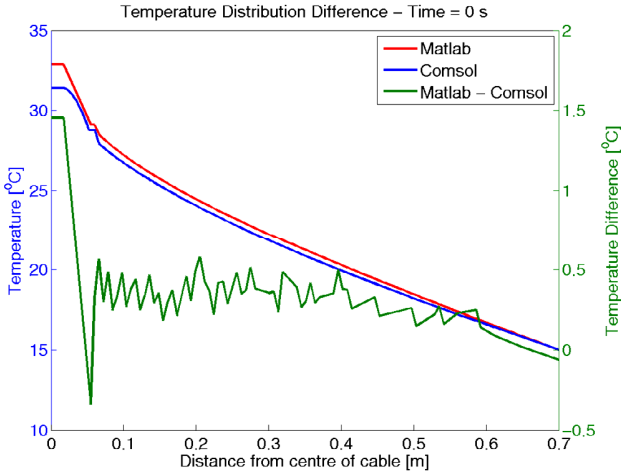

Fig. 7: Temperature distribution from the centre of the conductor, of the centre cable, to ground surface. Some differences are seen in the figure between the TEE model and the FEM model. The shown geometric temperature distribution is a snapshot at *t = 0* s as it is calculated for the load profile of Fig. 4.

It is seen in the figure that the temperature distribution modelled with TEE is very similar to that of the FEM simulation, showing deviations of maximum 1.5°C.

A similar accuracy in the TEE calculations can be found in Fig. 8. The figure, which shows the temperature distribution at the time $2x10^5$s (approximately two days and seven and a half hours), and proves that the TEE methodology enables fast and accurate calculations, deviations are below 1.5°C, of temperature distributions even under dynamic load conditions.

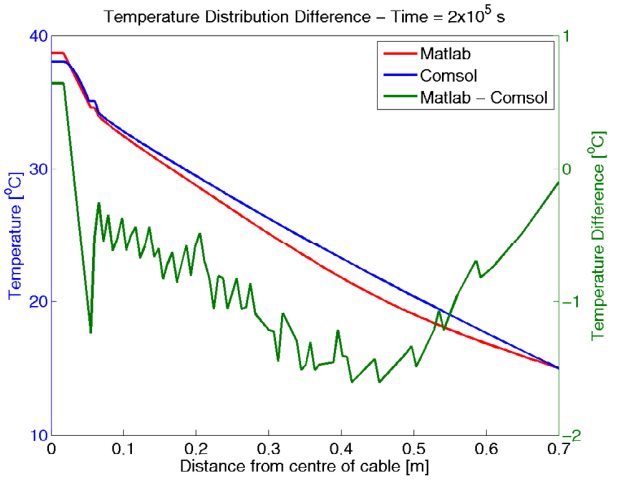

Fig. 8: Temperature distribution at time $t=2x10^5s$. It is seen that the TEE methodology enables accurate calculations of dynamic temperature distributions.

It has to be emphasised that increased accuracy can be obtained without the need for major changes in the

methodology. One of the inaccuracies lies in the calculated thermal resistances as calculated by the IEC standard. These inaccuracies are not further dealt with in this paper, as the inaccuracies could just as easily be in the FEM simulations.

Moreover it should be remembered that the thermal capacitance of the soil is approximated with a cylindrical shape which is not quite accurate.

Dealing with both of these issues is left for future research activities.

E. Temperature Estimation and Prediction

A difference exists between temperature estimation and temperature prediction.

Temperature estimation is concerned with estimating the temperature based on measurements of the current. This quantity can tell about the history of the thermal conditions of the cable, as well as determine whether an existing thermal state of the system is acceptable or not. Any inaccuracies in the temperature estimation thus lie in either the current measurements (not likely with today's SCADA systems) or in the thermal model.

Temperature predictions are concerned with the future, and predictions about the load profile are therefore necessary. The uncertainties in the temperature predictions are therefore at least two-fold, as they include both uncertainties in calculating the temperature and in the predictions of the load profile.

From the calculations point of view, it makes no difference whether the data input are existing measurements or predictions, and the same formulae can therefore be applied.

F. Loadability vs. Time

An obvious application of the methodology described, is to determine the emergency rating of transmission cables very quickly. This includes schemes which tells the operator of the cable how much he can overload the cable under the given conditions and for how long. Such calculations can be easily performed by using the TEEs.

If it for instance is assumed that the history of the temperature is as given in Fig. 5. At the end of the given temperature profile, a fault happens in the transmission system, causing overloading of the cable. The operator now has to know how much and for how long he can overload the cable. The TEE methodology described in this paper will, within less than one minute, be able to display Fig. 9, informing the operator about the available time for reaction and reconfiguration of the system.

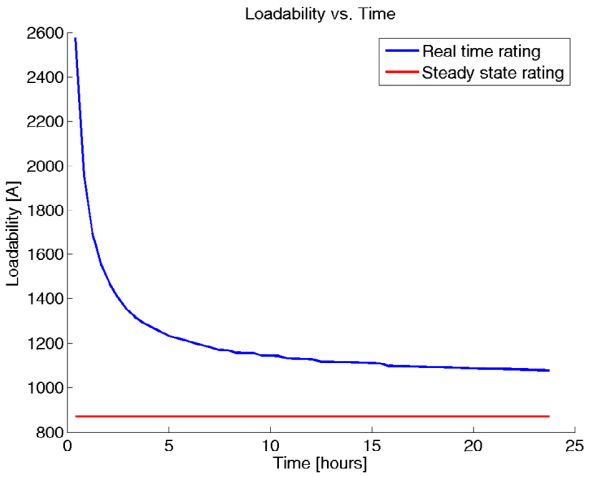

Fig. 9: Loadability of the cable vs. time. During a fault in the transmission system which causes an overloading of the cable, the figure will help the system operator to make proper decisions about how fast he needs to take action in order to prevent damage to the cable.

Faster calculations can of course be made by using fewer π-sections as a first response to a failure, and by including proper safety margins in the analysis, this might be sufficient. After such a fast, preliminary calculation, the more accurate one hundred π-section calculations and an even longer timeline, e.g. two weeks, can be given.

The latter is especially important when dealing with cable grids, as repair times usually are not measured in days but in weeks.

IV. Conclusion

The present study has introduced the basic ideas behind the use of fast thermo electric equivalents (TEEs), also denoted the lumped parameters model, within dynamic temperature simulations of transmission cables. The TEE methodology has shown to be capable of making accurate calculations when comparing to a finite element model (FEM), even for highly dynamic load variations.

In order to develop the true dynamic methodology, the authors had to adapt changes to the internationally accepted standard way of calculating the thermal resistance of the cable surroundings. Especially when dividing the cable surroundings into many π-sections, the methodology proved very accurate, while maintaining a low computational time.

The TEE methodology in the paper is shown to be capable of accurately determining both temperature distributions (geometric dependent) and temperature profiles (time dependent). This enables the operator of the cable system to supervise the current thermal state of the transmission system.

It is moreover shown in this paper that the TEE methodology is capable of helping the operator when failures occur in the system and overloading of the cable is necessary. The TEEs enables a reliable overview of how long and how much the cable can be loaded without risking thermal damage to the cable.

REFERENCES

[1] *IEC Electric Cables - Calculation of the Current Rating -Thermal Resistance - Calculation of Thermal Resistance.* International Electrotecnical Commission Standard 60287-2-1, edition 1.1, November, 2001.

[2] Y.C.Liang and Y.M.Li, "On-line dynamic cable rating for underground cables based on dts and fem," *WSEAS Transactions on Circuits and Systems*, vol. 7, No. 4, 229-238, April, 2008.

[3] M. Schmale, H.-J. Dräger, and R. Puffer, "Implementation and operation of a cable monitoring system in order to increase the ampacity of a 220-kv underground power cable,". 2010 Cigre Session Papers´, 21, rue d'Artois, F-75008 Paris, 2010. Cigre. B1-113-2010.

[4] Jerzy Gołębiowski and Marek Zaręba, "The simplified method for transient thermal field analysis in a polymeric DC cable," *Electrical Engineering*, Springer, vol. 93. No. 4, p. 209-216, May 2011.

[5] *IEC Calculation of the cyclic and emergency current rating of cables - Part 2: Cyclic rating of cables greater than 18/30 (36) kV and emergency ratings for cables of all voltages.* International Electrotecnical Commission Standard 60853-2, edition 1.0, July, 1989

[6] Ole Christensen, Differentialligninger og uendelige rækker, Technical University of Denmark - Institut for Matematisk Modellering, 2006.

[7] *IEC Electric Cables - Calculation of the Current Rating - Thermal Resistance - Calculation of Thermal Resistance.* International Electrotecnical Commission Standard 60287-2-1, edition 1.1, Nov., 2001.

[8] G. J. Anders, Rating Of Electric Power Cables, IEEE Press, 1997.

[9] NKT cables, *Produktkatalog Elforsyning 2010,* [Online], Available: http://www.nktcables.dk/~/media/Denmark/Files/Catalogue/Elforsyning%20katalog%202010.ashx, Nov., 2011.

V. BIOGRAPHIES

Rasmus Schmidt Olsen received his master of science in electrical engineering in 2010 from the Technical University of Denmark (DTU). His PhD project, which he began shortly thereafter, is concerned with dynamic load optimisation of cable based transmission grids and it is a collaboration between Energinet.dk and DTU.
His main interests are within thermal performance of transmission cables, how this performance can be increased and how asset management can be introduced for a more optimal utilisation of such cables and cable systems.

Joachim Holboell is associated professor and group leader at DTU, Department of Electrical Engineering. His main field of research is high voltage components, their properties, condition and broad band performance, including insulation systems performance under AC, DC and transients. Focus is also on wind turbine and future power grid applications.
J. Holboell is Senior Member of IEEE.

Unnur Stella Guðmundsdottir received her M.Sc. and PhD degree in 2007 and 2010 respectively, from Aalborg University in Denmark. Her PhD studies focused on modelling of underground cable system at the transmission level. She was a guest researcher at SINTEF in Norway in November 2008 and at Manitoba HVDC Research Centre in Canada during June-October 2009. Currently she holds a position as a cable specialist at Energinet.dk where she is a deputy manager for DANPAC, a research project focusing on undergrounding of almost the entire Danish transmission system.
U. S. Gudmundsdottir is a Member of IEEE.

F.2 Modelling of Dynamic Transmission Cable Temperature Considering Soil Specific Heat, Thermal Resistivity and Precipitation

Modelling of Dynamic Transmission Cable Temperature Considering Soil-Specific Heat, Thermal Resistivity, and Precipitation

Rasmus Olsen, *Student Member, IEEE*, George J. Anders, *Fellow, IEEE*, Joachim Holboell, *Senior Member, IEEE*, and Unnur Stella Gudmundsdóttir, *Member, IEEE*

***Abstract*—This paper presents an algorithm for the estimation of the time-dependent temperature evolution of power cables, when real-time temperature measurements of the cable surface or a point within its vicinity are available. The thermal resistivity and specific heat of the cable surroundings are varied as functions of the moisture content which is known to vary with time. Furthermore, issues related to the cooling effect during rainy weather are considered. The algorithm is based on the lumped parameters model and takes as input distributed temperature sensing measurements as well as the current and ambient temperature. The concept is verified by studying a laboratory setup of a 245 kV cable system.**

***Index Terms*—Cables, prediction methods, temperature, temperature control, transmission lines.**

I. Introduction

THIS PAPER describes how the temperature of power cables can be dynamically computed when the thermal models are dependent on the moisture content of the surroundings. It is shown how simple temperature measurements from an optic fiber can be implemented in the calculations and how the developed algorithm will estimate the dynamic evolution of the cable environment. This, in turn, will allow predictions about the future development of the temperature and can be utilized in dynamic rating calculations.

The background for developing the temperature estimation methodology is the decision, made by the Danish parliament, to underground all of the Danish transmission system below 400 kV and large parts of the 400 kV system as well. The decision was made based on two reports [1] and [2], which discuss different possibilities in performing such an undergrounding. Based on this decision, the Danish transmission system operator (TSO), Energinet.dk, started a research project investigating possible implementation strategies for dynamic rating of cable-based transmission grids. As Energinet.dk always installs fibres for distributed temperature sensing (DTS) measurements together with their cables, it was decided to investigate how such measurements could be used for improving the utilisation of an almost completely undergrounded transmission system.

The objective is to use the thermal models during normal operation, such that the transmission system operator can monitor the temperature of all cables in the grid. Furthermore, constant monitoring will enable estimation of the cables' real-time loadability, including the emergency rating and, thus, the system operator will gain increased flexibility, especially during contingencies.

In addition to these two purposes, the thermal models can be used for the prediction of the future thermal evolution of the cables. This means that the operator, based on the forecasted generation and consumption patterns, can determine if his transmission system can operate safely in the hours to come, or if he needs to perform control actions in order to prevent overloadings. The latter means that valid dynamic thermal models of the cables will enable Electrothermal Coordination (ETC)-based operation of transmission grids as discussed, for example, in [3] and [4].

In order to ensure accurate thermal modelling of the individual power cables, which is a necessity for ETC to become reality, the parameters of the thermal models should be as accurate as possible. Different studies have taken into consideration the changes of the thermal parameters of the cable surroundings by adapting the soil thermal resistivity while assuming that other thermal parameters are static, [5] and [6]. However, it should be realised that other thermal parameters, in particular, the specific heat of the surroundings, may also change over time.

The implementation of the time varying specific heat of cable surroundings in thermal modelling will be addressed in this paper. Furthermore, the effect of precipitation will be included in the analysis to improve accuracy of the thermal models.

All these considerations will be implemented in the thermal models by assuming that DTS measurements are available, such as will be the case for the future Danish transmission system. In case DTS measurements are not available, as might be the case for older cable systems, the thermal model will be able to work with measurements from thermocouples, which may easily be installed after commissioning of the cable.

It should be recognised that in addition to the moisture content, also the temperature of the cable surroundings affects the thermal resistivity [7] and specific heat [8] of the material. In this study, this temperature dependence of the thermal resistivity and

Manuscript received December 23, 2012; revised March 25, 2013; accepted May 08, 2013. Date of publication June 13, 2013; date of current version June 20, 2013. Paper no. TPWRD-01400-2012.

R. Olsen and U. S. Gudmundsdóttir are with the Section of Transmission Lines, Energinet.dk, Fredericia 7000, Denmark (e-mail: rso@energinet.dk; usg@energinet.dk).

G. J. Anders is with the Department of Electrical Engineering of the Technical University of Lodz, Lodz 90-924, Poland (e-mail: george.anders@bell.net).

J. Holboell is with the Department of Electrical Engineering, Technical University of Denmark, Kgs. Lyngby 2800, Denmark (e-mail: jh@elektro.dtu.dk).

Color versions of one or more of the figures in this paper are available online at http://ieeexplore.ieee.org.

Digital Object Identifier 10.1109/TPWRD.2013.2263300

specific heat is indirectly taken into account by the variability of the moisture content in the surroundings.

II. Moisture-Dependent Thermal Parameters

A. Thermal Resistivity

In [5] and [6], the estimation of the thermal resistivity of the surroundings is implemented in the analysis of the dynamically varying temperature of power cables, which, in turn, is utilized for determining the real-time ampacity of the cables. The thermal resistivity is in the studies adapted such that the computed temperature matches the measured temperature on the cable surface with a specified tolerance over a specified time period. The studies utilize the IEC step response approach to dynamic temperature calculations [9].

The thermal resistivity is exponentially declining with increasing moisture content; sample data are shown, for example, in [10]. However, the dependence of the thermal resistivity on the moisture content is not trivial as similar soil types may have very different properties. Thus, for ensuring accurate modelling, measurements of the thermal resistivity as a function of moisture content must be performed for the specific soil around the cables. It should be noted that the models discussed in [5] and [6] are not dependent on the measurements of the soil thermal resistivity as they only use the temperature and current measurements; and independently adapt the thermal resistivity to fit these measurements.

B. Specific Heat

As stated, the variation of the specific heat with moisture content in the soil is not considered in the studies of the real-time ratings of power cables; however, some studies within other research areas have dealt with this issue, [11]–[14].

It is argued in these studies that, because the weight contribution of gasses in sand and soil is negligible, the specific heat of porous materials (such as sands and soils) is linearly dependent on the moisture content (1), [14]

$$\mathcal{C}_{\mathrm{s,u,therm}}(M) = \frac{M}{100} \cdot \mathcal{C}_{\mathrm{water,therm}} + \left(\frac{100 - M}{100}\right) \cdot \mathcal{C}_{\mathrm{s,u,therm}}(0). \quad (1)$$

Here, $c_{\mathrm{s,u,therm}}(M)$ is the specific heat at moisture content M, in percentage $(\%_{\mathrm{w}})$ of the total weight, $c_{\mathrm{water,therm}}$ is the specific heat of water and $c_{\mathrm{s,u,therm}}(0)$ is the measured dry material-specific heat.

C. Precipitation

During cable loading, moisture will migrate away from the cables when the temperature is high, but it will be added to the cable surroundings during rainy weather. Reference [15] investigates how the thermal resistivity of soil and backfill is affected during and after rain. It concludes that rain can have, but it is not certain, an effect on the thermal resistivity.

In addition to the effect of precipitation on the thermal resistivity of the soil, the water may have further effects.

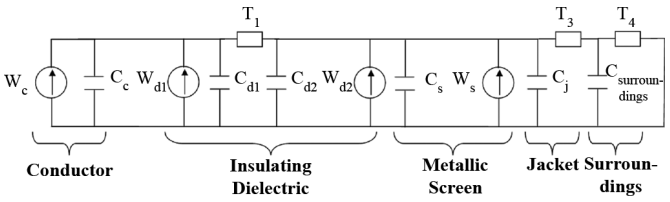

Fig. 1. Thermoelectric equivalent (TEE) of a transmission cable. TEE is the method that utilizes the resemblance between heat flowing in a thermal system with current running in an electric circuit, for calculation of the thermal response to a heat input.

First, the specific heat of the soil will be affected by the rain as shown in (1).

Second, precipitation can cause a direct cooling of power cables when the water flows down through the soil. Both of these effects have not been included in any previous studies. Therefore, one of the goals of this paper is to address these shortcomings.

III. Thermal Modelling of Transmission Cables

This section will briefly summarize the thermal model based on the thermoelectric equivalents (TEEs, also denoted as a lumped parameters model), used in this study, which is similar to the finite-difference model (FDM). For a full description of the modelling procedure, see [16]. Alternatively, see [17] and [18] which describe how other studies recommend similar approaches to thermal modelling.

The thermal model which is presented in this paper, and the concerns which are discussed, are all based on the choice of cables and installation procedures used in Denmark; however, with small modifications of the algorithm, the methodology will be applicable to most other transmission systems.

A. Thermal Model

TEE is the method that utilises the resemblance between heat flowing in a thermal network and current flowing in an electric circuit. All materials have a thermal resistivity and a specific heat, which in the electric analogy is electric resistivity and electric capacity. By modelling heat flow with a current in the electric analogy, the voltage at the different nodes inherently models the temperature. A diagram of a simple TEE of a transmission cable is shown in Fig. 1.

In order to ensure accuracy of the simulations, it is suggested that all subcomponents should be divided into multiple zones. The present study suggests dividing the insulation into 10 zones, the jacket into 3 zones, and the surroundings into 100 zones, such as suggested in [16]. The thermal resistance of all metal parts of the cable (e.g., conductor and screen) is assumed to be negligible; however, the thermal capacitance of the metallic parts must, of course, be included in the simulations.

Danish underground transmission cables are installed in an envelope of sand to improve the thermal environment and for protection from rocks during installation. This means that the cable surroundings are composed of two regions of different materials: sand (sometimes referred to as backfill) and soil. Because the sand is closest to the cables, it has the highest impact on their temperature and the previously described 100

thermal zones have therefore been distributed such that the thermal backfill will be divided into 50 zones and the soil into 50 zones.

B. Thermal Parameters

The calculation of the thermal parameters for the model will be performed and as follows.

1) Thermal Parameters of the Insulation: The thermal resistance of zone number x of the insulation is calculated as given in (2), and the thermal capacitance is given by

$$T_{1,x} = \frac{\rho_{\mathrm{d,therm}}}{2\cdot\pi}\cdot\ln\left(1+\frac{r_x - r_{x-1}}{r_{x-1}}\right), \quad x = 1,2,3,\ldots,n \tag{2}$$

$$C_{1,x} = c_{\mathrm{d,therm}}\cdot\pi\cdot\left(r_x^2 - r_{x-1}^2\right). \tag{3}$$

Here, $T_{1,x}$ is the thermal resistance of zone number x, $\rho_{\mathrm{d,therm}}$ is the thermal resistivity of the dielectric material, r_{x} is the radius (from the cable center) of zone x with r_0 equal to the conductor radius, n is the total number of zones in the insulation, $C_{1,x}$ is the thermal capacitance of the dielectric zone x, and $c_{\mathrm{d,therm}}$ is the specific heat of the dielectric material.

2) Thermal Parameters of the Jacket: Similar to the dielectric insulation, the thermal resistance of the different zones in the jacket is given by (4), and the thermal capacitance is given by

$$T_{3,y} = \frac{\rho_{\mathrm{j,therm}}}{2\cdot\pi}\cdot\ln\left(1+\frac{r_y - r_{y-1}}{r_{y-1}}\right), \quad y = 1,2,..,m \tag{4}$$

$$C_{3,y} = c_{\mathrm{j,therm}}\cdot\pi\cdot\left(r_y^2 - r_{y-1}^2\right). \tag{5}$$

Here, $T_{3,y}$ is the thermal resistance of zone y, $\rho_{\mathrm{j,therm}}$ is the thermal resistivity of the jacket material, r_{y} is the radius (from cable centre) of zone y, m is the total number of zones in the jacket, $C_{3,y}$ is the thermal capacity of jacket zone y, and $c_{\mathrm{j,therm}}$ is the specific heat of the jacket material.

3) Thermal Parameters of Cable Surroundings: Cables in flat formation (the most common way of undergrounding transmission cables in Denmark) will mutually heat each other, and this mutual heating is included in the evaluation of the thermal resistance of the surroundings [16], [19]. For cross-bonded cables, the center cable will be the hottest [20], and (6) gives the thermal resistance of zone number z, and (7) give its thermal capacitance. Other bonding type and cable formations will require modification of (6), depending on the specific conditions

$$T_{4,z} = \frac{\rho_{\mathrm{s,u,therm}}}{2\cdot\pi}\cdot\left(\ln\left(\frac{r_z}{r_{z-1}}\right)+\frac{\ln(2)+\ln\left(1+\left(\frac{2\cdot L}{s_1}\right)^2\right)}{k}\right), \quad z = 1,2,3,\ldots,k \tag{6}$$

$$C_{4,z} = c_{\mathrm{s,u,therm}}\cdot\pi\cdot\left(r_z^2 - r_{z-1}^2\right). \tag{7}$$

Here, $\rho_{\mathrm{s,u,therm}}$ is the thermal resistivity of the surrounding material of type u (depending on the zone number, u can be either sand or soil), L the burial depth of the cables, s_1 the axial spacing between the conductors, r_{z} the radius (from the cable center) of zone z, k is the total number of zones in the surroundings, $C_{4,z}$ is the thermal capacitance of the surroundings zone z, and $c_{s,u,therm}$ is the specific heat of the surrounding material of type u.

Equation (6) is seen to be the radial thermal resistance of a cylinder with an inner radius of $r_{\mathrm{z}-1}$ and an outer radius of r_{z} represented by the term $\ln(r_{\mathrm{z}}/r_{\mathrm{z}-1})$. However, due to the fact that there is more than one cable in a flat configuration, the influence of the outer two phases is included by adding the term $\ln(1+(2L/s_1)^2)$. The division by k is to evenly distribute the influence over the volume of the surroundings. Similarly, the term $\ln(2)/k$ takes into account the image of the cable itself above ground. It is seen that by summing up the thermal resistances for all k zones, the result is the IEC standard equation for T_4 with 100% load factor (9), [19]

$$T_4 = \frac{\rho_{\mathrm{s,u,therm}}}{2\cdot\pi}\sum_{z=1}^{k}\left(\ln\left(\frac{r_z}{r_{z-1}}\right)+\frac{\ln(2)+\ln\left(1+\left(\frac{2\cdot L}{s_1}\right)^2\right)}{k}\right) \tag{8}$$

$$= \frac{\rho_{\mathrm{s,u,therm}}}{2\cdot\pi}\cdot\left(\ln\left(\frac{2L}{\frac{D_e}{2}}\right)+\ln\left(1+\left(\frac{2\cdot L}{s_1}\right)^2\right)\right). \tag{9}$$

Since the TEE method is an attempt to model the 3-D reality in 1-D, it is necessary to represent the shape of the thermal backfill as a circle. A cross section of a Danish cable trench would show a trapezoidal area with sand around the cables. Because the width to height ratio (w/h) of the trapezoid is larger than 3, the trapezoid has in the simulations been adapted to a circle with a radius calculated as suggested in [20] and shown as

$$r_{\mathrm{backfill,eq}} = \frac{2L}{e^{G_b}} \tag{10}$$

where G_{b} is a geometric parameter dependent on the L/h and w/h ratios. The values of G_b are found in [20].

C. Losses

The joule and dielectric losses of cables will, in this study, be calculated as suggested in the standard IEC 60287 [19].

D. Calculation of the Dynamic Thermal Response

The dynamic thermal response to an applied current is calculated by solving a set of first-order differential equations as described in [16]. Expression (11) shows the equations for the simple TEE of Fig. 1, but the system which is solved in

the present study will obviously consist of a matrix containing 113×113 elements

$$\begin{bmatrix}\dot{\theta}_e\\ \dot{\theta}_s\\ \dot{\theta}_c\end{bmatrix} = \begin{bmatrix} -\left(\frac{1}{C_4T_3}+\frac{1}{C_4T_4}\right) & \frac{1}{C_4T_3} & 0\\ \frac{1}{C_3T_3} & -\left(\frac{1}{C_3T_1}+\frac{1}{C_3T_3}\right) & \frac{1}{C_3T_1}\\ 0 & \frac{1}{C_1T_1} & -\frac{1}{C_1T_1}\end{bmatrix} \cdot \begin{bmatrix}\theta_e\\ \theta_s\\ \theta_c\end{bmatrix} + \begin{bmatrix}0\\ \frac{1}{C_3}\cdot(W_{d2}+W_s)\\ \frac{1}{C_1}\cdot(W_c+W_{d1})\end{bmatrix}. \quad (11)$$

Here, θ_{e}, θ_{s} and θ_{c} are the jacket, screen, and conductor temperature increase, above ambient soil temperature, respectively, and $C_1 = C_{\mathrm{c}} + C_{\mathrm{d1}}$, $C_3 = C_{\mathrm{d2}} + C_{\mathrm{s}} + C_{\mathrm{j}}$, and $C_4 = C_{\mathrm{surroundings}}$.$W_{\mathrm{C}}$, W_{d}, and W_{s} are the losses in conductor, dielectric, and screen, respectively.

The solution to this equation is given in (12), [21] and [22]

$$\begin{bmatrix}\theta_e(t)\\ \theta_s(t)\\ \theta_c(t)\end{bmatrix} = c_1\bar{v}_1\cdot e^{\lambda_1 t} + c_2\bar{v}_2\cdot e^{\lambda_2 t} + c_3\bar{v}_3\cdot e^{\lambda_3 t} + \begin{bmatrix}\theta_e(\infty)\\ \theta_s(\infty)\\ \theta_c(\infty)\end{bmatrix} \quad (12)$$

where the initial conditions above ambient are $\theta(0)$, steady-state conditions above ambient are $\theta(\infty)$, λ's are the eigenvalues of the system matrix, $\bar{v}$'s are the corresponding eigenvectors, and c's are constants calculated by solving (13) with the boundary conditions

$$[\,\vec{v}_1 \quad \vec{v}_2 \quad \vec{v}_3\,]\cdot\begin{bmatrix}c_1\\ c_2\\ c_3\end{bmatrix} = \begin{bmatrix}\theta_e(0)\\ \theta_s(0)\\ \theta_c(0)\end{bmatrix} - \begin{bmatrix}\theta_e(\infty)\\ \theta_s(\infty)\\ \theta_c(\infty)\end{bmatrix} \quad (13)$$

$$\begin{bmatrix}\theta_e(0)\\ \theta_s(0)\\ \theta_c(0)\end{bmatrix} = \begin{bmatrix}\theta_e(0^-)\\ \theta_s(0^-)\\ \theta_c(0^-)\end{bmatrix} \quad (14)$$

$$\begin{bmatrix}\theta_e(\infty)\\ \theta_s(\infty)\\ \theta_c(\infty)\end{bmatrix} = \begin{bmatrix}(W_c+W_d+W_s)\cdot T_4\\ \theta_e(\infty)+(W_c+W_d+W_s)\cdot T_3\\ \theta_s(\infty)+(W_c+\frac{W_d}{2})\cdot T_1\end{bmatrix}. \quad (15)$$

Here, $\theta(0) = \theta(0^-)$ means that the temperature above ambient at the beginning of the present calculation time interval is set equal to the temperature above ambient at the end of the previous interval. $\theta(\infty)$ is the temperature above ambient which would be observed after having applied the present conditions (current, voltage, thermal resistivities, etc.) for an infinite period of time.

The native soil temperature is added to the results of (12) to obtain the cable conductor temperature. The native soil temperature can either be measured or modelled, as suggested, for example, in [23] or [24].

IV. Implementing DTS Measurements in the Tees

It should be recognized that the purpose of performing thermal modelling of cable systems is to:

1) estimate the conductor temperature (not measurable);
2) predict the future temperature evolution of the cable;
3) estimate the ampacity of the cable system.

In order to support the aforementioned three purposes, the DTS measurements are used in thermal modelling as a feedback mechanism. The principle is to calculate the cable surface temperature as a function of time using (12) and then compare the calculated fiber temperature with the measured temperature. If these temperatures are different, the thermal parameters of the surroundings are changed and the modelling is repeated until the computed temperature is within a predefined accuracy of the measured temperature. In this way, the properties of the environment are known and updated whenever needed, and the future thermal evolution can be predicted based on the actual real-time conditions.

A. Temperature Calculation Loop

The proposed algorithm computes the thermal evolution of the cables and their environment, such that the model will always use the most recent values of thermal and electric resistivity, specific heat, ambient temperature, and applied current. This means that the algorithm will use a set of these values for calculating the temperature evolution for a period Δt before the set of values is updated.

Δt is thus an important parameter as the modelling accuracy depends on it, and its choice should be based on the frequency of the measurements and expected rate of change of the cable, sand and soil parameters.

B. Temperature Check Frequency

1) Regular Temperature Checks: Since the thermal resistivity and specific heat of the cable surroundings can change in time, it is important to check at regular intervals if the thermal parameters of the model have to be updated. It is not expected that the thermal parameters will change rapidly during normal cyclic operation and, therefore, a comparison between modelled and measured fiber temperatures four times each day should be sufficient. However, there are exceptions from this general requirement when more frequent checks must be made.

2) High Loads: During periods of high load (e.g., 0.7 p.u. or higher), the jacket temperature may increase to a magnitude where moisture migrates fairly fast away from the cable, resulting in rapidly increasing thermal resistivity of the sand. In this case, temperature checks every hour or so could be enforced for ensuring reliable computations.

3) Load Changes: When the load changes by a significant amount, it may be necessary to perform the temperature checks more frequently. This is in order to ensure that the model follows the actual cable temperature during the entire load change. Furthermore, depending on how the temperature is measured, large load changes may result in the model wanting to decrease the moisture content (M) unrealistically fast. Thus, a maximum negative dM/dt should be enforced for modelling purposes, in this study $(-dM/dt)_{\max} = 1[\%_{\mathrm{weight}}/\mathrm{h}]$ is used.

4) Precipitation: In case of rain, the thermal parameters will require a more frequent update, since the thermal resistivity and specific heat can change almost instantaneously.

Furthermore, in heavy rain, the water can run past the cables and cool them beyond the effect of what can be modelled by simply changing the thermal resistance and capacitance of the soil. This means that the model must be able to include a cooling effect caused by the precipitation.

It is suggested that the model should try to adapt the thermal resistivity until a certain lower limit is reached. If the modelled

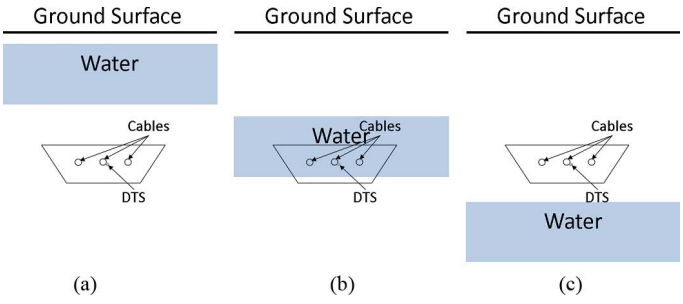

Fig. 2. Sketch of how heavy rainfall can influence the DTS measurements. Time increases from (a) to (b) and again from (b) to (c). It is seen in (b) that the temperature at the fiber pipe may decrease instantaneously while the conductor temperature will experience the cooling effect with a time lag. After the dense block of water has passed (c), the soil and backfill will most likely be saturated with water; however, the temperature of the soil does not necessarily decrease to the water temperature, and, therefore, the fiber temperature may increase again at (c) even with the cables out of operation.

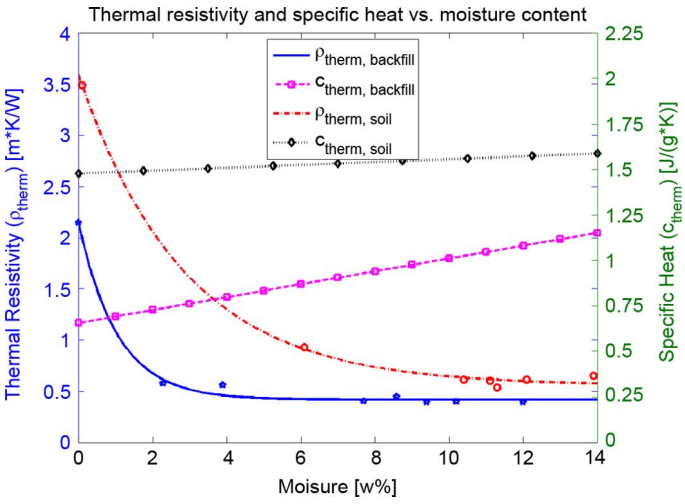

Fig. 3. Measured thermal resistivity and calculated specific heat as a function of moisture content (in % of the total weight) of sand and soil.

temperature still does not match the measured value, the algorithm should lower the computed temperature directly until the required match is obtained. This approach is based on the assumption that the thermal resistivity becomes almost constant beyond a certain value of the moisture content, and, therefore, the deviation between measured and modelled temperature can only be attributed to an external cooling.

The cooling effect of the water may decrease the readings of the temperature sensor more than the surrounding thermal backfill and soil. Thus, when the water has passed beyond the cables, the soil and thermal backfill are saturated with moisture, but a large amount of water and, thus, the instantaneous cooling of the sensor and the cables is gone. This, in turn, may require an increase of the modelled fiber temperature by readding some of the previously subtracted temperature. A sketch of the rain problem is shown in Fig. 2.

Fig. 2 shows cross sections of typical Danish cable trenches. It is noted that the DTS fiber is installed next to the center cable in an air-filled pipe.

C. Check of the Temperature Match

The methodology allows, in principle, for as good an accuracy of the modelled temperature as required by the TSO; however, when the allowed deviation between modelled and measured temperature decreases, the simulation time increases. Moreover, the accuracy of the measured DTS temperature is in the range of $1\,^{\circ}\mathrm{C}$ and, therefore, it is proposed that $\pm 1\,^{\circ}\mathrm{C}$ is the proper accuracy to be used in modelling the temperature of cable systems.

D. Adapting the Tee Model

The proposed methodology is built on the assumption that if the modelled and measured temperatures at, say, 12:00 are within an acceptable tolerance, the thermal parameters of the surroundings before 12:00 were obtained correctly. If later, for example at 18:00, the values do not match; the thermal parameters of the surroundings must have changed since 12:00. Thus, the thermal parameters are updated and the simulation is re-run for the time interval 12:00–18:00 until the measured and computed temperatures at the cable surface match.

Because a single DTS fiber only allows for temperature measurements at one specific distance from the conductor, the thermal resistivity and specific heat distribution in the backfill and the native soil cannot be directly determined. Therefore, the model assumes uniform thermal properties in each of the materials surrounding the cables.

Because the moisture content of the sand and soil are not necessarily equal, it is assumed, for simplicity, that the ratio $R_{\rho/\rho}$ between the thermal resistivity of the soil and sand is kept constant with time. Also, it is assumed that the ratio $R_{\mathrm{c/c}}$ between the specific heat of the soil and sand is constant with time.

Mass and heat transfer models could be used to determine the grading of the thermal resistivity and specific heat through the sand and soil, but including such models would unnecessarily complicate the algorithm and most likely will not increase the accuracy of the predictions.

1) Adaption of Thermal Surroundings: As stated before, the parameter, which, in reality, changes with time, affecting the cable rating, is the moisture content of the thermal backfill and the soil and because the thermal resistivity and specific heat are directly related to the moisture content, these parameters vary along with it.

On that basis, the algorithm, which has been developed for this study, varies the moisture content of the thermal backfill when the modelled temperature is out of the acceptable range $(\pm\Delta\theta_{\max})$ from the measured value. The new moisture content is then related to curves for the thermal resistivity and specific heat of the backfill and the soil, in order to obtain the new thermal parameters for the model. The present study has been based on measured data for one type of sand and soil typically used in Danish cable trenches, see Fig. 3. It should though be noted that the shape of the curves can vary significantly even for similar materials and, therefore, it is now common practice to obtain such curves for new high-voltage cable installations.

Based on the curves in Fig. 3, it is assumed here that $R_{\rho/\rho} = 1.5$ and $R_{\mathrm{c/c}} = 3$. These values are based on the authors' experience that the moisture content in the sand will be lower than that of the soil. The measured dry density is also higher for the soil $(2.6 * 10^6\ \mathrm{kg/m^3})$ than for the sand $(1.7 * 10^6\ \mathrm{kg/m^3})$.

2) Special Cases: As stated, there are special cases, such as during heavy rain, where the thermal model will not be able to adapt by simply changing the thermal resistance and specific heat of the surroundings. Furthermore, in order to account for special cases which may not be covered by the considerations discussed before, and include the fact that the real world does not always behave as theoretically expected, it is necessary to define a realistic interval (lower and upper boundaries) for the moisture content (for example 0–6%$_{\mathrm{weight}}$ for the sand), such that the model will always perform realistic calculations of the temperature. The complete algorithm for modelling the thermal behavior of transmission cables with temperature checks is shown in Fig. 4. Note that a working algorithm should contain a data validation and conditioning module, such that bad measurements do not affect the calculations. For simplicity, such a module is not included in Fig. 4.

E. Multiple Possible Hot Spots

It should be acknowledged that the TEE methodology only evaluates the temperature at a single point along the cable route. In the case of multiple possible hot spots, it is necessary to apply the algorithm of Fig. 4 for each such location.

This can especially be necessary in the case of seasonally changing or long term slowly developing hot spots along the route.

F. Other Temperature Measurements

Some cable manufacturers offer the possibility of integrating an optic fiber for DTS measurements in the cable's metallic screen. Such a measurement is easily included as the feedback instead of the fiber temperature in the pipe, which has been considered so far, as the metallic screen temperature is inherently modelled in the described TEE methodology.

Furthermore, all other temperature measurements (e.g., at the jacket) can also be utilized in the estimation of the temperature distribution; however, it should be recognised that the further the measuring point is from the cable, the less accurate the modelled temperature is likely to be.

V. Loadability Calculation

A. Steady-State Ratings

Even though this paper mainly focuses on dynamic calculations, it is also possible to use the algorithm to calculate the steady-state rating. By neglecting the capacitances in the thermoelectric analogy and summing up the resulting series resistances of (2), (4) and (6), one ends up with the steady-state ampacity equations of the IEC standard series 60287, [19]. This standard assumes a unity load factor; hence, if the predicted future load exhibits cyclic variations, the resulting rating can furthermore be multiplied by the cycling rating factor described in the IEC Standard 60853, [9].

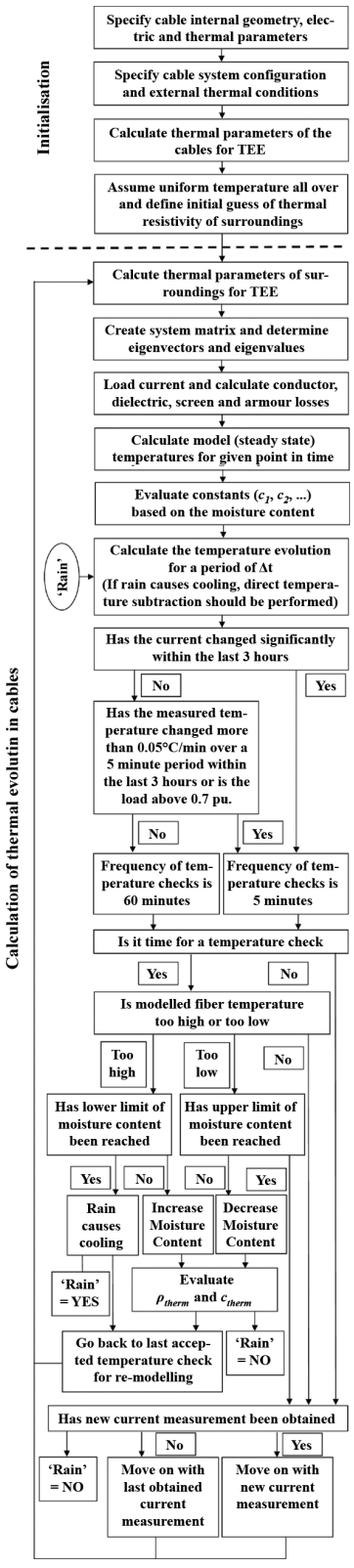

Fig. 4. Algorithm for calculating the temperature of power cables and including checks with measured temperature values. The parameter "Rain" can be either YES, if precipitation causes external cooling, or NO, if no external cooling is experienced.

B. Dynamic Ratings

The TEE method enables a fairly straightforward evaluation of the emergency rating, as the temperature is known for the entire cross section of the cable trench (from ground surface to cable conductor) in real time.

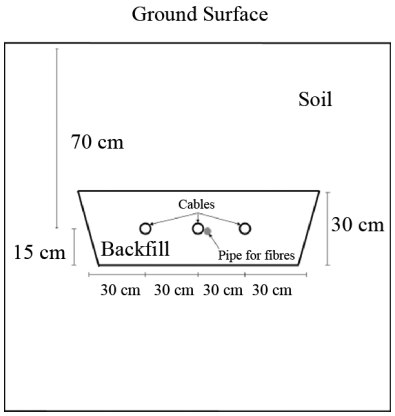

Fig. 5. Cable system modelled in the case study.

The authors suggest that the loadability of the cable system is given as a graph showing time on the abscissa and the maximum allowable current (for the specified emergency temperature), for this period of time, on the ordinate [16].

The calculations are performed by assuming that a specific constant current (I_{TEST}) runs in the cable. The transient temperature response is then calculated by (12). The calculations will be based on a static moisture content of the surroundings as well as a static (or predicted) θ_{amb} determined at the specific point in time of the rating period.

By finding the time where the limiting temperature (conductor or jacket) is reached, a data point (time and current) on the loadability curve is obtained. Thereafter, new currents are applied until a sufficient amount of data points for the loadability curve have been found.

The maximum time period that will be considered in this study is 24 hours since this is assumed to be a sufficient time horizon for an operator to take the required remedial actions. Furthermore, the thermal limit is set to 90 °C on the conductor.

The loadability curve can become an important tool in everyday operation of a transmission system as it can, in case of contingencies, directly tell the operator whether immediate control actions are necessary or if there is time before the thermal limits are reached. Since the loadability curve is a function of the assumed moisture content and ambient temperature, a series of such curves could also be produced with various values of these parameters.

VI. Case Study

To prove the validity of the method, the algorithm was tested on a power cable system (set up in a laboratory) as shown in Fig. 5. The current is varied over four months but for simplifying the measurement of the conductor temperature no voltage was applied across the insulation. Furthermore, screens are left floating, thus minimizing screen losses.

The DTS temperature is obtained from a fiber located in a pipe next to the center phase, and the measured temperature has been compared to the computed temperature at the same location. The cables specifications are given in Table I.

TABLE I
Specifications of the Cables in the Experiment

	Material	Outer diameter [mm]	Thermal resistivity [m·K·W^{-1}]	Specific heat [J·m^{-3}·K^{-1}]
Conductor	Aluminium	45.0*	0.0	$2.43 \cdot 10^6$
Insulation	XLPE	102.0*	2.8*	$2.57 \cdot 10^{6}$ *
Screen	Lead	106.5*	0.0	$1.44 \cdot 10^6$
Jacket	PE	112.0*	2.8	$2.57 \cdot 10^6$

* Specifications marked with a * are measured quantities.
The conductor is solid. The cable has semiconductive screens on conductor and metallic screen, but these are in the mathematical model assumed to be part of the insulation. It is assumed that the PE has similar thermal properties as XLPE. Electrical properties of the materials can be found in [19].

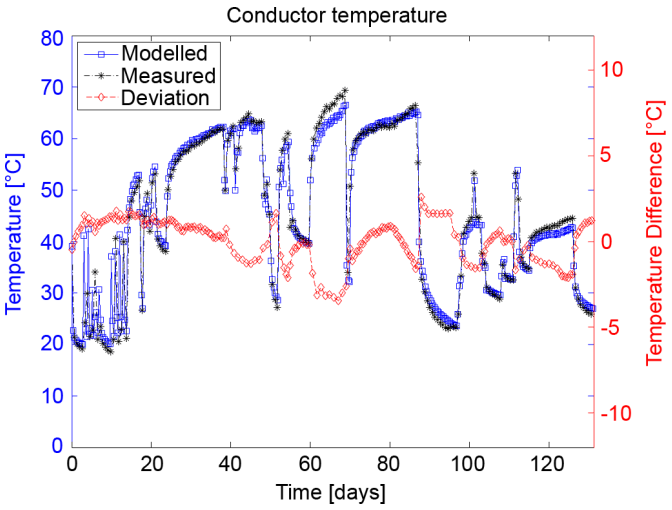

Fig. 6. Modelled and measured conductor temperature. We can observe that the deviations are within 2 °C for most of the modelled period of more than four months.

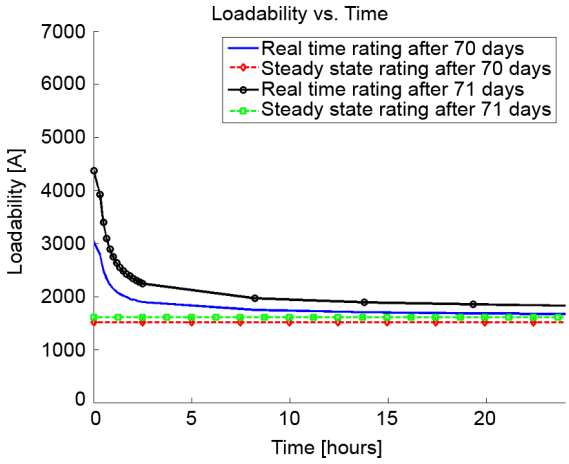

Fig. 7. Loadability as a function of time for the cable system for two points in time. The real-time monitoring of the cable system is seen to be important as the actual thermal state of the system has a major influence on the loadability.

The measured and modelled conductor temperatures are shown in Fig. 6.

The modelled temperatures generated for Fig. 6 utilize the adaption of thermal resistivity and specific heat, and it is seen

that the conductor temperature is computed with fairly good accuracy, better than $2\,^{\circ}\mathrm{C}$ for most of the time. Such temperature variations must be expected at the conductor as the $1\,^{\circ}\mathrm{C}$ accuracy between measurement and model is enforced on the fiber, which is located in a pipe outside the cable.

Furthermore, modelling of the cooling effect, caused by precipitation, proved necessary for the large temperature decrease which is seen after approximately 70 days. Without implementation of this cooling effect, the temperature difference between model and measurement would exceed $15\,^{\circ}\mathrm{C}$ but is now kept below $5\,^{\circ}\mathrm{C}$.

Fig. 7 shows the calculated real-time and steady-state loadability for two points in time (before and after rain). It is seen that it is important to monitor the cables in real time as the loadabilities can vary fairly much even within a short period of time. It is furthermore seen that it is possible to load the cable with a large current in case of emergency and, thus, dynamic temperature calculations will give the TSO a significant flexibility in controlling the system.

VII. Conclusion

This paper presents a new algorithm, based on TEEs, for implementing DTS measurements in the calculation of the dynamic temperatures of power cables by varying both the thermal resistivity and the specific heat of the cable surroundings with time. There are two important innovations implemented in the proposed algorithm.

First, the model varies both the thermal resistivity and specific heat of the surroundings when computing the dynamic temperature of power cable systems, where the varying specific heat has not been previously dealt with in any published studies. The moisture content of the surroundings varies with time and as the thermal resistivity and specific heat are directly related to the moisture content, these parameters vary along with it. The algorithm models the cable system's thermal response to the applied load, and the computed temperature is compared to the measured temperature. The moisture content of the surroundings is adjusted until the measured and computed temperatures match with desired accuracy.

The second important feature of the proposed algorithm is modelling the effect of precipitation since this can cause direct cooling of the cables. This feature is also not considered in any previous published model. As an observation of the experimental outcomes has shown, this might be a significant factor in obtaining correct cable temperature values.

Another important contribution presented in the paper is an idea describing how to create a loadability versus time curve. This can tell the cable operator, at any given point in time, how much the cables can be loaded and for how long. This feature can become important in case of network contingencies since the operator will gain additional information as to how the system might behave in the coming hours, and based on this, he or she can decide which control actions to take.

The developed algorithm is verified by application to a cable system setup in a laboratory environment.

References

[1] Energinet.dk, "Cable action plan," Tech. Rep., Mar. 2009. [Online]. Available: http://energinet.dk/SiteCollectionDocuments/Engelske%20dokumenter/Om%20os/Cable%20Action%20Plan%20-%202008-2009.pdf

[2] Energinet.dk, Improvement of the visual impact of the 400 kV grid Fredericia, Denmark, Tech. Rep., Apr. 2010.

[3] H. Banakar, N. Alguacil, and F. D. Galiana, "Electrothermal coordination part I: theory and implementation schemes," *IEEE Trans. Power Syst.*, vol. 20, no. 2, pp. 798–805, May 2005.

[4] N. Alguacil, H. Banakar, and F. D. Galiana, "Electrothermal coordination—Part II: Case studies," *IEEE Trans. Power Syst.*, vol. 20, no. 4, pp. 1738–1745, Nov. 2005.

[5] G. Anders, A. Napieralski, M. Zubert, and M. Orlikowski, "Advanced modeling techniques for dynamic feeder rating systems," *IEEE Trans. Ind. Appl.*, vol. 39, no. 3, pp. 619–626, May/Jun. 2003.

[6] S.-H. Huang, W.-J. Lee, and M. T. Kuo, "An online dynamic cable rating system for an industrial power plant in the restructured electric market," *IEEE Trans. Ind. Appl.*, vol. 43, no. 6, pp. 1449–1458, Nov. 2007.

[7] M. G. Alishaev, I. M. Abdulagatov, and Z. Z. Abdulagatova, "Effective thermal conductivity of fluid—saturated rocks—experiment and modeling," *Eng. Geol.*, vol. 135–13, pp. 24–39, May 2012.

[8] T. Hirono and Y. Hamada, "Specific heat capacity and thermal diffusivity and their temperature dependencies in a rock sample from adjacent to the taiwan chelungpu fault," *J. Geophys. Res.*, vol. 115, no. B5, 2010.

[9] *IEC calculation of the cyclic and emergency current rating of cables*, Int. Electrotech. Comm. Standard Series 60853, Jul. 1989.

[10] G. J. Anders, *Rating of Electric Power Cables in Unfavorable Thermal Environment*. Piscataway, NJ: IEEE, 2005.

[11] N. H. Abu-Hamdeh, "Thermal properties of soils as affected by density and water content," *Biosyst. Eng.*, vol. 86, no. 1, pp. 97–102, 2003.

[12] T. Ren, T. E. Ochsner, R. Horton, and Z. Ju, "Heat-pulse method for soil water content measurement: Influence of the specific heat of the soil solids," *Soil Sci. Soc. Amer. J.*, vol. 67, no. 6, pp. 1631–1634, Nov./Dec. 2003.

[13] J. Toman and R. Cerny, "Temperature and moisture dependence of the specific heat of high performance concrete," *Acta Polytech.*, vol. 41, no. 1, pp. 5–7, 2001.

[14] J. M. Basinger, G. J. Kluitenberg, J. M. Frank, P. L. Barnes, and M. B. Kirkham, "Laboratory evaluation of the dual-probe heat pulse method for measureing soil water content," *Vadosa Zone J.*, vol. 2, no. 3, pp. 389–399, 2003.

[15] J. S. Lyall, G. Nourbakhsh, and H. C. Zhao, "Underground power cable environment on-line monitoring & analysis," in *Proc. IEEE Power Eng. Soc. Transm. Distrib. Conf.*, 2000, vol. 1, pp. 457–462.

[16] R. S. Olsen, J. Holboell, and U. S. Gudmundsdóttir, "Dynamic temperature estimation and real time emergency rating of transmission cables," presented at the IEEE Power Energy Soc. Gen. Meeting, San Diego, CA, Jul. 2012.

[17] Working Group 08, "Calculation of temperatures in ventilated cable tunnels," *Electra*, no. Électra No. 143, Aug. 1992.

[18] J. Engelhardt, F. Hoppe, W. Pawlowicz, M. Huang, N. Parker, and J. Nierenberg, "Real-time ratings for a 115 kV submarine cable system," in *Proc. IEEE Transm. Distrib. Conf.*, 1999, pp. 26–31.

[19] *IEC Electric Cables—Calculation of the Current Rating—Current Rating Equations (100% Load Factor) and Calculation of Losses*, Int. Electrotech. Comm. Standard Ser. 60287–1, Dec. 2006.

[20] G. J. Anders, *Rating of Electric Power Cables*. New York: IEEE, 1997.

[21] Ole Christensen, *Differentialligninger og uendelige rækker* (in Danish). Kgs. Lyngby, Denmark: Polyteknisk Boghandel & Forlag, 2006.

[22] Z. S. Tseng, Systems of first order differential equations, Department of Mathematics, Pennsylvania State University, 2012. [Online]. Available: http://www.math.psu.edu/tseng/class/Math251/Notes-LinearSystems.pdf

[23] T. Kusuda and P. R. Achenbach, Earth temperature and thermal diffusivity at selected stations in the united states Washington, DC, USA, Tech. Rep. NBS Rep. 8972, Jun. 1965, U.S. Dept. Commerce/Nat. Bureau Standards.

[24] G. M. Williams, P. L. Lewin, and M. LeBlanc, "Accurate determination of ambient temperature at burial depth for high voltage cable ratings," in *Proc. IEEE Int. Symp. Elect. Insul. Conf.*, Sep. 2004, pp. 458–461.

Rasmus Olsen (S'12) received the M.Sc. degree in electrical engineering from the Technical University of Denmark (DTU), Lyngby, Denmark, in 2010.

His Ph.D. project is concerned with dynamic load optimization of cable-based transmission grids and it is a collaboration between Energinet.dk and DTU. His main interests are within thermal performance of transmission cables, how this performance can be increased, and how asset management can be introduced for a more optimal utilization of such cables and cable systems.

George J. Anders (F'99) has been involved in several aspects of power system analysis and design during his 36 years with Ontario Hydro, Canada, its successor companies, and as a consultant. He published more than 50 papers in IEEE TRANSACTIONS on this subject, wrote three books, and taught numerous courses on cable-rating issues. His main interests are in the field of ampacity calculations of electric power cables.

Dr. Anders is a co-convener of Working Group 19 of the International Electrotechnical Commission (IEC), which develops international standards for cable-rating calculations. He is the author of the computational algorithms implemented in the CYMCAP program. The program is now de-facto the industry standard for cable ampacity calculations and is used by more than 200 users in 40 countries on five continents. He is a registered Professional Engineer in the Province of Ontario.

Joachim Holboell (SM'11) is Associate Professor and Deputy Head of the Department of Electrical Engineering, Center for Electric Power and Energy, Technical University of Denmark (DTU), Lyngby, Denmark. His main research intertest are high-voltage components, their properties, and condition and broadband performance, including insulation systems performance under ac, dc, and transients. His focus is on wind turbine technology and future power-grid applications.

Unnur Stella Gudmundsdóttir (M'13) received the M.Sc. and Ph.D. degrees in electrical engineering from Aalborg University, Denmark, in 2007 and 2010, respectively.

Her Ph.D. studies focused on the modelling of underground cable systems at the transmission level. She was a Guest Researcher at SINTEF in Norway in 2008 and at Manitoba HVDC Research Centre, Winnipeg, MB, Canada, in 2009. Currently, she is a Senior Cable Specialist at Energinet.dk, where she is a Deputy Manager for DANPAC, a research project focusing on undergrounding of almost the entire Danish transmission system.

F.3 Electrothermal Coordination in Cable Based Transmission Grids

Electrothermal Coordination in Cable Based Transmission Grids

R. Olsen, *Student Member IEEE,* J. Holboell, *Senior Member IEEE,* and U. S. Gudmundsdóttir, *Member IEEE*

***Abstract* - Electrothermal coordination (ETC) is introduced for cable based transmission grids. ETC is the term covering operation and planning of transmission systems based on temperature, instead of current. ETC consists of one part covering the load conditions of the system and one covering the thermal behaviour of the components. The dynamic temperature calculations of power cables are suggested to be based on thermoelectric equivalents (TEEs). It is shown that the thermal behaviour can be built into widely used load flow software, creating a strong ETC tool. ETC is, through two case scenarios, proven to be beneficial for both operator and system planner. It is shown how the thermal behaviour can be monitored in real-time during normal dynamic load and during emergencies. In that way, ETC enables cables to be loaded above their normal rating, while maintaining high reliability of the system, which potentially can result in large economic benefits.**

***Index Terms*--Cables, finite element methods, load flow analysis, power cable thermal factors, power system simulation, prediction methods, temperature control, transmission lines**

I. Introduction

This paper introduces electrothermal coordination (ETC) in cable based transmission grids. ETC was introduced for overhead lines in [1] and covers temperature based dynamic operation of transmission systems and thermally based planning of such systems. Because of the short thermal time constant, it is in [1] argued that one can benefit mostly by introducing ETC for overhead lines. However looking into the future of e.g. the Danish transmission system, almost the entire grid will be undergrounded [2, 3], and the Danish Transmission System Operator (TSO), Energinet.dk, thus expects that much transmission capacity can be gained by utilising the ETC concept on cable based systems as well.

The issue of dynamic operation of transmission lines has been investigated by different researchers (e.g. [4, 5]), but many of these projects have focussed on the component level (for most overhead lines) with limited considerations about the influence on an entire system.

On the component level, dynamic operation is discussed by using the term Dynamic Thermal Rating (DTR). DTR is a calculation of the temperature in individual components and based on this temperature the operator decides on how to act.

Some of the research in DTR has in reality ended in pseudo DTR, meaning that even though the temperature is somehow estimated; network operation is still based on current instead of temperature as the limiting parameter. Such operation methodologies are executed by specifying a number of loadability levels which the operator can relate to during emergency and faulted operation.

The present paper introduces a method enabling operation of individual transmission cables based on temperature estimations (real DTR). The models developed for this DTR is then combined with load flow simulations, such that ETC becomes possible.

Distributed temperature sensing (DTS) technology allows for monitoring of the real time temperature in or around the cable. The DTS optic fibre can be implemented in the cable screen or, as it is done in Denmark, in a pipe laid close to the centre phase. However as the temperature on the conductor is the real limitation of the cable loadability, it is not sufficient with such external measurements when controlling transmission systems in real time. Modelling is thus necessary in order to obtain the real time conductor temperature. Furthermore, temperature measurements cannot directly be used to make predictions about the future evolution of the cable temperature and accurate thermal models are thus necessary in order to perform DTR and ETC.

Ref. [6] shows how DTS measurements can be integrated into the thermal models in order to increase accuracy; however some older cable systems are without temperature monitoring and the thermal model developed in [6] thus take temperature measurements as an optional input for increased accuracy.

The thermal models are developed with the scope of implementation in the Danish transmission system, where direct burial in flat formation is the preferred installation method for transmission cables. Since most cables are terminated above ground at a tower, in gas or in open air insulated substations, a discussion about the necessary thermal models for cables in air is also included in this study.

The installed cables are XLPE insulated and they are equipped with copper wire/aluminium foil metallic screens. However the thermal models will, with smaller adaptions, be applicable to other transmission systems as well.

As it is seen from the above description of ETC (see also [1]), a number of different models and principles are necessary for ETC to become operational. In order to provide a clear overview of the ETC methodology, the present paper is therefore divided into several sections, each covering a necessary part of ETC in cable based transmission systems.

II. Thermal Modelling of Transmission Cables

A. Choice of Thermal Model

The thermal models of [1] are, as stated, concerned with overhead lines; but as the thermal conditions of OHL and

R. Olsen is with Section of Transmission Lines, Energinet.dk, Fredericia 7000, Denmark (e-mail: rso@energinet.dk).

J. Holbøll is with the Dept. of Electrical Engineering, Technical University of Denmark, Kgs. Lyngby 2800, Denmark (e-mail: jh@elektro.dtu.dk).

U. S. Guðmundsdóttir is with Section of Transmission Lines, Energinet.dk, Fredericia 7000, Denmark (e-mail: usg@energinet.dk).

underground cables are very different, another thermal model is necessary for this study.

Different methodologies for temperature calculations on cables have already been developed, where the most common are: Finite Element Modelling (FEM, see e.g. [7]), Finite Difference Modelling (FDM, see e.g. [8]), Thermoelectric Equivalents (TEE, see e.g. [9]) and the Step Response Method (e.g. [10]).

It is clear from the ETC-application, that the thermal model to be selected must be fast, since the temperature has to be calculated for a large number of cables, and accurate, because the reliability of the entire transmission system depends on accurate rating calculations. Based on these two requirements, the TEE method was chosen for thermal modelling.

Compared to 2D and, in particular, 3D FEM simulations, performed with commercially available FEM software, TEEs can model the dynamic thermal behaviour of transmission cables both with a sufficient accuracy and fast, [11]. The accuracy of TEEs was proven in [6], where the modelled temperature of cables in a large scale experimental setup was compared to measurements.

B. Design of Thermal Model

The following briefly summarises dynamic temperature calculations by TEE.

1) Calculating the Thermal Parameters

TEEs utilise the resemblance between heat flowing in a thermal system and current flowing in an electric system. Thus thermal resistances of materials can be modelled by electric resistances, as well as thermal capacitances can be modelled by electric capacitances. The heat generated in conductor, dielectric, screen, etc. is resembled by current sources in the electric analogy.

When modelling the heat flowing through a resistance, with a current, the voltage drop will be equal to the temperature difference on the two sides of the thermal resistance. Fig. 1 shows the simplest case of a TEE for a directly buried cable.

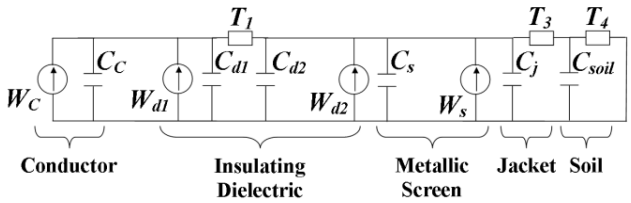

Fig. 1: Thermoelectric Equivalent, TEE, of a single phased cable without armour. W_c are joule losses in the conductor, the sum of W_{d1} and W_{d2} are the dielectric losses and W_s are the screen losses. The C's are the thermal capacitances and the T's are the thermal resistances of the respective subcomponents.

In the figure, the thermal parameters of each subcomponent (conductor, insulation, metal screen, jacket and surrounding soil) are lumped together into few components. As explained in [6] and [11], such a coarse division of the thermal parameters, as seen in Fig. 1, will result in deviations between the modelled dynamic temperature and the temperature of a cable in operation where the thermal parameters are continuously spread over the entire material. It was therefore suggested in [6] that the different subcomponents should be divided into multiple thermal zones. Such a division into zones is shown in Fig. 2 where the insulation for illustrative purposes is divided into three.

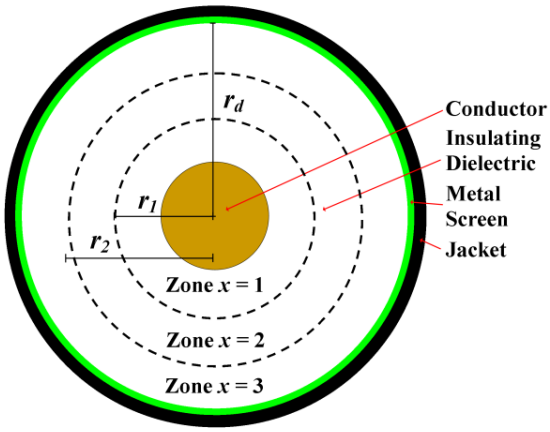

Fig. 2: Cable design used for thermal modelling. r_1 and r_2 illustrate the outer radius of Zone 1 and 2 respectively.

Throughout this paper, the assumption is made that all metal parts of the thermal network can be considered as being isotherms. This is a valid assumption due to the high thermal conductivity of metals as compared to dielectric materials.

The thermal resistances used for modelling the different subcomponents are calculated by using adapted versions of the guidelines given by IEC standard 60287-1 [12], as shown in the following.

The thermal resistance of zone *'x'* in the insulation is calculated as given in (1) and the thermal resistance of zone *'y'* in the jacket is calculated as given in (2).

$$T_{1,x} = \frac{\rho_{therm,d}}{2 \cdot \pi} \cdot \ln\left(\frac{r_x}{r_{x-1}}\right), x = 1,2,3,\ldots,s \qquad (1)$$

where $\rho_{therm,d}$ is the thermal resistivity of the dielectric material, r_x is the radius of zone x, r_0 is the conductor radius and s is the total number of zones in the insulation.

$$T_{3,y} = \frac{\rho_{therm,j}}{2 \cdot \pi} \cdot \ln\left(\frac{r_y}{r_{y-1}}\right), y = 1,2,3,\ldots,t \qquad (2)$$

where $\rho_{therm,j}$ is the thermal resistivity of the jacket material, r_y is the radius of zone y, r_0 is the screen outer radius and t is the total number of zones in the jacket.

The thermal resistance, $T_{4,z}$, of zone *'z'* in the surrounding soil is calculated as given in (3).

$$T_{4,z} = \frac{\rho_{therm,sur}}{2 \cdot \pi} \cdot \left(\ln\left(\frac{r'_{z-1}}{r_{z-1}}\right) - \ln\left(\frac{r'_z}{r_z}\right) + \frac{\sum_{k=1}^{n} \ln\left(\frac{d'_{pk}}{d_{pk}}\right)}{u} \right) \qquad (3)$$

$$z = 1,2,3,\ldots,u$$

where $\rho_{therm,sur}$ is the thermal resistivity of the surroundings, L the burial depth, r_z the radius of zone z (r_0 is the outer radius of the cable itself), r'_z the distance from zone z to the image of the cable itself above ground, d_{pk} is the distance from the cable under investigation, p, to cable k, d'_{pk} is the distance from cable p to the image of cable k above ground, n is the number of cables in vicinity of cable p and u is the total number of zones in the surroundings.

It is seen that the basic concept of Kennelly's hypothesis, stating that the ground surface is isothermal, is maintained in the calculation, as well as the thermal influence of the cables in the vicinity is seen also to be included in the calculation.

Note that by summing up $T_{1,x}$ over all x, $T_{3,y}$ over all y and $T_{4,z}$ over all z, one obtains the standardised equations of [12].

The thermal capacitances are calculated based on the cross section of the different zones (4). It is assumed that the cross section of the zones in the surroundings can be approximated by means of concentric circles.

$$\begin{aligned} C_{1,x} &= c_{therm,d} \cdot \pi \cdot \left(r_x^{\,2} - r_{x-1}^{\,2} \right) \\ C_{3,y} &= c_{therm,j} \cdot \pi \cdot \left(r_y^{\,2} - r_{y-1}^{\,2} \right) \\ C_{4,z} &= c_{therm,sur} \cdot \pi \cdot \left(r_z^{\,2} - r_{z-1}^{\,2} \right) \end{aligned} \tag{4}$$

Here $c_{therm,d}$, $c_{therm,j}$ and $c_{therm,sur}$ are the specific heat of the dielectric, jacket and surroundings respectively, $x=1,2,\ldots,s$, $y=1,2,\ldots,t$ and $z=1,2,\ldots,u$ is the number of the zone in the insulation, jacket and surroundings, respectively.

Subcomponents such as semiconductive layers, thermal backfill, etc. have been left out of the model. This is not a limitation in the methodology, but merely an attempt to simplify the description.

The joule losses in the conductor, dielectric losses in the insulation and induced joule losses in the screen have been calculated as described in IEC 60287 [12].

2) Calculating the Temperature

In the TEE model, which in its nature is discrete in space, the temperature increase above ambient at each node is calculated analytically by solving the differential equation system shown in (5). The specific equation in (5) relates to the simplest TEE as it is shown in Fig. 1.

$$\begin{bmatrix} \dot{\theta}_e \\ \dot{\theta}_s \\ \dot{\theta}_c \end{bmatrix} = \begin{bmatrix} -\left(\frac{1}{C_4 T_3} + \frac{1}{C_4 T_4}\right) & \frac{1}{C_4 T_3} & 0 \\ \frac{1}{C_3 T_3} & -\left(\frac{1}{C_3 T_1} + \frac{1}{C_3 T_3}\right) & \frac{1}{C_3 T_1} \\ 0 & \frac{1}{C_1 T_1} & -\frac{1}{C_1 T_1} \end{bmatrix} \cdot \begin{bmatrix} \theta_e \\ \theta_s \\ \theta_c \end{bmatrix} + \begin{bmatrix} 0 \\ \frac{1}{C_3} \cdot \left(W_{d2} + W_s\right) \\ \frac{1}{C_1} \cdot \left(W_c + W_{d1}\right) \end{bmatrix} \tag{5}$$

Equation (5) can in short be given as (6).

$$\dot{\vec{\theta}} = \underline{A} \cdot \vec{\theta} + \vec{W} \tag{6}$$

where A is the system matrix and $\vec{W}$ is related to the applied external influences, in this case the different losses.

The general solution to the differential equation system of (5) is as given in (7), [13].

$$\begin{bmatrix} \theta_e(t) \\ \theta_s(t) \\ \theta_c(t) \end{bmatrix} = c_1 \bar{v}_1 \cdot e^{\lambda_1 t} + c_2 \bar{v}_2 \cdot e^{\lambda_2 t} + c_3 \bar{v}_3 \cdot e^{\lambda_3 t} + \begin{bmatrix} \theta_e(t_\infty) \\ \theta_s(t_\infty) \\ \theta_c(t_\infty) \end{bmatrix} \tag{7}$$

where $\bar{v}_i$ are eigenvectors of the system matrix $\underline{A}$. Similarly λ_i are the eigenvalues which are all non-positive, since the TEE is a stable system. The constants c_i are calculated based on the end point constraints, as given in (8). The end point constraints are the initial ($\theta(t_0)$) and infinite ($\theta(t_\infty)$) steady state temperatures, which are simply calculated by removing the capacitances from the TEE and calculating the voltage drops across the thermal resistances.

$$\begin{bmatrix} \vec{v}_1 & \vec{v}_2 & \vec{v}_3 \end{bmatrix} \cdot \begin{bmatrix} c_1 \\ c_2 \\ c_3 \end{bmatrix} = \begin{bmatrix} \theta_e(t_0) \\ \theta_s(t_0) \\ \theta_c(t_0) \end{bmatrix} - \begin{bmatrix} \theta_e(t_\infty) \\ \theta_s(t_\infty) \\ \theta_c(t_\infty) \end{bmatrix} \tag{8}$$

Denoting the right hand side of (8) by $\theta(t_0)$-$\theta(t_\infty)$, the constants c_1, c_2 and c_3 are found by performing Gauss-Jordan Elimination on the matrix:

$$\left[\vec{v}_1 \quad \vec{v}_2 \quad \vec{v}_3 \middle| \vec{\theta}(t_0) - \vec{\theta}(t_\infty) \right] \tag{9}$$

The total cable temperature is then found by adding the results of (7) to the measured (or modelled, [14]) undisturbed soil temperature at cable depth.

As suggested in [6], this study utilises a division of the surroundings into 100 zones, the insulation into 10 zones and the jacket into 3 zones. The system matrix of (5) therefore becomes a 113 x 113 matrix, as well as the vectors of (5) and (7) will contain 113 elements. This will lead to 113 individual eigenvalues and eigenvectors. As there is no general analytical method for solving a degree 113 polynomial equation, the eigenvalues and vectors, have been determined numerically.

It should be noted that the electric resistivity, the thermal resistivity and the specific heat are temperature dependent properties; however in the present study the thermal parameters of the model have been treated as constant. This is not a limitation in the methodology, [6], but an assumption which is made for the purpose of simplification only.

It should be acknowledged that thermal modelling must be performed on hotspot locations as the hotspots will be the limiting operating points for the cable system. However the thermal model described above is well suited to deal with hotspots, as studies such as [15] proves that hotspots wider than 3 meters can be treated without considering axial heat flow. The assumption that hotspots are wider than 3 meters is valid, at least in the Danish transmission system, as hotspots are generally located when cables cross under roads, etc.

3) Cables in Air and other Special Conditions

As mentioned, underground cables are in most cases terminated above ground. The part of the cable in air will be subjected to different thermal conditions than the undergrounded part, and a different model must therefore be utilised. The thermal conditions for the internal parts of the cable are identical for the air part and underground part, but the surface of a cable in air can be subjected to solar radiation and the heat losses to the surroundings are highly nonlinear, i.e. most research within power cables assumes that the losses may be evaluated as given in (10), [9].

$$\begin{aligned} W_{rad} &= h_{rad} \cdot \left(\theta_e^4 - \theta_{air}^4 \right) \\ W_{conv} &= h_{conv} \cdot \left(\theta_e - \theta_{air} \right) \end{aligned} \tag{10}$$

where W_{rad} and W_{conv} are the losses caused by radiation and convection respectively, h_{rad} and h_{conv} are the radiation and convection constants respectively (each dependent on the materials and cable geometry) and θ_{air} is the air temperature.

Because of the nonlinearity in the heat balance equations, they must be solved with numerical solution methods or by linearizing the losses such as done in the step response method, [9].

In the remaining part of this study it is assumed that the bottlenecks of the cables are on the underground part, and that the temperature thus can be calculated by using (7), but it

should be pointed out that measures to mitigate possible hotspots above ground might be necessary.

C. Load Flow Calculations

The novelty of ETC lies in the close connection between temperature calculations and load flow simulations within the transmission system.

On the basis of the predicted future load flow scenario, it is possible to forecast the evolution of the temperature in all transmission lines in the system.

Relatively fast and accurate methods are available for load flow calculations and the present study uses the Newton-Raphson methodology.

D. Connecting Load Flow and Thermal Calculations

The thermal calculations and the load flow calculations are interdependent in several ways.

The temperature is via the joule heating directly related to the current passed through the conductor. However, the current based joule heating is also connected to the temperature because the electric resistance of the conductor is temperature dependent. Furthermore, this resistance is a part of the impedance of the transmission line, which again is an essential parameter in the load flow studies.

In the present study these interdependencies have been implemented as follows.

The temperature dependence of the electric resistance is included by adapting the electric resistance to the temperature calculated at the last time step. This approximation is assumed valid as long as a low time step is used compared to the time constant of the conductor temperature, screen temperature, etc. An iterative process for calculation of the resistance would be more correct, the gained accuracy hereof however is, due to the high thermal time constants involved, expected to be low compared to the computational time required.

III. Implementation in Load flow simulations

The thermal models of section II. have been implemented in the commercially available system analysis software DigSilent Power Factory (DSPF).

This software is widely used for load flow calculations by utility companies, transmission system operators, as well as many universities and other research institutions. The implementation of ETC in DSPF will therefore address a large part of the power industry.

One of the strengths of DSPF is the graphical interface, which enables the user to get an easy overview of the grid, including electrical variables, etc. In addition to the graphical interface, it is possible to change the grid parameters in two different scripting environments, DigSilent Simulation Language (DSL) and DigSilent Programming Language (DPL), which makes it a strong tool for a large variety of simulation purposes. The grid calculations are obviously inherent parts of the DSPF software, however the thermal calculations are not. Therefore the major part of the algorithm to be developed in the following clauses lies in this area.

Since ETC here is treated with no concern about stability (neither voltage nor frequency) related issues, the only grid calculations needed are load flow simulations. It is therefore possible to use the DPL instead of the DSL environment, which makes the algorithm both flexible and efficient. All grid quantities such as bus voltages, etc. of course have to be maintained within relevant regulations.

The AC-balanced load flow (positive sequence) calculations are performed by DSPF, which solves the classical power equations by using the Newton-Raphson method.

The connection between the load flow calculations and the thermal calculations is, as mentioned, primarily the conductor current. The actual load current of each cable in the grid is therefore written to a text file, which then is loaded by Matlab for the further thermal analysis.

The feedbacks from Matlab to DSPF are the calculated temperatures plus the resistivity of the individual cables in the grid, the latter is to be used in the next load flow calculation.

The implementation of this 'DSPF-Matlab ETC Package' is visualised in Fig. 3 and the individual parts are explained in the following.

The accuracy of the, dynamically evolving, calculated temperature is highly dependent on the losses, which again are highly dependent on the time step. The time step should therefore be carefully chosen as a compromise between computational time and accuracy.

i. To adapt component parameters via DPL it is necessary to initialise the grid by running a load flow calculation.

ii. A description of the transmission grid is written to txt-files. This includes load-names, line-names, etc.

iii. All parameters in the system can be changed via DPL-scripts. Changes will most often be the size of loads, lengths of cables, sizes of cables, sizes of generators, etc. It is assumed that all parameters of the grid have been static for a long time, such that the temperatures are in steady state before the dynamic simulation begins.
All cables are compensated by half at each end and the necessary compensation per phase is as given in (11).

$$Q = 2 \cdot \pi \cdot f \cdot C' \cdot l \cdot U_0^2 \tag{11}$$

Here Q is the reactive power, f is the system frequency, C' is the capacitance per length of the cable, l is the length and U_0 is the line-to-screen voltage.

iv. The eigenvalues and eigenvectors of (7) for all cables in the system are evaluated and the initial temperatures are calculated.

v. The temperatures are loaded into DSPF from a txt-file.

vi. The cable resistance is redefined.

vii. Having performed the load flow calculations, the current running in all cables is extracted and exported to a txt-file.

viii. The currents are loaded in Matlab where the conductor losses (W_c) and steady state temperatures are calculated for all lines.

ix. The temperatures are stored in a mat-file for later analysis and the temperatures which are important for DSPF are exported to txt-files.

x. Check whether the results have changed from the previous iteration to the present. If large differences exist in either load flow or temperatures, it is necessary to run the calculations again until they have stabilised. Stability here is defined as temperature differences below 0.01 K and load differences below 1 A.

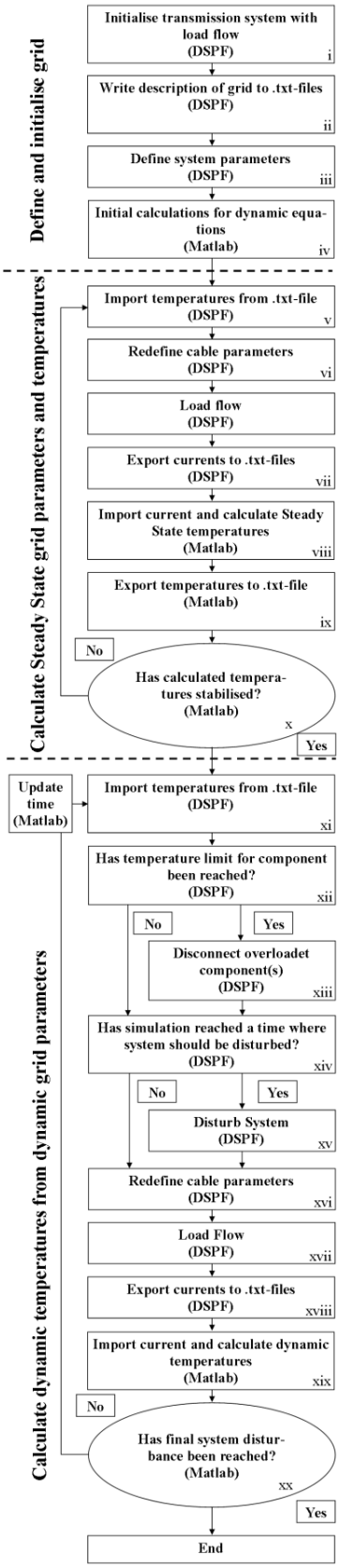

Fig. 3: Algorithm structure for integration of temperature calculations in load flow software. An in-depth description of the different parts is given in the text as indicated by the roman numbers. It is furthermore indicated which program handles the different parts of the algorithm.

xi. The dynamic simulation starts by loading the steady state temperatures into DSPF and adjusting the grid parameters (resistances) to these temperatures.
xii. Test if the temperature has exceeded the individual limits of these components.
xiii. If the temperature limit has been exceeded for one or more cables, the relevant lines are disconnected from the grid.
xiv. Check if it is time for disturbances of system.
xv. Disturb the system. This can for example be an N-1 case (a grid with a major single outage).
xvi. Knowing the temperatures, the cable impedances are adapted as in *vi*.
xvii. DSPF runs a load flow calculation.
xviii. The currents obtained from the most recent load flow are exported to txt-files.
xix. These currents are imported in Matlab and the thermal response to the current is calculated on the basis of (7).
xx. Finally, test whether or not the end time has been reached. If not, the algorithm runs the steps from *xi* to *xix* again.

It should be acknowledged that the described methodology has been developed in close cooperation with all stakeholders at the Danish TSO, and the software integration can thus be seen as technically ready for implementation into the Danish transmission system.

IV. Case Study

In order to maintain a clear overview of the benefits of ETC the basic case used in this study is a simple two-line system with two generators and one load, Fig. 4, which is also found to be the case studied in papers that have previously dealt with ETC [1].

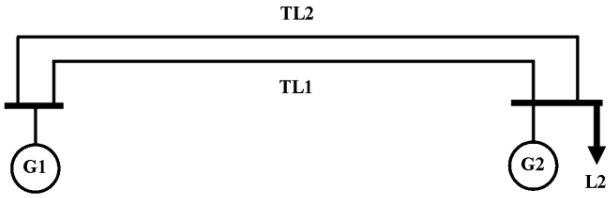

Fig. 4: Two line system used for case study.

The ETC software package has, with success, been tested on significantly larger systems than this two line test case, hereunder an adapted version of the IEEE 14-bus test network containing 20 cables, however the described two line system enables more comprehensible analysis, and discussing ETC as a concept is thus easier.

The base voltage (V_{base}) is 132kV. The cables are equipped with metallic screens, which may cause additional heating.

The transmission lines have been modelled with cable dimensions which are available online [16], and the most important geometric parameters are summarised in Table I.

The cables are 100 km long [1]. The reactive power generated by the cables is compensated by half at each end. The cable screens are assumed to be perfectly cross-bonded, which, together with negligible eddy currents, for simplicity means that screen losses can be neglected [12].

TABLE I
GEOMETRIC PARAMETERS OF TRANSMISSION CABLE
'TYPE (A)2XS(FL)2Y 1X1600 RMS/50' USED IN THIS STUDY [16]

Conductor cross section [mm^2]	d_c [mm]	t_i [mm]	Screen cross section [mm^2]	t_s* [mm]	t_j [mm]	D_e [mm]
1600	48.5 **	15/20 ***	110	0.4 ****	5.9	101

* t_s being the thickness of the screen
** Segmental aluminium conductor
*** The cable is equipped with semiconductive layers, which have been assumed to be 2.5mm thick. In the thermal studies these layers are assumed to have the same thermal properties as the XLPE insulation and the insulation thus has an effective thickness of 20mm.
**** The thickness of the screen is calculated on the basis of the screen area and the effective outer diameter of the insulation. In the electrical calculations the screen is a copper wire screen, however in the thermal calculations it is assumed that the screen is a solid material as illustrated in Fig. 2.

The load L2 is varying daily according to Fig. 5. The generator G2 is mainly supposed to supply the load with active power during peak hours as shown in Fig. 5.

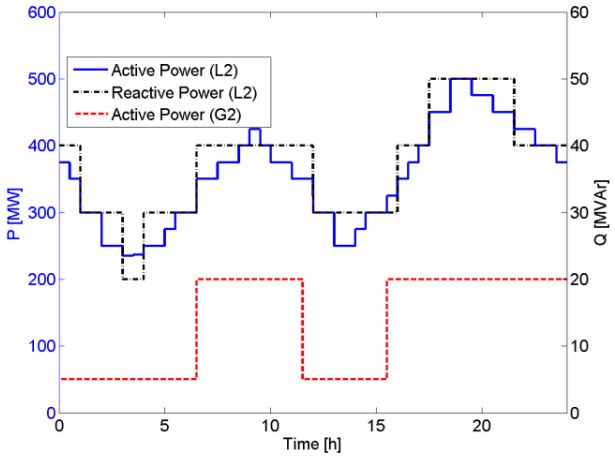

Fig. 5: Load (L2) and generation (G2) cycles of the components seen in Fig. 4. It is assumed that the same cycles are repeated indefinitely.

Generator G1 is forced to be slack and the reactive powers of G1 and G2 are controlled such as to keep the voltage at the nodes within the accepted limits.

It is assumed that the two cable systems (TL1 and TL2) are located far enough from each other, such that they can be treated as thermally independent.

The thermal parameters of the study are listed in Table II.

TABLE II
THERMAL PARAMETERS OF TRANSMISSION CABLE

Material	ρ_{therm} Thermal Resistivity [m·K/W]	c_{therm} Specific Heat [J/(m^3·K)]
Aluminium (Conductor)	0	$2.5 \cdot 10^6$
XLPE (Dielectric)	3.5	$2.4 \cdot 10^6$
Copper (Screen)	0	$3.45 \cdot 10^6$
PE (Jacket)	3.5	$2.4 \cdot 10^6$
Soil (Surroundings)	1	$1.9 \cdot 10^6$

It is assumed that the ambient temperature at cable depth is steady state 15°C, the methodology though allows for implementing varying ambient temperature. The following clauses will determine the consequences of running the system under the normal load cycle and during a fall out of TL2.

A. Normal Load Cycle

It is assumed that the normal load cycle in Fig. 5 is repeated infinitely, thus the figure is only a snapshot of one day. In the simulation process, this has been modelled by applying half the maximum allowed steady state current for an infinite amount of time, followed by applying the loads of Fig. 5 for twenty-nine days before the results are obtained. This procedure ensures the thermal system to be in dynamic equilibrium state before the results are produced.

The time step of the simulation is chosen in such a way that the entire loop of dynamic calculations is repeated every ten minutes. This means that the conductor losses of all cables are evaluated based on electrical resistances which are up to ten minutes old. However, as the temperatures are not expected to change significantly within this time the approximation is considered valid.

During normal cyclic operation, the thermal limit of transmission cables is a maximum jacket temperature of 50°C in order to avoid moisture migration [12]. The maximum steady state current (I_{max}) is calculated based on this temperature, here 839 A. The current in the cables of TL1 and the jacket temperature for the centre phase for the thirtieth day in the simulation, are shown in Fig. 6.

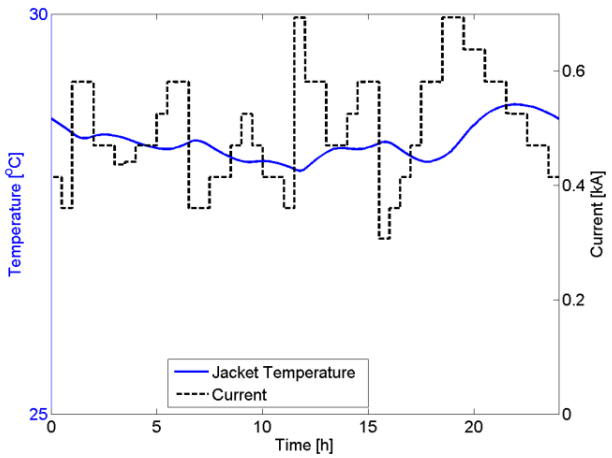

Fig. 6: Current and jacket temperature of cable TL1. An initial load of half the loadability has been applied for an infinite amount of time prior to simulation, resulting in steady state, thereafter applying the loading profile of Fig. 5 for twenty-nine days before the shown day. Based on the conventional steady state calculations the maximum allowable current would be 839A and the maximum temperature on the jacket 50°C.

As expected, it is seen from the figure that the jacket temperature follows the current with a small time lag.

In order to illustrate the benefits of using ETC as the operating methodology in the transmission system, instead of current based operation, the results of the simulations have been normalised according to the maximum steady state values, Fig. 7.

It is seen in Fig. 7 that the temperature lies almost steadily around 0.57 pu, while the current fluctuates highly between 0.35-0.85 pu. This illustrates very clearly the operational freedom gained by operating transmission systems based on temperature (ETC) instead of the current. In the specific case,

the operator could be allowed to increase the current above I_{max} for several hours on a daily basis without jeopardising the reliability of the system.

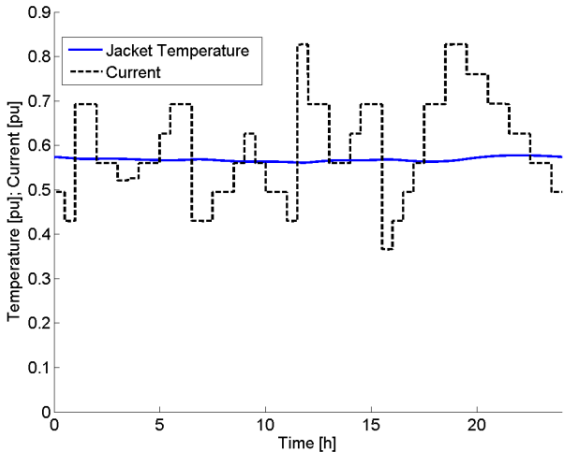

Fig. 7: Normalised current and jacket temperature of the data shown in Fig. 6. The current has been normalised based on the current that, during steady state conditions, would give a jacket temperature of 50°C. The jacket temperature has been normalised based on the maximum allowed temperature of 50°C. It is clear that the temperature is much below the maximal acceptable level for all times, whereas the current varies a lot and almost reaches the steady state operating conditions of 839 A.

B. *Failure of Transmission Line*

This clause will discuss the benefits of operating transmission systems based on ETC instead of currents when experiencing a failure in the grid.

Again it is assumed that the load and generation patterns of Fig. 5 have been applied for infinitely long time (twenty-nine days) prior to the day of the fault. At 17:00:00 a fault occurs in TL2 which forces the line to be disconnected where after the load is immediately taken over by TL1.

The Danish transmission system is operated based on current schemes and current levels up to 2 pu is normally allowed for maximally 1 hour during such emergencies, where after the line must be disconnected.

For transmission systems operated based on ETC, it is the conductor temperature which is the limiting factor during emergency operation. The transmission system is allowed to run uninterrupted until the critical conductor temperature is reached and the transmission line must be disconnected. During emergency operation, the limiting conductor temperature has here been set to 90°C, and it is assumed that this conductor temperature is allowed for as long as the emergency operation is necessary. This limitation may result in jacket temperatures higher than 50°C, however as emergency operation is expected to be short and because moisture migration of the surroundings is a process requiring some time to evolve, higher jacket temperatures may be allowed during emergency operation.

The ETC tool is seen to be flexible as any temperature limit can be used. Thus if the TSO e.g. only allows a jacket temperature of 50°C under emergency operation, this limitation can easily be implemented.

Fig. 8 shows how the temperature and current of TL1 evolves before and after the failure, when the system is operated based on ETC.

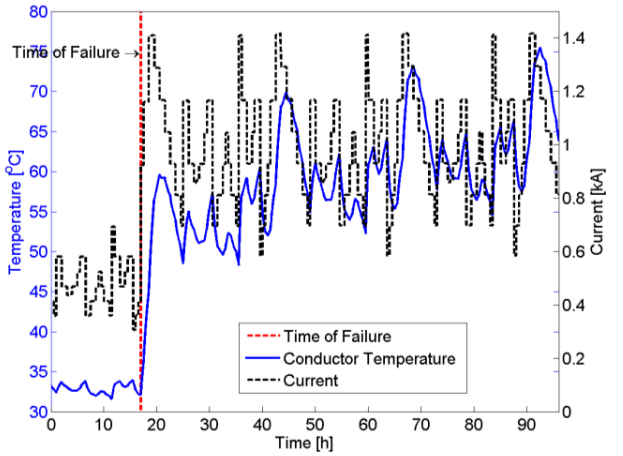

Fig. 8: Conductor temperature and current of cable TL1 when a failure occurs in cable TL2 after 17:00h. Even though the current exceeds the limit by 50% for several hours each day, the temperature is not critical, and the line can thus be kept operational.

It is seen that even though the current exceeds its limit by 50%, the system is in a safe state because the conductor temperature at most reaches approximately 60°C within the first hours and 75°C within the next three days. An extension of the time scale in Fig. 8 shows that the temperature will not reach 90°C within the first twenty days after the failure. This time frame can in many cases be sufficient to arrange the repair of the faulted line, or at least find other measures to reduce the extra loading of TL1.

It is from this example recognised that the transmission system becomes more flexible when operated on the basis of temperature than when operated on the basis of current. In current based operation, the operator is forced to disconnect TL1 at 18:00h, since the current still exceeds 1 pu after one hour, while the temperature based operation does not require disconnection of TL1.

In market based systems, which is how transmission systems in EU are operated today, the system would be in an economically optimal state prior to the failure of TL2. Disconnection of TL2 will not change this state considerably; however disconnection of both TL1 and TL2 will change the system to an economically non-optimal state. The benefits of implementing ETC in the system are thus obvious, as it enables flexible operation and optimisation of the costs.

V. Conclusion

It is shown in this study how dynamic calculations of the thermal conditions in transmission cables can be combined with load flow simulations of a power grid, enabling electrothermal coordination (ETC). This paper shows how dynamic temperature calculations can be implemented into commercially available power systems software, obtaining a strong tool for ETC based system planning and operation, allowing for a significantly increased loadability of the transmission lines. This implementation strategy was chosen in order to allow for easy integration of ETC into software which is already widely used by distribution and transmission companies. The software development has been closely

followed by the Danish TSO, Energinet.dk, and ETC is from Energinet.dk's point of view seen as ready for implementation into the Danish transmission system.

ETC based operation is in this paper studied and compared to the presently used current based operation of transmission grids. A two line transmission system is used as a case study to demonstrate how the temperature in all cables can be monitored during normal cyclic operation by utilising dynamic thermal calculations, thus giving a real time picture of the thermal state of the transmission system. By determining the real time thermal state of the transmission grid, ETC can predict the future thermal evolution of the system, and thus the reliability of the transmission system, based on predicted loads, can be foreseen. This is especially of great importance during faults in the system, where the loadability of all transmission lines can quickly be estimated via ETC, given the actual thermal conditions, and ETC can show the operator which actions should be taken.

It is emphasised that the ETC tool has been applied to larger systems with equal success, however in order to maintain a clear and comprehensive overview, the simple two line system was used in this paper for illustrating the effectiveness of ETC.

In summary, the transmission system operator can benefit from ETC in cable based transmission grids due to access to:

1. The thermal history of all cables
2. The present state of the system, including the consequences of possible control actions
3. The future evolution of the transmission system state, based on predicted load patterns

The predictions mentioned in 2 and 3 are only possible via modelling. Monitoring by measurements is thus not sufficient for ETC applications.

In addition to the above three elements, ETC might also benefit the planner of transmission grids, since especially cable based systems will experience a significantly increased loadability, both during the normal daily load cycle and during emergency operation.

REFERENCES

[1] H. Banakar, N. Alguacil and F. D. Galiana, "Electrothermal Coordination Part I: Theory and Implementation Schemes," *IEEE Trans. Power Systems*, vol. 20, No. 2, pp. 798-805, May. 2005.

[2] Energinet.dk, "Cable action plan," Tonne Kjærsvej 65, 7000 Fredericia, Denmark, Tech. rep., March 2009.

[3] Århus, Odense og Roskilde Miljøcentre, By- og Landskabsstyrelsen og Energinet. Dk, "Improvement of the visual impact of the 400 kV grid," Tech. rep., Tonne Kjærsvej 65, 7000 Fredericia, Denmark, ISBN: 978-87-90707-72-9, April 2010.

[4] J. Ausen, B.F. Fitzgerald, E.A. Gust, D.C. Lawry, J.P. Lazar and R.L. Oye, "Dynamic Thermal Rating System Relieves Transmission Constraints", *IEEE 11th International Conference on Transmission & Distribution Construction, Operation and Live-Line Maintenance*, Paper 25, 2006.

[5] M.J.C. Berende, J.G. Slootweg, and G.J.M.B. Clemens. "Incorporating weather statistics in determining overhead line ampacity," *2005 International Conference on Future Power Systems*, 2005.

[6] R. Olsen, G.J. Anders, J. Holboell and U.S. Gudmundsdóttir, "Modelling of Dynamic Transmission Cable Temperature Considering Soil Specific Heat, Thermal Resistivity and Precipitation," *IEEE Trans. Power Delivery*, vol. 28., no. 3, pp. 1909-1917, July, 2013.

[7] Faruk Aras, Cüneyt Oysu, and Güneş Yilmaz. "An assessment of the methods for calculating ampacity of underground power cables," *Electric Power Components and Systems*, vol. 33, No. 12, pp. 1385-1402, October 2005.

[8] Ajit Hiranandani. "Calculation of conductor temperatures and ampacities of cable systems using a generalized finite difference model," *IEEE Power Engineering Review*, Vol. 11, No. 1, pp. 15-24, January 1991

[9] G. Anders, "Rating of Electric Power Cables - Ampacity Computations for Transmission, Distribution and Industrial Applications", IEEE Press, 1997.

[10] *IEC Calculation of the cyclic and emergency current rating of cables.* International Electrotechnical Commission Standard Series 60853, July, 1989

[11] R.S. Olsen, J. Holboell and U.S. Gudmundsdóttir, "Dynamic Temperature Estimation and Real Time Emergency Rating of Transmission Cables", IEEE General Meeting 2012, July, 2012.

[12] *IEC Electric Cables - Calculation of the Current Rating.* International Electrotechnical Commission Standard Series 60287, December, 2006.

[13] Z.S. Tseng, "Systems of First Order Differential Equations," Pennsylvania State University – Department of Mathematics, 2012, [Online], Available: http://www.math.psu.edu/tseng/class/Math251/Notes-LinearSystems.pdf

[14] T. Kusada and P.R. Achenbach, "Earth Temperature and Thermal Diffusivity at selected stations in the united states," U.S. Department of Commerce/National Bureau of Standards, Tech. Rep. NBS Report 8972, June, 1965.

[15] H. Brakelmann and G. Anders, "Ampacity Reduction Factors for Cables Crossing Thermally Unfavorable Regions," *IEEE Trans. Power Delivery*, vol. 16, No. 4, pp. 444-448, October, 2001.

[16] NKT cables, "High Voltage Cable Systems - Cables and Accessories up to 550 kV," [Online], Available: http://www.nktcables.com/support/download/catalogues-and-brochures/high-voltage-and-offshore/~/media/Files/NktCables/download%20files/com/HighVolt_e_200309.ashx, Apr., 2012

VI. BIOGRAPHIES

Rasmus Olsen received his master of science in electrical engineering in 2010 from the Technical University of Denmark (DTU). His PhD project, which he began shortly thereafter, is concerned with dynamic load optimisation of cable based transmission grids and it is a collaboration between Energinet.dk and DTU. His main interests are within thermal performance of transmission cables and grids. R. Olsen is a student member of IEEE.

Joachim Holboell is associated professor and deputy head of center at DTU, Department of Electrical Engineering, Center for Electric Power and Energy. His main field of research is high voltage components, their properties, condition and broad band performance, including insulation systems performance under AC, DC and transients. Focus is also on wind turbine technology and future power grid applications.
J. Holboell is Senior Member of IEEE.

Unnur Stella Guðmundsdottir received her M.Sc. and PhD degree in 2007 and 2010 respectively, from Aalborg University in Denmark. Her PhD studies focused on modelling of underground cable system at the transmission level. She was a guest researcher at SINTEF in Norway in November 2008 and at Manitoba HVDC Research Centre in Canada during June-October 2009. Currently she holds a position as a senior cable specialist and group leader at Energinet.dk where she is a deputy manager for DANPAC, a research project focusing on undergrounding of almost the entire Danish transmission system. U. S. Gudmundsdottir is a Member of IEEE.

F.4 Electrothermal Coordination in Cable Based Transmission Grids Operated under Market Based Conditions

Electrothermal Coordination in Cable Based Transmission Grids Operated under Market Based Conditions

R. Olsen, *Student Member, IEEE,* J. Holbøll, *Senior Member, IEEE,* U. S. Gudmundsdóttir, *Member, IEEE,* C. Rasmussen

***Abstract*--Electrothermal coordination (ETC) is a fairly novel concept, where the temperature of all lines in the transmission grid is monitored in real time and can be projected on the basis of measured and predicted load conditions. Until now ETC has been of mainly academic interest, but this paper describes how ETC can be implemented in transmission systems as they look today, taking into account both political decisions and market based conditions such as the ones the European transmission systems are operated under. The description of implementation strategies is supplemented by studying real cases from the Danish transmission system, and it is shown that great benefits can be achieved when utilising ETC instead of the present conservative approach to transmission cable dimensioning and operation.**

***Index Terms*—Cables, current control, load flow analysis, power control, power system economics, power system simulation, prediction methods, SCADA systems, temperature control, transmission lines**

I. Introduction

This paper describes and addresses issues that must be considered when implementing Electrothermal Coordination (ETC) in transmission systems which are operated under market based conditions. As described in [1], ETC is a concept which enables the Transmission System Operator (TSO) to utilise the varying loadability of transmission systems in a way that combines dynamic thermal studies with knowledge about the flow of electric power.

Because the Danish transmission system operation is subjected to market based conditions, the fundamental Optimal Power Flow (OPF) concept, which optimises parameters such as transmission losses and/or total costs, cannot be applied.

The reason is that the market dictates all stakeholders to be provided with equal access to the grid no matter where they are located and it is the responsibility of the TSO to transport the energy from the sites of generation to the sites of consumption. Costs related to transporting the energy are not considered, when deciding which units are allowed to provide the grid with power, as only the price of the energy itself is included in this decision.

On that background the present study addresses the possibility of introducing ETC in transmission systems operated under marked based conditions such that planning and operation of the transmission system can be optimised as seen from the TSO's point of view.

In [2] the authors showed how it is theoretically possible to implement ETC in cable based transmission systems, including the thermal calculations and the necessary load flow simulations. This paper builds another layer to the methodology and shows that ETC is not only of academic interest, but that TSOs can benefit directly by implementation of it.

It should be noted that [2] is solely concerned with real-time operation of transmission systems as it focusses on how ETC can be beneficial during contingencies. This paper will therefore mainly be concerned with investigating other aspects of ETC and in specific this paper studies how ETC can contribute to day-ahead planning and grid expansion planning of transmission systems. This will show that ETC can benefit several areas of expertise within the TSO and on time scales from minutes to years.

In order to verify the methodology, this paper will use the Danish transmission system, owned by the Danish TSO Energinet.dk, as an example. Actual cases are analysed with ETC in order to increase validity and ensure that the method can be implemented in real operational transmission systems.

Because the future Danish transmission system will consist mainly of cables, this paper has focused on modelling cable based systems. However it should be acknowledged that with proper adaptions it will be possible to analyse overhead line based systems as well.

The implementation of ETC in the Danish transmission system, as it will be described in this paper, illustrates the potential of the methodology. The description includes principles relevant to several TSOs and ETC should thus also be implementable in other transmission systems.

II. ETC of Cable Based Transmission Grids

For the overall understanding of ETC, it is important to be familiar with the methodology of combining Thermoelectric Equivalents (TEE) and load flow simulations. However as it was described in detail in [2] only a brief summary is given in the following.

R. Olsen is with Section of Transmission Lines, Energinet.dk, Fredericia 7000, Denmark (e-mail: rso@energinet.dk).

J. Holbøll is with the Dept. of Electrical Engineering, Technical University of Denmark, Kgs. Lyngby 2800, Denmark (e-mail: jh@elektro.dtu.dk).

U. S. Guðmundsdóttir is with Section of Transmission Lines, Energinet.dk, Fredericia 7000, Denmark (e-mail: usg@energinet.dk).

C. Rasmussen is with Section of Grid Planning, Energinet.dk, Fredericia 7000, Denmark (e-mail: cra@energinet.dk).

A. Loadability of Power Cables

Firstly it must be acknowledged that the loadability of a power cable is limited by the conductor temperature.

The conductor temperature has to be limited as a high temperature on the conductor implies a high temperature of the insulating material with an increased risk of failure as a consequence. In order to ensure reliability, excessive conductor temperatures are thus to be avoided.

In addition, as high temperatures on the jacket will cause the surroundings to dry and dry surroundings have worse thermal properties than moist, a high jacket temperature may lead to a vicious circle where the conductor temperature exceeds the maximally acceptable. The jacket temperature is in Denmark therefore considered to be the limiting parameter for the cable loading and the steady state loadability of a cable can thus be calculated as given in (1), [3].

$$I_{\max} = \sqrt{\frac{\left(\theta_{e,max} - \theta_{amb}\right) - W_d \cdot T_4}{R_{AC} \cdot T_4 \cdot \left(1 + \lambda_1\right)}} \qquad (1)$$

where I_{max} is the steady state loadability, $\theta_{e,max}$ is the maximally allowed jacket temperature, θ_{amb} is the ambient temperature, W_d are the dielectric losses, T_4 is the cable's external thermal resistance, R_{AC} is the electrical AC resistance of the conductor and λ_1 is the ratio between screen and conductor losses.

During contingencies in the Danish transmission system, the current in cables is allowed to increase to 200% of the steady state loadability as it is assumed that short durations of high temperatures will not jeopardise cable integrity or cause significant drying of the surroundings. This 'emergency loadability' is in Denmark allowed for up to 1 hour.

The steady state and the emergency loadability are presently only calculated during designing of the cable. In this design phase, the loadability is for safety evaluated conservatively by assuming high ambient temperature, low moisture content, etc. which means that there is a potential for increasing the value of the loadability if the actual cable temperature is known.

The challenge of ETC is therefore to dynamically evaluate the current values which will result in the limiting temperatures.

In order to evaluate such dynamic loadabilities, it is thus necessary to know the limiting temperatures of the cables. The present study has focused on XLPE insulated cables for which cable manufacturers allow conductor temperatures of up to 90°C during normal operation. However in order to avoid moisture migration of the surroundings, the Danish TSO requires the jacket temperature to be limited to 50°C.

During emergency operation though, the conductor temperature may be allowed to increase to temperatures higher than 90°C for a limited period of time; [4] for instance allows 105°C. Similarly the jacket temperature is allowed to rise to 60°C during emergency operation as it is assumed that applying this temperature for only 1 hour will have limited effect on the moisture content of the surroundings, [5].

B. Dynamic Temperatures by Thermoelectric Equivalents

It was shown in [6]-[7] that TEEs are suitable for modelling of the dynamic temperature of a system of transmission cables. TEEs are simple to implement, the accuracy is relatively high and the computational time is low.

The concept of TEE builds on the resemblance between heat flowing in a thermal system and current flowing in an electric circuit. The heat generated in a transmission cable is conducted through the different subcomponents and the soil to the ambience above ground. All materials which the heat has to pass through have a thermal resistivity which in the electric analogy is resembled by an electric resistivity. Furthermore all materials have a specific heat which is the capability of storing heat. This thermal capacitance is, in the electric analogy, resembled by an electric capacitance. When modelling the heat with a current in such an electric analogy, the voltage drop across a resistance will automatically resemble the temperature difference across the component. For easing the understanding, the simplest thermoelectric equivalent for single phased transmission cables is shown in Fig. 1, [7].

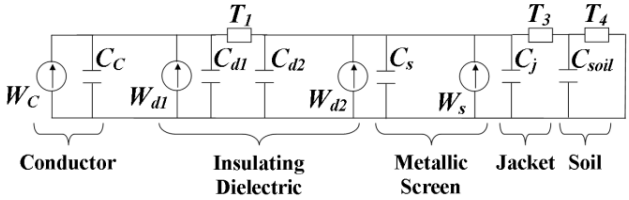

Fig. 1. Thermoelectric Equivalent of a single phased cable. W_c are the joule losses in the conductor, the sum of W_{d1} and W_{d2} are the dielectric losses and W_s are the screen losses. The *C*'s are the thermal capacitances of the respective subcomponents, as well as the *T*'s are the thermal resistances.

The spatial resolution of the TEE of Fig. 1 is poor. However, as it is shown in [6]-[7], it is possible to increase the resolution significantly, resulting in a far more accurate model.

The dynamic simulations performed with TEEs are conducted by solving (2).

$$\begin{bmatrix} \dot{\theta}_e \\ \dot{\theta}_s \\ \dot{\theta}_c \end{bmatrix} = \begin{bmatrix} -\left(\frac{1}{C_4 T_3} + \frac{1}{C_4 T_4}\right) & \frac{1}{C_4 T_3} & 0 \\ \frac{1}{C_3 T_3} & -\left(\frac{1}{C_3 T_1} + \frac{1}{C_3 T_3}\right) & \frac{1}{C_3 T_1} \\ 0 & \frac{1}{C_1 T_1} & -\frac{1}{C_1 T_1} \end{bmatrix} \cdot \begin{bmatrix} \theta_e \\ \theta_s \\ \theta_c \end{bmatrix} + \begin{bmatrix} 0 \\ \frac{1}{C_3} \cdot \left(W_{d2} + W_s\right) \\ \frac{1}{C_1} \cdot \left(W_c + W_{d1}\right) \end{bmatrix} \qquad (2)$$

Here θ_c, θ_s and θ_e are the conductor, screen and jacket temperature increases above the ambient soil temperature respectively, C_1=C_c+C_{d1}, C_3=C_{d2}+C_s+C_j, C_4=C_{soil}, W_C are the conductor losses, the sum of W_{d1} andW_{d2} are the dielectric losses and W_S are the screen losses.

The thermal resistances (*T*) and capacitances (*C*) are defined according to the design of the cable, [3] and [7].

The solution to the first order differential equation system of (2) is then as given in (3), [8].

$$\begin{bmatrix} \theta_e(t) \\ \theta_s(t) \\ \theta_c(t) \end{bmatrix} = c_1 \bar{v}_1 \cdot e^{\lambda_1 t} + c_2 \bar{v}_2 \cdot e^{\lambda_2 t} + c_3 \bar{v}_3 \cdot e^{\lambda_3 t} + \begin{bmatrix} \theta_e(\infty) \\ \theta_s(\infty) \\ \theta_c(\infty) \end{bmatrix} \qquad (3)$$

where *c*'s are constants evaluated based on the boundary conditions, *v*'s are eigenvectors of the equation system matrix and λ's are the eigenvalues of the equation system matrix.

All losses which must be estimated for these equations are calculated as specified in the international standards [3].

It should be noted that (3) is site specific, which means that when the cable passes through areas with varying external conditions (3) should be applied to each area in order to determine where the hotspots of the cable are. For this purpose [7] shows how distributed temperature sensing (DTS) measurements can be used to adapt the external thermal conditions for a conductor temperature accuracy of 2^{o}C.

C. Connecting TEEs with Load Flow Simulations

The purpose of performing load flow simulations is to estimate the current which will run in the different cables of the transmission system. Since the losses are directly related to the current flow, load flow simulations enable the prediction of the temperature evolution in all cables of the system. In [2] it is further argued, that load flow simulations are dependent on the conductor temperature of the different cables as the resistances are temperature dependent.

It is thus seen that there is a close connection between load flow studies and the temperature evolution of the individual transmission lines.

III. Implementation of ETC Considering the Market

As stated in the introduction, optimization of transmission systems have to address a large number of concerns and involves many different stakeholders, including energy producers, consumers, TSOs, politicians, etc. The present section is on this background dedicated to describing how ETC can be implemented in transmission systems while having the different concerns and stakeholders in mind.

It should be recognised that ETC can contribute to at least three areas of expertise within the TSO, each covering a certain time frame:

1. Real-time system control (minutes)
2. Day-ahead planning (days)
3. Grid expansion planning (years)

Suggestions to implementation procedures for each of these areas of expertise are given in the following.

A. Real-Time System Control

The Danish transmission system is monitored 24 hours a day, 7 days a week, by skilled personnel (denoted: the operator) trained in controlling the system, such that the supply of electric energy can be continuously secured.

The operator presently controls the system by ensuring that the current in each line is kept below its steady state loadability during normal operation.

During contingencies the operator must keep the current in each line below the emergency rating and, as soon as possible, reconfigure the system such that a new component failure can be allowed without the risk of blackouts.

By introducing temperature monitoring of the transmission system, by thermal simulations, it becomes possible to show the operator directly how hot the cables are, how the temperature will evolve and when the temperature will reach the limits. Furthermore, when unlikely events happen, such as two simultaneous component failures, the operator is expected to control the system based on experience, and here ETC will enable the operator to make decisions based on knowledge of the actual conditions instead of experience.

More specifically, ETC will be able to provide the operator with figures describing the loadability of the individual transmission cables as a function of time or/and the predicted temperature evolution in the hours to come. With these tools, the operator can focus on the most critical lines, without worrying about the rest of the system, because ETC will give an alarm in the case of potential overheating.

On this background it should be recognised that the combination of thermal modelling and load flow simulations is vital in predicting the thermal evolution, and this is the reason that ETC is a strong tool for the transmission system operator.

In case of an emergency situation the operator has fairly free hands for controlling the system and he can use the necessary means in order to maintain a reliable power supply to the consumers. This means that for ‘real-time system control’ power system integrity is more important than the costs for operating the system.

For the Danish transmission system it is suggested that ETC is implemented in the following way for real-time system control:

The implementation of ETC for emergency operation will require a continuous dynamic modelling of the temperature of all cables, such that the real-time temperature can be used in case of contingencies. This requires that the current of all transmission lines is measured, and that these currents are utilised to calculate the temperature via (3). In the case of a contingency, the ETC system will, based on the predicted production and consumption, calculate the load flow with the new grid configuration (after the fault) and this load flow will be used in the prediction of the temperature evolution.

B. Day-Ahead Planning

In Denmark, and the neighbouring countries, electric energy is sold and bought on market conditions. This means that the lowest priced energy will be sold first, and thereafter, if more energy is necessary, more and more expensive energy is sold. This selling and buying of electric energy is performed in hourly intervals for the coming day. Various political decisions may though result in deviations from the otherwise market based approach. In Europe the decision of increasing the amount of renewables is such a deviation, because even though e.g. wind turbines may produce expensive power; they have first priority to the grid, and renewable energy will thus always be sold first.

When everybody has bought the amount of energy needed, at the agreed price, the day-ahead market is closed and it is up to the TSO to transport the electric energy from site of production to site of consumption, hereunder maintain the flow on the cross-border lines that is the result of the day-ahead market agreements.

The above described market process takes place every day at noon (12:00), and covers the electric power system for the hours from midnight (00:00) to midnight (24:00) the following day. In Denmark, the TSO performs load flow simulations on

each hour of the market settled energy production and consumption in order to determine, if there are any violations of the loadability limitations of the individual transmission lines in the forecast.

Furthermore, in order to be able to sustain failures in the grid, an N-1 analysis is performed for each hour of the coming day. An N-1 analysis is a series of load flow simulation in which, one by one, each of the major components of the grid are assumed to be out of service. In each of these situations the grid must be able to operate with the steady state loadability limitation being respected for all components. If the N-1 criterion is not respected, the code prescribes the operator to take action in order to prevent overloadings and cascading failures in the grid. It should be remembered that such possible actions may be foreseen at least 12 hours before they appear and the operator can thus activate resources on market based conditions, i.e. the cheapest solution first.

The loadability limits, which are presently utilised to evaluate if the N-1 condition is respected, are static values of the maximum allowable current, (1). The present code may thus force the operator to act, even though the temperatures in the individual components are well below the limit.

By utilising ETC, the temperature can be modelled, (3), based on the market determined production and consumption patterns, and thus it can be foreseen if the predicted load flows will result in excess temperatures or not. This will allow the operator to utilise the full current carrying capacity which may be significantly higher than the loadability which was defined during purchasing of the component.

For the Danish transmission system it is suggested that ETC is implemented in the following way for the day-ahead planning:

The market is settled at noon on the day before operation, which means that the market predicts the energy exchange in the timeframe 12-36 hours into the future. A load flow simulation for each hour, with complete grid (the N situation), is performed and the temperature evolution throughout the coming 36 hours is calculated for all components in the system. For each cable the maximum predicted temperature from 00:00-24:00 is determined. Based on this maximum temperature a simulation is performed finding the current, which will result in a jacket temperature of 50^{o}C or a conductor temperature of 90^{o}C, whichever is reached first after 40 hours. This calculated current will be utilised as the loadability limit for the N-1 simulations for the coming day. Similar to the described 40 hours loadability, loadability levels for shorter time periods could be calculated, however 40 hours will enable the operator to control the system via market based decisions for the entire coming day of operation, and it is thus projected that a 40 hours loadability limit will benefit the operator mostly.

The maximum predicted temperature in the period from 00:00-24:00 is also utilised for determining the emergency loadability. The emergency loadability is defined as the current which result in the maximum allowable temperature after 1 hour. The present study allows for a maximum temperature of 105^{o}C on the conductor or 60^{o}C on the jacket, whichever is reached first. This 1 hour emergency loadability limit will only be utilized if an extreme situation, such as N-2, is experienced.

By utilising ETC in this way, the operator will not experience any difference in his daily work, as the operational boundaries are only changed once each day and thus simple control strategies can be maintained while enabling a better utilisation of the cables.

It is recognised that, by implementing ETC in the suggested way, the operator will not necessarily be allowed to use the full current carrying capacity at all times. However, given the restrictions set by politicians, in order to ensure a reliable power supply and given the restrictions set by the market based approach to transmission system operation, the methodology enables a significant increase in the utilisation of transmission cables, when comparing with today's system operation, which is based on static loadability limits.

C. Grid Expansion Planning

Today the Transmission Grid Planner (TGP) uses the standardised equations of [3] when choosing the proper cable size. However static loadability limits must be inherently conservative in order to ensure reliability and even when using the more dynamic approach of cyclic rating, such as described in the IEC standard 60853, [9], the specific history of the transmission cables will not be included in the analysis and thus also these calculations may result in underutilisation.

When planning new cable lines, the dimensioning criteria will generally not be the normal daily load cycle. Instead scenarios such as N-1-1 (e.g. one major component out for maintenance followed by one failure) and problematic external conditions including hot weather and high consumption are analysed. In such situations it can become beneficial to utilise ETC as the methodology for dimensioning of new cables, because each case can be dynamically investigated.

ETC simulations can potentially result in lowering the requirements for the cross sectional area of the conductor, than if the cross section was to be chosen on the basis of the static equations of [3]. Smaller cross sections may lead to a number of cost savings on both purchasing the cable, but also on accessories, transport, installation, etc.

For the Danish transmission system it is suggested that ETC is implemented in the following way for the grid expansion planning:

Implementing ETC in grid expansion planning will require that the TGP can set up realistic dynamic load profiles for the grid. The TGP will, via integration of thermal analyses in load flow simulations, be capable of predicting the thermal evolution during the dimensioning situations and, based on these analyses, determine if the investigated case gives a sufficiently reliable system or if larger cables are required.

IV. Case Studies

This section shows the potential of ETC when it is applied to two actual cases which are of major importance to the Danish transmission system.

The case studies uses publically available XLPE cable dimensions, electrical properties and thermal properties, [4], [10] and [11], for performing the thermal calculations.

It should be noticed that a case study of real-time system operation was discussed in [2] and because the system integrity is more important than the costs during emergency operation it is not necessary to investigate real-time system control with a special focus on the market implementation. The following cases are therefore only concerned with day-ahead planning and grid expansion planning.

A. Day-Ahead Planning

The Danish island of Funen is connected to the Jutlandic grid by means of two 400kV systems and one 150kV system, see Fig. 2.

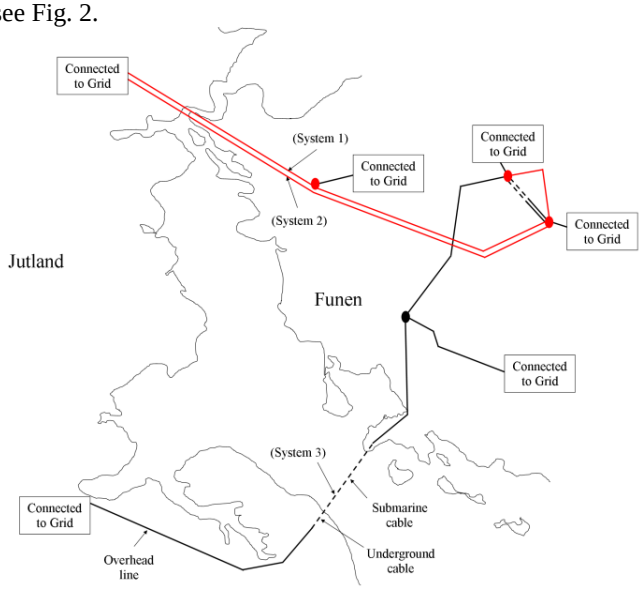

Fig. 2. Overview of electrical connections between Jutland and Funen. Dashed lines are cables and solid lines are overhead lines. In paranthesis is shown the denotation of the lines. System 1 and 2 are 400kV lines and system 3 is 150kV.

Funen has generation internally and can therefore in principle run in island mode. However, due to the market based conditions under which the transmission system is operated, it shall be strived to allow the cheapest produced energy to be transported to the consumers at Funen, and thus the electrical connection to Jutland are vital for ensuring the free market.

In the unlikely event of both 400kV connections being out of service, the TSO would like to know if it is possible to operate the transmission system with only the 150kV system to supply the required load or if it is necessary to purchase generation capacity, or generation reserves, on the Funen side on the day-ahead market. In the following it is assumed that the underground cable of the 150kV system is the limiting part of 'System 3'.

At 12 o'clock, the market is settled, and the TSO has to determine whether the N-1 criterion is respected in the coming day of operation. Based on the settled market, the predicted apparent power, *S*, transfer from Jutland to Funen for the coming day of operation is as seen in Fig. 3.

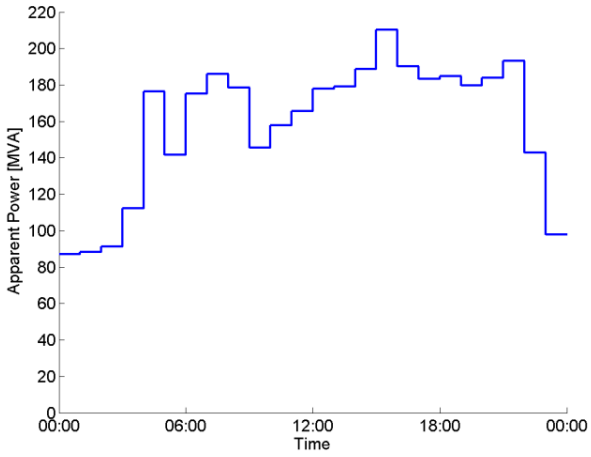

Fig. 3. Predicted apparent power, *S*, to be transmitted from Jutland to Funen in the coming day of operation.

'System 1' is to be taken out of operation for maintenance at 7:00, and the N situation from 7:00 and on-wards is thus that Funen and Jutland are only connected via "System 2" and "System 3".

The predicted load flow through these lines, given the predicted apparent power of Fig. 3, is thus as shown in Fig. 4.

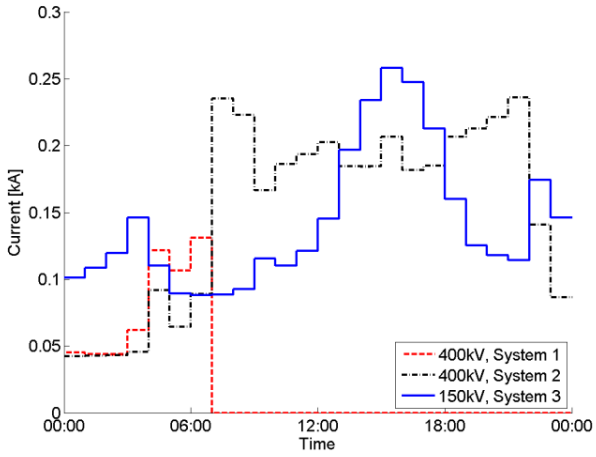

Fig. 4. Predicted current in the 150kV and the two 400kV transmission lines when one 400kV system is assumed to be taken out for maintenance at 7:00.

It is predicted that the weakest link of the remaining two lines is the 150kV underground cable in System 3. In order to determine the 40 hours loadability of this cable, the temperature in the line is to be estimated, and this requires knowledge about the properties of the involved component. This case study assumes that the cable is a 150kV copper conductor cable with a cross sectional area of 300mm^2. The cable characteristics have been taken from [4]. The cables are buried in flat formation (conductors spaced 0.3 meters apart) in a bedding of sand, such as is the normal installation procedure in Denmark. The burial depth is 1.4m and it is assumed that the ambient temperature is the seasonally highest of the normal temperatures in Southern Jutland and Funen: 20^{o}C, [12]. The current in 'System 3' which does not lead to

excessive temperatures is calculated, by using (1), to be 656A. Furthermore, 'System 2' is rated approximately 850 A.

Given these quantities, it is seen that with a complete grid (the N situation), the system is in a reliable state as the steady state loadability levels are respected.

Thereafter N-1 simulations are performed on the system for each hour. If "System 2" fails before 7:00, the maintenance of "System 1" will be postponed, however after 7:00 it is assumed that "System 1" cannot be restored within the day of operation. The N-1 load flow, assuming "System 2" failure in the hour between 7:00-8:00, thus looks as seen in Fig. 5.

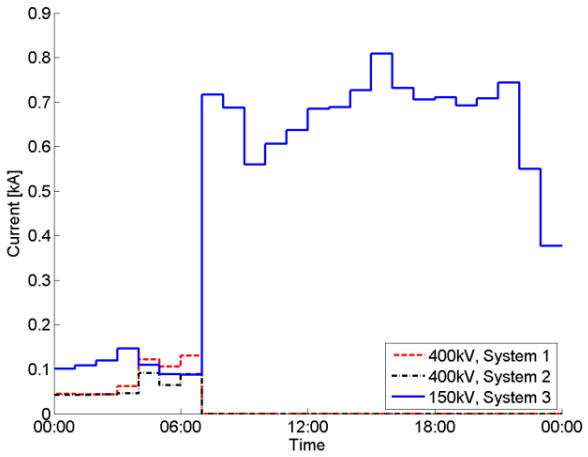

Fig. 5. Simulated load flow when System 1 is assumed out of operation and System 2 fails, i.e. N-1-1. It is seen that the load in the 150kV cable increases significantly and potentially above the emergency rating. The market based generation schedule is thus not acceptable why remedial actions, such as increasing generation at the Funen side, must be taken.

As mentioned, the present standardised steady state loadability of 'System 3' is 656A, and because the maximum of the current seen in Fig. 5 is 809A, the classical operation procedure concludes that the grid will reach an unacceptable state after failure of 'System 2'. When using the steady state loadability, it is therefore necessary to take remedial actions before 7:00 in order to avoid possible critical situations. These remedial actions can for instance consist of increasing the generation at the Funen side which is a costly procedure.

By implementing ETC in the day ahead planning, the 40 hours loadability limit can be evaluated by taking into account the actual conditions, which in this case result in a 40 hours loadability of 955A. ETC based operation would thus allow the TSO to operate the transmission grid under the given market settled generation and consumption patterns without the need to interfere.

Similarly to the 40 hour loadability, the 1 hour loadability can be evaluated based on the predicted load of Fig. 4. For the present case, the 1 hour loadability is 1428A, which is significantly higher than the presently used emergency loadability, which is defined as two times the steady state loadability, i.e. 1312A. In case of contingencies appearing in addition to the failure of "System 2", there is thus also additional operational freedom to be gained when utilising ETC.

On this background it should be clear that there may be large benefits to be gained by implementing ETC in the day-ahead planning of the transmission grid. In the present case study, remedial action can be avoided and thus costs to increased generation on the Funen side may be circumvented.

B.System Expansion Planning

In Fig. 6 a part of the Danish (Northern Zealand) transmission system, as it looks today, is shown. All lines at 50kV and above are included. It is seen that most lines are overhead lines and that the TSO has installed several lines in parallel at critical places for ensuring redundancy.

Besides the normal commercial and residential consumers in the rural area with mainly smaller towns, a large industrial electricity consumer is connected to the "VAL" node.

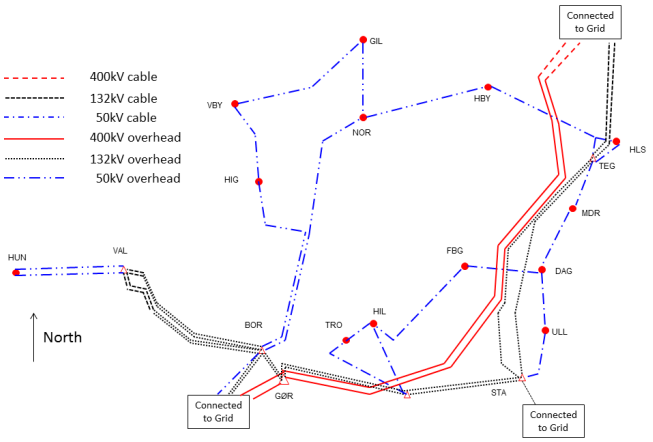

Fig. 6. Transmission system in the Northern Zealand as of 2009, including all lines from 50kV and up. It is seen that most lines are overhead lines, and many lines are installed in parallel for ensuring redundancy. The red dots represent connections to the lower voltage consumer grid and the connection to the transmission grid is presented as "Connection to Grid".

Fig. 7 shows a suggestion to the transmission system design as it could look in the year 2025.

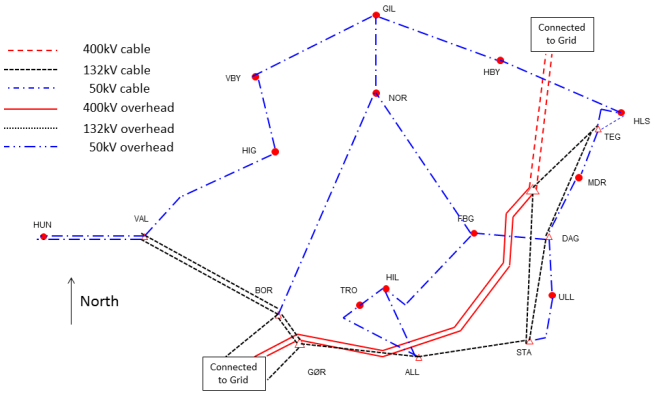

Fig. 7. Suggested transmission system design as of 2035. It is seen that most transmission lines are now cables, and that the system has become meshed to a more predominant extend than Fig. 6.

It is seen that the transmission lines are now mainly cables and that the system has changed to a more meshed design, as compared to Fig. 6, which shows a more radial structure.

It is seen from the two figures that the suggested transmission system will have a very different configuration than the existing; especially at the VAL node, where it is

suggested that the power should be redundantly supplied from HIG instead of purely from BOR.

It is projected that the most critical lines are the two 132kV systems between BOR-VAL, and in the unlikely event that both of these two systems are out of service (related or unrelated faults or maintenance issues), the required power should be transmitted via the 50kV system instead. The question is now, whether the new topology can handle the required stress in case of multiple faults or if it is necessary to build a third 132kV line to the VAL node.

In case of two faulted 132kV lines between BOR-VAL, all of the power must be transferred via the GIL-node through the grid all the way to HUN, and because there is no generation capacity on the VAL side of the faulted grid, the cable between GIL-VBY will be the hardest loaded and thus also the limiting link of the network.

A projected loading pattern for the cable GIL-VBY, in case of the two 132kV lines being out of operation, is shown in Fig. 8. It is for simplicity assumed that the current has been steady state 180A for infinitely long time prior to failure which happens after 48 hours. Thereafter the load instantly increases and varies between 600-1200A in the daily load cycle.

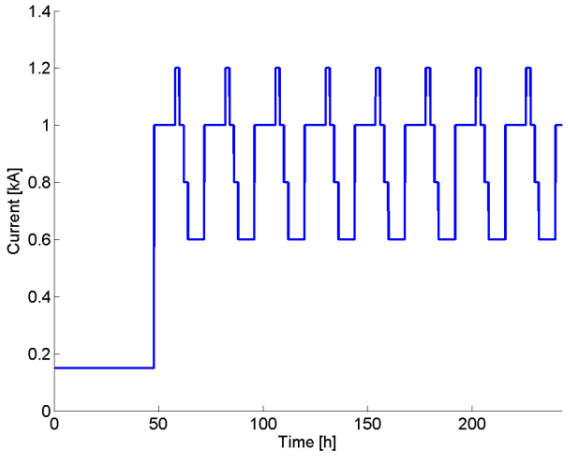

Fig. 8. Projected load profile of GIL-VBY cable in the case of two faulted 132kV systems between BOR-VAL.

In the conventional way, the 50kV cable would have to be dimensioned for a constant current of 1200A, because the load cycle includes 2 hours of 1200A each day, even though the dimensioning case is highly unlikely.

The loadability of the installed cables is calculated by assuming the same burial conditions as the previous case.

By using the parameters which are available in [10], considering a 72kV cable (driven at 50kV) with aluminium conductor, the maximally allowed steady state current for different cross sections of the cable will be as given in Table I. The thermal resistivity of soil is assumed to be 1Km/W and thermal resistivity of sand is set to 0.5Km/W.

TABLE I
LOADABILITY OF 50KV POWER CABLES OF DIFFERENT CONDUCTOR CROSS SECTION

Conductor Area [mm^2]	400	500	630	800
Steady State Loadability [A]	523	594	684	753

It is seen that none of the cables are even close to be capable of transporting the maximum current of 1200A continuously and a third 132kV system may thus be necessary. It is noticed that for the 400mm^2 cable three parallel systems are required and for the 630mm^2 two parallel systems are required.

When utilising (3) to calculate the thermal response to the load profile of Fig. 8 for the four different conductor sizes, the results will be as seen in Fig. 9.

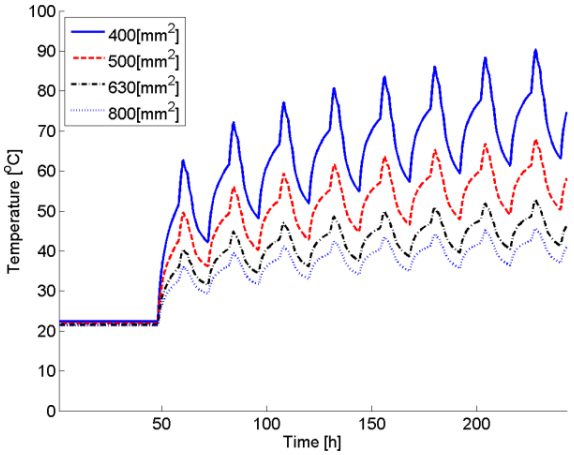

Fig. 9. Modelled jacket temperature of centre phase for four different conductor sizes, each exposed to the load profile of Fig. 8.

It is seen from the figure that the cables have a fairly large thermal inertia, and that some of the cables are capable of carrying the required load-profile for several days before the jacket temperature exceeds 50°C.

The conclusion to the results of Fig. 9 must therfore be that it is possible to conduct the required current for a significant period of time before the jacket temperature increases beyond the accepted 50°C, and thus the dynamic thermal calculations requires only for a single cable system to be installed which may result in a significant reduction of the costs, as when compared to installing two cable systems. The installation of a proper sized 50kV cable thus also implies that the TSO can omit building a third 132kV connection between the BOR and VAL nodes. For maximum system safety, and for minimising losses, the 800mm^2 cable should be chosen, because this allows for longer repair times of the two 132kV systems; however even the 630mm^2 cable is seen to be able to handle the required load profile for a substantial amount of time. It should be noted that the thermal model furthermore confirms that the conductor temperature does not exceed the 90°C limit for the 630mm^2 and 800mm^2 cables, for the investigated scenario.

IV. CONCLUSION

Electrothermal Coordination (ETC) is in this study shown to be implementable and beneficial in cable based transmission systems which are operated under market based conditions.

There are two important innovations in the presented study. Firstly, the definition of a 40 hours loadability which is used to evaluate if the day-ahead market can be allowed or if

operator interference is required, and secondly, the thermal analysis of the projected dynamically varying load for design of new transmission lines.

The paper furthermore gives thorough suggestions to the steps which must be taken in order to implement ETC in the transmission system operated under market based conditions.

Regulation requires all stakeholders to have equal access to the grid and thus conventional grid optimisation tools, such as Optimal Power Flow (OPF), may not be allowed.

ETC is therefore introduced in this paper as a way to enhance performance of the grid, such that the system operator can be allowed to increase loading above the conventional steady state and emergency rating values. It is shown in this study, that ETC can be beneficial for three areas of expertise within TSOs, firstly real time system control, secondly, day-ahead market planning and thirdly, grid planning.

A previously published paper showed, through a case study, that the TSO can benefit in the real time operation of transmission systems and an algorithm for ETC analyses was proposed. The present paper utilises the algorithm in the day-ahead planning and it is shown to be beneficial as increased loadability values can turn an otherwise not allowed market state into an allowed market state.

Furthermore, a second case shows that the grid planner can also benefit from ETC, as it allows for minimising the cross section of future cable lines while maintaining system reliability.

By utilising the techniques proposed in this study, TSOs will potentially be able gain economic benefits, both on investment in new transmission lines and on the operation.

Having these fundamental technical procedures in place, the next step will be to perform the actual implementation in the Danish transmission system operation which is a topic that Energinet.dk is presently looking into.

V. Acknowledgement

The authors would like to thank F. Christiansen, Energinet.dk, for his contributions to this publication.

References

[1] H. Banakar, N. Alguacil and F. D. Galiana, "Electrothermal Coordination Part I: Theory and Implementation Schemes," *IEEE Trans. Power Systems*, vol. 20, No. 2, pp. 798-805, May, 2005.

[2] R. Olsen, J. Holboll, and U.S. Gudmundsdottir, "Electrothermal Coordination in Cable Based Transmission Grids", *IEEE Trans. Power Systems*. Accepted for publication.

[3] *IEC Electric Cables - Calculation of the Current Rating - Current Rating Equations (100 % Load Factor) and Calculation of Losses - General*. International Electrotechnical Commission Standard 60287-1-1, edition 2.0, December, 2006.

[4] ABB, XLPE Land Cable Systems – User's guide, Sweden. April, 2010. [Online]. Available: http://www05.abb.com/global/scot/scot245.nsf/veritydisplay/ab02245fb5b5ec41c12575c4004a76d0/$file/xlpe%20land%20cable%20systems%202gm5007gb%20rev%205.pdf

[5] O. E. Gouda, G. M. Amer, and A. Z. E. Dein, "Effect of dry zone formation around underground power cables on their ratings," *International Journal of Emerging Electric Power Systems*, vol. 10, no. 3, 2009.

[6] R.S. Olsen, J. Holboell and U.S. Gudmundsdóttir, "Dynamic Temperature Estimation and Real Time Emergency Rating of Transmission Cables", IEEE General Meeting 2012.

[7] R. Olsen, G.J. Anders, J. Holboell and U.S. Gudmundsdóttir, "Modelling of Dynamic Transmission Cable Temperature Considering Soil Specific Heat, Thermal Resistivity and Precipitation," *IEEE Trans. Power Delivery*, Accepted for publication in 2013.

[8] Z.S. Tseng, "Systems of First Order Differential Equations," Pennsylvania State University – Department of Mathematics, 2012, [Online], Available: http://www.math.psu.edu/tseng/class/Math251/Notes-LinearSystems.pdf

[9] *IEC Calculation of the cyclic and emergency current rating of cables - Part 2: Cyclic rating of cables greater than 18/30 (36) kV and emergency ratings for cables of all voltages*. International Electrotechnical Commission Standard 60853-2, edition 1.0, July, 1989

[10] NKT cables, *Produktkatalog Elforsyning 2010*, [Online], Available: http://www.nktcables.dk/~/media/Denmark/Files/Catalogue/Elforsyning%20katalog%202010.ashx, Nov., 2011.

[11] NKT cables, *High Voltage Cable Systems - Cables and Accessories up to 550 kV*, [Online], Available: http://www.nktcables.com/support/download/catalogues-and-brochures/high-voltage-and-offshore/~/media/Files/NktCables/download%20files/com/HighVolt_e_200309.ashx, Apr., 2012

[12] Danish Meteorological Institute, *Climate Normals*, [Online], Available: http://www.dmi.dk/dmi/index/danmark/klimanormaler.htm

Biographies

Rasmus Olsen received his master of science in electrical engineering in 2010 from the Technical University of Denmark (DTU). His PhD project, which he began shortly thereafter, is concerned with dynamic load optimisation of cable based transmission grids and it is a collaboration between Energinet.dk and DTU. His main interests are within thermal performance of transmission cables, how this performance can be increased and how asset management can be introduced for a more optimal utilisation of such cables and cable systems.

Joachim Holboell is associated professor and deputy head of center at DTU, Department of Electrical Engineering. His main field of research is high voltage components, their properties, condition and broad band performance, including insulation systems performance under AC, DC and transients. Focus is also on wind turbine and future power grid applications.
J. Holboell is Senior Member of IEEE.

Unnur Stella Guðmundsdottir received her M.Sc. and PhD degree in 2007 and 2010 respectively, from Aalborg University in Denmark. Her PhD studies focused on modelling of underground cable system at the transmission level. She was a guest researcher at SINTEF in Norway in November 2008 and at Manitoba HVDC Research Centre in Canada during June-October 2009. Currently she holds a position as a cable specialist at Energinet.dk where she is a deputy manager for DANPAC, a research project focusing on undergrounding of almost the entire Danish transmission system. U. S. Gudmundsdottir is a Member of IEEE.

Carsten Rasmussen received his M.Sc. and PhD degree in 1997 and 2000 respectively, from DTU. His PhD studies focused on prototypes of terminations for superconducting cables. He has been working at Energinet.dk (formerly called Elkraft System) since 2001. The last 4 years in the Grid Planning section.

www.energinet.dk

Electricity Division
Electricity Transmission
Energinet.dk
Tonne Kjærsvej 65
DK-7000 Fredericia
Denmark
Tel: (+45) 70 10 22 44
Fax: (+45) 76 24 51 80
Email: info@energinet.dk

www.elektro.dtu.dk

Department of Electrical Engineering
Centre for Electric Technology (CET)
Technical University of Denmark
Ørsteds Plads
Building 348
DK-2800 Kgs. Lyngby
Denmark
Tel: (+45) 45 25 38 00
Fax: (+45) 45 93 16 34
Email: info@elektro.dtu.dk